Potential tsunamigenic sources in the Eastern Mediterranean and a decision matrix for a tsunami early warning...

Conference Paper · May 2011

CITATIONS
3

READS
66

1 author:

Amos Salamon
Geological Survey of Israel
39 PUBLICATIONS **477** CITATIONS

SEE PROFILE

CIESM Workshop Monographs

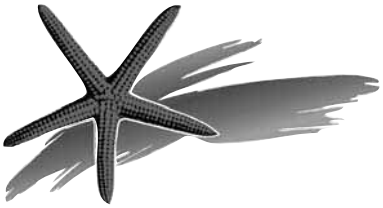

Marine geo-hazards in the Mediterranean

Nicosia, 2 - 5 February 2011

CIESM Workshop Monographs ◊ 42.

To be cited as: CIESM, 2011. Marine geo-hazards in the Mediterranean. N° 42 *in CIESM Workshop Monographs* [F. Briand Ed.], 192 pages, Monaco.

This collection offers a broad range of titles in the marine sciences, with a particular focus on emerging issues. The Monographs do not aim to present state-of-the-art reviews; they reflect the latest thinking of researchers gathered at CIESM invitation to assess existing knowledge, confront their hypotheses and perspectives, and to identify the most interesting paths for future action.

A collection founded and edited by Frédéric Briand.
Publisher : CIESM, 16 bd de Suisse, MC-98000, Monaco.

CONTENTS

I - Executive Summary

This synthesis, initiated during the meeting, was developed and coordinated thereafter by inputs received from all participants, under the coordination of Gert de Lange. Frédéric Briand, the Monograph Series Editor, reviewed and edited the entire volume, whose physical production was carried out by Valérie Gollino.

1. Introduction

Amongst the most devastating marine catastrophes that can occur in areas prone to seismic and volcanic activity, are earthquakes, volcanic eruptions and submarine slides, all of which can lead to tsunamis and/or additional hazards which may seriously endanger human society. Many such events are known and have been reported for the Mediterranean, a region where high-frequency occurrence of seismic and volcanic activity coincides with some of the most densely populated coastal areas in the world.

Acutely conscious of these potential marine geohazards, CIESM invited a selected group of scientists, covering the broad aspects mentioned above, at its 42nd International Workshop from 2-5 February 2011, at Nicosia, Cyprus. Following introductions by Frédéric Briand, Director General, and Gert de Lange, Chair of the CIESM Committee on Marine Geosciences, the group discussed not only past seismic, volcanic, and submarine slide generation, but also past tsunami activity, and potential present and future areas for tsunami origin and fate, based on field observations, historical records, and modeling studies. In addition, mitigation was considered for risk reduction purposes. The outcome of the workshop includes a state of the art review, conclusions, and recommendations for actions and for further research activities. These are synthesized in this Executive Summary and are presented with specific details in the full papers prepared by each of the workshop participants.

Note from the Editor:

On 11 March 2011, just a few weeks past the conclusion of this workshop, a major earthquake and a subsequent catastrophic tsunami hit the northeastern coastal region of Japan, taking thousands of lifes and leaving hundreds of thousand survivors homeless and desperate. The dramatic observations made in Japan (Kyoto University Team, 2011; Tokyo Earthquake Research Institute, 2011; Group on Earth Observations, 2011; Parashar *et al.*, 2011) served as a powerful reminder, if necessary, of the destructive nature of such events. They signaled the rapid and devastating impact in areas close enough to be struck within half an hour ... as would be the case for most locations of any such event in the closed Mediterranean Sea. Added to the lessons previously learned from the Indian Ocean tsunami of 26 December 2004, such observations are of much relevance to the Mediterranean setting and were therefore constantly in the mind of the group who drafted this synthesis thereafter. These two recent catastrophes have demonstrated the reality and plausibility of worst case scenarios, that tended to be previously considered as a hypothetical upper boundary. In addition, the magnitude and severity of the impact call for our urgent re-consideration of assessment of magnitude for geohazard events where recurrence rates now exceed several millennia.

Most marine hazardous events in general and in the Mediterranean in particular can be related to geological processes associated with plate boundaries and to active faulting or slope failure resulting in major slumps at continental margin areas. In the present-day Mediterranean configuration, it is the subduction of the African plate underneath the EurAsian plate (for details, see Mascle, this volume) that initiates the former and the shallow margin and steep unstable continental slopes (Fig. 1) that contribute to the latter event generation (for details, see Sallarès *et al.*, this volume; Ceramicola *et al.*, this volume; and Migeon *et al.*, this volume). The former large-scale geological processes not only lead to distinct volcanic arc activity (Sakellariou, this volume) but also to enhanced seismicity in discrete areas (see below, and Papadopoulos, this volume). Volcanoes and Earthquakes are two near-surface expressions of these deep geological processes that may lead on the one hand to catastrophic events directly and on the other hand to tsunami-related damage, indirectly. Massive slides may be triggered by an earthquake (Salamon, this volume) or by progressive *in situ* destabilizing processes.

Each of these generalized processes will be outlined in the next sections, followed by others on tsunami activity and detection, mitigation, and recommendations.

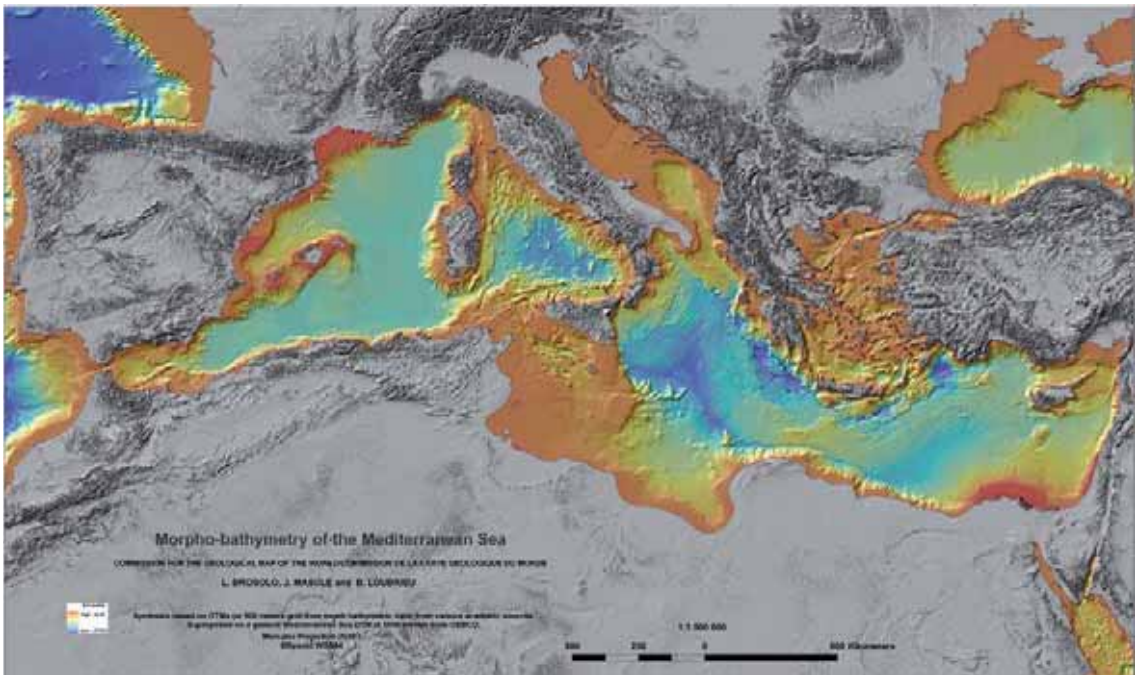

Figure 1. General morpho-bathymetry of the Mediterranean Sea DTM at 500 m.

2. Volcanoes

Mediterranean subduction-related volcanism occurs in the Tyrrhenian and the Aegean Seas with respectively the Aeolian and Hellenic volcanic arcs. Volcanic activity along these arcs has been known since prehistoric time and is still going on. Approximately 5% of the known tsunamis worldwide have been generated by processes connected with volcanoes. In general, volcanic activity-related tsunami triggering mechanisms may relate to the caldera formation, to the volcanic edifice collapse, to pyroclastic flows, to hot surges generated during eruption, and even to failure of volcanic deposits soon after their deposition on the seafloor (Gamberi and Marani, this volume; Sakellariou, this volume).

Caldera formation – submarine eruptions

Large volcanic eruptions may lead to collapse of the entire volcanic edifice and consequently to the formation of a caldera. Caldera formation has repeatedly occurred during the long eruptive history of Thera (Santorini) volcano, including the Minoan eruption in the 17th century BC. If such caldera formation is below sealevel, then huge quantities of seawater rush in to fill the new

cavity. The tsunami generated in that way spreads radially, like the tsunami triggered by the explosion of Krakatoa volcano in 1883, or of Sumiso volcano, Japan (Tani *et al.*, 2008). The same process is thought to have occurred during the Minoan eruption and subsequent caldera formation (Yokoyama, 1978; Goodman-Tchernov *et al.*, 2009; McCoy and Heiken, 2000; De Martini *et al.*, this volume; Sakellariou, this volume). Shallow-water submarine eruptions, like the AD 1650 Columbo eruption, just north of Santorini, are known to be able to cause hazardous phenomena like gas explosions, pyroclastic flows and tsunamis (Dominey-Howes *et al.*, 2000). Deep submarine eruptions probably do not constitute a major hazard since the pressure of the water column causes the material to be ejected mainly in the form of lava flows.

Pyroclastic flows

Pyroclastic flows are tightly associated with and constitute one of the most devastating phenomena of volcanic eruptions. They are hot surges, composed of hot gas and volcanic tephra, which travel down the volcanic slopes and spread laterally at velocities of hundreds of kilometres per hour. Recent studies have shown that pyroclastic flows, depending on their density and velocity, when entering the ocean are capable of triggering tsunamis. Very thick pyroclastic flow deposits of the Minoan eruption have been mapped on the seafloor at distances up to 30 km around Santorini (Sigurdsson *et al.*, 2006; Sakellariou, this volume), and may have triggered tsunami waves (McCoy and Heiken, 2000).

Volcanic edifice gravitational collapse / slope failure

An additional geohazard associated with most of the volcanoes in the Mediterranean is the process of structural failure and gravity collapse of the volcanic edifices. This hazard is inherent to the history of volcano growth that evolves through constructional phases to gravitational instability. This inevitably leads to an increase of the steepness of the edifice's flanks, of overloading and of potential instability. When the volcanic dynamics results in an excess critical instability, destructional phases punctuate the constructional processes, leading to structural collapses, often catastrophic, of the volcano's flank.

2.1 Tyrrhenian Sea

In the Tyrrhenian Sea, the Aeolian volcanic arc includes seven islands and several volcanic seamounts that do not reach the sea surface. Some of the Aeolian Island volcanoes are known to be active, as for example the well known Stromboli volcano that due to its continuing intermittent eruptions was known in the antiquity as "the lighthouse of the Mediterranean". Besides many accounts of past potential hazards from eruptions of these active volcanoes, their period of '*unrest*' in 2002 has shown that the submarine portions of these islands can be hazardous. This can be exemplified for Stromboli where after a period of intense activity, with lava flows emission, a large amount of pyroclastic material and lava had accumulated on the northern side of the volcano. Due to the weight of this new material and the steep gradient of the flank, huge downslope mass movements occurred on 30 December 2002. A first massive submarine landslide occurred just under the sea level followed by a subaerial landslide; both landslides produced tsunami waves. The tsunami had a run-up of about 10 m (Maramai *et al.*, 2005a), and the fact that there were no casualties was due to the low touristic season. Another example comes from Panarea Island. On 3 November 2002, three large whitish plumes suddenly appeared at the sea surface about 3 km eastward of Panarea. Submarine craters opened at the top of a 2.3 km^2 shallow rise of the seafloor, between –2 and –30 m below sea level. This event highlighted the unexpected revival of volcanic activity offshore Panarea Island a volcano generally considered to be extinct (Esposito *et al.*, 2006). In addition to Island arc volcanism, large volcanic seamounts are present in the Tyrrhenian back arc domain that have been possibly affected by large collapse and by explosive submarine eruptions at a depth of 500 m.

A further active volcanic region is located in the Sicily Strait where crustal extension in front of the Apenninic-Maghrebian chain is accompanied by magma ascent and volcanic activity. Here, historical reports on submarine volcanic activity are frequent. The most recent and well described ones correspond with the eruptions that lead to the formation of the ephemeral Ferdinandea Island in 1831 and the Foerstener submarine eruption of 1891 (Corti *et al.*, 2006). The case of the Ferdinandea Island has shown that in the area submarine eruptions can be hazardous associated with phreatomagmatic eruptions that also can generate local tsunamis.

2.2 Aegean Sea

The Hellenic Volcanic Arc has developed as a consequence of the active subduction and melting of the African lithosphere beneath the Aegean Sea. The trace of the volcanic arc is parallel to and about 150 km north of the Hellenic Trench, and is delineated by four main volcanic fields in the South Aegean Sea, namely Poros-Methana-Egina, Milos, Santorini-Columbo, and Nisyros-Kos. Major historically recorded eruptions took place mainly in the Santorini-Columbo volcanic field. The most recent major explosive eruption, the Minoan eruption of the Santorini volcano, took place in the 17th century BC (about 3600 years B.P.) and has been considered to be a main reason for the decline of the Minoan civilization on Crete (e.g. Marinatos, 1939), an hypothesis that is no longer generally accepted. Recent studies have shown that the Minoan eruption is the second largest one worldwide, after the Tambora 1815 eruption in Indonesia, and much greater than the 1883 eruption of Krakatau also in Indonesia (Sigurdsson *et al.*, 2006). It is widely believed and there is evidence proving this, that huge tsunami waves were generated as a consequence of the various eruptive phases, which inundated the coasts of the Central and Eastern Mediterranean (Marinatos, 1939; Yokoyama, 1978; Minoura *et al.*, 2000; Pareschi *et al.*, 2006a; Bruins *et al.*, 2008; Papadopoulos, 2009; Novikova *et al.*, 2011; De Martini *et al.*, this volume). A more recent, submarine eruption took place in September 1650, associated with the submarine Columbo volcano that is located a few miles northeast of Santorini. Tens of casualties were reported from the volcanic gases and the tsunami which followed this eruption (Dominey-Howes *et al.*, 2000). The Columbo volcanic field is comprised of about 20 small, submarine volcanic cones. Recent studies suggest that these cones may be younger than the main Columbo edifice and may thus constitute potential centers of future submarine eruptions.

2.3 Gaps of knowledge related to volcanic activity

Monitoring of hydrothermal activity, geochemical composition of emitted gas, seismicity and ground motion is well established on volcanoes located on land in the Mediterranean Region. In contrast, submarine volcanoes in the Mediterranean (such as in Columbo-field, or submarine cones in the Tyrrhenian Sea) are not being monitored by any means. Consequently, no risk assessment or prevision can be done for the marine domain.

3. Earthquakes

3.1 Geodynamics and seismo-tectonics

Earthquakes represent the most frequent hazardous events in the Mediterranean region. The main geodynamic process, which controls seismicity on Earth, is the continuous motion of rigid lithospheric plates. This mechanism is quite active in the region where complex interactions between the African and Eurasian plates, and several microplates (see Fig. 1 in Mascle, this volume), are associated with a variety of seismo-tectonic styles: *compression* due to lithospheric convergence in SW Iberian Peninsula, North Algeria, Calabria Arc in Italy, Hellenic Arc in Greece, Cyprus Arc in Levantine basin; *extension* in back-arc basins (e.g. Alboran Sea, Tyrrhenian Sea, Aegean Sea), as well as in more complicated areas such as the Apennines and the Messina Strait in Italy, and the Corinth Rift in Central Greece; *shear* associated with horizontal *strike-slip motion* of adjacent lithospheric blocks, for example along the North Anatolian Fault, in Eastern Ionian Sea (Cephalonia), and along the Dead Sea Fault; *oblique-slip* where compression, or extension, are combined with strike-slip motion, like *transpression* along the Eastern Hellenic arc, or *transtension* along the southern part of the Dead Sea Fault, and along the western segment of the North Anatolian Fault Zone. Most of this seismicity is relatively shallow and occurs in the upper 30 or 40 km of the lithosphere. Deeper earthquakes have however been recorded in Spain (up to about 660 km) as well as in the subduction zones of the Calabria (up to ~350 km), Hellenic (up to ~180 km), and Cyprus Arcs (up to ~120 km). Earthquakes associated coastal uplifts such as at Rhodes and Crete (Stiros and Pirazzoli, 2009; Stiros, 2010) are signatures of the convergence between Africa and Eurasian plates along the Mediterranean Arc Systems.

3.2 Distribution – short history

Although the seismicity, that is the level of earthquake activity, is not uniformly distributed in space and time, there is in fact no area in the Mediterranean Sea region which is free of earthquake epicentres (see Fig. 2 in Mascle, this volume) or its influence. The highest seismicity, however, is

concentrated in the eastern basin of the Mediterranean Sea. This is mainly due to a higher rate of tectonic deformation varying from 7 mm/yr, near the western Peloponesis, to 15 mm/yr around SW Crete (Hollenstein *et al.*, 2008) compared to the western Mediterranean. In the eastern Mediterranean the kinematics is dominated by a general motion towards the Hellenic trench, where the oceanic lithosphere is subducted beneath the Aegean continental crust at about 35 mm/yr while the North Anatolian Fault is taking up the westward motion of Anatolia relative to Eurasia which amounts on the order of 25 mm/yr (Reilinger *et al.*, 2006). The seismo-tectonic styles, as well as the distribution of the focal depth of earthquakes, are also different from one place to another. The Hellenic subduction zone is particularly capable of producing large earthquakes and large events may obviously be expected to occur in the future. Such large events would accordingly impact the coastline bounding the Aegean Sea and the Marmara Sea.

The occurrence of strong, usually disastrous, earthquakes is well known from the antiquity up to now. Some large earthquakes caused destructive or damaging tsunamis, including the events of 373 BC in Corinth Gulf (Sakellariou and Lykousis, 2003), of AD 365 and 1303 in the Hellenic Arc (Yolsal *et al.*, 2007; Fokaefs and Papadopoulos, 2007), of 1402 in the Corinth Gulf, of 1481 in Rhodes island, of 1956 in Amorgos in southern Aegean Sea (Okal *et al.*, 2009), of 551 and 1202 in the Levantine Sea (Salamon *et al.*, 2007), of 1222 in Cyprus, of 1627 at Gargano off the Adriatic coast (De Martini *et al.*, 2003), Italy, 1755 in Portugal, 1822 in Antiochia (Soloviev *et al.*, 2000), 1856 in Algeria, of 1783 and 1908 in the Messina Strait; of 479 BC, 330, 1859 in Thessaloniki and Imroz, of 1893 in Samothraki, 1983 at Lemnos in the northern Aegean (Soloviev *et al.*, 2000; Papadopoulos, 2009; Okay, this volume), of 447 and 1509 in Istanbul and Marmara Sea. Recent catastrophic earthquakes occurred in Izmit (Turkey) and Athens (Greece) in 1999 (Görür *et al.*, 2002; Tinti *et al.*, 2006a; Altınok *et al.*, 2011), in North Algeria in 2003 (which also triggered a tsunami), in L'Aquila (Italy, 2009) and in Lorca (Spain, 2011).

Most earthquake sources are located close to coastal zones. This is of particular importance from the point of view of tsunami hazard. Since the geodynamic processes that cause earthquakes continue for millions of years and are still ongoing, there is no doubt that large earthquakes will repeatedly occur in this area.

3.3 Seismic parameter determination – data bases

Information about the main source parameters of earthquake events, being the time of initiation, the epicentre, the focal depth and the magnitude, are available in catalogues usually arranged in chronological order. Furthermore, additional earthquake information is organized in data bases compiling other parameters related to seismic events such as driving mechanism, surface rupture and associated natural effects such as the resulting intensities and damage, etc.

The instrumental record of earthquakes started to develop about 100 years ago. Thanks to this instrumental monitoring, it progressively became possible to produce catalogues of seismicity for the instrumental period of seismology. The recorded and calculated parameters are improving with time due to gradual enhancements of monitoring and processing capabilities through seismograph networks. The catalogues thus become more and more complete, homogeneous and accurate. This yields important insight for the improved identification and characterisation of seismogenic fault, for the understanding of their geometry and kinematics, and for reconstructing the overall seismo-tectonic framework (e.g. Sallarès *et al.*, this volume). However, the identification of earthquake events that occurred prior to the instrumental era, is based only on historical and archaeological documentation, as well as on a variety of geological observations and methods. Palaeoseismology, for example, is one of the main geological methods which could be applied, but this has, so far, been done mainly on land (see Sallarès *et al.*, this volume). The data provided by these methods is less -complete, -homogeneous and -accurate as compared with the instrumental records. Nonetheless, the pre-instrumental information is invaluable since it provides evidence for at least some of the events, both on land and offshore, which otherwise would have remained unknown. In addition, the historical and geological methods also allow to extend the seismic catalogues far into the past. This is especially important for seismogenic structures for which the frequency of earthquake production is longer than a century. This not only improves the earthquake statistics, but even more importantly it is vital for hazard assessment of events with lower frequency (and often more catastrophic consequences). There is a clear need for information on past earthquakes

so as to permit a better evaluation of *(1)* the general irregularities of the time-space patterns of large earthquakes, *(2)* the common discrepancy between long-term plate boundary slip rates versus rates inferred from seismicity, *(3)* archaeological evidence for clustering of destructive earthquakes that is associated with the recurrence time.

The geological identification of tsunami sediment deposits in coastal areas is a newly developing discipline which provides useful and important information about palaeo-tsunamis and their causative earthquakes. In parallel, several geophysical methods that were developed to investigate the offshore environment, greatly contribute in the identification and characterization of submarine seismic faults and slumps.

3.4 Associated marine hazards

Large earthquakes (M>6.0) are usually damaging and can be destructive. The impact of earthquakes on human communities generally decreases with distance of populated areas to the epicentres. A characteristic deviation from this general rule can be found in cases of large (M>6.5) intermediate-depth earthquakes in the Hellenic Arc and possibly in the Cypriotic Arc, which may cause serious damage at large distances towards remote Mediterranean Sea localities. However, strong submarine earthquakes *per se* do not constitute a direct hazard of marine origin, as it is the secondary effects which induce the hazard. Examples of the latter are tsunamis directly related to co-seismic fault displacement and strong ground motion at the sea floor or indirectly to submarine and coastal landslides, all of them being triggered by strong ground motion (Fig. 2). Submarine slumps and coastal landslides may also result in the generation of local or regional tsunami waves. However, the majority of the basin-wide tsunamis are produced by shallow earthquake activity in the Mediterranean basins. Overall, the main tsunamigenic zones in the Mediterranean are associated with the main seismogenic zones and nearby continental slopes (Fig. 3). The triggering of tsunami waves by co-seismic processes and its impact on the communities along the coast of the Mediterranean Sea, is evaluated in Okay (this volume).

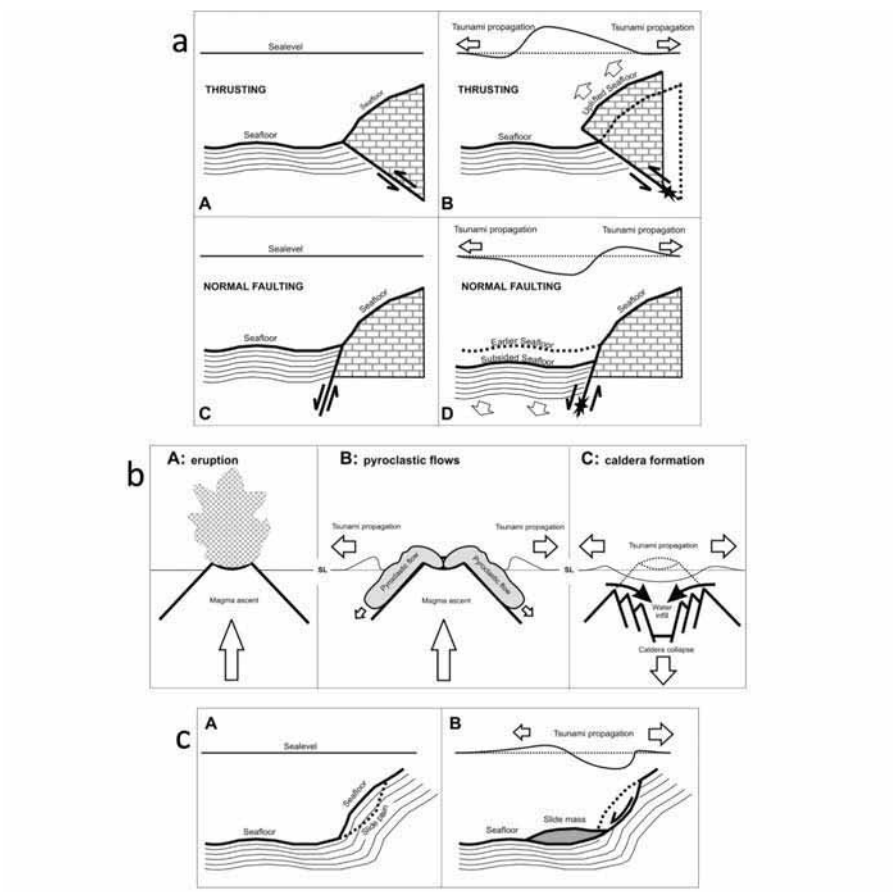

Figure 2. Sketches illustrating the origin of tsunami generated by: (a) faulting (ground displacement), (b) volcanic activities and, (c) submarine landslide.

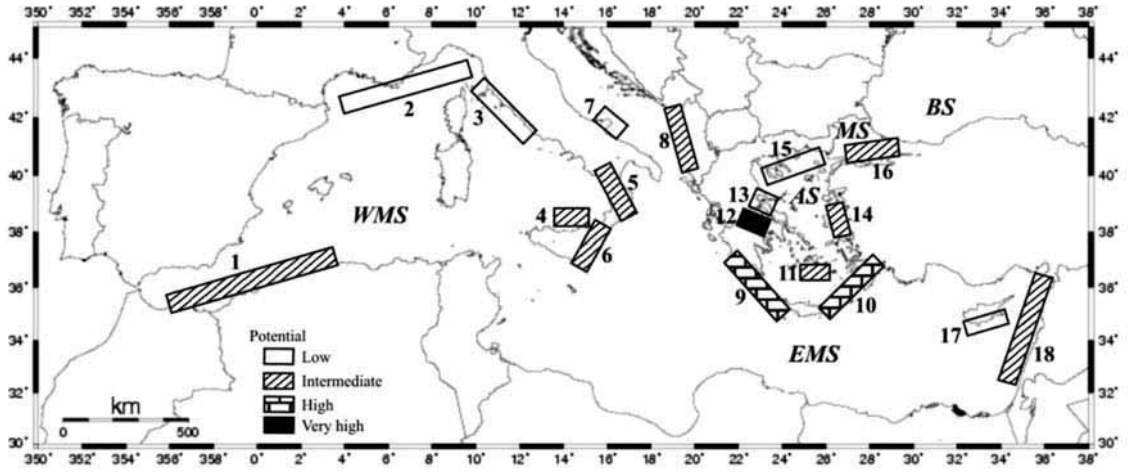

Figure 3. Tsunamigenic zones defined from documentary sources and their relative tsunami potential classification (Papadopoulos and Fokaefs, 2005; Papadopoulos, 2009): WMS=Western Mediterranean Sea, EMS=Eastern Mediterranean Sea, AS=Aegean Sea MS=Marmara Sea. Black Sea (BS) is not included in this study. Zonation key; 1 = Alboran Sea, 2= Liguria and Côte d' Azur, 3 = Tuscany, 4=Aeolian Islands, 5=Tyrrhenian Calabria, 6= Eastern Sicily and Messina Straits, 7=Gargano, 8=east Adriatic Sea, 9=west Hellenic arc, 10=east Hellenic arc, 11=Cyclades, 12=Corinth Gulf, 13=Maliakos Gulf, 14=east Aegean Sea, 15=north Aegean Sea, 16=Marmara Sea, 17=Cyprus, 18=Levantine Sea.

4. Submarine Landslides

In the Mediterranean Sea, the steep and narrow continental margins, tectonically active in majority, and fed by small mountain-supplied rivers, are highly affected by several slope failure processes (Figs. 2-4). Until now, about 600 scars related to submarine landslides and almost the same number of mass-failure deposits have been reported in the literature from specific studies realized around the whole Mediterranean basin (Camerlenghi *et al.*, 2010). These events are located in both tectonically active and quiet areas and have usually been triggered from shallow (about 50-100 m) to up to 2 km water depth. They involve remobilization of continental-slope deposits with volumes ranging from less than 0.001 km^3 to more than 1,000 km^3. Only few submarine landslides have been accurately dated so far, with ages ranging from within the last 100,000 years to very recent

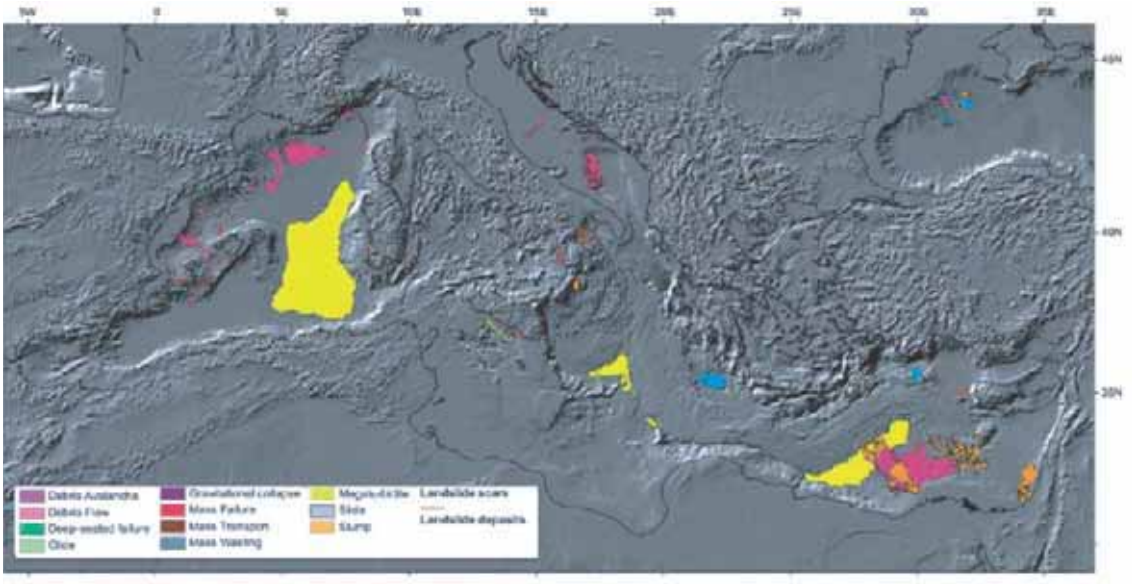

Figure 4. Location of the main submarine-landslide events reported around the Mediterranean margins and basins. Modified from Camerlenghi *et al.* (2010).

times. Therefore, the frequency of triggering and relationship with potential punctual events such as earthquakes are still a matter of debate. Moreover, there is still a lack of information for modern, "active", failures (i.e. the land reclamation failure into the sea at the Nice airport that affected the shelf edge in 1976 (Sultan *et al.*, this volume) or the Calabria failures that affected the Ionian margin (Ceramicola *et al.*, 2010a;b; Planinsek *et al.*, 2011), from which we could extract valuable parameters that will help to better understand past failures.

Depending on the volume of deposits mobilized by the failure event, the depth at which failure occurs, and the acceleration history of the failed mass, submarine landslides can generate tsunami waves at the sea surface that are known to have a local and damaging effect along the coastline, a few tens of kilometers around the location of the source of the landslide by comparison with earthquake-induced tsunamis that can affect a whole basin (Papadopoulos *et al.*, 2007a; Ioualalen *et al.*, 2010). However, simulations of landslide generated tsunami for the coast of Israel (Rosen, this volume) showed that also regional effects (beyond 150 km) can be encountered in some cases.

4.1 Slope movement stages and physical mechanisms

To evaluate the failure potential of a submarine slope, a clear understanding is needed of underlying physical processes associated to both predisposition and triggering factors. Examples of the latter are: slope gradients, high sedimentation rates, fluid seepages, lithological discontinuities, loose sand and liquefaction, leaching and high sensitivity clay, hydrates occurrence and free gas generation, etc. Three main types of triggering mechanisms can act in time and space to produce failure of submarine slopes: (1) tectonic factors related to the Mediterranean plate-tectonic reorganization (in the last 5 Ma) such as the Calabrian Arc and the Mediterranean Ridge subduction (i.e. vertical uplift of Calabria offshore shelf areas) and fore-arc extension (i.e. Crotone Spartivento Basins); (2) eustatic changes in sea level such as during the Messinian salinity crisis (6 Ma ago) and changes due to glacial-interglacial periods (such as the LGM, 20 Ka) where sea level drops were in the orders of hundred meters; (3) high storm waves inducing overloading on shallow underconsolidated sediments. An additional potential landslide mechanism (Rosen, this volume) may occur due to scouring of the lower part of the eastern flank of the Nile delta (consisting of huge unconsolidated sediment volumes) resulting from the increased bottom flow of much saltier and warmer waters coming from the Suez Canal, since its widening and deepening after the 1990s. A main initial slope failure event may be accompanied by subsequent mass movement processes at different stages (post-failure; retrogressive failure, and slope failure reactivation; Hampton *et al.*, 1996).

4.2 Observation, detection and precursory evidence

Great technological improvement in geophysical tools (multibeam bathymetry, AUV, ROV, side-scan sonar) during the last two decades has allowed to map seabed morphologies with a resolution never achieved before - up to cm resolution even at great water depths. This has allowed marine geoscientists to identify new features (cold water coral reefs, fluid vents, mud volcanoes provinces) as well as to characterize structures such as submarine failures at a higher resolution, and to assess their spatial distribution. Seabed mapping has hence shown to be an important tool not only to identify recent morphologies and active faults at the seabed, but also to integrate information from the morpho-bathymetric data (sea-bottom surface) with data coming from shallow to deep sediments (sub-bottom data, multichannel seismic reflection; see Ceramicola *et al.*, this volume; Migeon *et al.*, this volume). Tsunami-genic recent morphologies caused by deformation, erosion and depositional events that are observed at the seafloor can now be related to deep-seated structures that may represent the trigger (i.e. seismogenic faults, fluid/gas, rapid sediment loading). Slope failure processes are at first local, with formation of plastic and weak zones, then become more general (Leroueil, 2001). Therefore, sediments submitted to active deformation are characterized by specific litho-facies and typical geotechnical properties (weak zones). Collecting sediment cores is thus a necessary step to identify processes that usually start at the scale of the grains, i.e. at a millimetre scale. In addition, laboratory and *in situ* geotechnical measurements may constrain changes in physical properties characterizing the presence of weakness layers within the sedimentary column (see Nice airport case study, Sultan *et al.*, this volume).

Identification of potential precursory evidences of submarine landslides requires continuous temporal physical data acquisition and high spatial resolution imaging of the seafloor and sub-seafloor deformation features. High resolution morphological data and changes in geotechnical properties may give an indication on a deformation mechanism affecting progressively the superficial continental-slope sediment (i.e. creeping). The easiest recognizable/detectable precursor for submarine failures should be the formation of trains of small-scale low-elevation escarpments, few tens of cm high.

4.3 Gaps of knowledge associated with sedimentary mass movements

4.3.1 Submarine slides

Little is known about the early phases of submarine landslide initiation, the steady-state or transient conditions under which early deformation and subsequent slope failure may evolve. Also, the sediments from which slope failure originates have rarely been sampled, nor their physical properties determined. Moreover there is a lack of understanding on the early post-failure evolution of submarine slope failures, which is critical for assessing tsunami hazard from submarine landslides. Finally, a major gap in knowledge concerns the timing of failure processes and the precise age of failed sediment accumulations, i.e. recurrence rate.

4.3.2 Submarine faults and paleoseismic parameters

In submarine fault characterization (i.e. slip rate, segmentation and kinematics), large difficulties appear when dealing with slow-moving and reactivated faults located in low sedimentation rate areas. An important gap of knowledge concerns the identification of earthquake single ruptures and the occurrence of vertical and strike-slip components per event (i.e. co-seismic slip). This is based on the ability to recognize and date individual event horizons, as is done in trench techniques on land. Regarding the off-fault paleo-seismic studies, the use of turbidites as paleo-seismic indicators requires demonstrating that earthquakes are their most plausible triggering mechanism. Other gaps of knowledge are related to: the selection of sediment coring sites, as events may be missing or under-represented depending on the depositional location; the link between the turbidite thickness and the magnitude of an earthquake, the relation of which is not straightforward; and the limitations to obtain accurate ages using radiocarbon, due to the spatial and temporal variability of the ^{14}C reservoir age essential for date calibration.

5. Tsunamis

The word tsunami is a Japanese term derived from the characters “tsu” meaning harbor and “nami” meaning wave. It is generally accepted by the international scientific community to describe a series of travelling waves in water produced by the rapid displacement of a large amount of seawater such as can be associated with submarine earthquakes, volcanic eruptions, or landslides. The length of tsunami waves (i.e. the distance between two consecutive crests or troughs) ranges from 10-300 km and is much larger than that of waves generated by winds or by big storms. As for all ocean waves, their wave-period is proportional to the wave-length, and is typically comprised between 5 minutes and 1 hour. This is much larger than the period of wind waves, typically confined to the 1-15 sec band.

As discussed above, tsunamis are most frequently generated by large submarine earthquakes (about 75% of the cases according to tsunami catalogues), and less frequently by volcanic activity and by landslides (~5 and 10% respectively) (Tinti *et al.*, this volume). However, not every submarine disturbance generates a tsunami. Wiegel (1964) quotes Leet who stated that a catalog made in 1861 reported only 124 tsunamis during the interval that 15,000 earthquakes were observed along coastlines. According to Smid (1970), the Greek historian Thucydides was the first to relate tsunamis to submarine earthquakes, but the understanding of a tsunami’s nature remained low until the 20th century.

In addition to tsunami, in recent years (see Vilibic´ and Šepic´, 2009; Tinti *et al.*, 2004; Rabinovich and Monserrat, 1996) a new term appeared, “meteo-tsunami”, attributed to long water waves of similar periods and behavior (including coastal flooding), but being generated by meteorological factors such as by a travelling atmospheric disturbance. Since the meteo-tsunamis are not due to

geo-hazards, they will not be addressed in this summary. Their flooding risks and early detection and warning aspects, however, are similar to those due to geohazards.

As mentioned above, a tsunami is generated when the sea water is displaced within a very short time over a large region by a disturbance involving the sea bottom or the sea surface (Fig. 2a). An earthquake, which may be explained as the effect of the movement (slip) of two crustal blocks slipping one with respect to the other along a contact surface that is called seismic fault or rupture surface, causes a deformation of the sea floor even if the fault is buried and does not reach the surface. The shallower the earthquake, the greater is its impact; the larger the deformation, the larger is the extent of the area involved. When a large sector of the sea bottom is displaced vertically (upheaval or subsidence) in a very short time , then the ocean watermass experiences the same displacement as the ocean-floor and consequently, the sea surface also deforms and is forced out of the equilibrium. In this way initial crests (or troughs) form in correspondence to zones of sea bottom upward (or downward) movement and then propagate as tsunami waves. The initial amplitude of tsunamis in a source region ranges from a few cm for small earthquakes (M= 5.5) to a few meters for large magnitude earthquakes (M > 7.5).

Mass movements (e.g. coastal and submarine landslides, pyroclastic flows) generate tsunami waves when they involve a large volume of material over an extensive area (Fig. 2b,c). A mass sliding along the ocean floor with a sufficient speed displaces water in the front and draws or sucks water in at the rear. If the slide front is wide enough, then the water cannot escape laterally but is pushed upward. So in general, crests and troughs are continuously formed during the motion of the sliding mass, and then propagate across the ocean. The larger the thickness of the landslide, the larger is the amplitude of crests and troughs. The tsunami is the result of complex interactions between all such waves. Dense pyroclastic flows can be interpreted as masses moving along the sea bottom and therefore their tsunami generation mechanism is the same as for landslides. Lighter components of pyroclastic flows with a density less than that of water are not able to penetrate, and float at the sea surface. Their quick motion determines tangential stresses and overpressures, that are larger than the ones produced by winds and that are capable to produce tsunami waves at the surface, usually however of small amplitude.

Volcanic slope collapses can be assimilated to mass movements (submarine or coastal), while the collapse of a volcanic caldera can be schematically seen as a sudden downward displacement of a sector of land that goes underwater: the rapid extension of the sea domain causes the seawater to flow in and fill the caldera, and starts the tsunami (Fig. 2c). Both events can involve volumes up to 1-10 km^3 and have the potential to generate large amplitude tsunamis. Explosions of submarine volcanoes can also initiate water waves, but usually most of the energy is dispersed in turbulent motions and only small amplitude waves are formed.

Tsunami waves propagate across the ocean with a speed that increases with the water depth h and that, when the wavelength is much larger than h, is proportional to the square root of h. It ranges from 700 km/h in the deep ocean to a few km/h in shallow water close to the coast. Consequently, tsunami wave propagation is strongly influenced by the ocean topography, with two main effects: 1) they slow down when they approach the coast, and their wavelength diminishes since crests offshore travel faster than crests nearshore; 2) their fronts tend to deform and bend due to wave shoaling and refraction.

The amplitude of the tsunami waves strongly depends upon their origin. Tsunamis induced by earthquakes have initial amplitudes at most up to a few meters in the source region, but they can be much larger when they are generated by large landslides. Tsunami amplitude increases when they approach the coast, the amplification factor depending mainly on the sea floor slope, sea-bottom roughness, the tsunami wavelength and the configuration of the coastline. Because of their large wave periods and corresponding large wave lengths, tsunamis may amplify 2-10 times when they impact a coast and therefore their potential of flooding is quite large. For a low-lying coast, they can penetrate for hundreds of meters inland reaching run-up heights (that is the maximum topographical altitude touched by the wave onshore) of some tens of meters above sea level. For example, the recent earthquake-related tsunami event in Japan (11-March-2011) had an initial height of ~ 6m but the run-up waves have in many places reached heights of 15-18 m (even upto

37.9 m; Kyodo News, 2011), and in some cases, moved more than 4 to even 10 km in-land (e.g. Kyoto University Team, 2011; Parashar *et al.*, 2011; EOS, 2011).

According to the available tsunami catalogues, 10-15% of the known tsunamis did occur in the Mediterranean. The presence of coastal and submarine seismic zones, of coastal, island and submarine volcanoes, and of unstable ocean margins ensures that all the causative processes are active. In the Mediterranean and in the NE Atlantic there is a potential for the generation of very large tsunamis that can travel across the ocean over very great distances. The 1755 M=8.5 earthquake in the Gulf of Cadiz produced a tsunami that penetrated along the river Tagus estuary with catastrophic effects in Lisbon and that was observed as far as the British Islands in the north and as far as the Caribbean Islands to the west. In the Mediterranean, basin-wide tsunamis are expected to be generated by seismic sources north of Algeria, by earthquakes in the Calabrian Arc and along the Hellenic Arc. On the western segment of the Hellenic Arc, a 365 AD earthquake is believed to have occurred in western Crete producing a tsunami that, according to historical records and to recent geological findings, propagated in the whole eastern Mediterranean and reached Greek coastal zones, Israel, Gaza, Egypt, Libya, eastern Sicily and the Adriatic Sea. The large 1303 tsunami, caused by a M~8 earthquake that ruptured the eastern segment of the Hellenic Arc, had a similar propagation. (Fokaefs and Papadopoulos, 2007). Basin-wide tsunamis can be produced also by the Mediterranean volcanoes. The tsunami produced by the Santorini Minoan eruption has been well studied and seems to have affected most of the eastern Mediterranean and the Ionian Sea (McCoy and Heiken, 2000; Goodman-Tchernov *et al.*, 2009; Bruins *et al.*, 2008; Papadopoulos, 2009; De Martini *et al.*, this volume). Holocene slope collapses of Stromboli and Ischia volcanoes (Maramai *et al.*, 2005a) are speculated to have produced tsunamis affecting the whole Tyrrhenian Sea. Moreover, along most of the margin of the Mediterranean Sea very large, mostly Pleistocene, landslide deposits have been identified that had the potential for basin-wide tsunami generation (Salamon, this volume).

Since most of the tsunamigenic sources are found close to the coast in the Mediterranean region, the minimum tsunami lead-time is quite short. The highest waves can reach the nearest coast in only a few minutes. The 2002 Stromboli tsunami that was caused by a 15 million cubic meter submarine landslide sliding along the Sciara del Fuoco, took less than three minutes to attack the entire coast of the island, and five minutes to strike the Panarea coasts 20 km away from the source. For the 1908 Messina catastrophic tsunami, most of the witnesses reported that the tsunami reached the shore of the Messina Strait less than 5 minutes after they felt the earthquake. The large 1956 South Aegean Sea tsunami arrived in nearby islands within less than 10 minutes. The Mediterranean is a small basin compared to the large oceans, consequently tsunamis generated near one coast can reach the opposing shore of the basin in about 1-2 hours. Observed and computed travel times confirm that the 2003 tsunami generated in north Algeria took 70-80 minutes to reach the coast of southern France. Less than one hour is taken by tsunamis generated in Italy to reach Greek Ionian coasts and *vice versa*, and about one hour for tsunamis generated in the eastern Hellenic Arc to reach the Egyptian coast. Propagation time is of course even shorter for tsunamis that occur in smaller basins like the Marmara Sea or in narrow gulfs like the Gulf of Corinth and Patras, or the Gulf of Izmit. Short tsunami travel times pose very severe and demanding constraints to tsunami early warning systems (TEWSs) in the region. This is one of the main concerns of the IOC-UNESCO Intergovernmental Oceanographic Coordination Group for the Tsunami Early Warning and Mitigation System in the North-eastern Atlantic, the Mediterranean and connected seas (ICG/NEAMTWS in short) since its establishment in November 2005. This activity is strongly supported by CIESM, in particular through the upgrade of the MedGLOSS sea level stations to real time sea level data transmission.

6. Risk reduction: preparedness and mitigation

Due to the increasing coastal developments and population, potential economic and social impacts of natural disasters continue to increase. Preparedness and mitigation against geohazards involve a series of risk reduction actions. Such actions include the establishment of TEWSs, of evacuation and emergency systems, as well as developing short- medium- and long-term strategies and sectorial plans (UNESCO, 2008; Murata *et al.*, 2010; Okay, this volume).

Until 2004, only the Pacific Ocean was covered by a TEWS which has been operating since the 1960s under the supervision of the IOC-UNESCO. More recently, other systems were also developed there. The national delegations participating at the General Assembly of IOC in June 2005 took decisions for the development of TEWSs in the North East Atlantic and the Mediterranean Sea, in the Indian Ocean, as well as in the Caribbean Sea. The three systems are under construction and still in the pre-operational stage.

The systems mentioned above are designed for issuing warnings only in the regional and transoceanic domain (coastal zones threatened by tsunami waves that may arrive more than one hour after its generation). They will report only to the national authorities in each country, whereas only national authorities will decide upon dissemination of warnings to their countries inhabitants. This is the case of tsunamis generated by fault displacements induced by major earthquakes. However, the most commont tsunami sources around the world are situated very close to the coasts, which is in the near-field domain (coastal zones threatened by tsunami waves within a few minutes and certainly less than one hour after their generation). The afore-mentioned systems are inadequate in providing timely warnings for the near-field domain and in addition, such warnings remain the sole responsibility of the national authorities in each country.

Global statistics shows that more than 80% of tsunamis victims are caused during the first hour of tsunami wave propagation (Gusiakov, 2009). Hence the issue of near-field early warning of tsunamis is today a hot topic (e.g. Murata *et al*., 2010). Following the 2004 Indian Ocean catastrophe, the German Indonesian Tsunami Early Warning System (GITEWS) was initiated in conjunction with the Indonesian TEWS (InaTEWS) (Lauterjung *et al*., 2010; Behrens *et al*., 2010), and designed for both regional and near-field tsunamis.

In the Mediterranean region nearly all coastal zones are threatened by near-field tsunamis (Fig. 2 in Mascle, this volume; and Fig. 3) and until now no answer has been given on how to issue a warning message within the first 5 - 30 minutes, which is the most common time window for the arrival of the first tsunami wave. So far, only a simple local tsunami device has been installed at Stromboli, intended only for the needs of this island. In addition, the national French project RATCOM develops a demonstrator, pre-operational local TEWS in the area of Ligurian coast and Corsica Island. The development of such TEWS's for near-field tsunamis is a realistic goal in the Mediterranean region that can be achieved by utilizing traditional and modern technologies such as sea-bottom seismometers, near-field tide-gauges, tsunameters, CGPS, GPS buoys, fast wave simulation tools and others (Rosen, this volume). The improvement of reliable and accurate earthquake catalogues, as well as the understanding of the tsunamigenic sources and mechanisms, are also crucial for modelling earthquake sources and tsunami generation and propagation, and are expected to contribute substantially for early-warning operations.

Effective early warning systems require a strong commitment of national and local authorities. Risk mitigation plans increase the capacity of local communities with the development and implication of risk reduction strategies and measurements (UNESCO, 2008; Murata *et al.*, 2010). Tsunami warning and evacuation systems, public awareness, risk mitigation measurements are the ultimate goal to build coastal disaster resilient communities around the Mediterranean (Okay, this volume). There is a need for identifying and monitoring marine geo-hazards and risks and improving early warnings as a priority. Series of continuous multiple risk reduction and mitigation efforts, such as short- to long-term actions, must be taken to reduce the structural and social vulnerabilities and to build up the capacities of communities (Okay, this volume).

For the short-term actions, strengthening of evacuation systems including evacuation plans for early warning are essential and should be linked with coastal inundation and evacuation maps. Particular attention should be given to the continuous improvement and upgrading of the evacuation exercise, emergency communication and response systems. Preparedness and public awareness will be enhanced through such education and training for geohazards and risk.

For the medium to long-term actions, the reduction of structural vulnerabilities and strengthening of coastal infrastructures as well as designing codes for coastal infrastructure and buildings, and inspecting coastal roads, railways and airports against tsunami heights, and protecting hazardous facilities such as nuclear power plants from tsunamis, and implementing structural mitigation

measurements including constructing seawalls, tsunami towers, vertical evacuation structures as well as educating for good constructing practices are important components of an overall structural risk mitigation action plan.

For the long-term actions, the increase of institutional capacity by improving communication, coordination, cooperation among the govermental offices plays a significant role. In addition, attention needs to be given to non-structural mitigation actions including risk transfer strategies (e.g. insurance, financial tools), investment in disaster prevention, focusing on policy development, legislation and organizational development of partnership (local authorities, business sector, media and volunteer organizations), targeting at land-use best practices (restricted coastal buffer zones) as well as networking of local knowledge centres along coast zones.

7. Recommendations

In the last seven years the world has suffered three major devastating tsunamis: 2011 in Japan, 2010 in Chile, and 2004 in Sumatra, with many thousands of casualties. Still, there are large areas where geo-hazard identification, and risk reduction systems are under-developed or even non-existent. Hazard identification and risk analysis provide the first step for the development of risk reduction and disaster resilient capacities.

As detailed above, several types of marine geohazards exist in the Mediterranean Sea, the most important of which are earthquakes, landslides, tsunamis and volcanism. Although some of them occur infrequently, their potential impact cannot be underestimated. For example, nuclear power plants are often located in coastal areas because of the nearby source of cooling water. Therefore, marine geohazards should be studied in depth and be taken into account in hazard analysis, risk assessment, and mitigation plans, by utilizing all available instrumental, historical, geological and other data. In order to reduce risks this information is the key for building policies and prevention measurements (mitigation). Hazard and risk identification involve series of scientific investigations and research through understanding hazard, vulnerabilities and risk elements. Current scientific knowledge on the main sources and generation mechanisms of marine geohazards in the Mediterranean region is still incomplete and uncertain (see above). Therefore, there is a need to acquire geophysical, geological and geotechnical data in order to better determine the location, size and kinematics and average frequency of occurrence for the potential sources of marine geohazards.

The purpose of improving and extending the coverage of high-resolution sea-floor mapping, coastal bathymetry (including river estuaries and inlets) and local beach and land topography, is of great importance in simulating better realistic generation, propagation and inundation of tsunami waves. These are all essential tools to support hazard mapping and early warning.

Considering that the regional Tsunami Early Warning System (TEWS), now under construction within the coordination of IOC-UNESCO, is meant to cover basin-wide and regional tsunamis, the need to develop specific near-field TEWS is of the highest priority. Priority should also be given to the densification of already existing instrumental networks in potential tsunamigenic areas, and the improvement of the capabilities for real-time data transmission and processing. There is also a need for further development and implementation of offshore monitoring systems of earthquake activity, volcanoes, unstable submarine masses and sea level changes. As travel time from source to coast is short, improved knowledge of the seafloor coupled with realistic simulations of potential hazard scenarios, and inundation maps besides TEWS, is needed to guide the preparation and mitigation of tsunami hazards. Risk mitigation actions should include proper planning and design of building codes to account for these geohazards in the design and construction standards, public education, preparedness and evacuation plans, and legislation for risk mitigation practices.

Time is an important variable in risk management, especially when it concerns extreme events (Beer and Ismail-Zadeh, 2003). The success of risk reduction actions is dependent on risk communication between scientists and local authorities as well as operational people. The Geoscience community has a responsibility to educate the engineers, and urban planners, authorities, media and public to build disaster resilience (Okay, this volume). In parallel, similar consistency should be established between early warning and evacuation systems. For a timely

evacuation, tsunami warning should be linked with the magnitude of earthquakes. Local authorities must prepare communities to understand warnings and to respond adequately. Coastal infrastructure, roads, railroads, airports, industrial facilities and plants such as shore-based power plants based on seawater cooling, need to be sufficiently protected from potential tsunamis impacts.

SUGGESTED ROADMAP

Identification, characterization, and potential generation mechanisms of main sources for marine geohazards have been summarized in Table 1. In addition, actions and tools as well as mitigation of risks are recapitulated.

Table 1. Summary of marine geohazards in the Mediterranean and suggested potential mitigation actions. *(*): EQ = earthquake; F = fault; L = landslide; V = volcano; VP=Volcanic Processes; T = tsunami.*

AIMS	OBJECTIVES	ACTIONS	TOOLS
UNDERSTAND PHENOMENA	**Identify and characterize the main sources of marine geo-hazards: EQ/F, L, VP, T (*)**	Identify hazardous submarine geological features (F, L, V, T) Define source models including structure, geometry, size and age (F, L, V) Quantify sediment/rock properties, composition and pore pressures (F, L) Infer their likely evolution and kinematic patterns (F, L)	Seabed mapping Sub-seafloor imaging and modeling Seafloor and sub-seafloor sampling (analysis and dating) Seafloor and sub-seafloor geotechnical measurements Seafloor seismological monitoring
	Understand the mechanisms of generation	Improve understanding of the generation mechanism of EQ, L, VP Improve understanding of energy transmission from seafloor to water to generate tsunamis depending on source mechanism Simulate the generation mechanisms and energy transmission including observations	Seafloor and sub-seafloor stress and strain monitoring Seafloor seismological monitoring Numerical models of rupture dynamics, failure, sliding, collapse Numerical and empirical models of energy transmission at the solid/liquid interface Analog models
REDUCE THEIR EFFECTS	**Assess the associated hazards**	Simulate the process of tsunami generation, propagation and inundation and compare with observations (T) Produce detailed tsunami hazard maps (arrival time, run-up, inland penetration distance) (T) Evaluate time evolution of key active faults, volcanoes, and unstable slopes including estimation of recurrence intervals (EQ, L, VP) Develop and implement probabilistic methods for hazard analysis and integrate with on land hazard models (EQ, L, VP) Identify and recognize possible precursory signals (EQ, L, VP)	Numerical models of wave propagation including near-shore effects Include source kinematics and energy transmission models Include near-shore bathymetry and coastal DEM (*) data Paleo-seismic tsunami records (on-/off-shore) High-resolution bathymetry and DEM Long-term seafloor and sub-seafloor monitoring of key active faults, volcanoes, and unstable slopes Compile historical and instrumental catalogs with information on location, magnitude and timing of the hazards (EQ, L, VP)
	Mitigate the risk	Design and implement near-field tsunami warning systems Assess vulnerability and risk for T, EQ, L, and VP Develop improved tsunami design codes for marine and coastal infrastructures and constructions Integrate systematic education and training Improve communication strategies	Real-time access to data from seafloor monitoring instrumentation Tsunami impact scenarios for the main sources Hazard maps Data bases of socio-economic, infrastructure and building attributes

II - WORKSHOP COMMUNICATIONS

Geo-hazards and the Mediterranean Sea

Jean Mascle

Geoazur, Villefranche-sur-Mer, France

For almost 4,000 years, since historical times, we know that geo-hazards have played a major role in the evolution of human societies around the Mediterranean Sea. The Santorini explosion around 1800 BC, the Pompeii disaster in 79, the collapse of Alexandria pharos around 700, the Messina earthquake and tsunami in 1908, are among the better known catastrophic impacts due to geo-hazards on human settlements. Dozen of volcanic eruptions, hundred of earthquakes and may be more tsunamis have however continuously affected the Mediterranean coasts and nearby areas.

Today similar catastrophic, or less damaging, events may obviously re-occur in and around the Mediterranean Sea and it still remains difficult to predict them. This is the consequence of two main characteristics of the Mediterranean environment: at first a very specific geological/geophysical setting including a progressively closing oceanic space; secondly, the presence of a dense

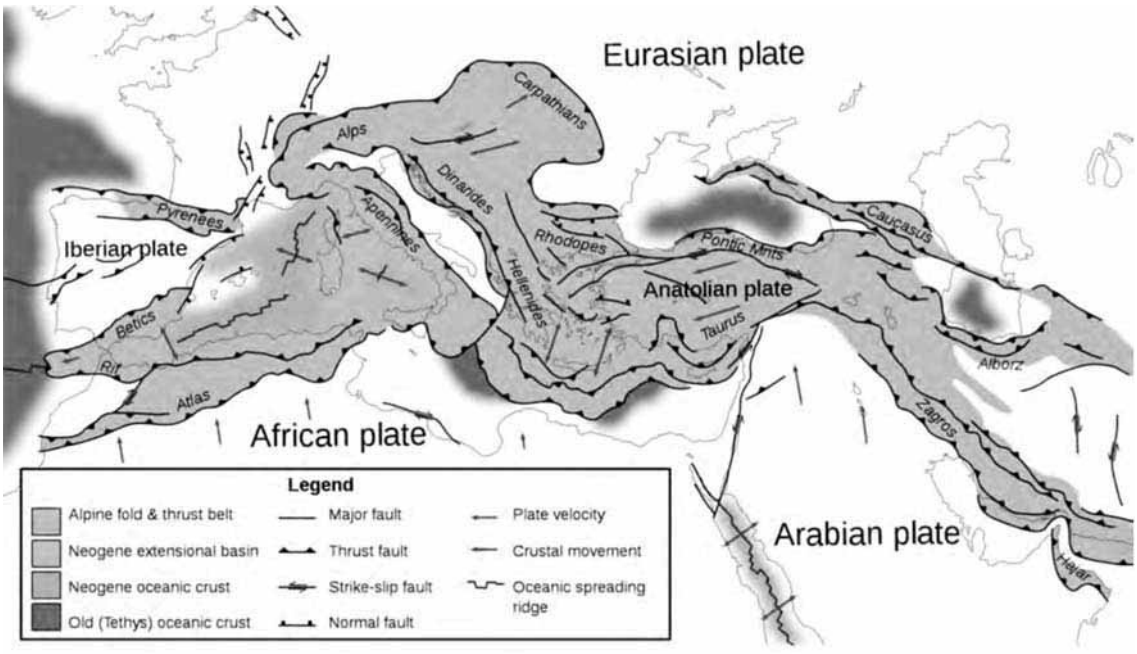

Figure 1. Tectonic setting of the Mediterranean Sea.

[see original colour illustration in Annex at end of volume]

population, and of important economic activities around and across the Mediterranean Sea surrounded by 22 bordering countries and where almost 25% of the world maritime traffic occurs.

What are the main catastrophic geo-hazards to which the Mediterranean Sea coasts could be submitted? They are no different than elsewhere: earthquakes, tsunamis, volcanic eruptions; one of the specificities of the Mediterranean is that they do occur in areas where almost 500 million people, including 160 millions directly on the seashore, are permanently living, and moreover on areas visited each year by more than 300 million tourists! So the Mediterranean Sea, which represents the cradle of our Western civilization, is particularly sensitive to natural geo-hazards.

Plate tectonic configuration and main geological characteristics (Figure 1)

Most of the catastrophic geo-hazards occurring in the Mediterranean Sea are due to its specific plate tectonic configuration, itself inherited from a long geological evolution, which started more than 200 Ma ago. Today the Mediterranean Sea is made of two main basins of strongly different ages (more than 150 Ma and less than 30 Ma respectively for the Eastern and Western basins) almost totally surrounded by mountain chains, which result from the subduction of former oceanic spaces and of collision of their continental margins. As a consequence of this long term history three converging major plates are almost in contact, the Eurasian, African and Arabian plates; several micro-plates are slightly moving, or almost stuck, between these plates: the Anatolian and Iberian micro-plates; former micro-plates have been incorporated either to Europe or to Africa: Apulian and Sinai blocks for example.

Seismic activities

A direct consequence of plate motion in the Mediterranean Sea is its intense seismicity (Figure 2); The epicenters repartition map (seisms from magnitude 3) show that the seismic activity widely

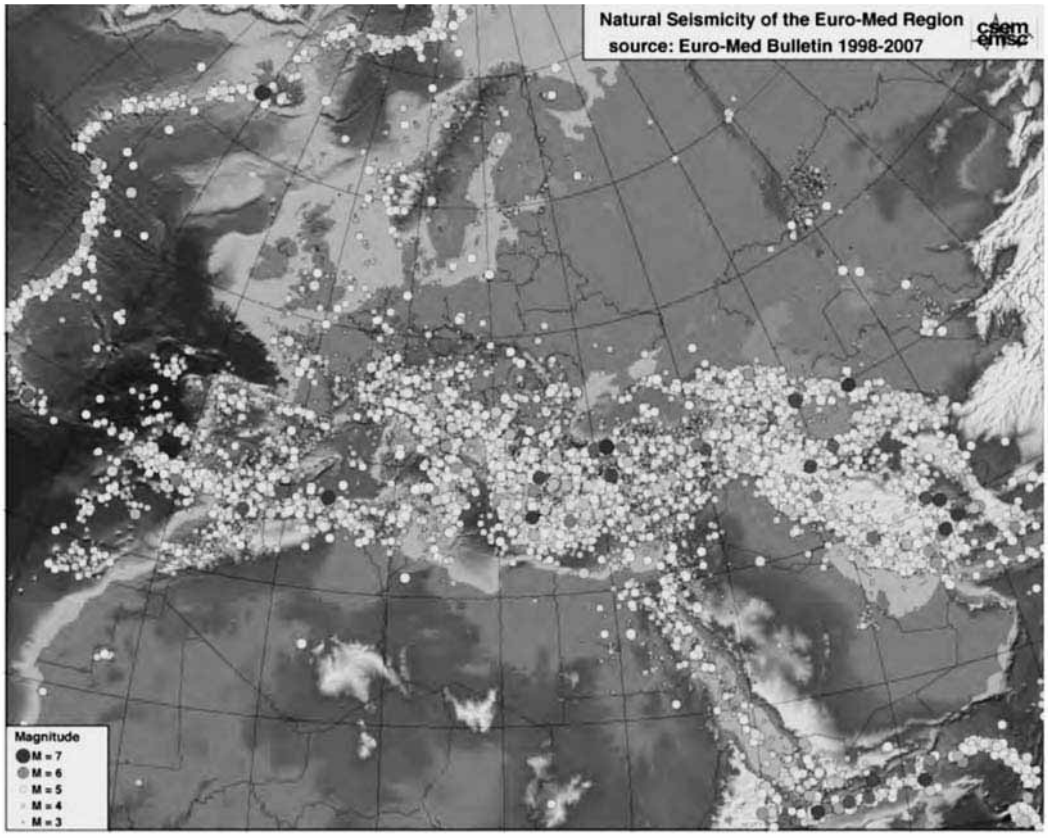

Figure 2. Repartition of seismic activity (epicenters of seisms from magnitude 3 to 7) on the Mediterranean domain and nearby areas.

[see original colour illustration in Annex at end of volume]

but not equally distributed over the area. A cloud of seisms, including some with magnitude higher than 7 is totally superposed to the Anatolian and Aegean regions; this intense activity is due to three main causes: the subduction of the African plate beneath Eurasia, the left lateral escape with respect to Europe of the Anatolian micro-plate and the progressive stretching or the Aegean continental crust. This seismic activity is clearly in trend with the seismic belt, which affects the Eastern border of the Arabian plate already in collision with Asia. Westwards the Aegean seismic nest connects with a less active seismic belt passing through the various Alpine mountain chains, and the Apennines. Another intensively active seismic zone can be seen over southern Italy; it underlines the subduction of the African lithosphere beneath Europe, and particularly beneath the Tyrrhenian Sea, and connects through Sicily with a new belt of seisms more or less superposed to the North African coastal chains and the Atlas mountains. To the west the Iberian micro-plate is almost totally surrounded by moderate seismic activity, which itself connects progressively with the seisms occurring on the Mid Atlantic Ridge through a diffuse seismic zone more or less superposed on a Gibraltar-Acores Islands axis and delineating the southern border of the European plate in the area.

Active or recently active volcanoes

Another consequence of plate convergence and active subduction processes in the Mediterranean Sea is the presence of active, or historically active, chiefly andesitic-type and explosive, volcanoes. Two active volcanic arcs are known in the domain: the Aegean volcanic arc and the Aeolian Islands, which both result from the subduction and melting at depth of the African lithosphere. Santorini Island is by far the most famous volcano of the Aegean volcanic arc. Its last historic catastrophic explosion occurred about 1800 years BC where its strongly impacted the Minoan civilization; other volcanoes such as Milos and Nysisros have been active in recent geological past but do not show strong activity at present. The Aeolian Islands volcanoes, are either inactive (Lipari, Salina, Filicudi, Alicudi, Panarea), dormant (Vulcano) or quite active (Stromboli). Most of them have been submitted to large-scale explosions within recent geological times. Two other volcanic zones, not directly related but interfering with subduction processes, are particularly active in the area: the Vesuvius and the Phlegraean fields nearby Naples and Mount Etna in North-Eastern Sicily. Both systems represent permanent risks which have to be continuously monitored.

Figure 3. Main active, or recently active, volcanoes in the Mediterranean Sea, and location (in red) of the main earthquake-triggered tsunami areas and of main potentially impacted coastal zones (in yellow) within the Mediterranean Sea.

[see original colour illustration in Annex at end of volume]

TSUNAMIS

Among the catastrophic events which affect from time to time the Mediterranean coasts, tsunamis have been until recently often neglected mainly since their geological records remain difficult to assess. Tsunamis seem however to rank among the most frequent catastrophic events and have induced important destructions known in both historical and recent times. It has been proposed that the collapse of the Alexandria pharos was the result of an earthquake and subsequent tsunami, which were also likely the cause of much destruction of coastal cities in the Antiquity. The Messina disaster, in 1908, was also the combined result of an earthquake and of a related tsunami.

Most of the major tsunamis are triggered by earthquakes, and the resulting waves are crossing regional basins such as the Western or the Eastern Mediterranean basins before to hit the opposite, northern or southern, coasts tens of minutes later. Being generated by important seismogenic ruptures, either off North Africa or south of the Hellenic arc, their effects concern mainly the southern coasts of Western Europe or the northern coasts of Africa within the Eastern Mediterranean. More local tsunami may be generated as consequence of submarine sedimentary or volcanic failures; such events may quickly (few minutes later) impact the neighboring coasts where they may also induce important damages. Most of the continental slope of the Mediterranean continental margins being either quite steep, or highly sedimented, may be submitted to large-scale destabilizations and therefore may be considered as areas to be surveyed for slope stability.

Catastrophic (instantaneous) geo-hazards are the most spectacular and as such remain in the historical memory and are even sometimes at the origin of myths (see CIESM, 2003). Other natural, but slower, geological events have however to be considered when trying to evaluate the various marine-related risks occurring in the Mediterranean Sea; the most obvious of them relates to the sea level fluctuations and particularly to sea level progressive rise, itself related to climatic fluctuations.

Marine geohazards associated with active geological processes along the Hellenic Arc and Back-Arc region

Dimitris Sakellariou

Institute of Oceanography, Hellenic Centre for Marine Research, Anavyssos, Greece

Abstract

The Hellenic Arc and Back-Arc region (Aegean and Ionian Seas) is the site of long-term geodynamic processes and crustal movements, which frequently give birth to violent, short-term, catastrophic geological events. Large earthquakes, seafloor ruptures, uplift or subsidence of shorelines, submarine landslides, submarine or island volcanic eruptions occur within the various geotectonic settings of the area and have triggered many tsunamis, some of them with catastrophic impact. This paper describes the genetic relationship between such geohazards and the dominant geotectonic setting in key areas of the Aegean and Ionian Seas.

Geodynamic Setting

The Hellenic Arc and Back-Arc region (Fig. 1) has been for several million years, and continues to be, the site of long-term geodynamic processes and crustal movements, which frequently give birth to violent, short-term, catastrophic geological events, called hereafter geohazards. The westward extrusion of Anatolia continental block along the North Anatolian Fault, the NNE-ward subduction of the Eastern Mediterranean lithosphere beneath the Hellenic Arc, the subsequent SSW-NNE extension of the Aegean back-arc region, the collision of NW Greece with the Apulian block in the northern Ionian Sea north of the Kephalinia Fault and the incipient collision with the Libyan promontory south of Crete are the main, ongoing processes which dominate the geodynamic evolution of the Hellenic Region (McKenzie, 1970; 1978; Dewey and Şengör, 1979; Le Pichon and Angelier, 1979; Le Pichon *et al.*, 1982; Meulenkamp *et al.*, 1988; Mascle and Martin, 1990; Meijer and Wortel, 1997; Jolivet, 2001; Armijo *et al.*, 2004; Kreemer and Chamot-Rooke, 2004).

Building up of stresses along the boundaries and in the interior of the crustal blocks involved leads to brittle (and ductile) deformation in the upper crust, expressed with normal, reverse or strike slip faulting and large earthquakes. Submarine landslides are very often triggered by strong earth tremors. Melting of the subducting East Mediterranean lithosphere underneath the Aegean produces magma which rises to the surface through existing weak zones (faults) forming the active volcanic centers of the Hellenic Volcanic Arc. Volcanic eruptions, sea-floor faulting and submarine landslides have triggered numerous, small or large tsunamis, some of which have devastated large parts of the Aegean, Ionian and Eastern Mediterranean coastlines.

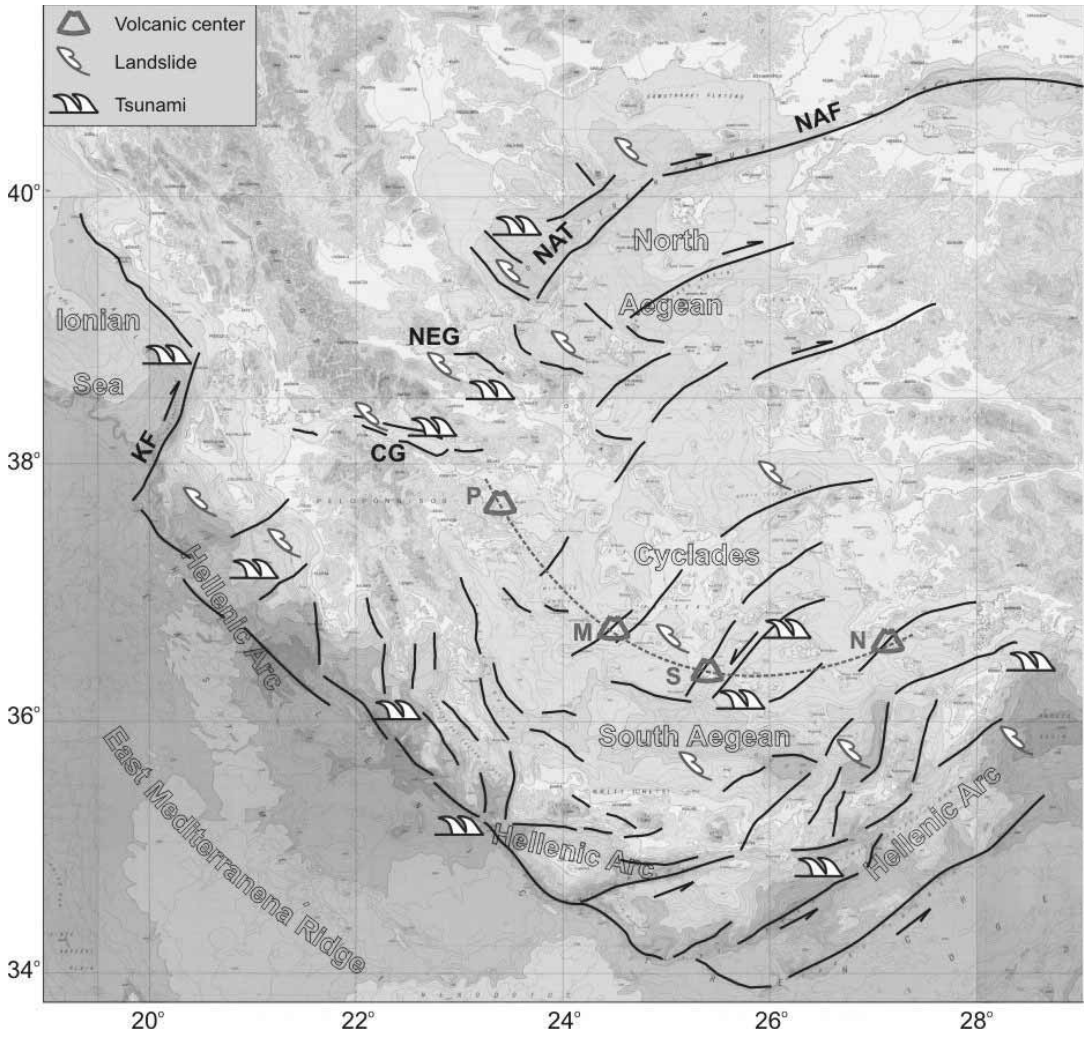

Fig. 1. Geodynamic structure of the Hellenic Arc and Back-Arc region with areas of major marine geohazards. Bathymetry extracted from the IBCM/IOC.

[see original colour illustration in Annex at end of volume]

The aim of this work is (i) to outline the specific areas in the Aegean and Ionian Seas where marine geohazards have repeatedly occurred in the past and/or are likely to occur in the future as a consequence of the active geological processes and (ii) to highlight some cases of catastrophic events originated at the sea in Late Holocene, particularly in historic times.

NORTH AEGEAN SEA – NORTH AEGEAN TROUGH (NAT)

The most striking feature in the North Aegean Sea is the North Aegean Trough. It comprises a series of separate tectonic depressions resulting from an apparent transtensional deformation along the westward prolongation of the right-lateral North Anatolian Fault into the Aegean (Mascle and Martin, 1990). Detailed swath bathymetric survey revealed the accurate morphology and geometry of the trough, with steep, faulted slopes and more than ten subbasins up to 1,600 m deep (Papanikolaou *et al.*, 2002). The northern, steep slope of the trough separates the series of the depressions from the thickly sedimented North Aegean shelf.

Regional seismic hazard and slope stability analysis has shown that the upper and middle slopes of the North Aegean trough are highly unstable. Lykousis *et al.* (2002) studied a large submarine slide developed on the south-facing slope of the trough to the south of Thassos Island. The failure zone extends at depths between 300 - 850 m and covers an area of 85 km^2. The mean thickness of

the slide is about 55 m and the total volume of 3.8 km^3 of late Pleistocene sediments has slid a distance of 6-7 km. Chronostratigraphic analysis of the seismic stratigraphy suggests that the major and secondary glide planes have developed in the transitional zones between a lower sequence of stiff, relatively coarser sediment layers deposited during low-sea-level-stands and the overlying weaker muddy layers of lower shear strength deposited during high-sea-level-stands. The major glide plane is assumed to have been developed within a muddy layer that was deposited about 170-245 ka BP. Stratigraphic, sedimentological data and AMS dates indicate an early Holocene age of the major failure event (between 5.5 and 7 ka BP).

Marine geological, sedimentological and seismological conditions like the ones described by Lykousis *et al.* (2002) prevail along long segments of the northern margin of the North Aegean Trough, like south of Thermaikos and Strymonikos Gulfs and between Thassos and Samothraki islands.

It is thus a reasonable assumption that similar landslides may occur again in the North Aegean Trough. Searching through the various tsunami catalogues (e.g. Papadopoulos and Fokaefs, 2005) one finds about 10-12 tsunami events in the North Aegean Sea, which may be related to slumping along the steep slopes of the North Aegean Trough or of the other basins of North Aegean (Fig. 1).

Hellenic Volcanic Arc

The Hellenic Volcanic Arc has developed in the back arc region of the Hellenic subduction zone, parallel to and about 150 km north of the Hellenic Island Arc (McKenzie, 1970; Le Pichon and Angelier, 1979). The trace of the volcanic arc is delineated by the four main volcanic fields in South Aegean Sea, namely Poros-Methana-Egina, Milos, Santorini (Thera) and Nisyros-Kos.

Santorini volcano – Minoan eruption

The most recent major explosive eruption in Greece, the Minoan eruption of the Santorini volcano about 3,600 years B.P., is one of the largest volcanic events known in historical time and has been the subject of intense volcanological and archeological studies (Druitt *et al.*, 1999; Friedrich, 2000). A marine geological survey conducted recently (Sigurdsson *et al.*, 2006) included about 1,000 km of air-gun profiles and revealed the distribution of pyroclastic deposits on the sea floor around the volcano, up to 30 km away from Santorini, ranging in thickness from 10 to 80 meters (Fig. 2). The results indicate that the submarine flows from the Minoan Bronze Age eruption may be of the order 40 km^3, yielding a volume of about 60 km^3 for the explosive eruption. Thus, the Minoan eruption is comparable in volume to the largest known historical eruption, that of Tambora in Indonesia in 1815 (Sigurdsson and Carey, 1989) and many times than the 1883 eruption of Krakatau in Indonesia, where approximately 10 km^3 of pyroclastic flows entered the ocean around the volcanic island (Sigurdsson *et al.*, 1991). These results, in relation to the 1883 Krakatau eruption, imply that the direct hazard from pyroclastic flows from the Minoan Eruption entering the sea is likely to be much greater than previously considered.

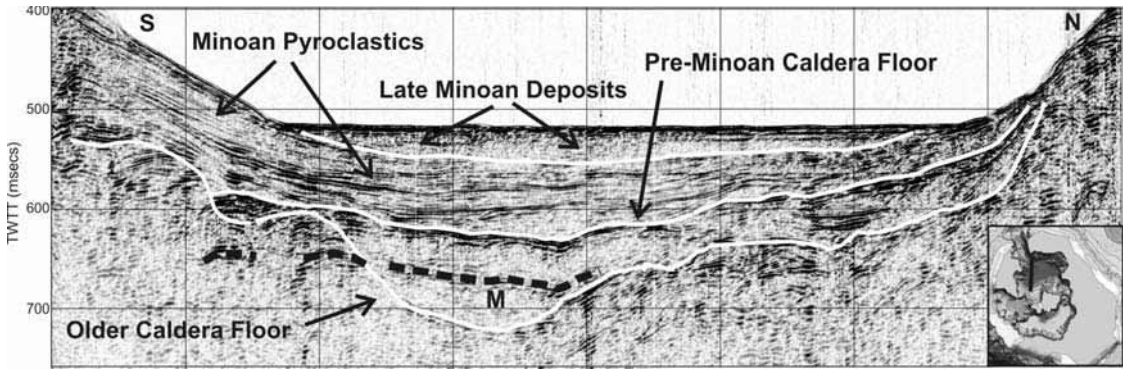

Fig. 2. Single channel Airgun 10c.i. seismic profile through the northern basin of the Santorini caldera. Up to 60-70 m thick pyroclastic deposits of the Minoan eruption have flown from the center of the caldera (left), which is now occupied by the recently built Kameni Islands, on the pre-Minoan caldera floor. The transparent, 10-15 m thick top-layer may represent deposition of floating and suspended ash and pumice.

Pyroclastic flows are among the most destructive and dangerous forms of volcanic eruptions. They are avalanches of hot ash, pumice, rock fragments, and volcanic gas that rush down the side of a volcano as fast as 200 km/hour or more with temperature as high as 500° C or more. Such flows were particularly destructive in the 1902 Mt Pelé and 1980 Mt St Helens eruptions. If such a flow reaches the sea it can behave in similar manner to a fast moving landslide and trigger a tsunami. There is testimonial evidence from the 1883 eruption of Krakatau, supported by modelling and experimental evidence (Delange *et al.*, 2001; Freundt, 2003), that pyroclastic flows can cross significant bodies of waters, displace similarly large water masses and hence trigger large tsunamis.

Numerous papers in the last 40 years have suggested tsunami generation triggered by the Minoan eruption, But surprisingly little robust onshore field evidence for Minoan tsunami deposits has been found so far in the Aegean specifically and the eastern Mediterranean region in general. Dominey-Howes (2004) has reexamined the original arguments and questioned the hypothesis of a mega-tsunami, favoring the occurrence of local, near-field tsunamis. Recently, Bruins *et al.* (2008) reported the discovery of extensive tsunami deposits at Palaikastro in north-eastern Crete, recorded and preserved as geoarchaeological deposits in Late Minoan human settlement. The tsunami deposits were dated as coeval with the Minoan Santorini eruption and were preceded by wind-transported volcanic ash. Field evidence suggests that tsunami waves at Palaikastro were at least 9 m high.

Following the findings and conclusions of Bruins *et al.* (2008) we can reasonably assume that tsunami generation did occur during the Minoan eruption and was most likely associated with the development of the massive pyroclastic flows and possibly also with the final collapse of the main volcanic edifice.

Kolumbo submarine volcano

The Santorini volcanic field extends 20 kilometers to the northeast, as a line of more than 20 submarine cones. The line of craters lies within a transtensional basin developed along the Kolumbo strike-slip fault zone (Sakellariou *et al.*, 2010). By far, the largest of these submarine craters is Kolumbo, a three-kilometer-diameter cone with a 1500-meter-wide crater, a crater rim as shallow as 18 m, and a crater floor 505 m deep. Kolumbo last was active in 1650 A.D., when an explosive eruption produced hot surges across the ocean surface that caused 70 deaths on Thera (Fouqué, 1879). The activity in Kolumbo started in March 1650 when violent earthquakes were felt in the area and lasted six months. The eruption started on 27 September, when dense clouds of smoke and flame were seen rising from the sea, which was covered with pumice. Explosions continued and culminated on 29 September, when dense smoke rose and rock fragments were ejected from the emergent crater. The eruption produced a tsunami with 20 m run up along the coasts of the nearby Ios Island.

A widespread hydrothermal vent field was discovered on the floor of the Kolumbo submarine crater during the recent marine survey (Sigurdsson *et al.*, 2006). High-temperature venting occurs in the northern part of the crater, with vigorous gas emission plumes more than 10 meters above the crater floor, and fluid temperatures up to 220ºC from vent chimneys up to four meters in height that are constructed of polymetallic massive sulfides and sulfates. Detail seismological surveys indicate that the main cluster of local seismicity is located near the northeastern edge of the Santorini Island, beneath the Kolumbo submarine volcano (Dimitriadis *et al.*, 2010).

CORINTH GULF

Marine geological expeditions have been conducted repeatedly in the Gulf of Corinth and yielded a wealth of data on the morphology of the seafloor, the character of the sedimentation and the sedimentation rates, the tectonic structure, the long term deformation, the slope stability, tsunami generation and impacts. Main active normal faults trend E-W and are aligned along the slopes of the Gulf of Corinth basin. Maximum observed fault length on the seafloor does not exceed 17-20 km. Sequence stratigraphic interpretation of the seismic data in association with sediment coring and geological data indicate maximum subsidence rate of the basin floor of about 3.6 m/kyr in the central part of the Gulf. Slip rates of up to 1.6 m/ka have been estimated for the main faults in the central Gulf of Corinth (Lykousis *et al.*, 2007a). Mean subsidence of 2.4-2.75 m/kyr has been

obtained for the basin of the Alkyonides Gulf, mainly overtaken by the southern basin bounding faults (Sakellariou *et al.*, 2007a). Although seismic fault geometry and kinematics may be well constrained, magnitude of single events associated with these faults and recurrence intervals need more data to be better assessed.

The Gulf of Corinth is characterized by a unique record of large earthquakes and tsunamis dating back to more than 2000 years before present. The oldest, historically reported earthquake and tsunami disaster in the Gulf occurred in 373 BC and led to the total destruction and submergence of the Ancient Helike, while the two most recent destructive earthquakes took place in the Western and Eastern Gulf in 1995 and 1981 respectively.

Extensive Gilbert – type fan delta deposits were developed along the Gulf of Corinth steep, faulted slopes. The offshore fan deltas are well pronounced along the southern slopes which are characterised by high sediment fluxes and rapid tectonic uplift (Brooks and Ferentinos, 1984; Ferentinos *et al.*, 1988; Lykousis *et al.*, 2007b). Deltaic sediments in the Gulf of Corinth have failed several times during the last 4-5 kyr after or during the deposition (progradation) of the HST fan delta. Small-medium size sediment failures with volumes of 10^6-10^7 m^3 have been mapped with high resolution (200 kHz) multibeam systems particularly along the steep southern margin of the Western Gulf of Corinth. The majority of the observed failures are downslope debris flows/avalanches. The failure scarps are shallow (10-50 m depth), located close to (100-200 m) the coastline and are usually associated with coastal zone retreat and submergence, due to upslope (cross shore) retrogression.

Recent (late 0.1-0.15 kyr) prodelta failures in the Gulf of Corinth are evidenced by the destruction of telecommunication cables, coastal collapse and the initiation of destructive tsunami waves (i.e. 1963 AD). The frequency of failure events in the W. Corinth Gulf is estimated to 2-3 events per 100 years (Lykousis *et al.*, 2007b). Slope and coastal failures are usually associated with earthquakes and may have triggered at least some of the known tsunamis in the area. The most recent catalogue reports a total of 17 probable and definite tsunami events, which have occurred within the Gulf of Corinth (Papadopoulos, 2003a). With the exception of the first event of 373 BC, the remaining 16 out of 17 tsunami events are reported to have occurred since 1402.

North Evia Gulf

Systematic single channel seismic profiling and swath bathymetric survey of the North Evia Gulf resulted in a detailed mapping of the offshore active faults in the North Evia Gulf basin. Tectonic subsidence of the submarine basin is mainly driven by the northeastern normal faults. Maximum observed fault length on the seafloor does not exceed 15-17 km (Sakellariou *et al.*, 2007b). Geometrical characteristics of the fault planes are relatively well constrained but slip rates of individual faults or fault segments have not been estimated yet.

Thorough analysis and interpretation of swath bathymetry and seismic profiling data highlighted several sites of slope failure and submarine landslides, which may have served as source areas of tsunami generation or may trigger tsunami in the future. The most important submarine landslide observed in the Gulf is located NW of Arkitsa on the southwestern, moderately steep slope of the basin. About $3x10^6m^3$ of sedimentary material was detached from the upper slope leaving behind a spoon-like scar with its scarp at 150 m water depth. The debris slid downslope through a channel for a distance of 4-5 km and accumulated in the deep basin of the Gulf at 400-450 m water depth. The accumulated sediment mass is covered by a very thin, mm-thick, sedimentary drape, indicating that this event is fairly young. We assume that the Arkitsa landslide triggered the tsunami which drowned the coasts of the North Evia Gulf right after the main shock of the 1894 Atalanti earthquake.

Hellenic island arc

The Ionian Islands, the western and southwestern part of Peloponnese, Kythera and Antikythera islands, Crete and Gavdos, Kassos, Karpathos and Rhodes islands form the uplifted parts of the Hellenic Island Arc. It runs parallel to a series of elongated basins which all together were called the Hellenic Trench because they were thought to delineate the boundary between the overriding

Aegean plate and the downgoing East Mediterranean oceanic crust. It is now known that they are aligned on right-lateral (in the western branch) and left-lateral (in the eastern branch) strike-slip zones developed within the forearc domain (Jongsma, 1977; Le Pichon and Angelier, 1979; Le Pichon *et al.*, 1982; Mascle *et al.*, 1982) as a consequence of incipient collision of the Hellenic Forearc south of Crete with the Libyan promontory (Mascle *et al.*, 1999).

Armijo *et al.* (1992) report E-W extension overtaken by N-S normal faulting along the Island Arc, while Ten Veen and Kleinspehn (2003) propose that deformation of the central part of the arc is controlled by sinistrally dominated 070º faults and secondary 020º extensional oversteps. This is particularly evident on the relief both on Crete and offshore, in the eastern and western Cretan Straits (Fig. 3). At the same time and at a lower crustal level thrusting and underplating is responsible for strong and very strong earthquakes (Shaw *et al.*, 2008).

The Hellenic Arc and Trench is the source region for the most devastating tsunamis in the Eastern Mediterranean during historic times (Papadopoulos and Fokaefs, 2005).

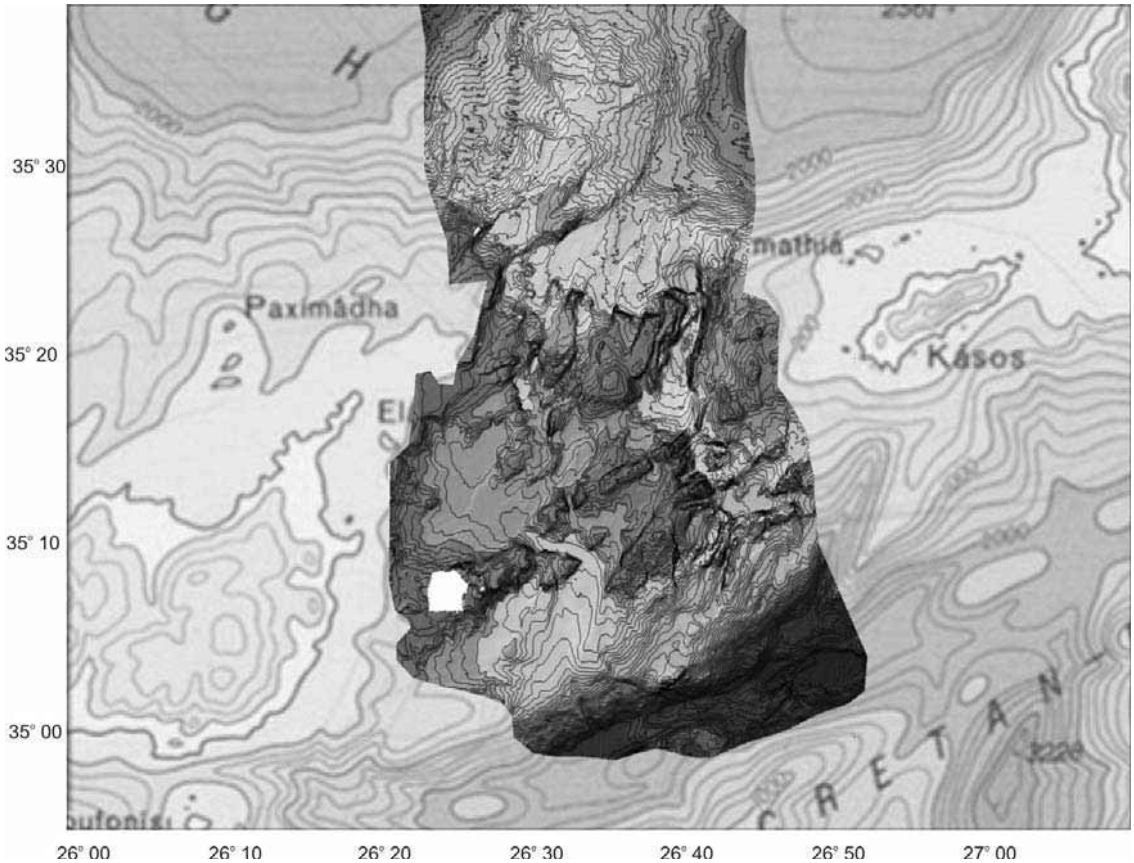

Fig. 3. Recently acquired swath bathymetry data in the Eastern Cretan Straits show extensive N70º faulting and N-S step-faulting. General bathymetry extracted from the International Bathymetric Chart of the Mediterranean IOC.

[see original colour illustration in Annex at end of volume]

The famous AD 365 earthquake which was felt throughout the Eastern Mediterranean, caused up to 10 m uplift of southwestern Crete and triggered tsunami which inundated coastal sites in Africa, the Adriatic, Greece and Sicily (Shaw *et al.*, 2008) occurred off southwestern Crete, on a low-angle, NEward dipping thrust fault within the overriding Aegean plate. Other tsunamis, like the 1303 one, which was generated off southeastern Crete, are still enigmatic and less studied. It is assumed that both aforementioned tsunami events (365 and 1303) were of tectonic origin. In other

words they were triggered by the sudden rupture and vertical dislocation of the seafloor due to motion on the respective seismic fault.

Further to the east, on the island of Rhodes, up to eight stepped Late Holocene shorelines have been recognised and studied along the east coast (Pirazzoli *et al.*, 1989). Two successive phases of submergence-emergence have been revealed and give evidence of the occurrence of positive and negative vertical movements. The strike slip character of the plate boundary along the eastern sector of the Hellenic Arc is not sufficient to explain the uplift of the island. Kontogianni *et al.* (2002) propose that the earthquakes which are responsible for the vertical displacement of the shorelines are probably associated with a major reverse fault offshore, running all along the coast of Rhodes. The 227 BC earthquake, which is responsible for the demolition of the Colossus of Rhodes may have also occurred on the proposed offshore fault.

Along the western branch of the Hellenic Arc more than 15 tsunami events have been reported (Papadopoulos and Fokaefs, 2005). Voett *et al.* (2006; 2007) report a series of at least four tsunami impacts on the coast between Lefkada Island and the entrance of the Amvrakian Gulf since the first millennium BC. This coincides with the area of highest seismic activity in Europe which includes the central Ionian islands of Lefkas, Ithaca, Kephallinia and Zakynthos. A significant portion of the seismic activity is associated with the right lateral Kephallinia Fault. Although strike slip faulting does not favor tsunami initiation, ground shaking from large earthquakes, like the 1953 one may generate unstable sediment masses to slide and trigger devastating but local tsunamis.

Recent swath bathymetry survey off the western coasts of Zakynthos and Kephallinia islands revealed extensive submarine slumping along the upper and middle slope and rolling of boulders derived from the steep, rocky shorelines.

Discussion

Large earthquakes, seafloor ruptures, uplift or subsidence of shorelines, earthquake triggered or aseismically developed submarine landslides, major or minor submarine or island volcanic eruptions occur within the various tectonic settings of the Aegean and Ionian Seas. Some of these marine geological processes in the near past have triggered small or large tsunamis, some of which were catastrophic for the Aegean, Ionian or even Eastern Mediterranean coastal region.

Information on the effects of the past disasters are very diffuse, especially if they took place in earlier times, and the reliability of the available tsunami catalogs has been questioned and reexamined (Ambraseys and Synolakis, 2010). But even so, similar processes are expected to, and will, occur in the near or far future. If we consider that the coastline of Eastern Mediterranean Sea is much more densely populated than it was in the past, it is easy to imagine the tremendous disaster they can cause.

It is thus of great importance that scientists from all different disciplines – marine geologists, seismologists, modelers, engineers, etc. – join forces, resources and efforts to better understand and forecast tsunami generation, propagation and impact.

Potential tsunamigenic sources in the Eastern Mediterranean and a decision matrix for a tsunami early warning system

Amos Salamon

Geological Survey, Jerusalem, Israel

Abstract

The tsunami decision matrix constructed by the IGC/NEAMTWS (2009; 2010) in order to issue a warning message as soon as a potential tsunamigenic earthquake occurs, focuses mainly on regional and basin-wide tsunamis. Unfortunately, most of the historical tsunamis that hit the Levant are considered local and as such are outside the mandate of the NEAMTWS. Moreover, the proposed matrix failed to capture most of the historical tsunamis that were generated by on-land earthquakes along the Dead Sea Transform, with an origin further than 30 km away from the coast.

Understanding the tsunamigenic architecture of the eastern Mediterranean helped to modify the proposed matrix according to the typical conditions in the Levant, especially the need to relate to seismogenic submarine landslides. The matrix was calibrated to suit the maximal distance (100 km) and minimal magnitude (M~ 6) of the assumed epicenter and magnitude of those historical tsunamigenic earthquakes. Non-earthquake tsunamis including sea waves from submarine seismogenic slumps are not covered yet. Hence, alerting volcanic and spontaneous slump tsunamis cannot be considered until a real-time monitoring of sea level is introduced into the warning system.

Since the majority of the tsunamis in the Levant will most probably originate from local M>6 earthquakes, the first warning signal will be the strong shaking. Therefore, there is no need to wait until a sophisticated warning system gets into operation and people should be taught to protect themselves from a tsunami by moving away from the sea as soon as they feel the strong shaking. The second natural warning signal, although may not always appear, is a drop in the sea level and retreat of the water. Indeed, some tsunamis may arrive from remote sources that will not be strongly felt and may start with a rise in sea level, but these are the minority of the events.

1. Introduction

Understanding the tsunamigenic architecture of the Eastern Mediterranean enables to formulate a decision matrix that can help determine in near-real-time whether an occurring earthquake is potentially tsunamigenic and, if necessary, issue an early warning message. Such a matrix has already been constructed by the IGC/NEAMTWS (Intergovernmental Coordination Group for the Tsunami Early Warning and Mitigation System in the North Eastern Atlantic, the Mediterranean and Connected Seas, 2009, updated in 2010), in accordance with worldwide experience, and it focuses mainly on large-scale earthquakes that may generate regional and basin-wide tsunamis. However, most of the historical tsunamis that hit the Levant are considered local (Table 1) and as such fall outside the mandate of the NEAMTWS. The urgent need to establish early warning

systems to local tsunamis originated from both earthquakes and submarine landslides is addressed by Papadopoulos (this volume) and Rosen (this volume). Nonetheless, the formulation and establishment of such systems may take some time.

This paper fills the gap and reconstructs the tsunamigenic framework of the eastern Mediterranean in terms of the location and threshold magnitude of all the potential sources. It then proposes a decision matrix that is both compatible with NEAMTWS requirements and suits the typical conditions in the Levant, especially the need to relate to seismogenic submarine landslides.

Table 1. Historical and modern tsunamis that affected the Levantine coast.

The list includes the significant historical and modern tsunamis that occurred in the eastern Mediterranean basin and affected the Levant coasts, from Egypt in the south to the Bay of Iskenderun in the north, and Cyprus (modified mainly after Guidoboni *et al.*, 1994; Guidoboni and Comastri, 2005; Salamon *et al.*, 2007; and Ambraseys, 2009). The Santorini (Thera, Late Minoan) tsunami, although pre-historical, is also included.

Event	Tsunami range*	Tsunamigenic cause	Affected coasts	Comments
1627-1600 BC	Basin wide?	Eruption of the Santorini (Thera)	Crete, Greece, Turkey	May have affected Levant, but evidence needs to be verified
1365±5 BC	Local	Unknown	Ugarit (Syria) flooded and half destroyed	
Mid 2nd century BC	Local	Unknown	Sea rose between Tyre and Acre	Coast was flooded
23±3 BC	Local	Unknown	Tsunami between Alexandria and Pellusium?	
115 12 13 morning	Local	On-land earthquake in northwestern Syria	Tsunami along the coast between Caesarea and Yavne, Israel	Doubtful tsunami, historical sources are not clear
365 07 21 before sunrise	Basin wide	Strong earthquake in Crete (Hellenic Arc)	Major tsunami in Alexandria, Peloponnese, Adriatic and Sicilian coasts	Loss of lives and much damage in Alexandria
551 07 09	Local	Earthquake offshore Lebanon	Tsunami in Lebanon, between Tyre and Tripoli	Damage in coastal cities of Lebanon, significant drawback of the sea
746 01 18 morning	Local	Earthquake in the Jordan Valley	Tsunami, possibly on the Levant coasts	Affected coasts were not mentioned, possibly in the Mediterranean
802 12 30 - 803 12 19	Local	Earthquake nearby Massisa	Massisa coasts, near Gulf of Iskenderun	
1033 12 05 before sunset (1034 01 04?)	Local	Earthquake, possibly in the Jordan Valley	Tsunami in Acre, and possibly nearby coast	Port of Acre dried for a while
1036 03 12 - 1037 03 11	Local	Earthquake nearby Cilicia	Sea in Cilicia billowed back and forth	
1068 05 29	Local	Earthquake in (southern?) Israel	Sea in southern Israel receded and returned	
1202 05 20 0240 UT	Regional–Local?	Earthquake in southern Lebanon and northern Israel	Severe tsunami on Levant coast and Cyprus	Damage in Acre
1222 05 11 06:15 UT	Local	Earthquake in southern Cyprus	Tsunami in Cyprus: Limasol and Paphos	Port of Paphos dried for a while
1303 08 08 03:30 UT	Basin wide	Strong earthquake in the Hellenic Arc	Widespread tsunami in eastern Mediterranean, including Acre	Acre was flooded
1408 12 29	Local	On-land (?) earthquake in northwestern Syria	Tsunami, near Mt. Cassius, western Syria	Boats were thrown on shore
1546 01 14 afternoon	Local	Earthquake, possibly in the Jordan Valley	Sea withdrew and returned, southern Israel	
1759 10 30 03:45 LT	Local	Earthquake in southern Lebanon, southern Syria and northern Israel	Sea waves flooded Acre and docks at Tripoli	Streets of Acre were flooded up to 2.5 m
1759 11 25 19:23 LT	Regional–Local?	Earthquake in southern Lebanon, southern Syria and northern Israel	Sea waves in Acre and as far as the Nile Delta	Damage in Acre
1870 06 24 17:00 UT	Regional	Earthquake in the Aegean Sea?	Port of Alexandria was flooded	
1872 04 03 07:40	Local	On-land earthquake in northwestern Syria	Sea rose and flooded the coast near Antakya	
1908 12 28 05:20 UT	Regional–Local?	Earthquake (and submarine landslide?) in the Straits of Messina	Tsunami in Messina Straits and nearby seas	Heavy loss of lives and damage in Messina
1953 09 10 04:06 UT	Local	Earthquake southwest of Cyprus	A series of tidal waves in Cyprus	Caused no damage
1956 07 09 03:12	Regional	Earthquake (and submarine landslide?) in the Aegean Sea	Tsunami in the Aegean Sea, recorded in Jaffa	Damage in Aegean Isles, not felt in Jaffa port

* Tsunami range according to ICG/NEAMTWS definitions.
LT: local time; UT: Universal Time.

2. Working approach

The many unknowns and uncertainties prevent detailed parameterization of tsunami generation for the Levant area. Field evidence is limited, sometimes unequivocal, and so far the constraint is mainly two millennia of descriptive records and a century of modern records of seismic and tsunami activity. Thus the geometry, orientation, mechanism, location, depth, repeat time and other characteristics of the tsunami generators can only be inferred from the existing data, relying on best judgment.

The seismotectonics and bathymetry of the eastern Mediterranean are reviewed in order to identify and parameterize all the main potential tsunamigenic sources. In most cases, the data are extracted or extrapolated from the published literature. For example, worst-case scenarios are estimated according to the tectonic setting, and repeat times are constrained by the geological and seismological findings. Uncertainties regarding submarine landslides are even greater, including the relations between the seismic source and the resulting landslide, the expected volume of the collapsed material and its elevation at start and rest, steepness of the slope and the sliding distance, the repeat time of events, etc.

Table 2. Characteristics of the tsunamigenic sources that may affect the Levant coast.

The table is based on the existing literature as well as on personal judgment where needed. Recurrent rates are conservative and were calibrated with the historical and recorded data. The historical record, two millennia long, is shown for comparison and verification. The table is modified from Thio (2009) and Galanti *et al.* (2009; 2010a).

Region	**Tsunamigenic source**	**Estimated tsunami recurrence rates** (in years)	**Comments and references**	**Reports of past tsunamis** (in Israel)
Continental margins of Israel	Seismogenic landslide, triggered by on-shore M>~6 earthquake, as far as 80-100 km away from the coast	Large ls 1:100,000 Small ls 1: 300	Large volume landslides according to Frey-Martinez *et al.* (2005). Small landslides: historical records of Israel show 7 local tsunamis in 2,000 years: 2 in south and 5-6 in the north.	115?, 746, 1033, 1068, 1202, 1546, 10/1759, 11/1759
Cyprus Arc	Earthquake	M≥6 1:100	There are five records of M≥~6 events during the last century in and around Cyprus (Salamon *et al.*, 2003), three of them in the sea, some are of strike-slip mechanism. Only the 1953 generated a local tsunami.	None
Crete and the NE Hellenic Arc	Earthquake	M≥8 1: 800-1,000	Shaw *et al.* (2008): Mw 8.3-8.5 thrust event, estimated repeat time of the 365 is ~ 5,000 yrs, and about 800 yrs if this type is typical to the entire Hellenic Arc (e.g. 1303). Papadopoulos *et al.* (2009): two M8-8.3 events per 2,000yrs.	1303
Aegean Sea	Earthquake Landslide Volcanic	? ? 1:25,000	The tsunami of the 1956 M7.5 earthquake was destructive in the Aegean but detected in Israel by instruments only. Perissoratis and Papadopoulos (1999) and Beisel *et al.* (2009): combined mechanism of earthquake and landslide. Santorini type of tsunami may occur once in 25,000 years.	1956 Evidence of the Santorini (1627-1600 BC) event in Israel is doubtful
Nile Delta	Landslide	1:10,000	Garziglia *et al.* (2008) estimate for the Rosetta province a rate of 1:27,000 yr for landslides of 3-500 km^3.	None
Offshore Egypt	Earthquake	?	Modern records show 2 M6 earthquakes (per century) with no record of a tsunami.	None
Beirut thrust	Earthquake	M7.5 1:1,500	Elias *et al.* (2007): event per 1,500 - 1,750 yr.	551
Italy, Sicily (Messina)	Earthquake	M7.5 1: ~1,000	After Valensise (2004) and Barbano *et al.* (2007). The 1908 tsunami arrived as far as western Egypt (Ambraseys, 1962).	None
Italy, Sicily (Etna)	Landslide	1: >10,000	After Pareschi *et al.* (2006b,c; 2007).	~8,000 B.P.

Comments: the estimated recurrence rates refer directly to a tsunamigenic event, thus ignoring the unknown relations between the total number of earthquakes and the 'successful' tsunamigenic ones. Triggers for the 2nd century BC and 23± BC tsunamis are not known. Ls- Landslide.

For each of the potential sources we list the past tsunamis it may have possibly generated, describe its probable dimensions, assign its threshold magnitude capable of producing a considerable tsunami, and estimate its return period (Table 2). The collected data were used to formulate the tsunami decision matrix for the Levant. For consistency, the scheme of the matrix was adopted from the ICG/NEAMTWS (2009; 2010) and tested against the historical tsunamis listed to have occurred in the Levant. The matrix was then modified to suit the typical conditions of the Levant and then again validated against the historical list.

3. The tsunamigenic framework of the Levant

3.1 Tectonic sources

As expected, plate boundaries are the major active tectonic elements in the eastern Mediterranean, and those that are in the sea are potentially tsunamigenic, either directly by sea floor deformation or by the release of submarine landslides. Continental seismogenic structures that are close enough to the continental slope are capable of triggering submarine slumps and therefore should also be considered. Several studies have already examined and simulated the potential tsunamigenic sources in the eastern Mediterranean region (e.g., Papadopoulos *et al.* (2007b) in the Hellenic Arc; Yalciner *et al.* (2007) in the Mediterranean; Fokaefs and Papadopoulos (2007) in and around Cyprus; Yolsal *et al.* (2007) for the eastern Mediterranean; Tinti and Armigliato (2003) in southern Italy; Tinti *et al.* (2005a) in the Mediterranean, Lorito *et al.* (2008) in southern Italy, including a rupture of the western Hellenic Arc, as was probably the case in 365 AD). Yet none of them compiled a comprehensive scheme that is relevant to the Levant.

3.1.1 Far sources

The Hellenic Arc has already generated the largest known earthquakes and basin-wide tsunamis in the eastern Mediterranean, most probably by shallow thrusts beneath the trench, and therefore is the most hazardous. The 2004 Sumatra experience demonstrated the break of a whole arc in an instance, thus portraying the potential break of the half, or even the whole Hellenic Arc as the worst-case scenario of an earthquake-generated tsunami in the eastern Mediterranean basin. The repeat time of such an extreme scenario, if at all probable, is not known, although the exceptional large offset (20 m!) suggested by Shaw *et al.* (2008) for the 365 earthquake is on a scale similar to that of the 2004 Sumatra earthquake.

The Cyprus Arc is the closest subduction zone to the Levant, but evidently is smaller, slower and less active than the Hellenic Arc. Large earthquakes that produce local tsunamis do occur there from time to time but so far no significant basin-wide tsunami is known to have originated from there. Yet the tectonic setting of the Cyprus Arc does not rule out the potential occurrence of a much larger event that could rupture a large segment of the arc to a depth of several tens of kilometers. Therefore, this hazard should not be overlooked, especially because the Levant coast faces large parts of that arc.

Sicily and Italy are the most distant tsunamigenic source that may affect the Levant. The tsunami that followed the Mw7.1, 1908 Messina earthquake (Pino *et al.*, 2009) was reported from as far away as western Egypt (Ambraseys, 1962). Favalli *et al.* (2009) suggested that the tsunami was driven by a combined seismic and landslide source which may have intensified its effect.

3.1.2 Near tectonic sources

The Dead Sea Fault System: although continental, the Dead Sea Transform (DST) turns out to be the most 'productive' source, for most of the tsunamis in the Levant followed DST earthquakes, possibly due to the triggering of submarine landslides. Altogether, about 60 moderate to large (M>~6) earthquakes were listed since about the mid 2nd century B.C. in and around the DST, from the Gulf of Aqaba in the south until it meets with the East Anatolian fault in the north (Salamon *et al.*, 2007; Salamon, 2010). Of these, about a quarter to a third of the largest and a seventh of the moderate earthquakes were tsunamigenic (Salamon *et al.*, 2007). The most distant coasts affected by a tsunami that originated from an earthquake along the DST were in Cyprus (in 1202) and Egypt (11/1759).

Dead Sea Transform secondary structures: additional parts of the DST are also capable of producing a tsunami. Such is the tsunami that followed the 551 Beirut thrust earthquake (Elias *et al.*, 2007). Other tsunamigenic examples are the October and November 1759 earthquakes that apparently ruptured the Rachaya and Serghaya faults, respectively (Gomez *et al.*, 2001; Daëron *et al.*, 2005). The motion along these secondary faults is slower than that of the main transform, implying a larger recurrence time of strong earthquakes and tsunamis.

Other nearby seismogenic structures are the Northeast Mediterranean Triple Junction which may have produced tsunamis in the Iskenderun Bay (802/3 and 1036/7); faults offshore Egypt and Sinai which, which as far as we know have not yet generated a tsunami, but the proximity to the Nile sedimentary cone poses the potential for tsunamis, for vast slumps are well recognized there throughout the recent geological record (e.g., Garziglia *et al.*, 2007; 2008). Additional elements that are not known to have produced a tsunami in the Mediterranean, but with tsunamigenic potential worth investigating, are the Palmyra in northeastern Syria (1042 AD), the southern Suez Rift (mb7.0, 1969) and the Gulf of Aqaba (Mw7.1, 1995), the last two did disturb the water in the gulfs (Ben-Menahem, 1991; Wust, 1997).

3.2 Submarine slumps

The bathymetry and shallow seismic profiles along and across the continental margins of the Levant show numerous scars typical of landslide morphology, and hilly topography and slide bodies at the foot of the continental slopes (Almagor, 1993). Similarly but on a larger scale, this is also seen around the Nile Cone (Garziglia *et al.*, 2007; 2008; Folkman and Mart, 2008). In a predictive sense, since no drastic changes have occurred in the depositional system of the Levantine margins in recent times, it is reasonable to assume that slope failure will continue in the future. Learning from the past, future tsunamis will most likely hit opposite the damage zone of large earthquakes.

3.2.1 Near sources

Offshore the northern Levant: Almagor (1993) described the morphology of this narrow shelf as cliffs about 1 km high, intensively cut by deep submarine canyons, and identified large slabs of detached sediments along the canyons. Evidently, it reflects intensive failure of the continental slopes, and therefore also its vulnerability to tsunami generation.

Offshore the southern Levant: Almagor and Garfunkel (1979) described scars that appear all along the Levant continental shelf in shallow water, with chunks of the failed material sampled as deep as 900 m. Frey-Martinez *et al.* (2005) discovered many slump complexes, the largest group extends over 4,800 km^2, buried within the Late Pliocene succession and reaching a volume of up to 1,000 km3. An increasing number of smaller slumps appear in younger strata, up to the Holocene. More importantly, the presence of proto-slumps within the very same area suggests that there is still a potential of slope instability.

3.2.2 Far sources

The Nile Delta is the largest submarine body of sediments in the eastern Mediterranean. Sediments are still accumulating and large scars as well as large volumes of slumps are well known there (Austin, 2006; Garziglia *et al.*, 2007; 2008). Although most of the information is derived from research on the western side of the cone, it seems that the eastern side is no different (Folkman and Mart, 2008).

The eastern Mediterranean, Aegean Sea and Italy: it was proposed that the Messina 1908 tsunami (Ortolani *et al.*, 2005; Billi *et al.*, 2008) that was reported from western Egypt (Ambraseys, 1962) and the 1956 tsunami of the Aegean (Perissoratis and Papadopoulos, 1999; Beisel *et al.*, 2009) that was recorded in the Jaffa harbor (Goldsmith and Gilboa, 1986; Van Dorn, 1987) and possibly also in Haifa (Shalem, 1956), were generated by submarine slumps immediately after a large M~7.5 earthquake.

In addition, modeling of a tsunami resulting from the sector collapse of the Etna volcano in prehistoric times (Pareschi *et al.*, 2006b,c; 2007) suggests its arrival to the Levant, although its possible impact on local settlements has been strongly exaggerated (Galili *et al.*, 2008). Another

large submarine slide was identified near the Anaximander Seamount (ten Veen *et al.*, 2004), but its tsunamigenic potential has not yet been investigated.

4. The decision matrix

In order to verify the ICG/NEAMTWS matrix for the specific conditions in the Levant, it was tested against each of the identified tsunamigenic sources and the historical tsunamis to see whether the matrix would have 'captured' them all. The matrix was found capable of covering the regional and basin-wide tsunamis originated from marine earthquakes, but surprisingly, most of the on-land tsunamigenic earthquakes were missed (e.g., 115?, 746, 1033, 1068, 1202, 1546, 1759/10, 1759/11)! The reason is that those earthquakes were most probably originated along the DST which is located more than 30 km away from the sea, and of lower magnitudes than stated by the matrix. Thus, the matrix should be modified specifically for the Levant.

The calibration proposed hereby consists of extending the maximal distance from the coast of the tsunamigenic earthquakes to 100 km and lowering its minimal magnitude to M~ 6 (Table 3, modifications are marked in black with white letters). In addition, a new row is added in order to introduce a message, "advisory" and "watch", in the case of a local tsunami. Upon re-testing the matrix against the historical tsunamis, one finds that they are all covered now with none escaping unnotice. The modified matrix is presented in Table 4 by the tsunami message type, according to the keywords recommended. Recently, the ICG/NEAMTWS (2010) adopted the changes proposed here. It is now clear which type of a message should be issued, as a function of the type of tsunamigenic earthquake.

Non-earthquake induced tsunamis, such as orphan (e.g. in the 2nd century BC), volcanic (Late Minoan, Santorini) and spontaneous events, are not meant to be covered by the decision matrix. Once the tsunami warning integrates real-time monitoring of sea level, the matrix can be updated and set to cover the non-earthquake tsunamis.

Table 3. The modified decision matrix, tested against historical events of the Levant.

Depth	Location	(Mw)	Tsunami Potential	Bulletin Type	Validation test for the Levant
< 100 km	Sub-sea or very near the sea (< 100 km)	5 to 5.5	Negligible potential for a local tsunami	Information Bulletin	-
		5.5 to 6.0	Small potential for a local tsunami	Local Tsunami Advisory	-
		6.0 to 6.5	Potential for a destructive local tsunami < 100 km	Local Tsunami Watch, Regional Tsunami Advisory	115?, 551, 746, 802, 1033, 1036, 1068, 1222, 1408, 1546, 10/1759, 1872, 1953
		6.5 to 7.0	Potential for a destructive regional tsunami < 400 km	Local Tsunami Watch, Regional Tsunami Watch, Basin-wide Tsunami Advisory	1202, 11/1759, 1870
		≥ 7.0	Potential for a destructive basin-wide tsunami > 400 km	Local Tsunami Watch, regional Tsunami Watch, Basin-wide Tsunami Watch	365, 1303, 1908, 1956
	Inland (> 100 km)	5.5 – 7.5	No tsunami potential	Information Bulletin	
≥ 100 km	All locations	≥ 5.5	No tsunami potential	Information Bulletin	

4.1 Decision maps

The proposed matrix (Table 4) is associated with a map (Figure 1) that enables issuing a tsunami alert as soon as the preliminary source parameters (magnitude, location and depth) of the occurring earthquake are determined. There are three hazard zones on the maps:

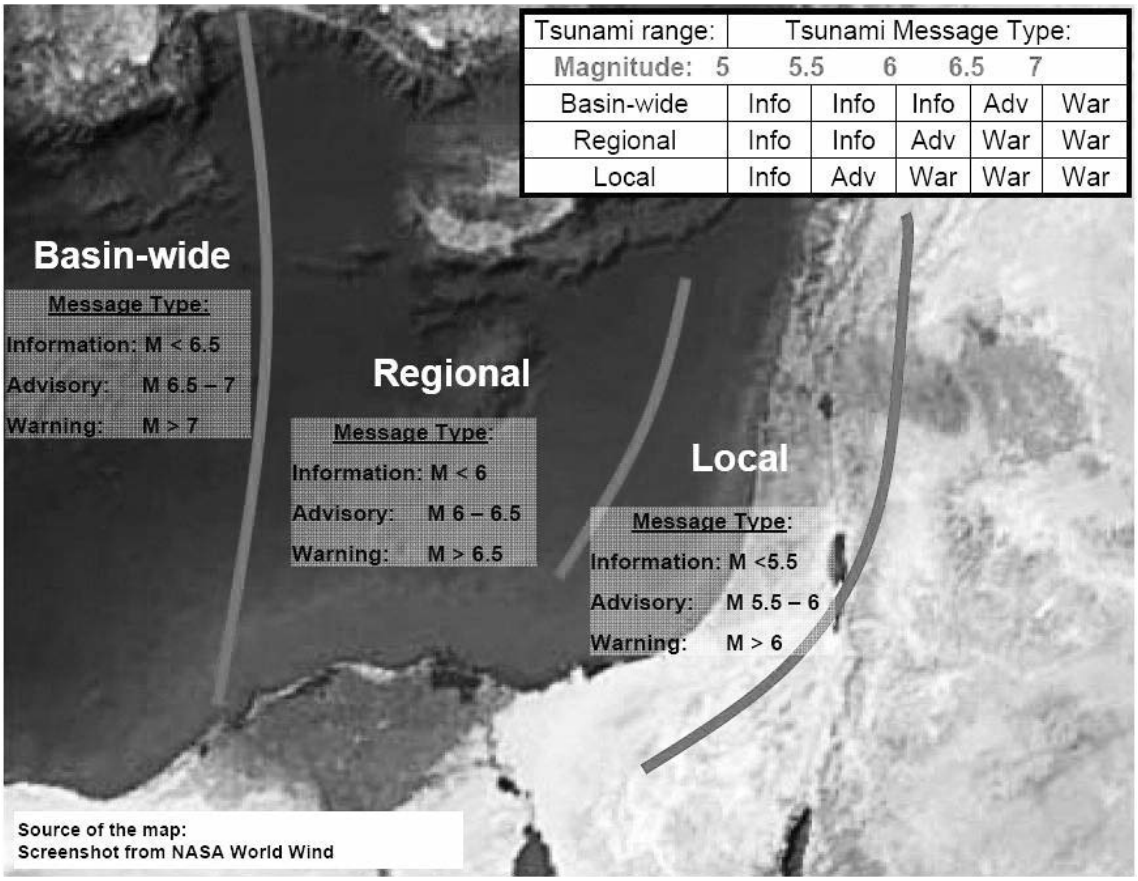

Figure 1. Threshold magnitude zones for tsunami early warning in the Levant.
The type of message presented on the map follows the modified decision matrix (Table 4).

Table 4. The modified decision matrix, by the type of the tsunami message.

Depth	Location	(Mw)	Tsunami Potential	Tsunami Message Type		
				Local	Regional	Basin-wide
< 100 km	Sub-sea or very near the sea (< 100 km)	5 to 5.5	Negligible potential for a local tsunami	Information	Information	Information
		5.5 to 6.0	Small potential for a local tsunami	**Advisory**	Information	Information
		6.0 to 6.5	Potential for a destructive local tsunami < 100 km	**Watch**	**Advisory**	Information
		6.5 to 7.0	Potential for a destructive regional tsunami < 400 km	**Watch**	**Watch**	**Advisory**
		≥ 7.0	Potential for a destructive basin-wide tsunami > 400 km	**Watch**	**Watch**	**Watch**
	Inland (> 100 km)	5.5 – 7.5	No tsunami potential	Information	Information	Information
≥ 100 km	All locations	≥ 5.5	No tsunami potential	Information	Information	Information

- Local (L) - the area vulnerable to earthquakes which may trigger a local tsunami or larger;
- Regional (R) - the area vulnerable to earthquakes which may trigger a regional tsunami or larger;
- Basin-wide (B) - the area vulnerable to earthquakes which may trigger a basin-wide tsunami.

The threshold magnitude for each type of message set for each of these regions, is presented on the map, according to the modified decision matrix (Table 4). Should an event with a magnitude larger than stated occur, a tsunami alert should be issued. For smaller earthquakes only a tsunami information message is needed. The map supports alerts coming from any Regional Tsunami Watch Centers (RTWCs) of the NEAMTWS, as well as issuing an independent alert by the local National Tsunami Warning Centers (NTWC).

5. Education – the already available tsunami warning system

Since the majority of the tsunamis that may affect the Levant will most probably originate from earthquakes along the Dead Sea Fault System, and the relevant events are expected to reach M6 and above, the first warning signal will be the strong seismic shaking. Therefore, and with no regard to when and where a sophisticated warning system gets into operation, people should be taught to protect themselves from a tsunami by moving away from the sea as soon as they feel the strong shaking. The second natural warning signal, although it may not always appear, is a drop in the sea level and retreat of the sea. Indeed, some tsunamis may arrive from remote sources that will not be strongly felt in the Levant area and may start with a rise in sea level, but these are the minority of the events.

Acknowledgment: the present study was conducted within the framework of the Inter-ministerial Steering Committee for Earthquake Preparedness in Israel, contract no. 28-02-014.

Earthquake triggered landslide tsunami simulations at the Israeli coasts and a proposed approach to early warning from landslide tsunamis

Dov S. Rosen

Israel Oceanographic & Limnological Research, Haifa, Israel

Abstract

Introduction

The tsunami event of December 2004 in the Indian Ocean and its disastrous impact of the coasts rose awareness also in regards to the feasibility of tsunamis in the Mediterranean basin, resulting in the establishment of the Intergovernmental Coordination Group for the Tsunami Early Warning and Mitigation System in the North-eastern Atlantic, the Mediterranean and connected seas (ICG/NEAMTWS) in November 2005 and upon it to the initiation of the development of the tsunami early warning system for the NEAM region. Since the 1st meeting, followed by another six official meetings to which CIESM also participated, there has been significant progress in the development of the warning system, expected now to become fully operational by 2013. The system is dedicated for regional to basin-wide tsunamis and is developed basically on the assumption of direct earthquake induced tsunamis. The warning for local tsunamis has been left to the responsibility of each country. Also earthquake triggered landslide tsunamis, as well as landslide tsunamis induced by other factors, are basically not included in the terms of reference of NEAMTWS, because such events are very difficult to detect, and because the warning times are relatively very short (in the order of minutes). Furthermore, in certain cases it has been shown that such tsunami events have shorter wave lengths/wave periods and are dissipating more rapidly, posing (perhaps?) less hazard to remote coasts.

Numerous theoretical and laboratory studies (physical and numerical) and fewer field studies have been conducted so far. It has been shown that tsunamis induced by landslides can be generated in a number of ways and of varying strength, depending for example on the strength of the initial impact inducing the landslide, on the material properties of the sliding matter, on the slope of the shelf, on the final sea bottom depth, on the final velocity, etc.

Fokaefs and Papadopoulos (2007), Papadopoulos *et al.* (2007c) and Salamon *et al.* (2007) among others have investigated tsunami events in the Eastern Mediterranean (EM). The latter have shown that among the 21 verified tsunami events in the EM, about half have been generated by earthquakes at the Dead Sea Transform, some of them on the Israeli shelf, others on the Lebanese or Syrian shelf. Earthquakes occurred in the past on the Egyptian coast, but so far there is very little knowledge about landslide induced tsunamis at the extensive deposition of unconsolidated sediments on the submerged part of the Nile delta, in spite of the real potential for such encounters. Furthermore, recent detailed bathymetric survey by multibeam of the Gulf of Aqaba, Red Sea by

IOLR and foreign partners (Tibor *et al.*, 2010), has shown signs of significant landslides on the Israeli shelf of the Gulf. It is suspected that these may have induced tsunamis if they occurred as shock events following earthquakes in the area, located on the Afro-Syrian fault.

Landslide tsunami simulations at mediterranean and red sea coasts

In order to investigate the impact extent of landslide induced tsunamis at the Israeli coasts, a number of simulation studies of landslides at the Mediterranean coast of Israel have been conducted and published (Galanti *et al.*, 2009; Galanti *et al.*, 2010; Thio, 2009). Recently, IOLR started numerical model simulations of landslide induced tsunamis at the Red sea coast of Israel (in the Gulf of Aqaba). In contrast to the simulations of Thio (2009), run with a relatively coarse grid at the coast (35m) and with an URS in house developed model, those carried by Galanti *et al.* have been with a much finer grid cell size (5 m), using the GEOCLAW model (LeVeque, 2006) which is part of the CLAWPACK internationally developed software package. The GEOCLAW package was shown to provide high quality simulation results, comparable to the leading tsunami models available nowadays (Lynett, 2009). Figures 1 and 2 from the results of Galanti *et al.* (2009) and Galanti *et al.* (2010) respectively show examples of the computed earthquake induced landslide inundation at the coasts of Tel Aviv and of Haifa Bay, while Figure 3 shows the inundation at the Gulf of Aqaba/Elat coasts due to a similar event on the Israeli shelf (run however with a coarser grid cell size at the coast). They demonstrate that the extent of maximum inundation may reach significant heights and may induce severe impact. Furthermore, the simulation at the Mediterranean coast of Israel has shown that the impact of the earthquake induced landslide tsunami may reach at more remote coastal areas of neighboring countries, probably due to the geometry of the coastal shelf in this region, enabling combined reflection and re-refraction of the tsunami waves towards neighboring coasts.

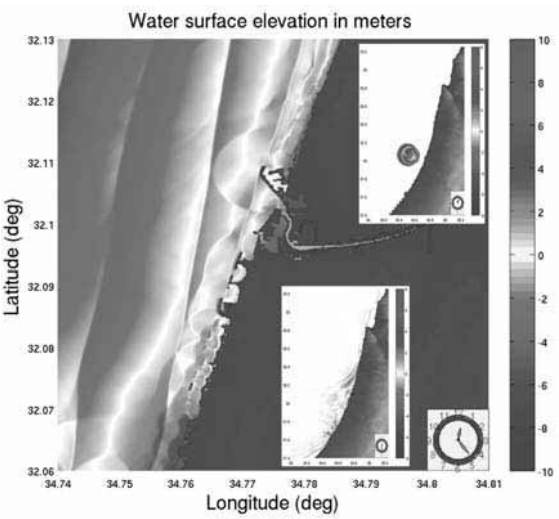

Figure 1. Example of earthquake induced landslide tsunami at the coastal shelf of Tel Aviv and the resulting inundation at the coast (after Galanti *et al.*, 2009). Landslide characteristics: volume 0.625 km^3 (50 m high x 2.5 km wide x 5 km long); initial fall speed 50 m/s. In the small frames are shown an earlier instance and a later instance of the tsunami wave, reaching neighboring countries coasts.

[see original colour illustration in Annex at end of volume]

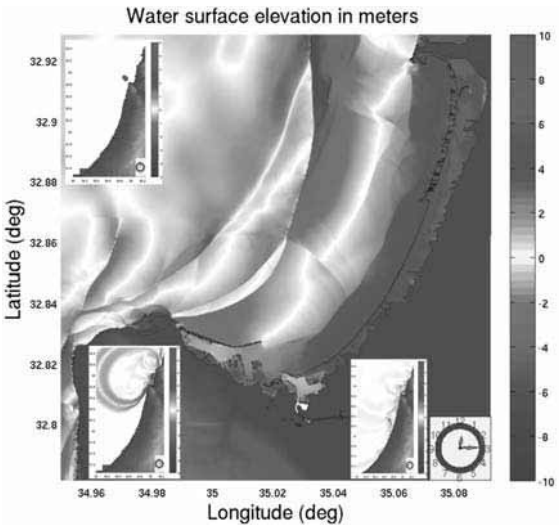

Figure 2. Example of earthquake induced landslide tsunami at the coastal shelf of Haifa and the resulting inundation at the Bay of Haifa coasts (after Galanti *et al.*, 2009). Landslide characteristics: volume 1.60 km^3 (50 m high x 4 km wide x 8 km long); initial fall speed 50 m/s. In the small frames are shown an earlier instance (up left) and two other instances of the tsunami wave.

[see original colour illustration in Annex at end of volume]

The GEOCLAW software accepts two types of inputs as tsunami generating source. The first is a time domain description of the water surface. The second option is by describing the spatial change in time of the bathymetry at the tsunami generation source, enabling simulation of the wave development and propagation due to the solid-liquid interaction at the source and the examination of the contributions of various geometric and physical parameters.

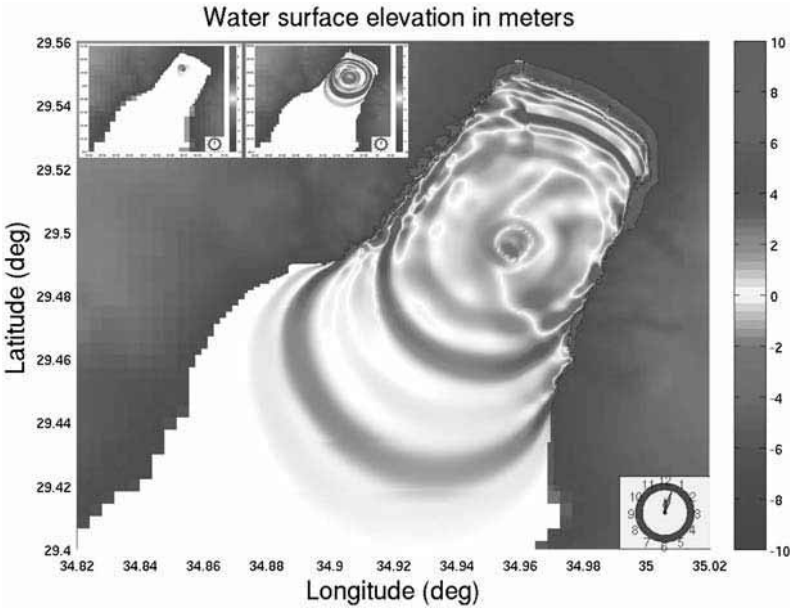

Figure 3. Example of earthquake induced landslide tsunami at the coastal shelf of the Gulf of Aqaba/Elat and the resulting inundation at the Gulf coasts. Landslide characteristics: volume 0.03 km^3 (30 m high x 1 km wide x 1 km long); initial fall speed 50 m/s. In the small frames are shown two earlier tsunami instances.

[see original colour illustration in Annex at end of volume]

A relatively novel feature of the landslide simulations carried out by Galanti *et al.* (2009) was the ability to simulate the changing shape of the landslide mass with time, which is applicable for coasts with relatively soft, unconsolidated bottom material or material which is likely to disintegrate from solid (cemented sand rock) to unconsolidated state. For the landslide simulation of soft material, Galanti developed a dedicated software, describing the sliding material mass as half of an elliptical hyperboloid facing the sea bottom and sliding down along its long axis, changing its shape along the shelf slope. The shape change is done in order to obtain a more natural change of the sliding material block moving downwards on the slope by adding a white noise random generator to the original shape. In addition the velocity at the initial and final stages of the slide change uniformly from 0 to a finite value, and at the end from the final velocity attended to 0.

Proposed approach to early warning of landslide tsunamis

As mentioned above, landslide induced tsunamis are events of fast propagation to local shores, leaving short warning times in the order of a few minutes to a few tens of minutes. In spite of the localized nature of such events as described in literature (particularly due to rock block slides), the simulations results obtained by Galanti *et al.* (2009) indicated that for certain shelf conditions such as these of the Mediterranean shelf of Israel, the tsunami waves induced by a landslide on the Israel shelf as unconsolidated mass, would affect at least the coast of Israel and those of its neighbors (Lebanon, Egypt) and probably even Cyprus.

A similar effect is estimated by the author for a landslide occurring at the Nile delta (Figure 4). As indicated by Rosen (2009), the widening and deepening of the Suez Canal since the 1990's has increased the discharge of very saline and warm sea waters entering the Mediterranean via the Suez Canal. In spite of the scarce published data, the author estimated that the present annual flow through the Suez Canal is about 100 to 120 km^3, larger than the present Danube yearly flow, and that this flow in the Mediterranean is expected to further increase, when the published plans for further deepening and widening of the Suez Canal would be implemented in coming years. This would induce, to the author's estimate, to significant cumulative bottom scouring of the eastern flank of the lower part of the Nile delta, eventually leading to a landslide and consequent tsunami.

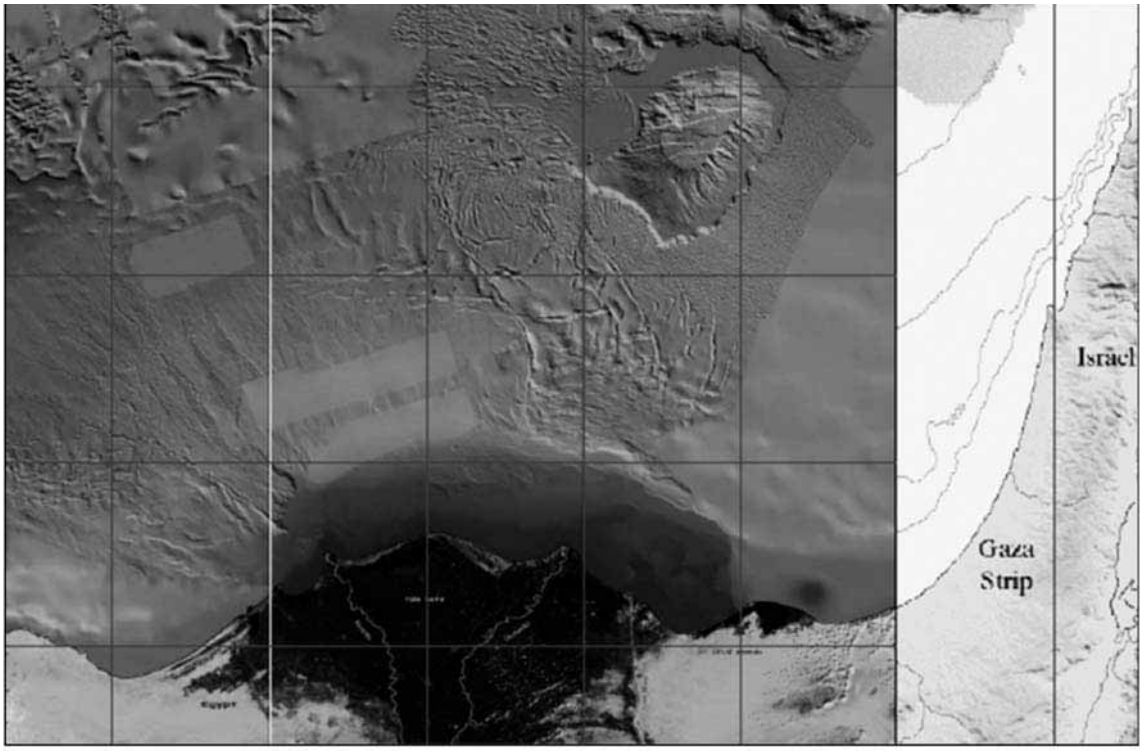

Figure 4. Underwater Nile delta fan as potential source of landslide induced tsunami for the Levantine basin (after Sardou and Mascle, 2003).

[see original colour illustration in Annex at end of volume]

Due to the short duration from the slide occurrence to the arrival of the tsunami waves at the coast, a local monitoring, detection and early warning stations system should be developed and installed. One alternative for such a system would be to installstations for early detection and warning at the upper part of the shelf (at about -50m depth) at sites assessed as potentially geologically unstable or at constant distances along the coast sector possessing land sliding potential hazard (~ each 25 km). These stations would be equipped with seismic sensors and with sea level pressure gauges and with quick release buoys with fiber-optics thin data transmission cables, which can detect sea level changes and start transmission of the data upon triggering by the encountered earthquake seismic waves, above a scale 6 magnitude threshold. In case of a strong local earthquake over that magnitude (which is expected to be detected and located within less than 2 minutes by the national seismic monitoring systems), the data would be immediately transmitted via the buoys released by the earthquake triggered stations and received at the national tsunami warning centers and analyzed for secondary shocks due to a local landslide and significant shifts in the local sea level at each buoy.

If such landslide is detected, then a warning based on the landslide location and pre-computed simulations of landslide induced tsunamis would be disseminated to the national authorities and via them to the potentially affected public. Detection of the tsunami waves from the data transmitted by the stations would be analyzed using the approach proposed by Rosen (2007) and by Rosen and Raz (2010).

Another option for landslide induced tsunami detection would be using HF radars. Among these we may quote the multi frequency beam forming HF radar (e.g. WERA radar system and the CODAR system). The WERA system, in contrast to the other existing systems, performs a continuous data gathering and analysis and enables early detection of tsunami thanks to the development of a special tsunami detection software. The radars are able to detect the high orbital surface velocities associated with tsunami waves in relatively shallow water (shallower than about

100 m and up to distances of about 250 km offshore). Recently, the WERA system was able to detect the tsunami wave arriving from the March 11, 2011 Tohoku tsunami in Japan at the offshore Chilean coast (Helzel Messtechnik, 2011). The radar systems require in general data gathering for a sufficient period of time, and thus WERA producers have developed the continuous gathering and processing mode which enables early tsunami detection and warning, particularly when the shelf is relatively wide. Consequently, for coastal areas with very thin coastal shelves, the radar systems may not be suitable for warning from local landslide induced tsunamis but only from remote seismic induced tsunamis.

Another tsunami detection method proposed is the NESTRAD (NEar-Space Tsunami RADar) concept, which consists of a real aperture radar accommodated inside a stationary stratospheric airship providing continuous monitoring of tsunamigenic oceanic trenches (Börner *et al.*, 2010). This method however apparently lacks again the capability for early warning when landslides occur at narrow shelves. According to these authors, a TEWS based on such system for the whole Mediterranean Sea would require 4 stationary airships.

Finally, a novel acoustic method has been proposed by Prof. Boris Katsnelson of Haifa University (pers. comm.) for detection of tsunami waves, based on a low frequency acoustic transmitter and a receiver array located at the edge of the coastal shelves. However, the sound noise generated by such systems was been assessed to be potentially dangerous to marine mammals and further investigation/development was presently ceased.

In conclusion, it is the author opinion that a combination of a HF radar system (WERA) and an array of submerged sea level stations released when a strong earthquake is encountered would provide a redundant solution for early warning of local earthquake induced landslide tsunami.

Preliminary field and GIS-based assessment of tsunami hazard on Cyprus

Jay S. Noller [1], Z. Zomeni [2] and I. Panayides [2]

[1] *Oregon State University, USA*
[2] *Cyprus Geological Survey*

Abstract

Cyprus has a long history of tsunami activity, as noted in written, archaeological and geological records. Records compiled thus far show that Cyprus experienced at least a moderate tsunami on average once every 30 years over the past two thousand years. Nearly all of the coastal sites display one or more of the geological/geomorphological indicators of past tsunami activity. We interpret these records to indicate that every part of the Cypriot shore has at one time been inundated by a tsunami. With that assumption in mind, GIS was used to create inundation maps based on coastal topography and hazard maps based on population density.

Introduction

The shallow earthquakes off the coast of Cyprus are accommodated often enough by seismogenic sea waves, more widely known as tsunamis. Kelletat and Schellmann (2001) were the first to identify the tsunamogenic depositional nature of large blocks and foraminifera-rich bimodal sand-gravel deposits on the coasts of Cyprus. More recent studies have mapped imbricate tsunami blocks and other features suggesting that seismic waves have reached almost the entire Cyprus coast (Noller *et al.*, 2005). Dated tsunamites off the coast of Caesarea in Israel correlating closely in age with the Thera eruption of 1630 -1550 B.C., provide concrete evidence for the past occurrence of tsunamis in the whole eastern Mediterranean (Goodman-Tchernov *et al.*, 2009). Similarly, the A.D. 365 western Crete earthquake destroyed Alexandria and killed thousands. With no doubt, these two events must have also affected Cyprus.

Much of the tsunami evidence comes from historical accounts dating back to Greek scriptures but also recent writings. Ogerius Panis and Marchisius Scriba, wrote in AD 1294 about a tsunami event in Lemesos and Pafos which is believed to have taken place in May AD 1222 (Rohricht, 1882):

> ... at Cyprus, the sea was lifted up by the shock and rushed inland; the sea in places opened up in huge masses of water big as mountains and surged inland, razing buildings to the ground and filling villages with fish ... Baffa (Pafos), they say, suffered most ... the harbor dried up and then the town was submerged by the sea ... the town and its castle were completely ruined and its inhabitants wiped out.

This account leaves no doubt about the occurrence of a tsunami for the May AD 1222 event. Archaeologists, historians but mainly seismologists and geomorphologists have often tried to collect and evaluate these past events. Nevertheless, it was not the scope of this study to provide

a new tsunami catalogue for Cyprus but to provide a map of areas at risk of inundation and identify populations and land uses which are vulnerable in the risk areas.

Regional geological setting

The tectonic framework of the Eastern Mediterranean and Middle East region is dominated by the collision of the Arabian and African plates with the Eurasian plate (McKenzie, 1970) and more specifically the northward subduction of the African plate along parts of the Hellenic and Cyprus arcs (Figure 1). In the vicinity of the Cyprus arc, the African plate penetrates below the locally oceanic Mediterranean crust (Makris, 1983) in the western part of the arc, in the proximity of Anaximander and Florence continental crust Seamounts and this is evident from the deep earthquakes in this region (Ambraseys, 1992a,b,c; Ambraseys and Adams, 1992). The Cyprus arc becomes more of a collision boundary in its central part where the Eratosthenes seamount, a continental crust microplate, and the Cyprus Island are undergoing intensive shallow deformation. In the eastern part, there is a wide zone of wrench faulting (Ben-Avraham *et al.*, 1995) in the vicinity of the Latakia ridge which extends all the way to the Syrian coast. On land, the Troodos ophiolite (Troodos Terrane) is the main orographic feature of the island containing all components of an ophiolitic sequence, an ultramafic core, a diabase sheeted dyke complex, a volcanic sequence of mostly basaltic pillow lava flows and topped with iron and manganese rich hydrothermal sediments. The allochthonous Mamonia Terraneis juxtaposed on the southern part of the island and the Keryneia Terrane on the north. The base of the Circum - Troodos sedimentary succession is marked by clays and sandstones, extensively exposed in western Cyprus, and topped with pelagic chalks and cherts indicating slow emergence of Cyprus as an island in the Miocene. The deposition of gypsiferous marls dates to the Messinian Salinity Crisis of the Mediterranean and the Pliocene marls the subsequent flooding and shallow sea formation. The Quaternary uplift of the island has formed thick and extensive fanglomerates on the early Pleistocene foothills of the Troodos ophiolitic mountains. Prominent and extensive marine and alluvial terraces span the whole Pleistocene.

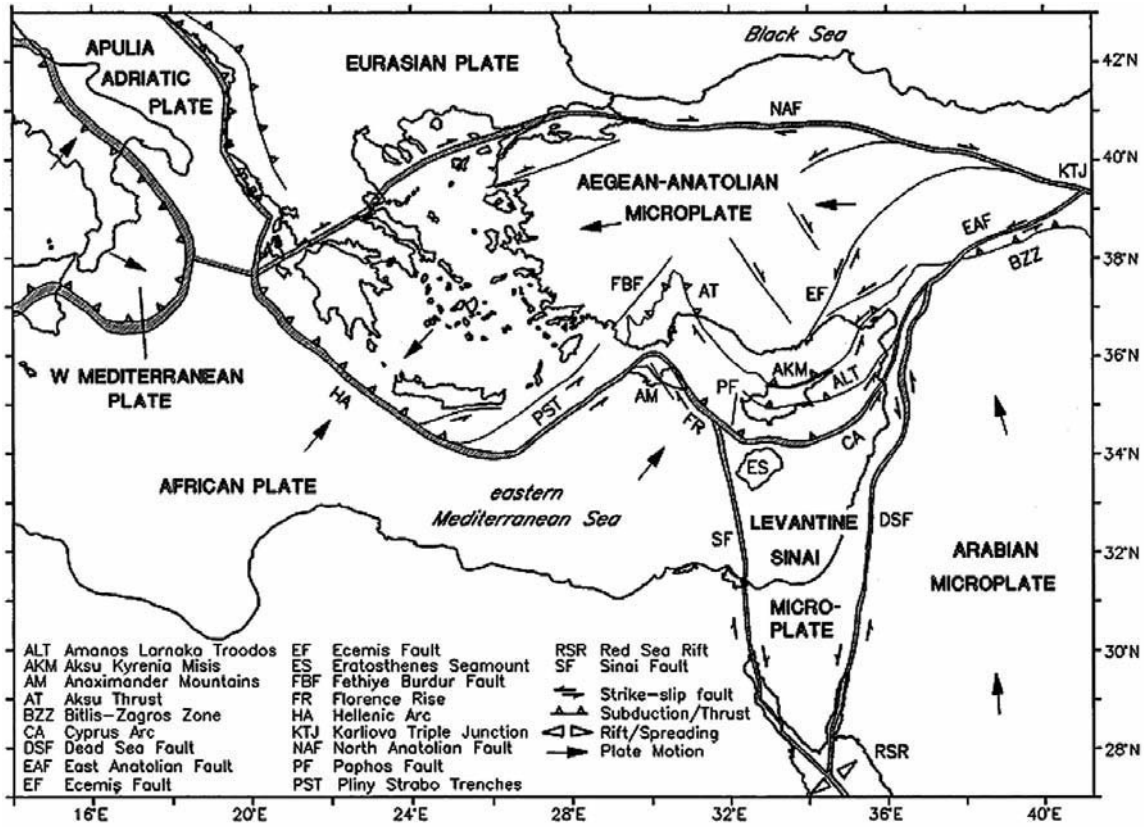

Figure 1. Tectonic setting of the Eastern Mediterranean showing the inferred location of the present-day Cyprus Arc (Aksu *et al.*, 2005).

METHODOLOGY

Reports of tsunami features presented here are the result of coordinated field and office study. This study applied geomorphological methods of field work, involving vehicle and foot travel to reach remote parts of the island. Field work was conducted between September 2003 and June 2004, with a short visit to field sites during the first week of February 2005, shortly after the tsunami event in Indonesia. Much of the coastal zone of Cyprus was studied in reconnaissance fashion, that is, areas accessible by 4WD vehicle and foot or within a short distance of a road (ca. 500 m). All of the major capes were inspected in detail, and many parts of the shorelines between these major landforms were inspected.

Geographic Information System (GIS) software (ArcGIS™, ESRI) and digital data were used to plan, compile and analyze the tsunami feature data. Data used during our analyses include topography and bathymetry, coastline, streams, roads, built-up areas, and satellite imagery (LandSat ETM and QuickBird). The DEM was clipped onshore at 1,500 m from the shoreline, and the bathymetry was clipped at several hundred kilometers distance. The onshore portion of the DEM was contoured at 5 meter intervals.

RESULTS

The tsunami record on Cyprus comes from several sources, involving the disciplines of history, archaeology, geomorphology, soil science and geology. In the past some past strong earthquakes were associated with tsunami waves, the most important of them in 92BC, 551AD, 1034, 1068, 1202, 1222, 1303, 1546 and 1759 (Fokaefs and Papadopoulos, 2007). More recently, the earthquakes of 18 June 1949 and 10 September 1953 were reported to have caused small local tsunamis.

A recent computer simulation of the 1222 AD event (Yolsal *et al.*, 2007), models a 7.0-7.5 magnitude earthquake with an epicenter off the southwest coast of the island, a focal depth of 15 km, a 3m co-seismic displacement along a 50 km long fault. The propagation of the wave was generated using non-linear shallow water theory and produced results of wave height and arrival times for the whole eastern Mediterranean coast including the coasts of Cyprus. With an initial wave of about 1 meter at sea, tsunami waves reach the Cyprus coast in less than a minute and vary in height from 30 cm at Cape Akamas to 190 cmat the Pafos Airport. It also becomes evident from Yolsal's results that maximum wave heights occur at the capes, a phenomenon being verified with field work. An impressive 82 cm high wave reaches Alexandria in Egypt in approximately 71 minutes. Historical accounts do mention the castle at Pafos collapsing and the earthquake causing damage in Alexandria (Ambraseys *et al.*, 1994). Similarly, an 8.0 magnitude earthquake off the southeast coast of Crete will result in a 90 cm high tsunami on the western Pafos coast and smaller waves elsewhere on the Cyprus coast.

Large rock blocks (20 to 50 ton) lifted up by tsunamis and deposited on higher ground constitute the most impressive form of tsunami evidence. Similar findings are recorded on the coasts of Cyprus (Figure 2). These blocks are found on Cape Kormakitis, Cape Plakoti on the coast of Gialousa, Cape Greco, Agia Napa, Pafos Airport, Kissonerga coast, Lara Bay and the whole Akamas peninsula north of Lara bay. Nearly all of the coastal sites visited displayed one or more of the indicators of tsunami activity and so the overall picture is one of many tsunamis having struck the shores of Cyprus. The presence of these large rock blocks is almost always out of geological context, located inland at a distance much further than any possible storm deposit and many times displaying inverse stratigraphy. Records of these "tsunami blocks" have been used worldwide as indicators of tsunami activity. Scicchitano *et al.* (2007) record tsunami blocks located 2-5 m amsl, reaching 182 t in weight, isolated or stacked and having a variety of features suggesting that they were dragged from the mid-sublittoral or mid-supralittoral zones. Rock block analysis was also conducted for modern tsunami events, the 2004 Indian Ocean and the 2009 South Pacific tsunamis which help identify and interpret palaeo-tsunami imprints on many coastal landscapes (Etienne *et al.*, 2011).

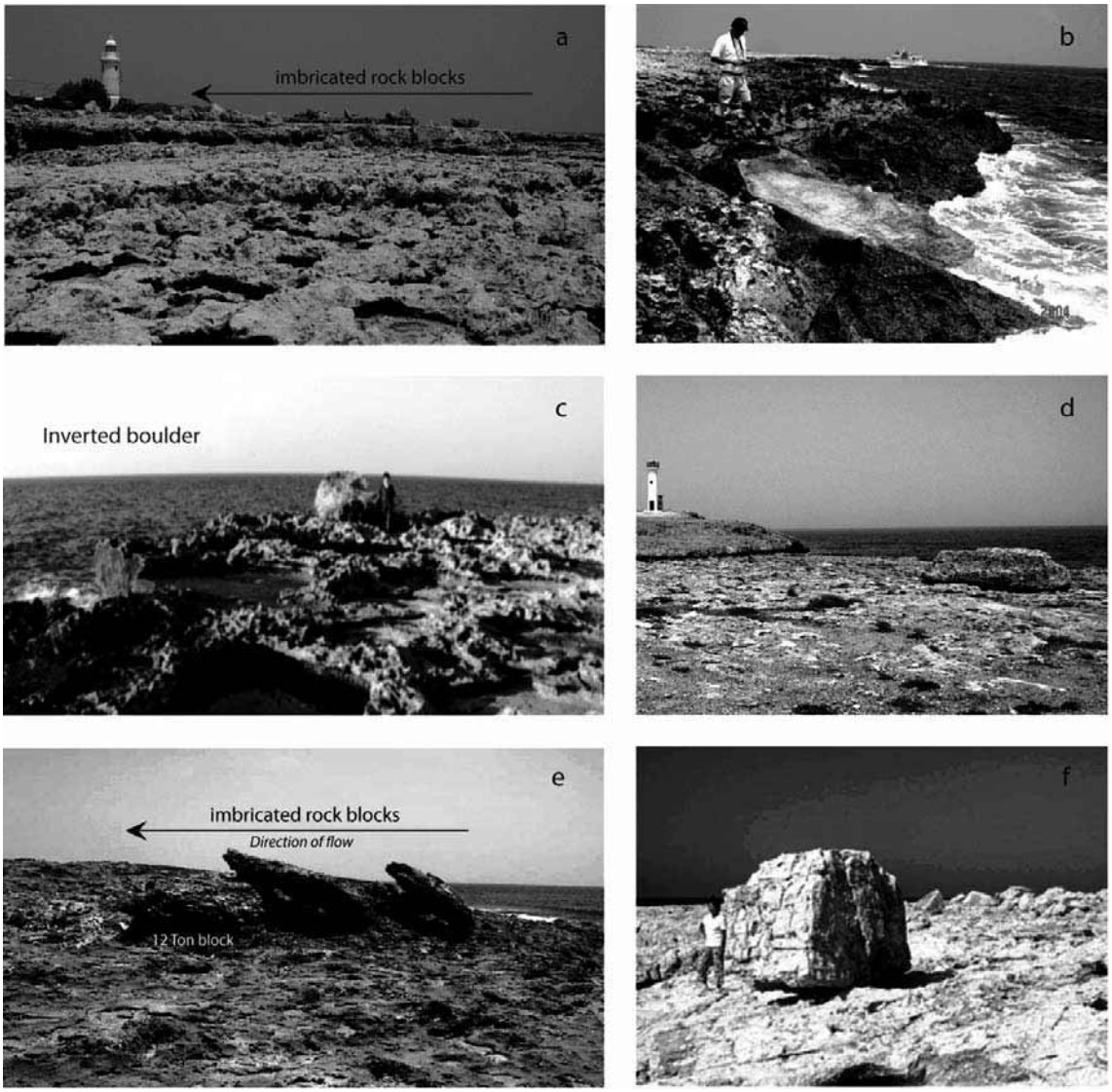

Figure 2.**a**. At Cape Greco a long line of imbricate boulders of Pleistocene calcarenite sandstone lies at an elevation of 4 m amsl. **b**. At Cape Greco, this recently dislodged boulder now lies about 15 minland. **c**. Area along shore at Davlos village is littered with large boulders. This boulder is inverted (top down). **d**. At Cape Plakoti in Karpasia, the area is scoured of soil and is littered with large boulders. The boulder in the photo lies 30 m inland **e**. View looking southwest at Cape Kormakiti. Here four 12 ton boulders originating from at or below sea level, with marine weathering features, are stacked in an imbricate manner. **f.** One of many examples of large tsunami blocks on the rocky coast of Akamas.

Cape Kormakitis presents the broadest expanse of landforms and deposits that are clearly developed by tsunamis. It is at this cape that one realizes storm waves cannot possibly explain the presence and orientation of large boulders (Figure 2e). The cape is barren of soil, with different sediment consisting of a bimodal particle size distribution of shelly sand and large boulders. Cape Plakoti in Karpasia is also largely barren of soil with some of the largest 'tsunami' boulders documented on Cyprus (Figure 2d). The distribution of marine-altered (e.g. bored by mollusks) artifacts of Neolithic and earlier age suggests deep-seated waves may have scoured the offshore region as well.

At Agia Napa the coastal aeolianite ridge hosts many large boulders at elevations approaching 8 m a.m.s.l. (Figure 3f). The aeolianite is scoured of soil, has a discontinuous shelly sand cover sediment, and has many marine-worn artifacts indicative of sudden marine deposition on the ridge top and inland. Many other areas of aeolianite all around the island have similar features, especially

the entire coast from Cape Greco to Cape Pyla (Figure 3e). Much of the southern escarpment of Akrotiri (Lemesos) is stripped of soil and sediment (Figure 3d). Large boulders on some terraces, up to 30 m elevation, are suggestive of tsunami deposits. However, mass wasting processes and differential erosion could have created these deposits and features here.

Figure 3. **a**. Tsunami boulders, many with marine features indicative of extraction from the sublittoral zone at Eremiti bay.**b**. View looking south at Cape Zephyros with infilled quarries and offshore rock blocks. **c**. Invertedtsunami blocks at Eremiti bay. **d**. View looking north at Akrotiri *Aetokremnos*. Area is scoured of soil and is littered with large boulders up to 30 m elevation.**e**. Tsunami boulders on the bare shoreface of Ormidhia, east of Larnaka. **f.** View looking east along the accordant ridges of aeolianite along the coast of Agia Napa. Baseball cap for scale in foreground. Cape Greco is in the background.

Cape Zephyros is blanketed by a cover of sediment consisting of shelly sand and rounded cobbles that locally infill archaeological (Roman?) quarries and cover red soil up to at least 5 meters above sea level (Figure 3b). Blocks offshore, shown on photograph of Figure 3b could have been displaced by tsunamis. Cape Geronisos displays an excellent example of the impact of tsunamis on soil distribution. Near the coastline soil is stripped off the surface. Further inland, soil appears locally in deep, protected pits in the underlying calcarenite, and lichens are present on many rocks. Several hundred meters inland the soil and vegetation are thick, and lichens are large in size and

cover nearly all exposed rock surfaces. Large boulders are present in at least two bars, one inland of the other, suggesting two phases of deposition or possibly two tsunami events.

Eremiti Bay, well documented by Kelletat and Schellmann (2001) and Whelan and Kelletat (2002), hosts impressive deposits of imbricate boulders, boulder bars, stripped soil boulder-armoured soil, lag gravels and other features. The evidence here strongly indicates a tsunami with a 15 m run-up (Figure 4).

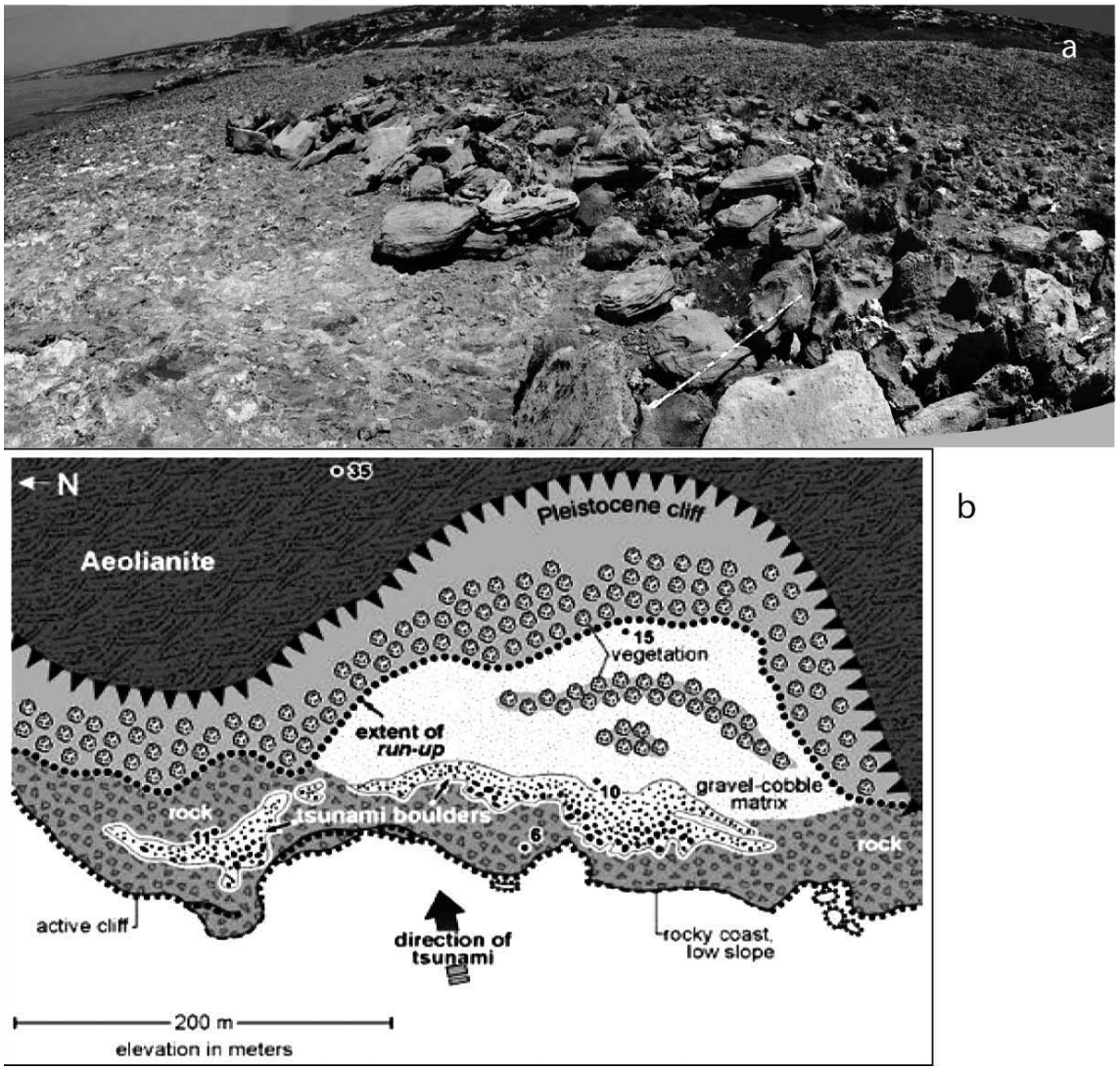

Figure 4 **a**.Eremiti Bay hosts an excellent display of tsunami deposits. **b**. Graphical representation of the deposits by Kelletat and Schellmann (2001).

Summary of field observations

Tsunami impact well explains the diverse, distributed nature of landscape features in the coastal zone of Cyprus (Figure 5). In general, the coastal zone within 100 to 400 m of the shoreline presents one of the following features: (1) slopes barren of soil; (2) a discontinuous, thin cover of sediment consisting of a bimodal particle size distribution of shelly sand and large boulders; (3) oriented large boulders tens of meters from shoreline; (4) particles showing marine indications such as vermetid borings, coralline algae deposits, pitting, and marine erosional landforms. Although compelling, other agencies of surficial processes could be responsible for many of the

features documented herein, including wind erosion, soil erosion, human activities, very-large storms, tectonism, mass wasting, river action and so forth. Only with concentrated efforts, such as a drilling program in estuarine environments, will tsunamis be more firmly established and dated.

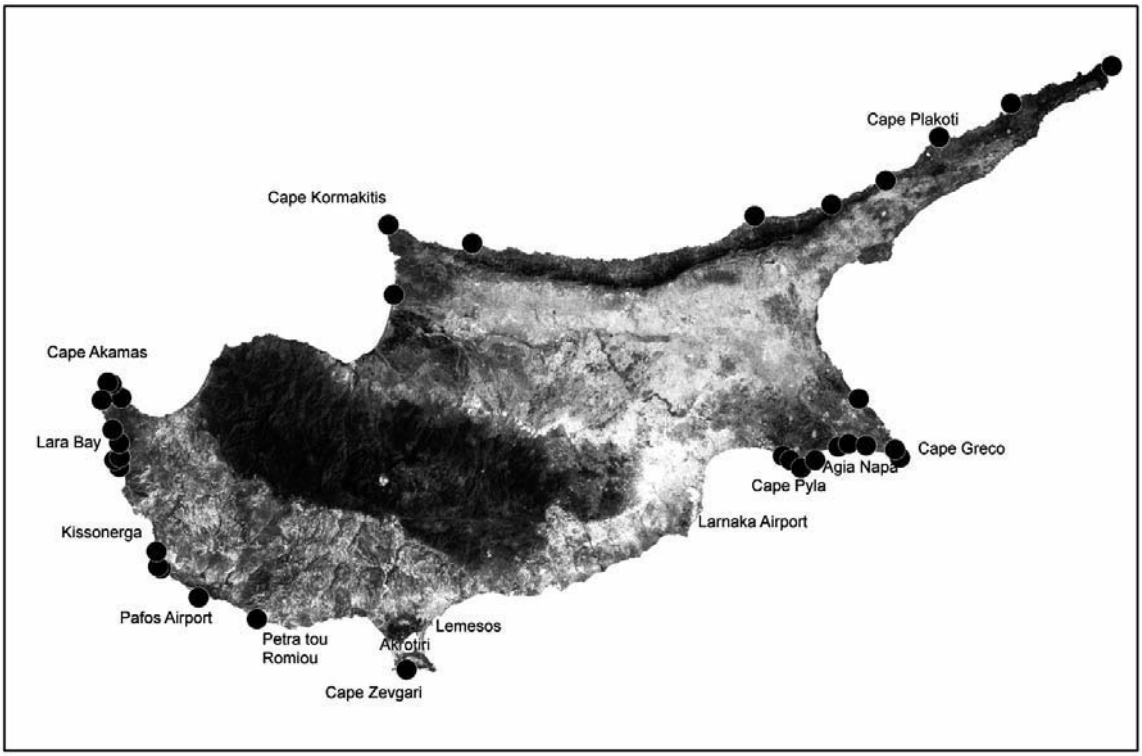

Figure 5. Landsat image of Cyprus with locations mentioned in text, showing distribution of geomorphological features indicating or suggesting tsunami processes.

Analysis of field results

Tsunamis were one of the many natural hazards that occurred in the ancient world and were recognized by early writers as extraordinary phenomena. Because of the work of Ambraseys (1962) *et al.*, there exists a rich bibliography of a literary record relating to tsunamis in the Eastern Mediterranean. Most recorded tsunamis struck within hours the ports and coastal population centers of Cyprus, Syria and Egypt, where most original written materials are found. With respect to the geological evidence of tsunamis on Cyprus, such as boulder deposits, the dates of Whelan and Kelletat (2002) and Kelletat (2002) cluster into four periods. There is an apparent coincidence inseveral of the timing of historical tsunamis with that of the geologically determined events.

Tsunami risk

Microzonation mapping is a key part of multidisciplinary assessment of the impact of natural hazards to population. Tsunami hazard becomes important because six of the seven densely populated areas on the island are on the coast and supporting one major economic sector of Cyprus, that of tourism. Large and important infrastructure is located almost entirely within a few meters from the coast, such as power plants, airports, water desalinization plants and oil refineries. Tsunami hazard maps produced here are a first approximation of the areas at risk, and relative caution should be taken.

A classified land use map was developed showing six classes of occupancy. The land use map was developed in ArcGIS™ using 2003 Quickbird™ images (having 60 cm pixel size) set as basis for drafting boundaries. Occupancy is based on the estimated number of persons per unit area and

duration of occupancy of the area in a zone 1,500 m from the coast. For example, the land use areas with high-rise apartments, house the most people per map unit area and have the highest rate of occupancy. To estimate the population at risk to tsunamis we calculated the area affected by tsunamis and then determined the minimum number of people affected by such an event. We then chose the 5 m contour as a first approximate distance of tsunami penetration, and used it to clip, that is select, only the portion of built-up areas within this zone. Areas of each land use class were tallied and estimated land use densities were calculated (Table 1).

Table 1. Matrix of land use zones and estimated population densities.*

Land Use Zone	Population Density (per m^2)	Category
1-2 story buildings	0.0048	1
2 or more story buildings (town centers)	0.025	2
Hotels and tourist apartments	0.0143	3
Summer homes and summer recreation areas (water parks, restaurants)	0.012	4
Industry (industrial zones, fish farms)	0.0055	5
Infrastructure (ports, airports, power stations, petroleum depots)	0.01	6

Vulnerability was high in lowland coastal areas on all the coastal cities including the western and eastern beaches of Akrotiri peninsula. The eastern beach, known as Ladies Mile beach is the busiest beach in the summer with thousands of bathers. Assuming a wave run-up of 5m, the coastal population at risk is about 200,000. At the time of an event the actual population at risk depends on the source of the tsunami and the variable affect it will have on the whole coastline, i.e. an earthquake with a southwestern epicenter will not create a tsunami wave on Keryneia coast and an earthquake in the southeast will similarly not affect Kormakitis Cape. Lemesos and Larnaka display the highest vulnerability because the historical centers of these cities are located right on the coastline. Other towns like Pafos and Agia Napa respond differently to the hazard since their tourist centers are on the coast but the town centers on higher ground, in Pafos being well over the 5 m assumed tsunami run-up. Figure 6 shows an example from the town of Larnaka.

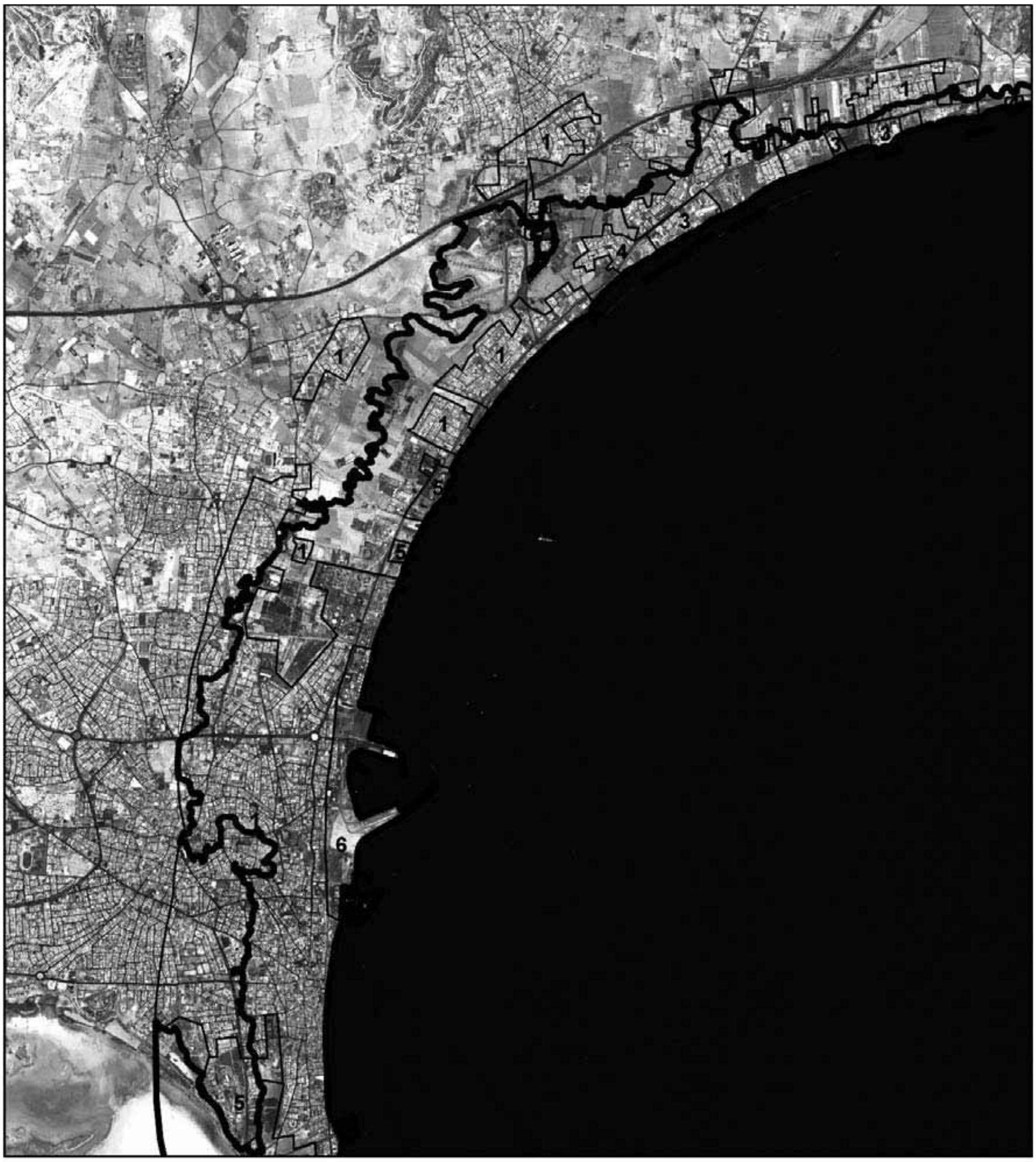

Figure 6. Map superimposed on satellite image showing areas of risk to tsunami damage in the town of Larnaka. The thick black line is the 5 m elevation line and marks the upper limit of local tsunami penetration, especially along channels and inland of low-sloping beaches. Boxed areas within a 1,500 m buffer from the coast show land use categories (marked from 1 to 6 according to Table 1).

Summary and conclusions

Cyprus has a long history of tsunami activity, as noted in written, archaeological and geological records. We interpret these records to indicate that every part of the Cypriot shore has been inundated by tsunamis. As such, the record compiled thus far shows that Cyprus experienced at least a moderate tsunami on average once per 30 years over the past two thousand years. Some, of these events must have been damaging in nature. Similarly, probabilistic studies by Fokaefs and Papadopoulos (2007) with updated tsunami catalogues estimate an average recurrence of 30, 120 and 375 years for moderate, strong and very strong tsunami occurrence.

Given the importance of the coastal resource in Cyprus' economy it is vital that the vulnerability of the tourism, commerce and residential sectors to tsunami be fully characterized so that mitigation measures may be designed and implemented. The very next step towards realizing this would be an intensive field study involving drilling of coastal sediments and dating of tsunami features to characterize the hazard of tsunamis. Attention to the historical and archaeological records is obviously an important part of establishing the ages of these events.

Acknowledgements: this work was funded partly by the Fulbright Commission and partly by the Cyprus Geological Survey.

Seabed mapping for marine geohazard assessment on the Ionian Calabrian margin

S. Ceramicola [1], M. Coste [1], P. Planinsek [1], D. Praeg [1], E. Forlin [1], A. Cova [1], S. Migeon [2], F. Fannucci [3], S. Critelli [4] and E. Colizza [3]

[1] Istituto Nazionale di Oceanografia e di Geofisica Sperimentale, Trieste, Italy
[2] Université de Nice-Sophia Antipolis UMR6526; GéoAzur Observatoire Océanologique, Villefranche/mer, France
[3] University of Trieste, Department of Geosciences, Italy
[4] University of Calabria, Cosenza, Italy

Abstract

The principle mass wasting processes occurring on the slopes of the Ionian Calabrian margin have been investigated using shallow geophysical datasets (swath bathymetry and subbottom profiles). Four types of mass wasting phenomena are recognized: 1) mass transport complexes (MTCs) within intra-slope basins, 2) slide scars on open slopes, 3) possible gravity sliding, 4) canyon headwall failures. Evidence of recurrent failures (types 1 & 2) suggests a history of mass wasting, triggered by seismo-tectonic activity and/or slope steepening due to the rapid late Pleistocene uplift of Calabria. Geohazard assessment suggests mass wasting processes of types 1, 2 and 3 as most likely to represent a geological risk for deep sea areas, whereas type 4 may constitute a marine geohazard for the adjacent coastal areas.

Introduction

Mass wasting processes on continental margins have strong relevance both for geohazards in coastal areas and for the emplacement and monitoring of deep sea infrastructures. The seabed dynamics of the Ionian Calabrian Margin (ICM) is currently examined in the context of the Italian project MAGIC (Marine Geohazard along the Italian Coasts). The objective of the project is the definition of seabed elements that may be associated with geological risks for adjacent coastal areas.

The ICM is a tectonically-active margin, the structures of which reflect two main processes: frontal compression and fore-arc extension during the SE advance of the Calabrian accretionary prism since the late Miocene (Sartori, 2003); and rapid uplift (up to 1 mm/yr) of onshore and shallow shelf areas since the mid-Pleistocene (Westaway, 1993). These processes are reflected in different tectonic in settings around the ICM, which is characterized by a relatively narrow continental shelf (max. width 7 km) above a slope that extends across depths of 150-2,000 m and varies in morphology from north to south. In the north, a broad, irregular slope is dominated by ridges and

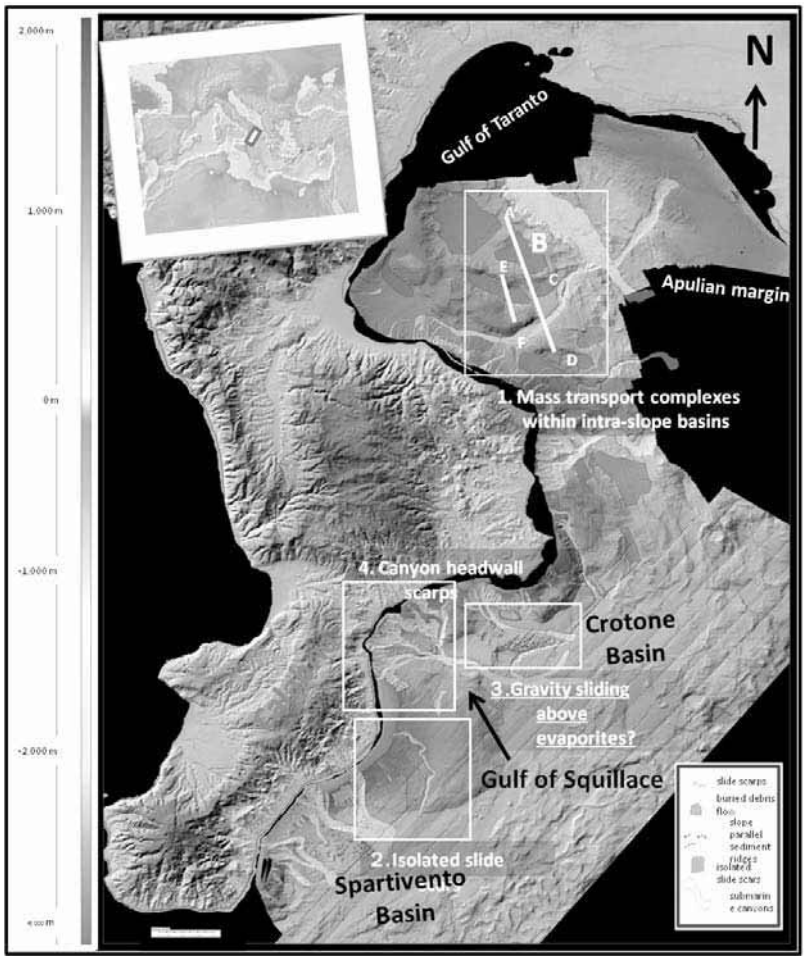

Fig. 1. Map of study area.

[see original colour illustration in Annex at end of volume]

intervening basins that are offshore extensions of the southern Apennine fold-and-thrust belt; in the south, a narrower slope descends steeply towards the deep-water Crotone and Spartivento fore-arc basins.

Here we present the results of mapping major features of mass wasting on the slopes of the ICM, and considering possible trigger mechanisms. The study is based on an integrated analysis of multibeam morpho-bathymetric data and Chirp subbottom profiles, acquired by OGS between 2005-2009, which together allow the recognition of four main types of mass wasting phenomena along the slopes of the ICM. These phenomena may represent a geohazard for the coastal as well as for the deep sea areas.

Results: different types of submarine mass wasting

1. Mass transport complexes (MTCs) within intra-slope basins

MTCs are identified on the northern ICM in association with the intra-slope ridges and basins: seabed imagery shows the slopes of the ridges to be marked by numerous small arcuate scarps (up to 10 m high) that record widespread failures; Chirp profiles show the intervening basins to contain unstratified bodies indicative of debris flows buried beneath stratified sediments. Multiple debris flows are observed in several basins, indicating recurrent episodes of failure, which may be linked to seismo-tectonic activity on the faults controlling these thrust-fold structures.

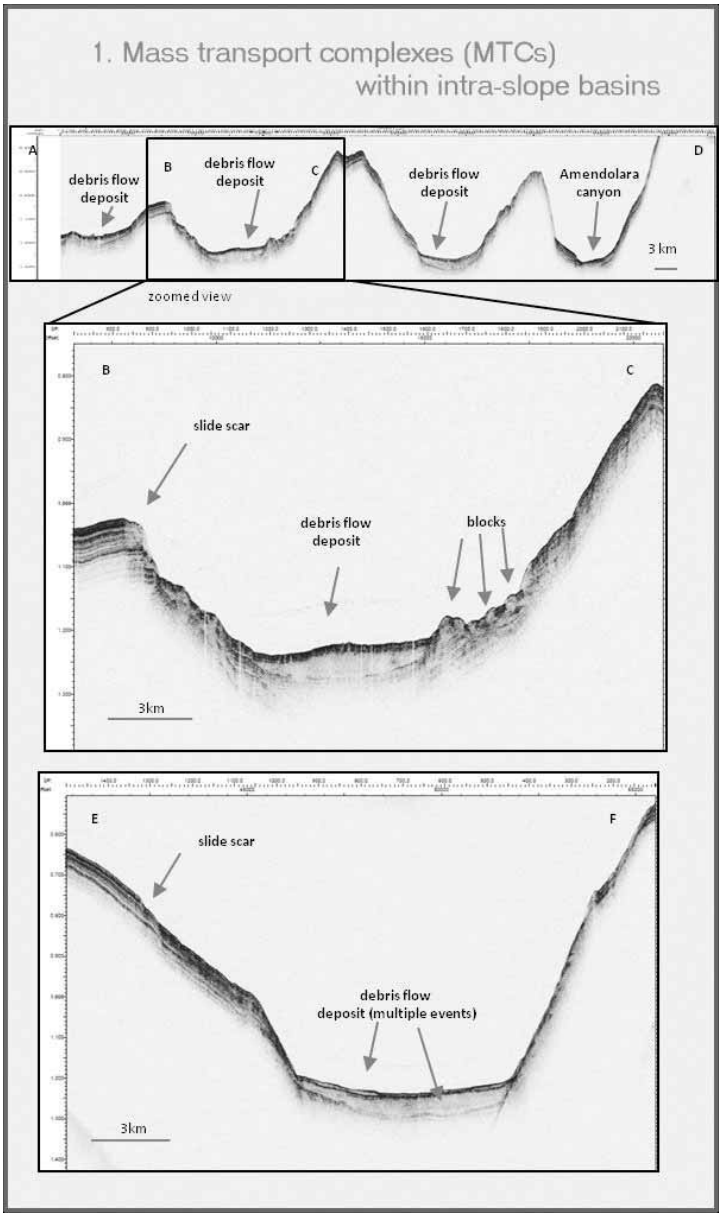

Fig. 2. Mass transport complexes (MTCs) within intra-slope basins. Location of sub-bottom profiles in Fig 1.

2. Slide scars on open slopes

Slide scars are recognized at seabed along the relatively steep southern Calabrian slope. Detailed studies are being undertaken of the Assi slide, which is bounded by arcuate seabed scarps up to 40 m high, defining a seabed feature ca. 7 km wide and 18 km long that extends from water depths of ca. 300 m to the base of the slope at 1,400 m; to the east, it is in part bounded by a canyon (the Assi canyon). The slide includes upper and lower headwall scarps; Chirp profiles suggest the lower scarp cuts unstratified deposits below the upper scarp, so that the lower slide is younger. Scarps and deposits of earlier failures are also observed in the subsurface beneath and beyond the Assi slide. The volume of material that has detached from the slope below the upper scarp is estimated to be of the order of at least 2 km^3. The seabed and buried slides are assumed to be linked to deposits within the adjacent deep-water basin that are yet to be identified. Analyses of the dynamics of the failure as well as a simulation of the possible tsunami that might have generated are in progress. Recurrent failure of the southern Calabrian slope may reflect seismic activity, as well as steepening of the slope in response to the late Pleistocene uplift of Calabria.

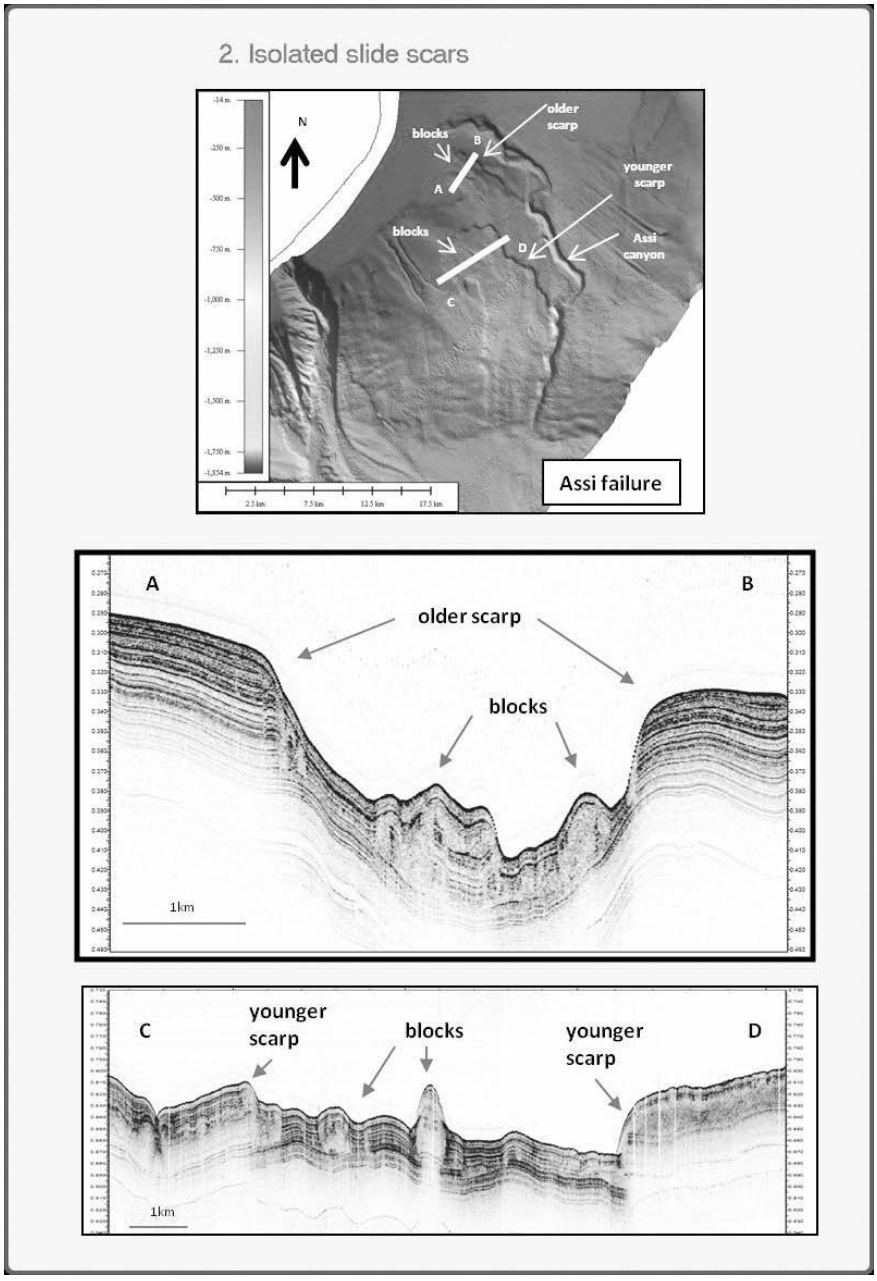

Fig. 3. Slide scars on open slopes. Location of swath bathymetry and sub-bottom profiles in Fig 1.

[see original colour illustration in Annex at end of volume]

3. Gravity sliding

In two areas of the southern Calabrian slope, elongate seabed features oriented subparallel to contours are observed, forming ridges and depressions up to 50 m high, 4 km long and 0.5-1 km in wavelength. Chirp profiles show stratified sediments with anti- and syn-forms; in one area these ridges have been previously observed on seismic profiles and shown to be associated with subsurface diapiric structures, interpreted to record upward movement of Messinian evaporites (Rossi and Sartori, 1981). Mud volcanoes also occur in the area, but are circular features of unstratified sediments distinct from the elongate ridges. We speculate that the seabed ridges may record a form of downslope sediment sliding above Messinian evaporites, resulting in features analogous to the cobblestone topography of the outer Calabrian Arc; such a process may have been enhanced by late Pleistocene slope steepening.

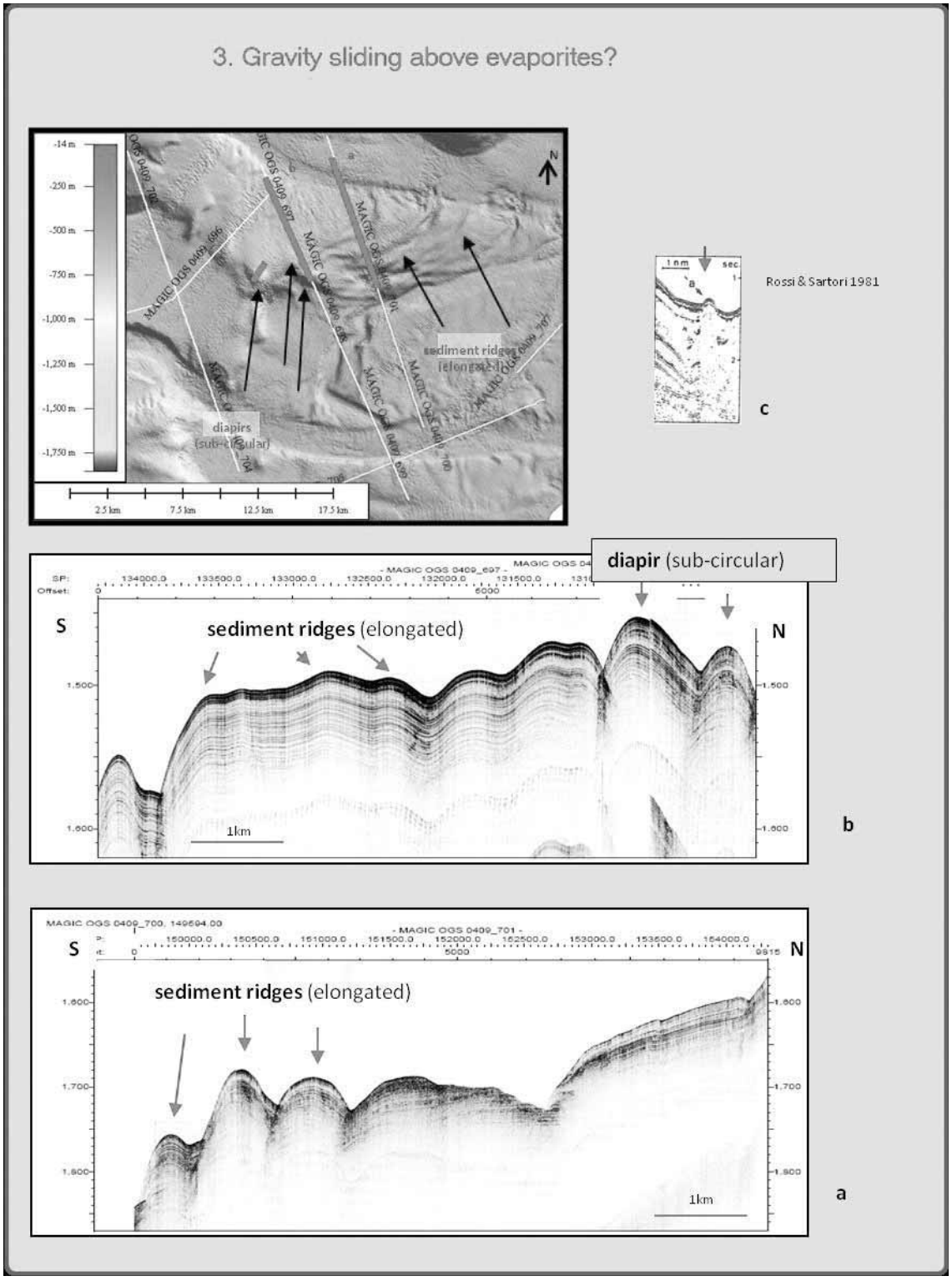

Fig. 4. Location of swath bathymetry and sub-bottom profiles in Fig 1.

[see original colour illustration in Annex at end of volume]

4 . Canyon headwall retrogressive activity

The ICM is incised by more than 40 canyons and intervening channels, which vary in their morphology from north to south along the margin. Many canyons, predominantly in the southern

areas, are characterized by a complex headwall geometry (cauliflower shape) that contains or is bordered by numerous small scarps, up to 50 m high. Water depths of canyon headwalls range from 10 m (i.e. Cirò) and 100 m. The presence of these scarps at seabed is interpreted to be consistent with retrogressive activity of the canyons.

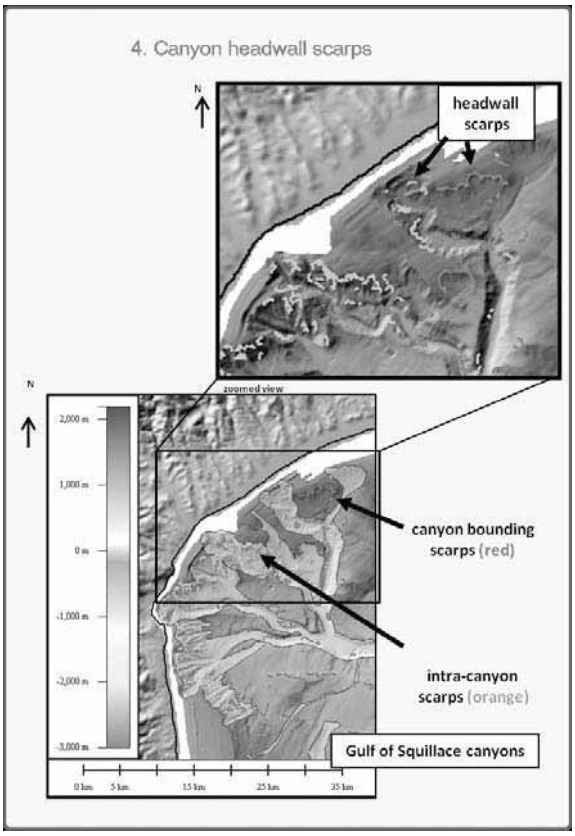

Fig. 5. Canyon headwall scarps. Location of swath bathymetry and sub-bottom profiles in Fig 1.

[see original colour illustration in Annex at end of volume]

Conclusions

• The Ionian Calabrian Margin is characterized by several different phenomena of submarine mass wasting that represent potential geohazards for adjacent coastal areas.

• Evidence of multiple failure events suggests a long and ongoing history of downslope sediment transfer around the margin.

• In the intra-slope basins of the northern part of the ICM, stacked failure deposits may reflect recurrent seismo-tectonic activity along faults underlying thrust-fold structures.

• On the steeper slopes of the southern part of the ICM, in addition to seismic activity, late Pleistocene differential uplift is a potential driver for recurrent slides and possible features of gravity sliding above evaporites.

• Canyon headwalls are associated with failures indicative of retrogressive landward growth; the main geological risk identified along the margin is due to activity within those close to the coastline in the southern area. Isolated failures, gravity sliding and MTCs may represent hazards for deep sea infrastructures.

Acknowledgements: the seabed dynamics of the Ionian Calabrian Margin (ICM) are being examined in the context of the project MAGIC (Marine Geohazard along the Italian Coasts, 2008-2012), led by Prof. Francesco L. Chiocci, University Sapienza, Rome and funded by the Italian

Civil Protection. The data in the study area have been acquired during several geophysical campaigns of the OGS Explora: in 2005 for the HERMES project (Hotspot Ecosystems Research in the Margins of European Seas) and in 2009 for MAGIC, PI Silvia Ceramicola (OGS); the 2005 MESC project (Morphology and Evolution of the submarine canyon in the Ionian margin of Calabria), PI Ester Colizza, (University of Trieste); the 2005 WGDT project (Morphology and Architecture of the Western Portions of the Gulf of Taranto: a Study of Submarine Instability in a Tectonically Active Margin), PI Salvatore Critelli (University of Calabria).

Distribution and causes of recent submarine landslides along the Ligurian margin (northwestern Mediterranean) inferred from very high-resolution data: some insights into geohazard assessment

Sébastien Migeon [1], Antonio Cattaneo [2], Virginie Hassoun [1], Christophe Larroque [3], Nicola Corradi [4], Francesco Fanucci [5], Bernard Mercier de Lepinay [3], Françoise Sage [1] and Christian Gorini [6]

[1] UMR GéoAzur, Université de Nice-Sophia Antipolis, CNRS, OCA, Villefranche/mer, France
[2] IFREMER, GM-LES, Plouzané, France
[3] UMR GéoAzur, Université de Nice-Sophia Antipolis, CNRS, OCA, Valbonne, France
[4] University of Genova, Dip.Te.Ris, Genova, Italy
[5] University of Trieste, DiGe, Italy
[6] UMR ISTeP, Université Pierre et Marie Curie, Paris, France

Abstract

Based on new multibeam bathymetric data, seismic-reflection profiles and side-scan sonar images, a great number of submarine failures of various types and sizes was identified along the northern margin of the Ligurian Basin and characterized with four distinct end-members concerning their location on the margin, sedimentary processes and possible triggering mechanisms. High sedimentation rates related to hyperpycnal flows, faults and earthquake activity, presence of a mobile evaporite layer at depth, together with sea-level fluctuations are the main factors invoked to explain the distribution and sizes of the different types of failure. Both small-scale failures (volume about 10^6-10^7 m^3) triggering at shallow water depth and large-scale failures (volume greater than 10^9 m^3) triggering on the lower continental slope are able to generate tsunami waves 5-50 km around the location of the source of the failures and could thus represent a high hazard potential.

Keywords: Ligurian margin, Submarine landslides, Geohazard.

Introduction

Submarine failures have been described for many years in a wide range of climatic and tectonic settings, from glacial to subequatorial areas (Huhnerbach and Masson, 2004; Imbo *et al.*, 2003; Laberg *et al.*, 2000; McAdoo *et al.*, 2000; Piper *et al.*, 1997) and along both passive and active margins (Collot *et al.*, 2001; Goldfinger *et al.*, 2000; Moore *et al.*, 1989; Urgeles *et al.*, 1997). Triggering factors can be thus as different as sea-level fluctuations, earthquakes, high-sediment supply leading to under-consolidated deposits and overloading, fluid charging and more (Sultan *et al.*, 2004). The recognition and discrimination between several factors is of major importance

for the geohazard assessment in a given area. In the Mediterranean Sea, steep and narrow margins tectonally active and fed by small mountain-supplied rivers are highly affected by severe landsliding processes. The Ligurian Basin experienced recently such phenomena: in 1979, a failure (8×10^6 m^3) occurred in shallow-water depth during infilling operations seaward of the Nice airport (Gennesseaux *et al.*, 1980) and generated three successive waves, 2-3 m height, that broke along the coastline between the cities of Nice and Antibes. Three historical tsunamis are also well-known in the area (1564, 1817, 1887 AD) and are closely related to historical earthquake events. Earthquakes could have been responsible for other tsunamogenic failures in the Ligurian Sea.

The present study focuses on the northern margin of the Ligurian Sea where a remarkable number of submarine failures of various sizes has been identified on the continental slope between the cities of Antibes (France) and Genova (Italy). To analyse their morphologies and distribution on the slope, and to identify their triggering mechanisms, a large dataset including Simrad EM300/EM2000 multibeam bathymetry, seismic-reflection profiles, echo-sounder profiles, deep-tow side-scan sonar and cores was acquired in the frame of the MALISAR cruises (2006, 2007, 2008, 2009). Our goal is to present the characters of the continental slope to outline the main features of the submarine failures and factors controlling their distribution. These results will help improving our ability to predict such geohazards along the Ligurian Margin.

Methods

Seafloor shaping and failure morphology have been studied using multibeam bathymetry collected using a hull-mounted Simrad EM300 and an EM2000 mounted on an AUV (Autonomous Underwater Vehicle). Volumes of slided deposits have been estimated using a DTM with a spatial resolution of 25 m. As the headwall scars were always well defined on bathymetric data, it was possible to calculate the volume of sediment missing in the scar area by firstly reconstructing a pre-slide seafloor topography and then subtracting the pre- and post-slided topographies using the Caraibes and GMT softwares.

Seafloor texture and micromorphology were investigated using side-scan sonar images and 3.5 kHz echo-sounder profiles collected using the deep-towed SAR (Système Acoustique Remorqué) system. The SAR is a side-scan sonar towed about 80-100 m above the seafloor, at an average speed of 1 ms^{-1} (2 knots). The system provides a 1,500 m wide swath of the seafloor with a spatial resolution of 25 cm, and 3.5 kHz profiles with a vertical resolution of about 80 cm.

The internal architecture of slope deposits, failure scars and mass-transport deposits have been studied using seismic-reflecting profiles of various resolution collected using a 300 m long 24-channels streamer and two mini-GI air gun (one 75/75 ci and one 40/40 ci), and a 450 m long 72-channels streamer and six mini-GI air gun (three 25/25 ci and three 15/15 ci).

Results

The integration of observations coming from both bathymetric data and seismic-reflection profiles allowed distinguishing several types of slope instabilities along the northern margin of the Ligurian Sea.

Type-1 failures are mainly superficial and reworked the first 30 to 90 m of deposits below the seafloor, representing volumes less than 10^8 m^3 on average. They are mainly located
(1) on the upper slope in the vicinity of the main feeding rivers, like the Var and Paillon rivers (Fig. 1); there, the slope gradient is 10 to 15° and about 150 landslides have been discriminated,
(2) on the walls of canyons eroding the slope where the seafloor slope angle exceeds 20°,
(3) on open slope environments, far from sediment supply and canyons but close to epicentral areas like the one of the 1887 earthquake, where the slope angle is about 5°. Whatever their location on the continental slope, the scars mainly exhibit an ellipsoidal or amphitheatre-like morphology. In few cases, scars are more complex, and consist in several coupled amphitheatre-like morphologies, as observed at the shelfbreak for the scar of the 1979 event. Each scar is continuing on the slope by a gully that evidences the erosive power of the failed mass remobilized in the scar. The gullies are more or less straight in the direction of the main slope angle in their downslope part, whereas they exhibit a low-sinuosity pattern in their upstream part. They are few hundred meters

to 5 km long. The gullies show a width comparable to that of the scars in the upper reach, then enlarge to 200-400 m and deepen to 40-80 m downslope. Several gullies gradually coalesce downslope, resulting in a single and larger gully. In some cases, several scars evidencing multiple failure events are observed at different locations along a single gully. The width and depth of each scar gradually increase downslope within the gully. In most cases, mass-transport deposits (MTD) are not found downstream from the scars, in the gullies, evidencing that the remobilized deposits are completely evacuated to the base of the slope. Few examples of well-developed MTD were identified where the slope angle decreases rapidly downstream from the scars, mainly at the transition between the canyon walls and the canyon floors.

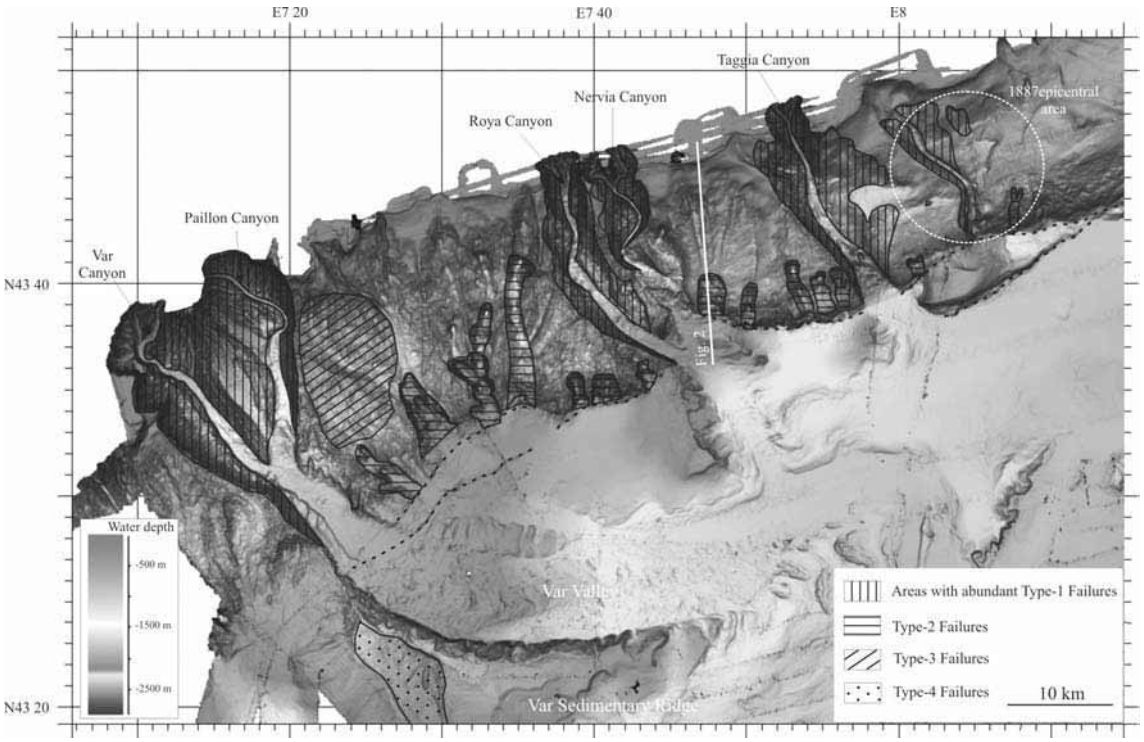

Figure 1. Bathymetric map illustrating the distribution and sizes of the main types of failures (see text for explanation) along the western segment of the northern Ligurian Margin.

[see original colour illustration in Annex at end of volume]

Type-2 failures like the so-called "Cirque Marcel" are large scars affecting the base of the continental slope, between 1,700 and 2,200 m of water depth (Fig. 1), where the slope angle is less than 6°. Twelve failures of type 2 have been identified along the segment of the slope comprised between the cities of Nice (France) and Imperia (Italy). They are 2 to 4 km wide, 4 to 6 km long. Seismic-reflection profiles suggest these large failure-related scars affected in some cases the whole Plio-Quaternary deposits, 300 to 500 m thick, and the slip plans correlate with the top of the Messinian conglomerates (Fig. 2). Volumes of remobilized deposits decrease gradually eastward from 2-2.6 x 10^9 m^3 to less than 25 x 10^6 m^3. In plan view, they exhibit a complex amphitheatre-like morphology resulting from several nested scars. In the Cirque Marcel, from the top to the base, four scars are present with heights ranging from 100 to 300 m. They are separated by flat areas 1 to 2 km wide. These areas exhibit themselves evidences of erosional processes, revealed by the presence of smaller-scale scars and scours. Upslope from the scars, the slope exhibits either an erosion related to the presence of large gullies or the presence of irregular morphologies indicative of sediment mobilization. In the area offshore Nice to Imperia, the base of the slope is also strongly affected by faults (Fig. 2). The deepest ones broke and shifted vertically the Messinian conglomerates, but the penetration of the seismic-reflection profiles did not allow the observation

of these faults at greater depth. Vertical displacements could be in the order of 300-400 m. The shallowest faults affect the Plio-Quaternary deposits and the present-day seafloor, revealing a recent activity. Vertical displacements along these faults are less than 50 m.

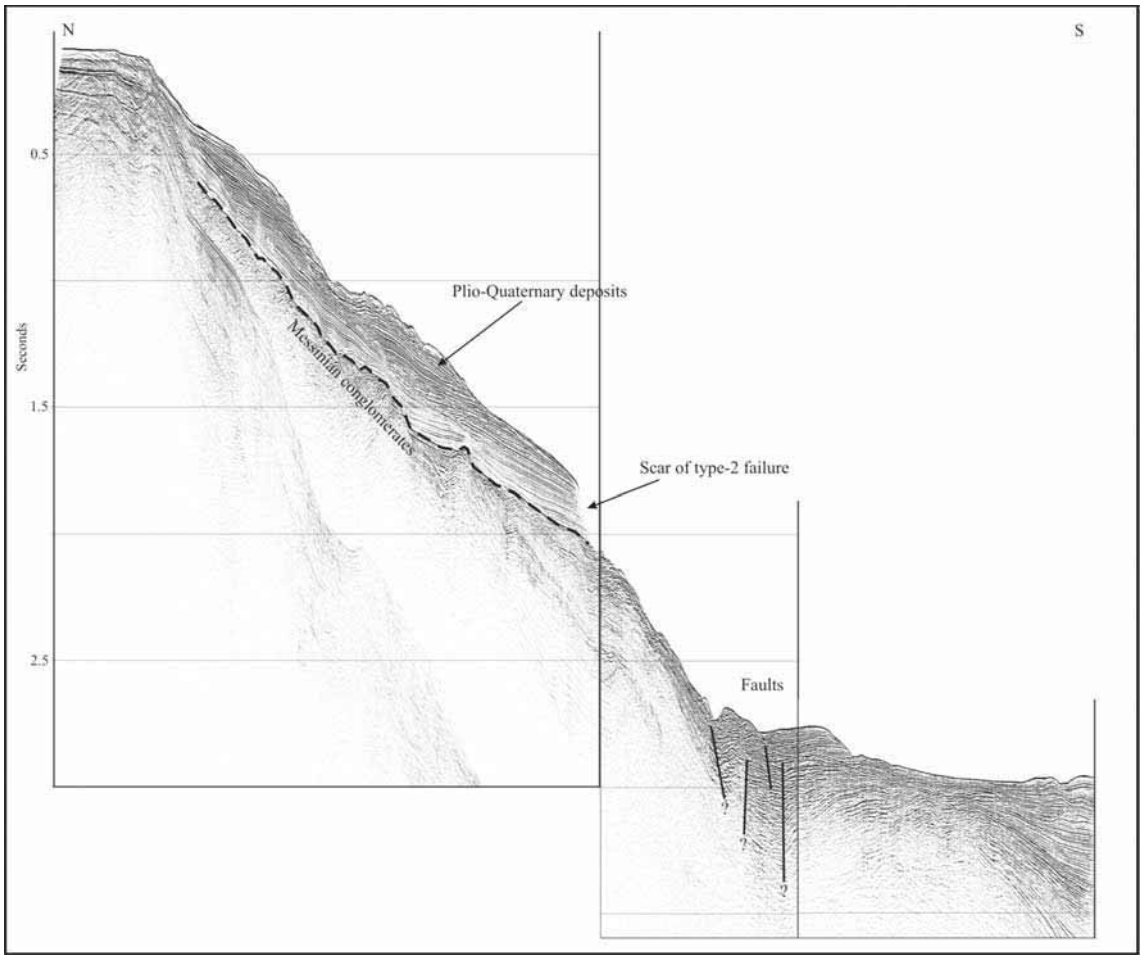

Figure 2. High-resolution seismic-reflection profile crossing the scar of a failure of type 2. Note the whole Plio-Quaternary deposits have been affected by the failure, the slip plan correlating with the top of the Messinian conglomerates. Profile location shown in Figure 1.

Type-3 failures correspond to escarpments up to 60 m in height and 5 km long. They are mainly developed in the segment of the slope comprised between Cap Ferrat (France) and the Principality of Monaco (Fig. 1), where the slope angle is about 7-8°. These escarpments are more or less oriented parallel to the isobaths (Fig. 3). They are not linear but exhibit a more indented pattern resulting from the presence of successive amphitheatre-like morphologies of various sizes along a single escarpment. From the seismic-reflection profiles, these escarpments developed in an area where the continental slope deposits are the thickest due to the concave profile of the Messinian surface that generated a slope basin-like structure (Fig. 3). The escarpments are probably only the superficial evidence of the intense destabilization affecting that sector of the continental slope as they correlate at depth with shear plans inducing slight rotational movements of the first 50-100 m of deposits below the seafloor (Fig. 3). All these features could be interpreted as a slow lateral spreading deformation related to creeping.

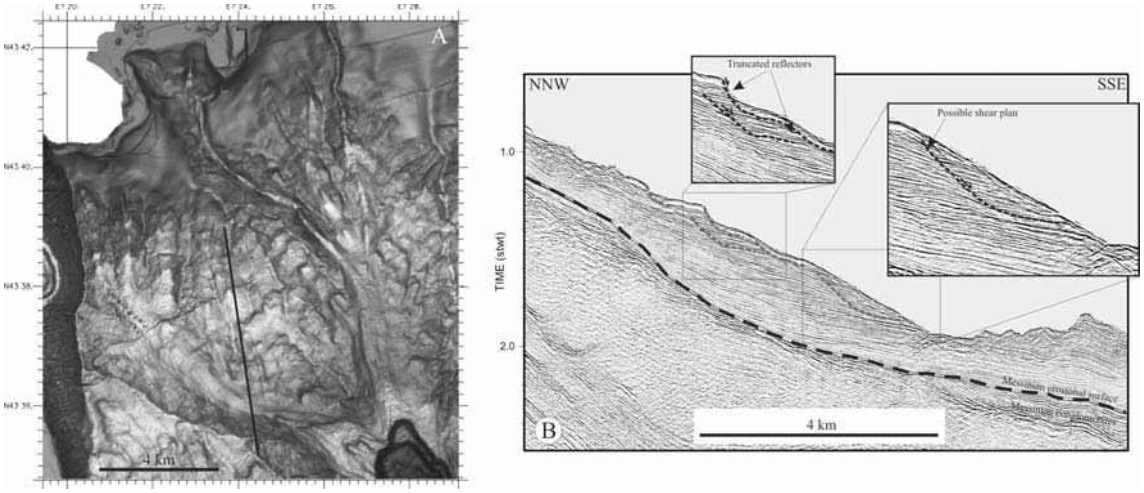

Figure 3. Shaded bathymetric map (A) and high-resolution seismic-reflection profile (B) illustrating the failures of type 3 located offshore Monaco.

[see original colour illustration in Annex at end of volume]

Type-4 failures are the largest ones. They consist of a scar 200-300 m height, located on the upper part of the continental slope off the Genova area and on the Var Ridge (Fig. 1), followed at its base by a MTD about 20 to 200 m thick. In most cases, MTD extends about 10 km downstream from the scar and 5 km laterally. The internal architecture of the MTD partly exhibits the original organisation of deposits evidenced by the presence of well-layered moderate-amplitude reflections. The change of reflection dip along the whole MTD suggests a slight rotational movement of the remobilized deposits. The best example of such failures is the Portofino Slide, located at the eastern limit of the bathymetric survey.

DISCUSSION

The specific location of each failure type along the Ligurian Margin could give hints on the controlling factors influencing their formation, including the structure of the margin, the presence of faults, the areas of highest sedimentation rate or of highest earthquake activity.

Effect of sedimentation rates and hyperpycnal currents. Sedimentation rates are high in the surrounding areas of the mouths of the main feeding rivers like the Var, the Paillon, the Roya, the Taggia. There, sediment deposition mainly results from direct supply by hyperpycnal flows, inducing sedimentation rates as high as 1-2 m/100 yrs (Mulder *et al.*, 2001a). Due to angles of 10-15°, failures of type 1 are thought to occur regularly but small volumes of deposits are involved for each episode of failure. Hyperpycnal flows are also involved in the gradual erosion of the base of the canyon walls, leading to local oversteepening responsible for the triggering of failures of type 1.

Effect of faulting processes and earthquakes. Areas of the highest earthquake activity mostly correlate with the presence of the faults affecting the base of the continental slope in the western part of the Ligurian Margin. Although the origin of these faults is still poorly known, they are associated with important vertical displacements that could correlate with earthquakes. The generation of deep decollement surfaces and the triggering of the huge type-2 failures are thought to result from the combination between earthquake events, rapid slip movements along faults and cyclic loading affecting sediment cover.

A recurrent earthquake activity is also well-known to favour the creep even along gentle slope as it may reduce the critical shear strength of sediment. The cumulative effect of low-magnitude events is thus prone to initiate or facilitate the slow deformation related to failures of type 3.

The strongest earthquake events are also probably responsible for the direct and rapid triggering of landslides through processes of shacking and loading, as for failures of type 1 identified in the epicentral area of the 1887 event, or for the large failures of type 4. It is possible that the presence of layers or surfaces of contrasting lithology provide preferential weak planes where failure may originate.

Effect of sea-level fluctuation. On passive margins, the triggering of large-scale failures is quite often closely connected to phases of sea-level rising or lowering (Garziglia *et al.*, 2008; Maslin *et al.*, 2005). In the absence of direct dating, it can be only speculated that failures of type 4 affecting segment about 5 km long of the upper slope, at water depth ranging from 50 to 100 m, could have been triggered by the latest phases of sea-level lowering during the Last Glacial Maximum, or sea-level rising during the early Holocene.

Effect of the presence of a mobile evaporite layer. The location of large failures of Type 2 at the base of the continental slope also correlates with the transition between the Messinian conglomerates deposited on the continental slope and the Messinian evaporites deposited in the basin. All over the Mediterranean Sea, the Messinian evaporites are considered as a mobile layer that affects the overlying Plio-Quaternary succession in numerous ways (Mascle *et al.*, 2006). The slow downslope movement of the evaporite layer to the deep part of the Ligurian basin resulted in a decompression at depth and the formation of normal syn-sedimentary faults that could have triggered failures of Type 2.

Insights into geohazard assessment. Along the Ligurian margin, factors promoting submarine landslides act at specific locations. Correlation between the types of factors and the types of submarine failures could help discriminate between areas that are prone to low-to-high geohazards.

Type-1 failure scars correlate with areas of both high slope angle and direct high particle-supply by hyperpycnal flows. These two factors promote high-frequency failures, with volumes classically lower than 10^8 m^3. As these two factors are closely connected with river discharges and seafloor erosion, these failures are restricted to small areas localized in the vicinity of river mouths and on the inner flanks of canyons. As a consequence, they do not strongly impact the morphology and the erosion of the whole margin. However, from the example of the 1979 Nice-airport landslide, such failures are able to generate a tsunami despite their small volume because they occur at shallow water depth (Ioualalen *et al.*, 2010). Type-1 failures could thus have a low-to-high hazard potential, not necessarily linked to regional seismicity as in the case of the 1979 Nice event (Dan *et al.*, 2007).

Type-2 failure scars correlate with the uplifting area of the margin and with the presence of main fault planes where earthquakes are also mainly concentrated. We infer that these three factors are responsible for the triggering of low-to-mid frequency failures with large volumes, ranging from 1 to 3 km^3. These failures affect the base of the continental slope along the whole western Ligurian margin (between E7°20' and E8°10' in latitude) and thus have a strong impact on its evolution in time and space. Despite their location at water depth ranging from 1,700 to 2,000 m, such failures could potentially generate a tsunami several metres high when assuming the worst possible conditions in the tsunami-simulation scenario, i.e. remobilisation of large volume (> 10^9 m^3) during a single failure event (Ioualalen *et al.*, 2010). As these failures occurred about 20 km offshore from the coastline, the tsunami would be able to propagate within the whole western Ligurian basin and to affect the coastline in an area 20-50 km long around the location of the failure (Ioualalen *et al.*, 2010). Type-2 failures could thus have a high hazard potential, especially in thesingle event scenario.

Type-4 failure scars are always associated to the presence of clearly identified MTDs and seem to represent single main failure-events in which large volumes (> 10^9 m^3) of deposits could have been remobilized. The VSR slide is very deep (> 2,000 m water depth), possibly associated with the presence of deep faults, and, owing to its depth, unlikely to have generated significant tsunami waves. The two large submarine landslides identified in the eastern Ligurian margin (Finale and Portofino Slides) represent probably large events. Because they triggered at 250-700 m water depth, these failures could have been responsible for significant tsunami waves but more detailed investigations are still needed to assess their potential geohazard.

Conclusions

Recent cruises conducted in the frame of the MALISAR project provided a huge dataset including multibeam bathymetry, Chirp echo-sounder profiles, 24- and 72-channels seismic-reflection profiles, deep-tow side-scan sonar and cores along the whole northern margin of the Ligurian Basin, from Antibes (France) to Genova (Italy). Analysis revealed that the margin is affected by a remarkable number of slope instabilities of different morphologies and sizes. The superficial failures of type 1 are mainly located in the areas surrounding the mouth of mountain-supplied rivers like the Var and the Paillonrivers, and along the walls of canyons eroding the continental slope. High sedimentation rates related to hyperpycnal flows and gradual basal erosion of canyon walls are thought to be the main trigger mechanism of such failures. Huge scars corresponding to failures of type 2 are located at the base of the continental slope, between 1,700 and 2,200 m of water depth. Their location correlates with the presence of faults that are also the areas of highest earthquake activity. Failures of type 3 correspond to escarpments 5 km long that are the superficial evidence of the slow creeping of the whole Plio-Quaternary deposits of some portions of the continental slope. The cumulative effect of low-magnitude earthquake events on continental-slope deposits should be responsible for that gradual and slow spreading deformation. Large-scale scars and MTDs from failures of type 4 are located on the upper part of the continental slope and affected segment of the margins several kilometres long at a water depth ranging from 50 to 100 m. Triggering factors for such landslides could be the strongest earthquakes as well as sea-level fluctuations related to the Last Glacial Maximum or the early Holocene.

Investigating submarine landslides through geotechnical testing, *in situ* monitoring and numerical modelling: case of the Nice slope

N. Sultan, S. Garziglia and S. Stegmann

Ifremer, Département Géosciences Marines, Plouzané, France

Abstract

We present here an integrated approach for landslide investigation based on multi-disciplinary studies including (i) observation and description, (ii) *in situ* measurements, (iii) monitoring and numerical modelling to improve submarine landslides and geohazards assessment. This approach was used during the last decade to evaluate the main factors controlling sediment instabilities on the Nice shelf edge/upper slope. Based on a comprehensive data base it was finally possible i) to show the start-up of a progressive failure mechanism in the study area and ii) to suggest the possibility of a direct or indirect role of pore water in the observed deformation features and signatures.

Keywords: piezocone, sediment properties, shear zone, submarine landslides, weak clays.

Introduction

"If a landslide comes as a surprise to the eyewitnesses, it would be more accurate to say that the observers failed to detect the phenomena which preceded the slide".

Since 1950, this eloquent statement of Karl von Terzaghi has endured as a milestone in the continuing efforts to learn how to detect and interpret the precursory signs of landslides in order to react and prevent the threats they pose to human lives, and high societal values. In that sense, Leroueil *et al.* (1996) proposed the "Geotechnical Characterisation of Slope Movements" as a multi-disciplinary approach to answer the need of assembling complex phenomena into a framework that can be used to maximise the knowledge of the causes of landslides. This involves the geomorphological and geotechnical characteristics but also the understanding of sediment mechanics. As a consequence landslide hazard and risk assessment requires the characterisation of three basic elements of the process: (1) the mechanical behaviour of materials, (2) the movement types, (3) the movement stages and their respective controlling laws and parameters. From the pre-failure, the failure, the post-failure to the reactivation stage, each phase of the process depends on a set of predisposing, triggering (or aggravating) and revealing factors that are in turn control variables of the movement types (Vaunat and Leroueil, 2000). Such interdependencies of the mechanics of landslide processes imply a progressive attainment based, as indicated by Picarelli (2009), "on site investigations and monitoring, and on laboratory testing and physical modelling interpreted in the light of theoretical considerations". The present paper aims to outline the observations, measurements and technological developments made by IFREMER in the context

of submarine landslide studies. Special emphasis is put on the integrated efforts made to unravel the diverse mechanisms controlling slope sediment failure on the Mediterranean continental margin offshore of Nice, France.

The Nice continental slope: a natural laboratory for geohazards studies

Located in the tectonically complex and seismically active area of the Ligurian Basin, Western Mediterranean, the continental margin of Nice shows a morphology primarily shaped by the system of the river Var system (Figure 1). Unravelling the processes of turbidity currents and deposition of this small sandy system has been the subject of intensive studies since the sixties (see Mas *et al.*, 2010; Jorry *et al.*, 2011 and references therein). Early works of Gennesseaux (1962) led to the idea that portions of the seafloor in between the very narrow shelf (0.2 to 2 km wide) and steep continental slope (>10°) offshore Nice were instable. His hypothesis was unfortunately confirmed on 16 October 1979, when a slope failure event took place, involving a portion of the Var River delta and runaway fill of the Nice airport extension under construction (Gennesseaux *et al.*, 1980). This event that initially involved ~10 million m^3 of fill materials and Quaternary silty-clays, sands and pebbles, resulted in a tsunami, the loss of human lives and significant damage such as the breaking of submarine cables across the distal part of the Var turbidite system (Gennesseaux *et al.*, 1980; Seed *et al.*, 1988; Savoye and Piper, 1991; Mulder *et al.*, 1997; Dan *et al.*, 2007). The burst of interest triggered by the so-called "1979 event", led to a suite of geological, geophysical and geotechnical investigations that resulted in the compilation of regional landslide hazard maps (Cochonat *et al.*, 1993; Mulder, 1992; Mulder *et al.*, 1994; 1997; Habib, 1994; Klaucke and Cochonat, 1999; Klaucke *et al.*, 2000).

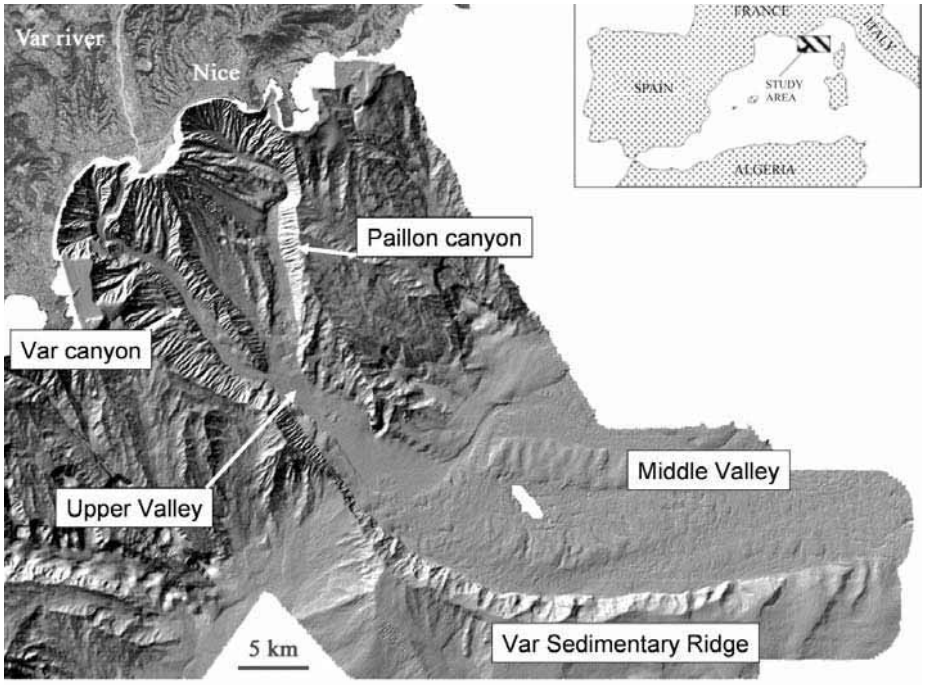

Figure 1. Bathymetry of the Nice continental slope (modified from Leynaud and Sultan, 2010).

By pointing out a great number and variability of factors controlling slope failure processes (seismicity, groundwater charging, presence of weak sedimentary layers, high-sediment accumulation rates and anthropogenic modification of the shores), these investigations emphasised that the continental slope offshore Nice provides an ideal natural laboratory for studying the interrelationships between depositional settings, triggering mechanisms and failure types. Several

studies have provided insight into the understanding of the failure mechanism and sediment mechanics on the shelf edge/upper slope area offshore Nice (e.g. Dan *et al.*, 2007; Leynaud and Sultan, 2010; Sultan *et al.*, 2010; Stegmann *et al.*, 2011). It is the scope of the following work to highlight how these recent, integrated studies afforded by technological developments allowed to overcome limitations inherent to underwater investigations, bringing the assessment of submarine slope failure hazard to a level comparable to that achieved on land.

The use of multi-disciplinary integrated approach

The use of integrated approaches based on multi-disciplinary studies ranging from observation and description to measurements, monitoring and modelling is today essential to improve submarine landslides and geohazards assessment. For the Nice study site, an integrated approach was developed and used during the last decade in four stages:

Stage 1: **Identification** / location of deformation and destabilisation phenomena based on geophysical data;

Stage 2: **Evaluation** of suspected processes by (*in situ*) measurements and monitoring of relevant parameter (e.g. sediment strength, pore pressure)

Stage 3: **Prediction** of different failure scenarii (from causes to consequences) based on numerical modelling;

Stage 4: **Integration** of the first three stages in order to concentrate geophysical investigations on restricted areas, to optimize (in terms of time and space) measurements and monitoring and ultimately to converge towards the most probable deformation scenario.

Ifremer developed three advanced geotechnical tools: CPTu piezocone, sonic piezocone and a modular piezometer system (details about those tools are given in the following paragraph). Those three tools provide essential capabilities for geohazard investigation, which overcome the descriptive approach and simplistic interpretations about triggering mechanisms of observed sediment deformations and submarine landslides.

Identification and location of deformation phenomena (Observing)

Indices of the effect of external factors on sediments and submarine slope stabilities can be detected from seafloor and sub-seafloor imagery. Figure 2 a summarizes bathymetric data from different oceanographic cruises in the last 30 years. The first swath bathymetric survey was performed in November 1979 after the 1979 failure (Pautot, 1981) based on a compilation of SeaBeam, EM1000 and EM300 multibeam sonars. In Figure 2 a, red broken lines indicate the uppermost identified landslides showing horseshoe-shaped headwall scars. Steps (or possible cracks) in the bathymetry are highlighted by light blue broken lines in Figure 2 a and are oriented perpendicular to the slope contours.
Figure 2 b shows an example (profile CH43001) of the available 3.5 kHz profiles from the study area. Piezocone sites PFM11-S3 and PFM11-S4 locations are projected on the CH43001 profile. Three important features can be identified from the seismic profile in Figure 2 c: 1- two seismic reflections between traces 3700 and 3900 converge in a landward direction with a pinch out at 14 m water depth, 2- at that position, a small morphological step imprints the seafloor; its formation seems to be related with these internal surfaces and 3- the presence of possible gas plume or fresh water flow in the water column above the seafloor terrace and associated major seismic reflection. The gas wipeouts observed on the seismic section are blanking the underlying stratigraphic organisation.
Those seafloor (multibeam bathymetry) and subseafloor (seismic profiles) data show the presence of several areas subject to potential weak areas which may be prone to failure: seismic reflections (discontinuities, slip planes?), landslide scars and presence of morphological steps, gas plume, gas wipeouts and cracks. In order to go further in the interpretation of the observed signatures, it is essential to complement observations by ground truth and mainly *in situ* geotechnical measurements and monitoring.

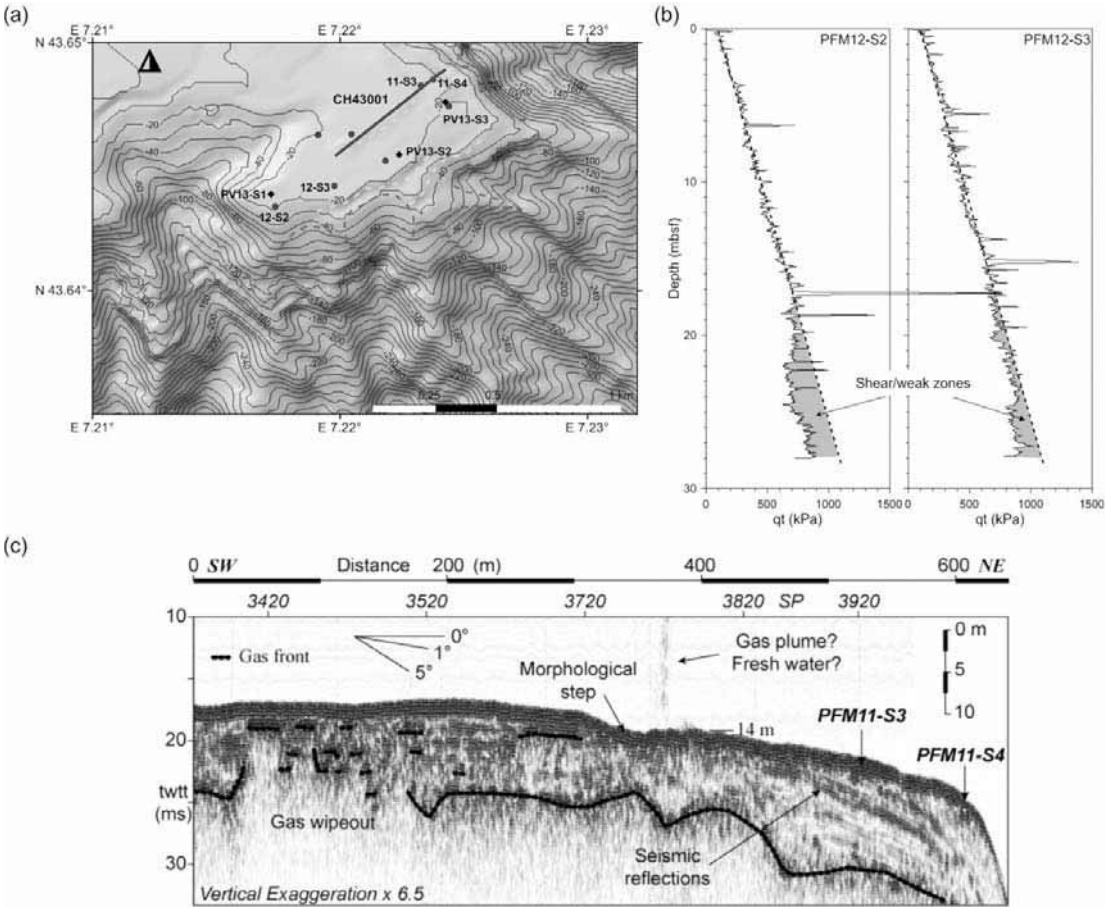

Figure 2. Nice slope study area: a) location of CH43001 Chirp sonar profile and available *in situ* geotechnical measurements projected on a shaded bathymetric map. Red dashed polylines indicate the uppermost headwall scarps of landslides and light blue dashed polylines highlight seafloor morphological steps. b) CPTu *in situ* data: corrected tip resistance (qt) versus depth from PFM12-S2 and PFM12-S3. For the 2 sites, shaded areas indicate significant decrease of the corrected tip resistance (possible shear zones). c) Profile CH43001 showing the presence of two seismic discontinuities to the NE at the edge of the slope. The two discontinuities fit with small seafloor morphological steps and correspond to a decrease in the sediment resistance measured at PFM11-S3 and PFM11-S4 (shear zones). A gas plume or fresh water flow can be observed in the water column above the morphological depression (trace: 3660-3670).

[see original colour illustration in Annex at end of volume]

Evaluation of suspected processes (Measuring)

Geotechnical data: from in situ measurements to laboratory testing

In situ measurements and monitoring were planned in order to complement indirect observations and to potentially detect i) the presence of sandy layers which are suspected to be the main conduits for fresh water circulation, ii) the presence of sensitive clay, which could be a direct consequence of the fresh water circulation and leaching phenomena, iii) the presence of *in situ* free gas and its potential effect on the degradation of the shear resistance of the surrounding sediments and iv) the presence of shear zones which is a direct indication of active shearing processes.

i) The presence of sandy permeable layers was already suspected thanks to available geophysical data. In order to calibrate geophysical data and to confirm the presence of sandy permeable layers, *in situ* geotechnical measurements were carried out in 2007 (Sultan *et al.*, 2008) using the Ifremer CPTu piezocone (called PENFELD). The Ifremer piezocone is designed to work at depths of up to 6,000 metres. It is equipped with a rod which penetrates the sediment to a maximum depth of 30 metres. The electric cone (10 cm^2) used gives a continuous measurement of the tip resistance

(qc), sleeve friction (fs) and excess pore pressure (Δu2) measured by means of a porous filter located immediately behind the cone (called U2 type cone). The Ifremer CPTu uses a hydrostatically compensated system where the cone load sensor is unaffected by the hydrostatic pressures leading to greater accuracy and sensitivity measurements in soft sediments (Andersen *et al.*, 2008). Sedimentary layers with low Δu2 values and high corrected cone resistance and friction are usually interpreted as an indicator of the presence of silty-sandy layers (e.g. Lunne *et al.*, 1997). Several sandy layers were detected in the non-failed sediments adjacent to the Nice/1979 failure (blue points in Figure 2 a - Sultan *et al.*, 2008). Tip resistance peaks shown in Figure 2 c correspond to some of the detected sandy layers. Shallow sandy layers were also recovered by coring (Dan *et al.*, 2007 and Stegmann *et al.*, 2011).

ii) Detection of sediments with high sensitivity is also possible using the CPTu piezocone. Indeed, low values of sleeve friction are often linked to the sensitivity of the clay. For the Nice study site, it was essential to determine the location of those sensitive clay layers in order to study the potential link between fresh water circulation, leaching and the sensitivity of clay layers. Dan *et al.* (2007) have used piezocone data acquired by industry along the coast and have shown a potential link between the depth of the 1979 slope failure and the presence of clay layers with high sensitivity. Additional work is in progress in order to determine the spatial distribution of clay layers with high sensitivity based on the CPTu data acquired in 2007 (Sultan *et al.*, 2008).

iii) Free gas partially saturating the sediment from the studied shelf was suspected from available geophysical data and detected by *in situ* sonic piezocone measurements. The used sonic piezocone is a technology improvement to the standard piezocone. The end of the classical piezocone coiled tubing holds two tips where the first contains a high-frequency compression wave source (1 MHz) and the second the receiver. The distance between receiver and source is equal to 0.07 m (more detail in Sultan *et al.*, 2007). As for the standard piezocone, the sonic piezocone is pushed into the sediment layers at a constant rate. A continuous measurement of the P wave velocity (Vp) and the attenuation is made. P wave velocities are very sensitive to free gas and decrease drastically with the increase of the degree of gas saturation.
Free gas may have an important impact on the clay shear strengths. Gas expansion and exsolution in clayey formations lead very often to the damage of host sediments. Figure 3 shows a sedimentary core acquired from the Nice shelf and where the presence of *in situ* dissolved and free gas led to

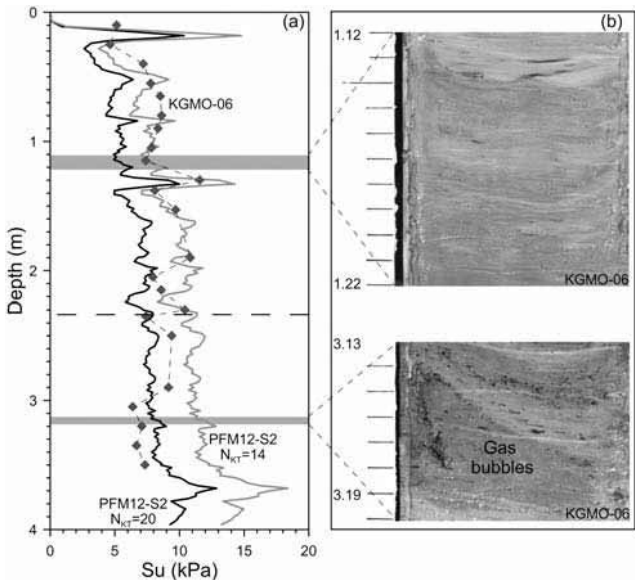

Figure 3. Free gas exsolution and expansion and degradation of the sediments' shear resistance: a) Undrained shear strength, Su, profiles derived from the piezocone test PFM12-S2 for empirical cone factor NKT of 14 and 20 compared with the Su values measured from laboratory vane shear tests. b) Photos of selected intervals from core KGMO-06 showing the vertical heterogeneity of the sediment. Note the disrupted sediment structures in the lower part of KGMO-06 and gas bubbles that exsolved during core retrieval.

[see original colour illustration in Annex at end of volume]

gas bubble growth and exsolution during cores recovery. This gas expansion has had a direct impact on the shear strength Su of the sediment as can be seen from Figure 3 a: the rate between the cone tip resistance (proportional to the *in situ* shear strength) and the shear strength measured on board after core recovery increased significantly (from 14 to 20) between the upper 2.30 m (no gas expansion) and the bottom of the core (gas expansion and sediment damage, see Figure 3 b).

iv) CPTu piezocone can be also used to detect shear zones along which upper mass sediments may move in a slope failure zone. Indeed, Leroueil *et al.* (1995) and Demers *et al.* (1999) demonstrated in zones of high shearing where the clay was remoulded that both the penetration tip resistance and the penetration pore pressure were low relative to the undisturbed clay at the same depth. This observation was confirmed by Mahmoud *et al.* (2000) showing that the CPTu can be used to identify softened zones within a marine clay deposit. For CPTu measurements carried out along the Nice shelf edge, the drop in cone resistance and friction was observed at several sites (Figure 2). The two examples presented in Figure 2 c show that the drop in cone resistance was observed between 18 and 28 m for PFM12-S2 and 17 and 28 m for PFM12-S3. Shear zones are normally considered as a clear indication of the presence of active shearing processes. However, shear strength degradation generated by *in situ* cyclic gas expansion and exsolution could be also another source of those weak zones.

In addition to the classical geotechnical laboratory tests needed to define the intrinsic sediment parameters, some advanced geotechnical laboratory tests are also essential to complement *in situ* geotechnical data. For instance, the use of advanced constitutive models needs a number of mechanical parameters that can be only determined from laboratory tests. Specifically, for the study area, it is essential to carry out long-term creeping tests in order to consider the strain softening behaviour of sensitive clay and its potential effect on slope instabilities.

In situ observing systems

In situ geotechnical measurements suggest the presence of several geohazard indices directly linked to fluid circulation: sandy layers as permeable conduits, high sensitivity due to freshwater sediment leaching, free gas expansion and exsolution directly linked to pore pressure and finally shear zones (or weak zones) that could be either the result of active shearing process or gas expansion and exsolution. Thus, pore pressure monitoring is the main missing key factor to study active processes occurring in the study site.

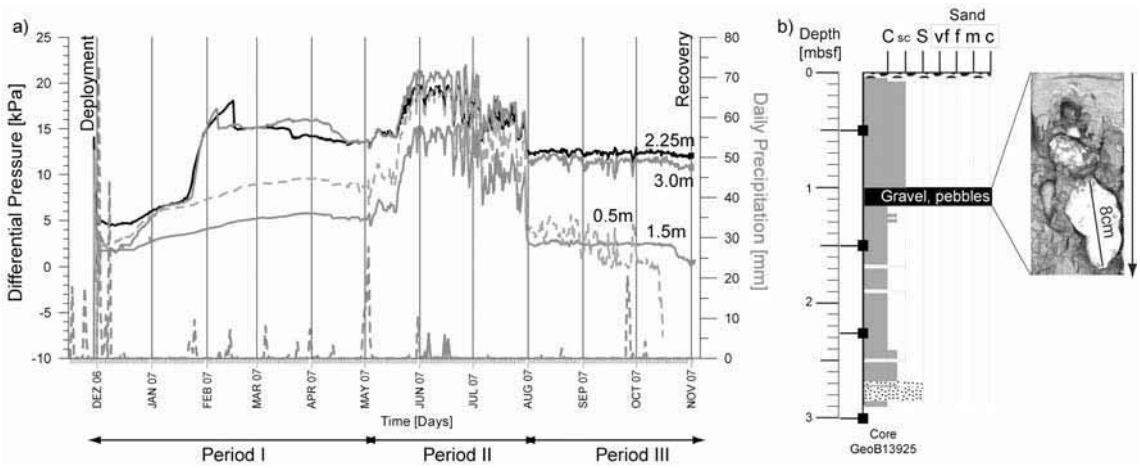

Figure 4. Excess pore pressure detection and quantification (from Stegmann *et al.*, 2011): a) Long-term pore pressure monitoring (1 year). Each curve represents one level of measurement (the corresponding depth is given in the graph). Annual pore pressure course is linked with hydrology by comparison with the daily precipitation rate measured at Nice Airport during the installation of the piezometer (<www.meteofrance.fr> b) Coarse-grained sediments and gravel recovered in the vicinity of the piezometer position. High permeable coarse grained portions imbedded in clayey-silty sediments favour the flow of fluids, due to the contrast of permeability hydraulic gradients. Pore water analyses here attest the occurrence of fresh water (Kopf *et al.*, 2009; 2010).

[see original colour illustration in Annex at end of volume]

For that reason, in recent years, three seagoing expeditions (M73-1 cruise on RV Meteor led by MARUM Bremen, Germany - Kopf *et al.*, 2008; PRISME cruise on RV L'Atalante led by Ifremer Brest, France - Sultan *et al.*, 2008 and P386 cruise on RV Poseidon led by MARUM Bremen, Germany - Kopf *et al.*, 2009) focused on the hydro-geological regime of the Nice study site. *In situ* pore pressure measurements using different systems of free-fall piezometer devices were performed as a key element during each of the cruises. The main results of these three cruises show: (i) a strong link between pore pressure transients and local precipitation (ii) overpressure at levels where groundwater flow occurs (coarse intervals containing sand and gravel); and (iii) fluidised fractures and channels that indicate high pore pressures at least temporarily. These observations, detailed in Stegmann *et al.* (2011), confirm the major role of pore pressure in deformation processes occurring at the shelf edge/upper slope area offshore Nice.

Prediction of different failure scenarii (Modelling)

Using numerical calculations Dan *et al.* (2007) and Leynaud *et al.* (2010) have tested some of the potential scenarii that could destabilize the sediment from the shelf edge and the upper slope offshore Nice. Based on a Finite Element Model Dan *et al.* (2007) show that sediment leaching by freshwater and the induced sensitivity could be one of the main sources of the 1979 accident. Leynaud *et al.* (2010), using a 3-D model based on the upper bound theorem of plasticity, illustrate the impact of the weak zone and its very low shear strength on the Nice slope stability. Considering homogeneous lateral extension of the shear zone, Leynaud *et al.* (2010) postulate a high critical probability of failure for the Nice slope (Figure 5). Of course weak zones are not yet continuous but will progressively propagate with time, leading to a highly metastable slope.

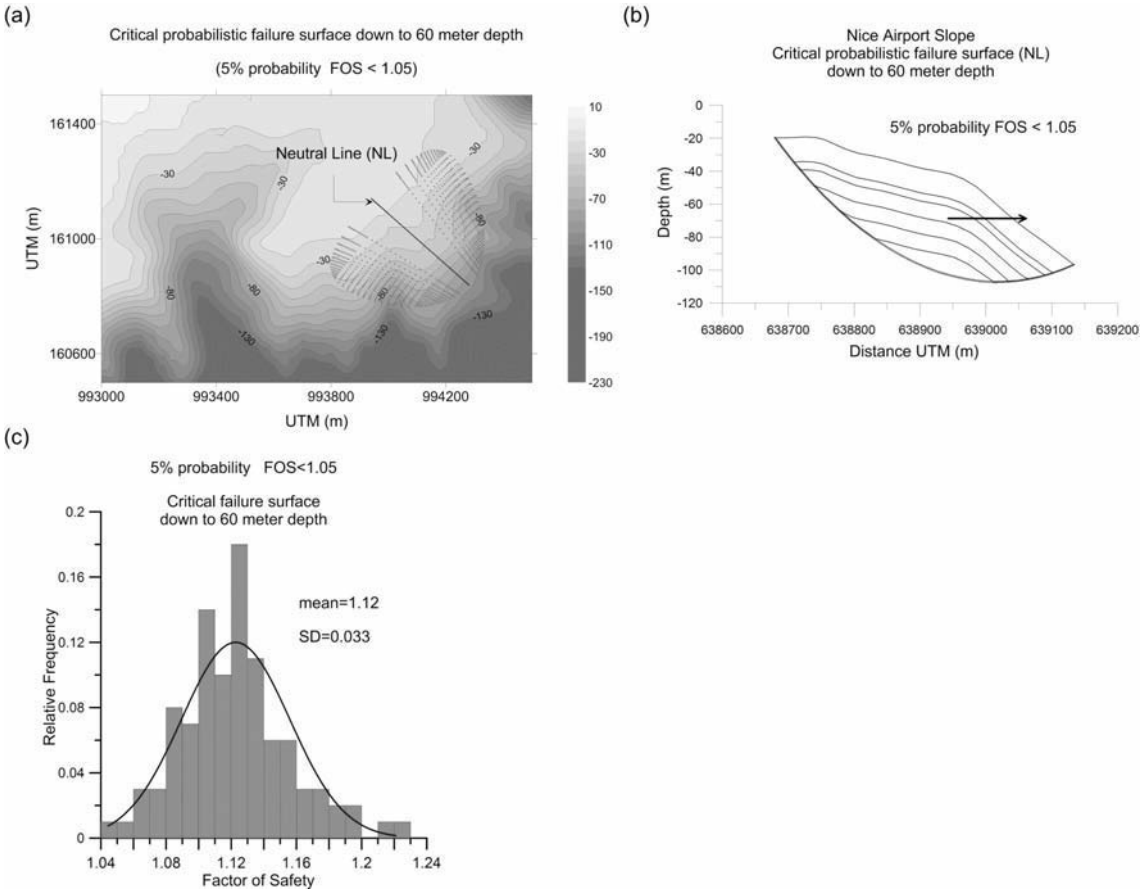

Figure 5. Detection of a theoretical critical failure surface using modelling (modified from Leynaud and Sultan, 2010): Example of probabilistic approach used to assess the 3D stability of the Nice slope under gravity loading.

Integrate information for better understanding

Based on the multi-method approach (*in situ* pore pressure data, the high quality *in situ* geotechnical data (CPTu and sonic cone) presented here, laboratory testing and numerical modelling) it is now possible to combine different scenarii. This allows testing the relevance of each of the possible external mechanisms for the stability of the Nice slope. Moreover, *in situ* geotechnical data show that weak zones are mainly present on the border of the plateau to the south-east of the 1979 failure area (Sultan *et al.*, 2010 – Figure 2). Numerical modelling also shows that the probability of slope failure is higher at the edge of this same plateau (Leynaud *et al.*, 2010 – Figure 5). Therefore, future investigations and monitoring will concentrate on this unsafe area in order to identify, as accurately as possible, the main factor controlling the stability of the Nice slope.

The way forward

Available geological, geophysical and geotechnical data from the shelf edge/upper slope area offshore Nice suggest the start-up of a progressive failure mechanism confirming that every failure process is, at first, local, with formation of plastic zones, then general (Leroueil, 2001 and Urciuoli *et al.*, 2007). In addition, the Nice slope study area which is a relatively small and well constrained natural laboratory provides the variability of involved mechanisms (seismicity, groundwater charging, presence of weak sedimentary layers, high-sediment accumulation rates, anthropogenic impact by construction, slope oversteepening, free gas) needed to improve our understanding of progressive slope movements in the marine domain. It is today urgent to complement the available data from the Nice shelf and slope site by continuous monitoring of sediment deformation and of pore fluid activities, in order to assess the danger of evolution from possible pre-failure stage of the slope to general catastrophic slope failure. Indeed, the available geotechnical and geophysical data do not constrain the timing of deformation and notably the transition from local plastic zones to general failure. This time period can be only predicted by monitoring the displacement rate of the sediment body above the slope failure surface. For the present study site, the main specific future scientific questions will focus on the four questions:

- What is the time scale of the progressive slope movement in the Nice study area?
- Is there link between fluid-escape activities and the slope displacement rate?
- What are the interactions between the recognised external mechanisms?
- What is the probability that such a progressive slope movement leads to a catastrophic failure in the next years?

As soon as September 2011, a vertical 3D tiltmeter will be installed on the shelf to the south-east of the 1979 slope failure (see Figure 5 c) in order to detect and monitor any possible sediment deformation above and through the detected shear zones. The displacement data derived from the 3D tiltmeter will be used to calibrate the numerical modelling and to update our working hypotheses in order to converge towards the most probable deformation scenario.

Due to the lack of the properties and distribution of the deeper strata of the Nice Slope as a source for inflow of fresh water (Guglielmi and Mudry, 1996), a drilling campaign by the Integrated Ocean Drilling Program (IODP) has been proposed for the near future. Both core recovery and long-term *in situ* measurements (e.g. pore pressure, temperature, tilt) in some of the boreholes will shed light on the potential landslide triggers at the Ligurian Margin, and on the transient changes in physical properties governing slope stability in general.

Conclusions

The continental slope offshore Nice provides an ideal natural laboratory for studying the interrelationships between predisposing, triggering/aggravating and revealing factors of submarine landslides. The use of an integrated approach based on multi-disciplinary studies was able to detect several phenomena which could be considered as precursor to slope failure. *In situ* geotechnical measurements and numerical modelling show that weak zones and unstable slopes are mainly present on the border of the plateau to the south-east of the 1979 failure area. The direct or indirect role of pore water in the observed deformation features and signatures was also shown. In the near future, 3D tiltmeter will be deployed to detect and monitor any possible sediment deformation above and through the detected weak/shear zones. Those displacement data will be used to calibrate numerical modelling and to converge towards the most probable mechanism at the origin of the observed weak/shear zones.

Combining inland and offshore paleotsunamis evidence: the Augusta Bay (eastern Sicily, Italy) case study

Paolo Marco De Martini, Alessandra Smedile and Daniela Pantosti

Istituto Nazionale di Geofisica e Vulcanologia, Roma, Italy

Introduction

Eastern Sicily (Italy) was repeatedly hit by tsunami waves related to large local historical earthquakes (e.g. 1908, 1693, 1169, CPTI Working group, 2004) as well as to far-field sources (e.g. AD 365 Crete earthquake, Jerome, 380). Along the eastern Sicily coasts, we selected the Augusta Bay (Fig. 1), a natural gulf about 15 km wide and with a 25 km-long shoreline, as the key area of this study because information available from historical written reports on tsunami effects (Gerardi *et al.*, 2008) and local geomorphology both suggest it is very favorable for the research of the geological signature of past tsunamis. We are all aware of the fact that tsunami sedimentation can take place in both off-shore and in-land environments and since the tsunami behaviour depends strongly on bathymetric and topographic configurations, different sedimentation patterns can occur depending on the differences in these environments (Sugawara *et al.*, 2008), asking for a multidisciplinary approach. Lowlands and lagoons characterize the Augusta Bay coastal area,

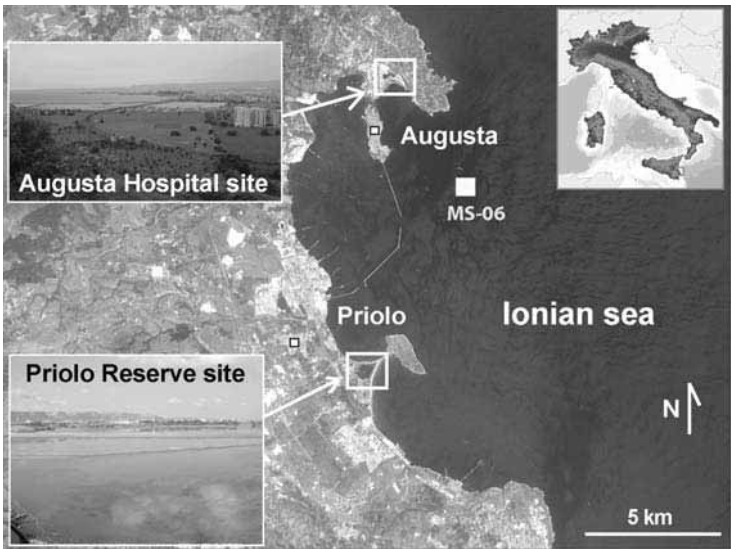

Figure 1. The Augusta Bay area in eastern Sicily, Italy. The Augusta Hospital and Priolo Reserve sites are marked with white empty rectangles, while a white square locates the offshore coring site (MS-06). Two panoramic pictures of the in-land investigated sites are also shown.

providing an excellent and convenient restricted condition for recognizing and identifying tsunami deposits (Shiki *et al.*, 2008), while a relatively wide continental shelf with a thick late-Holocene record has been investigated offshore through the acquisition of a tight grid of CHIRP-sonar profiles. Well-targeted sediment samples have been collected both offshore and inland. The integrated interpretation of the geophysical and geological data has been carried out in order to recognize, date and correlate key-layers in the sediment column that may be directly or indirectly related to tsunami events.

In-land evidence for tsunamis

As for the inland research we adopted an approach that includes:

a) detailed re-analysis of all the available historical reports on tsunami effects (hit localities, inundated areas and run-up distribution) along the Augusta Bay and surroundings;
b) geomorphologic and geological studies of the Augusta Bay, through aerial-photographs, satellite images interpretation and field surveys, to identify sites favorable to sedimentation, preservation and dating of tsunami deposits;
c) coring campaigns, using both hand auger equipment and a vibracoring (gasoline powered percussion hammer), always accompanied by GPS surveys for its exact positioning with respect to the present shoreline;
d) laboratory analyses on collected sediments (X-ray, physical properties, grain size, micropaleontological, radiometric datings and morphoscopic and glass chemistry on thepra).

Historical data

From the historical records we learned that the investigated area experienced at least four tsunamis (in 1908, 1693, 1542 and 1169) during the past millennium (period for which we believe that the historical tsunamis record can be considered complete, at least for the main events). As already known from the Italian seismic historical catalogues, the Middle Age period is quite scarce of information due to unstable social and economical conditions and thus the historical tsunami record is very poor before 1000 AD. However, it is well known that the large 365 AD Crete earthquake-generated tsunami hit the Augusta Bay area (Jerome, 380) as supported also by numerical modeling (Lorito *et al.*, 2008; Shaw *et al.*, 2008). An historical average tsunami recurrence interval (ATRI) of about 250 years for the past millennium in the Augusta Bay can be derived from written reports (a ~400 years long ATRI is obtained considering the ca 2 ka long historical dataset).

Geological data

Given the high variability in the nature of tsunami sediments, it is not surprising if tsunami deposits are not uniquely identifiable, as other kinds of deposits, storm- or hurricane derived, may share most of their characteristics. In recent years, only a few studies were designed to compare sedimentological characteristics of historical tsunami and storm deposits at the same or nearby site (Nanayama *et al.*, 2000; Goff *et al.*, 2004; Tuttle *et al.*, 2004; Kortekaas and Dawson, 2007). A recent review (Morton *et al.*, 2007), on the physical criteria for the abovementioned distinction, uses several modern examples to describe idealized tsunami and storm deposits. The presence of a relatively thin deposit (average <25 cm), often made by normally graded sand consisting of a single (or few) structureless bed, sometimes with rip-up clasts, strongly suggests a tsunami origin; on the other hand, a moderately thick sand bed (average >30 cm) composed of several planar laminations with foreset and ripples clearly favors a storm origin. Moreover, the geological approach may be complicated by erosion/deposition process related to storms (Morton *et al.*, 2007) and by the possible presence of a tsunami-related erosion/bypass zone (no deposition), usually as far as 150 m inland (Gelfenbaum and Jaffe, 2003).

In order to avoid most of these problems we selected only sites wide enough to perform our coring campaigns starting from a minimum distance of 200 m from the present shoreline and moving further inland as possible. We concentrated our study on the sites of Augusta Hospital and Priolo Reserve, about 10 km apart (Fig. 1). The Augusta Hospital site is placed on an alluvial surface (1 to 5 m a.s.l.) gently dipping towards a large salt marsh bounding the sea, while the Priolo Reserve site is a 0.5 km^2 shallow coastal lagoon separated from the sea by sand dunes, up to 4.5 m high.

A total of 22 cores were collected inland in these two sites, at a maximum distance of 530 m from the present coastline (De Martini *et al.*, 2010). The dominant fine to very fine stratigraphy is intercalated by at least six high-energy depositional layers, repeatedly found in several cores. These relatively thin (about 10 cm) single massive and structureless beds with abrupt erosional lower contact are made of coarse to fine sand with sharp basal contacts (Fig. 2A) and present a bioclastic component (sometimes predominant) made of microfauna (benthic and planktonic foraminifera, from both shallow and open marine environment) and shell fragments, both suggestive of a marine provenance (Fig. 2B).

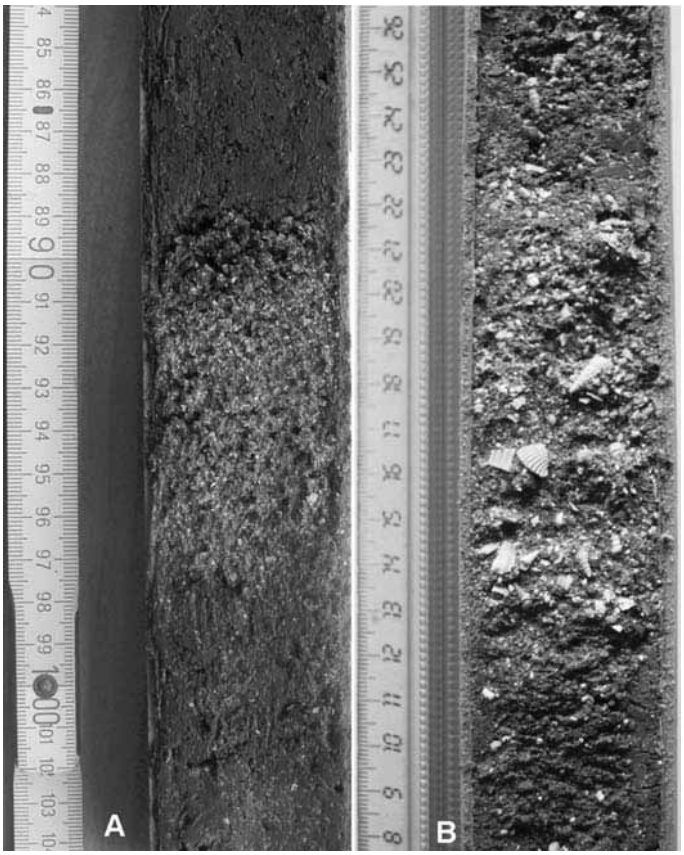

Figure 2. Two tsunami deposits found in the Augusta Bay sites. A) picture of a yellowish bioclastic layer (event AU-02) composed by few whole gastropods (*Hydrobia* spp., *P. conica*), abundant shell fragments (mollusks, corals and echinoderms), few ostracods, often broken benthic (*Ammonia* spp., *Bolivina* sp., *Cassidulina laevigata*, *Cibicides lobatulus*, *Haynesina germanica, Pullenia bulloides*, *Rosalina* spp., miliolids) and few badly preserved planktonic (*Globigerina* spp., *Globigerinoides* spp., *Globorotalia inflata*, *Turborotalita quinqueloba*) foraminifera; this layer shows a sharp erosional basal contact and no evidence for layering or grading. B) picture of a bioclastic layer with sharp (probably erosional) basal contact (event PR-02), with a huge amount of shell fragments, gastropods (*Pirenella conica*, with abrasions probably due to high energetic transport) and ostracods, benthic and few planktonic foraminifera (with a peculiar increment in the benthic foraminifera specific diversity with respect to adjacent deposits).

[see original colour illustration in Annex at end of volume]

Chronological constraints on the age of these deposits are based on eight AMS radiocarbon datings and on the attribution of a tephra layer to the 122 BC Etna eruption (thanks to petro-chemical and morphoscopic analyses). C14 derived data include measured and calibrated ages (according to Calib REV5.0.2 by Stuiver and Reimer, 2005) of the samples collected in the cores. For the marine shells we adopted the reservoir correction for marine samples (400 yrs according to the calibration data set marine04.14c, see Calib REV5.0.2 by Stuiver and Reimer, 2005) and a difference ΔR in reservoir age of the study region, to accommodate local effects.

On the basis of the combination of all the data collected on the marine inundations that hit the Augusta Bay area, we suggest that evidence for at least six tsunami events was found at the Augusta

Hospital (AU- events) and Priolo Reserve (PR- events) sites during the past 4 ka (De Martini *et al.*, 2010). In terms of tsunamis timing, we could list them as follow: younger than 1420-1690 AD (PR-01), 650-770 AD (AU-00), 160-320 AD (PR-02), 600-400 BC (AU-01), 800-600 BC (PR-03), 975-800 BC (AU-02) and 2100-1635 BC (PR-04). Three of the tsunami deposits found at the Priolo Reserve site may be associated to historical tsunamis: PR-01 to the 1693 local event, PR-02 to the 365 AD Crete event and PR-04 to the ca. 3600 BP Santorini event. These results appear to confirm studies performed on inland-displaced boulders (Scicchitano *et al.*, 2007; Barbano *et al.*, 2010) and coarse marine sediments (Scicchitano *et al.*, 2010) developed in the same area and surroundings on the 1693 tsunami. For the 365 AD Crete tsunami and the Late Minoan Santorini event, our findings may represent the first onshore evidence in the central-western Mediterranean area. On the basis of these results we can assume a geologic ATRI of about 600-700 years for the past 4,000 years in the Augusta Bay (De Martini *et al.*, 2010).

Offshore evidence for tsunamis

As for the offshore research we adopted an approach that includes:
a) geophysical survey of the Augusta Bay, through close-spaced grid of seismic reflection chirp-sonar profiles covering the 150 km^2 of the bay (morphobathymetry, seismic reflection, seafloor reflectivity), to identify an ideal location to sample a potentially complete stratigraphic record;
b) coring campaign, in order to collect a long sediment gravity core;
c) laboratory analyses on collected sediments (X-ray, physical properties, grain size, micropaleontological, radiometric datings and morphoscopic and glass chemistry on thepra).

Geological data

Offshore studies offer an interesting alternative to the investigation of tsunami's signatures because marine environments can assure a relatively undisturbed continuous record and, therefore, are potentially more sensitive to anomalous events (i.e., earthquakes and tsunamis). Although the marine environment might represent a new source for field-based tsunami evidence, very little has been done on the study of tsunami transport and deposition in offshore zones or in shallow-shelf areas (Weiss and Bahlburg, 2006; Dawson and Stewart, 2007). Coarse-grained deposits and, more generally, high-energy processes were used as offshore evidence for past tsunamis (Van der Bergh *et al.*, 2003; Reinhardt *et al.*, 2006; Abrantes *et al.*, 2008; Goodman-Tchernov *et al.*, 2009). In addition, these studies highlighted the difficulty of differentiating a tsunami effect from that of normal storms, and faced the problem of a subtle mixing of the two processes in the nearshore zone. With the aim of exploring new offshore approaches for the paleotsunami research, we started an investigation off the shore of Augusta Bay (Smedile *et al.*, 2011). We planned to integrate local in-land tsunami studies (De Martini *et al.*, 2010) with offshore coring, to highlight any subtle anomaly in sediments, fauna assemblages, physical properties, etc., that could represent a proxy for tsunami occurrence.

Differently from previous offshore studies in this area (Di Leonardo *et al.*, 2007; Budillon *et al.*, 2005; 2008) that considered only the recent part of sediments (i.e. the first 30 cm bsf), we presents new data (Smedile *et al.*, 2011) from a 6.7 m-long piston-core (MS-06) sampled 2 km offshore the Augusta harbor at 72 m water depth, in the northern part of the bay (Fig. 1), in shelf mud deposits where no evidence of gravitational processes and anthropogenic disturbances (both in terms of sediment quality and of local sedimentation rate due to dumping) exist. The MS-06 core is made of 6.7 m of almost homogeneous mud, interrupted by a 3-4 cm thick black medium-coarse sandy layer at ~3 m below the top (Fig. 3C). A quite thick *Posidonia oceanica* rich layer appears as a discrete interval just below the top core, also highlighted as a darker horizon by X-Ray imaging (Fig. 3A). Further dark layers, likely related to the compaction of *P. oceanica* remains, are recognizable in a qualitative way along the core from X-ray imaging, as well as localized concentrations of molluscs (mainly *Turritella communis*), sometimes arranged without directional pattern (Fig. 3B). The gamma density profile shows a homogeneous pattern with minor fluctuations, confirming that the core was sited in a low energy environment with a monotonous deposition dominated by fine-grained sediments (Fig. 3). The magnetic susceptibility profile shows the presence of a single layer very rich in magnetic minerals, suggesting its volcanic origin (Fig. 3).

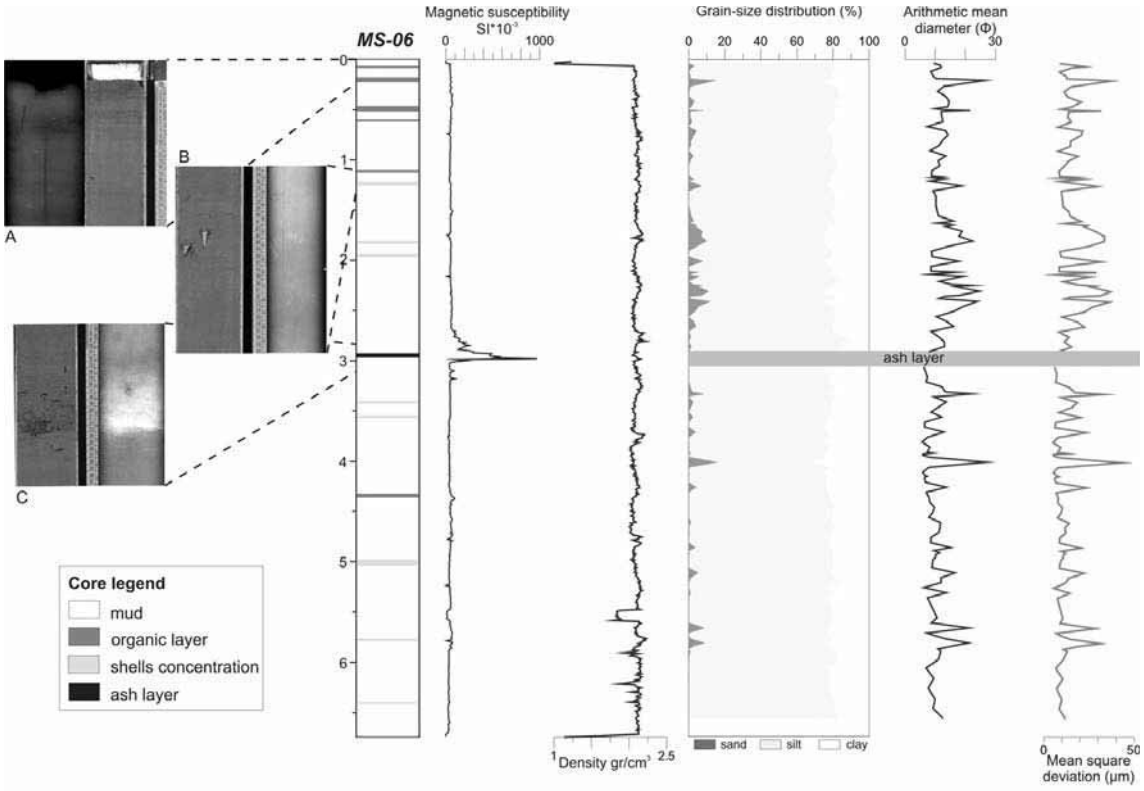

Figure 3. Simplified lithology of MS-06 core coupled with magnetic susceptibility, γ density logs and grain size distribution with some derived parameters (modified after Smedile *et al.*, 2011). On the left side some details of sediments and X-ray; images A) uppermost portion with organic rich layer in *Posidonia* fibers, B) shells concentration layer and relative X-ray image, C) ash layer consisting of black fine lapilli and coarse ash.

Through the analysis of tephrostratigraphy, ten AMS radiocarbon datings and radioactive tracers (^{210}Pb and ^{137}Cs), the entire core sequence has been dated back to the last 4,500 yrs. C14 measured ages were dendrochronologically corrected according to the radiocarbon calibration program OxCal 4.1 (Bronk Ramsey, 2009). Moreover, the marine palaeo-reservoir effect was subjected to the local effect (ΔR offset) that, in the Mediterranean Sea, appears to be relatively constant for the past 6 or 7 ka (Reimer and McCormac, 2002). The appropriate ΔR offset can be selected from the Chrono Marine reservoir Database (Reimer and Reimer, 2001). Moreover, results from benthic foraminiferal assemblage analysis (Smedile *et al.*, 2011) have shown up to 12 intervals in which displaced epiphytic foraminifera are present with abundance >25% of this whole assemblage. An opposite trend was found in the P/B ratio that shows a negative deflection in correspondence of almost all benthic displacement cases. Moreover, the sedimentological analysis (Smedile *et al.*, 2011) highlights sandy inputs in these 12 anomalous intervals. These microfaunal anomalies were generally accompanied by significant amount of vegetal remains in the washed fraction, by localized concentration of mollusks and/or by darker organic-rich stripes. Thus, the 12 anomalous layers should have been caused by high-energy events, with back-wash tsunami waves as best candidates, related to an uncommon mechanism able to transport epiphytic species at greater depths (72 m bsl), relative to their living zone (up to 35-40 m bsl considering the depth limit of the *P. oceanica*), along with some amount of sand characterized by a peculiar bimodal grain-size distribution (interpreted as the result of different depositional mechanisms and/or different sources for the sand). In terms of tsunamis timing, we could list them as follow: AD 1820-1920 (E1), AD 1430-1810 (E2), AD 930-1170 (E3), AD 590-800 (E4), AD 430-660 (E5), AD 90-370 (Ex), BC 350-130 (E6), BC 580-320 (E7), BC 660-400 (E8), BC 800-560 (E9), BC 1130-810 (E10), BC 1720-1200 (E11). One further element that supports the tsunami driven mechanism is the coincidence between five of the event ages (E1, E2, E3, Ex and E11) and the known tsunamis that hit the area (1908, 1693, 1169, AD 365 Crete, ca. 3600 BP Santorini). Considering the whole set

of events occurred during the past 3700 yrs, a first approximate offshore ATRI of 330-370 yrs for tsunami inundations in the Augusta Bay can be estimated (Smedile *et al.*, 2011).

These results suggest that our approach in the study of tsunami records is promising to define a cause-and-effect relationship between tsunamis and displaced epiphytic foraminifera rich layers. A comparative study between transport modeling of sediments during storms and tsunamis could also be a useful tool to better discriminate these phenomena in shallow-shelf areas.

Final considerations

Coastal tsunami hazard evaluations include modeling of expected inundations and their frequency in time at a specific site. Therefore, a detailed knowledge of the distribution of past, inundated areas and their timing is critical. The Augusta Bay area represents a unique case study because it allows a comparison between geological (both inland and offshore) and historical records. We obtained three different Average Tsunami Recurrence Interval values [250-400 yrs from historical data, 600-700 yrs from inland studies (De Martini *et al.*, 2010) and 330-370 yrs from offshore findings (Smedile *et al.*, 2011)] that may ask for few short considerations, potentially relevant to environmental risk management and Civil Protection applications, taking into account that the Augusta Bay area is a major national industrial and military site.

Historical data, although generally too limited in time and space to be used as the sole reference to forecast the effects and frequency of future tsunami events, are very useful in giving directions for the selection of the best tsunami research area and for a first estimate of peculiar tsunami parameters like run-up height or inundation distance.

The in-land research for tsunami deposits is for sure able to detect evidence for large tsunamis but medium-small size events could be easily missed. In fact, it suffers the difficulties related to the intense human activity along the coastline as well as to superficial erosional processes that may remove tsunami signatures/deposits and thus the related record is usually far from complete.

Finally the marine environment was clearly the best performing for the identification and dating of tsunami signatures, even if we believe that only a combination of the three approaches discussed above may furnish robust results also in densely populated areas.

We hope that our study could give new perspectives in the paleotsunami research and for the development of innovative approaches, which could be tested and applied in several other Mediterranean sites prone to tsunami hazard.

Submarine volcano geohazards in the Tyrrhenian Sea

Fabiano Gamberi and Michael Marani

ISMAR Bologna, CNR, Italy

1. Introduction

Submarine volcanic landforms have been shown to result, in part, from processes similar to those commonly observed in terrestrial volcanic settings. All land-based lava flow morphologies have been recognized in the marine environment, while the products of the range of explosive eruption styles have been documented even from the deep ocean at >3,000 metres water depth (Head and Wilson, 2003). Volcanism at subducting plate boundaries represents about 25% of the Earth's magma production (Sigurdsson, 2000), mainly developed within the volcanic arc environment. Subduction zones are thus characterised by the development of large volcanic edifices both in island arc and backarc basin environments hosting 80% of the currently active volcanoes of the planet (Chester, 1993).

Due to the characteristics of their magmas, often rich in volatiles, subduction zone volcanoes are particularly associated with geohazards. This also holds true for volcanoes developed in the marine environment, comprising coastal volcanoes, volcanic islands and submarine volcanoes. In these settings, the main processes that lead to geohazards are primarily the catastrophic collapse of volcanic edifices and submarine eruptions, both having the potential for generating far-reaching tsunamis.

Catastrophic collapse of volcanic edifices

The principle geohazard connected with volcanoes in the submarine environment arises from the processes of structural failure and collapse of the volcanic edifice. This hazard is intrinsic with the growth history of volcanoes that evolve through cycles of constructional phases and periods of gravitational instability with related edifice destruction. The growth of a volcano in the marine environment takes place with a continuing modification of its morphology caused by the production of new material both through endogenous (central intrusion and dykes) and exogenous processes (effusion and eruption) that can eventually lead to the formation of a volcanic island. These processes inevitably cause an increase of the steepness of the edifice's flanks and overloading, that lead to potential instability. When the volcanic dynamics overcome the threshold of critical gravitational stability, destructional phases are triggered and structural collapses, often catastrophic, of the volcano's flanks occur.

The main issue that distinguishes volcanic seamounts (inclusive of coastal volcanoes, island volcanoes and submarine volcanoes) in terms of raised instability lies in the basic asymmetry of the stress field in the interior of the edifice caused by the lack of buttressing forces towards the deeper seafloor sector. A further factor promoting instability is the presence of horizons that can act as weak layers, functioning as basal shear surfaces of the collapsing masses. Hyaloclastite or clay levels, horizons charged with hydrothermal fluids or highly altered by hydrothermal

circulation are some of the main processes by which layers in the marine sedimentary section can develop into weak layers. These sliding surfaces promote the lateral spreading of the edifice that in turn can result in catastrophic collapse. Other elements that weaken volcanic edifices are: sub-volcanic basement tilting, neotectonics, and active fracturing and fissuring.

A large-volume collapse, involving the major part of a volcano, causes instantaneous decompression of the magma and volatile surficial plumbing system, resulting in a shallowing of the fragmentation level and thus increasing the probability of paroxystic explosive eruptions more energetic than those usually expected.

Submarine eruptions

In general, submarine eruptions, contrary to subaerial ones, are not associated with large hazards since the pressure of the water column causes the material to be ejected mainly in the form of lava flows. Nonetheless, the hazards increase when the submarine volcanic centres are located at only

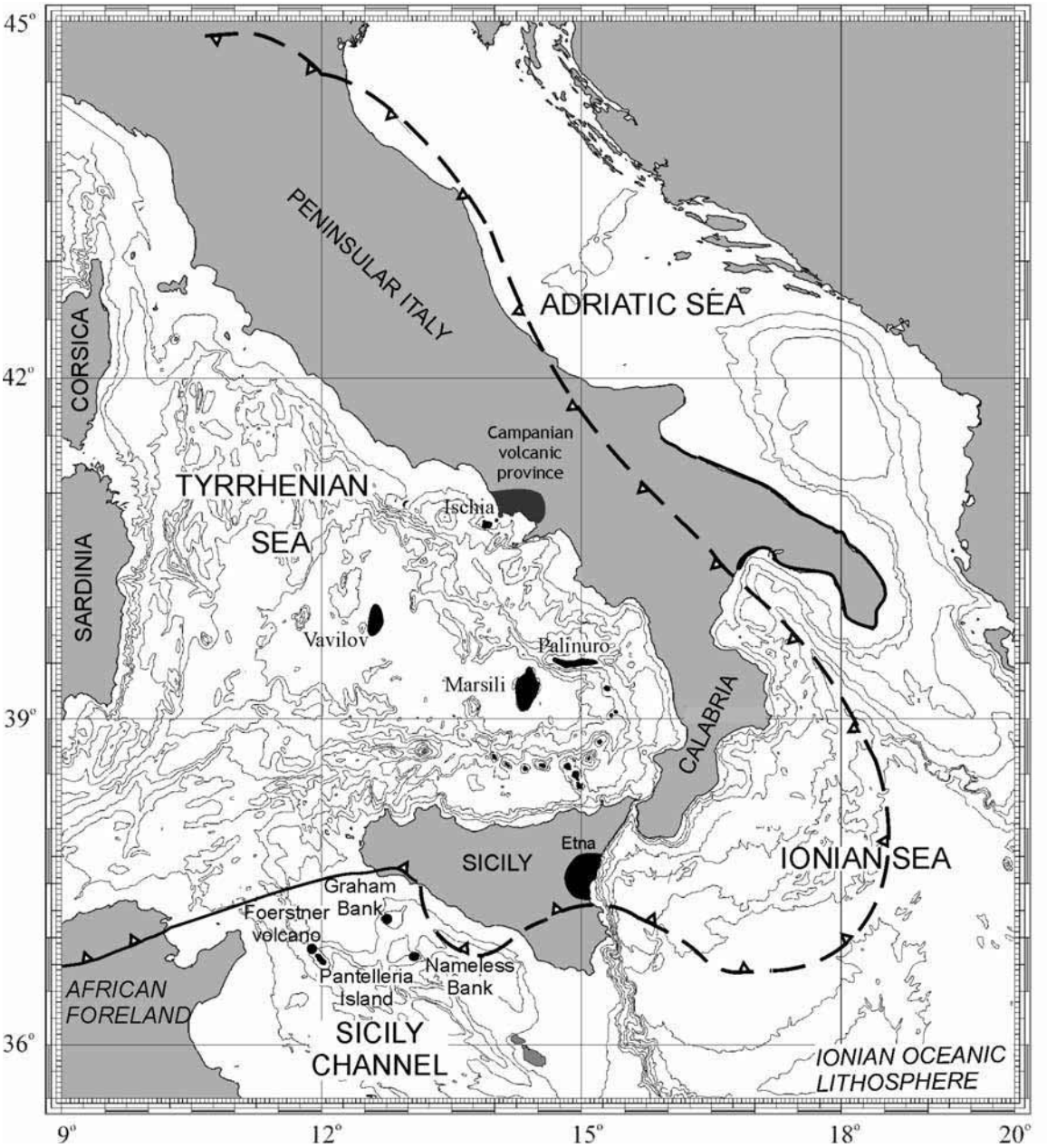

Fig. 1. Map outlining the areas treated in the text.

few hundreds of meters of depth. In this case, catastrophic phreatomagmatic eruptions and pyroclatic flows can occur also below the marine surface. Explosive phreatomagmatic activity has been recognized as a cause for 19% of the tsunamis generated in the volcanic environment. In the case of coastal volcanoes, tsunamis caused by the entrance of pyroclastic flows into the sea have also been recorded.

Tsunamis

Approximately 5% of the known tsunamis are originated by processes linked to volcanoes. Major sector collapses of large-volume submarine volcanoes or islands and submarine or coastal eruptions are some of the main causes of tsunami generation in the submarine volcanic environment. Furthermore, volcanic activity is often associated with increased seismicity. Thus, both volcanic and seismic activity can be primary tsunamigenic events. These processes can also destabilise the surrounding seafloor, causing secondary landslides that in some cases have been shown to be the major triggers for tsunamis.

Aims of paper

The use of swath bathymetric mapping as a remote sensing tool, augmented by steadily increasing ground truthing by means of sampling and direct observations, has profoundly increased our knowledge about the unique characters of submarine volcanism, concerning both edifice morphology and the structural instability of volcanic constructs inherent to the underwater environment. In the present paper, the morphologies of the Tyrrhenian Sea submarine volcanoes and the submerged portions of several volcanic islands are illustrated as well as a description of the volcanic region straddling the Straits of Sicily (Fig. 1). The results of this analysis are then used to infer the geohazards connected with the marine volcanic environment, comprising submarine and coastal volcanoes and volcanic islands.

2. Geological setting

The Italian region is characterized by a plate convergence setting, characterized by a subduction zone and active seismicity and volcanism that are often developed in the marine environment.

The Tyrrhenian Sea, bordered to the east and south by the Apenninic-Maghrebides mountain belt and to the west by the passive Sardinian margin, formed as a consequence of rifting and backarc extension of the Alpine/Apennine suture above the north-westerly subducting Ionian oceanic slab (Kastens *et al.*, 1988; Kastens *et al.*, 1990; Sartori, 1990; Jolivet, 1991). An eastwards migration of crustal thinning and oceanic accretion affected the Tyrrhenian area since the lower-mid Miocene (~15 Myr). First, production of oceanic crust occurred westward, during the Pliocene spreading of the Vavilov basin (4.3-2.6 Myr), where the large centrally located Vavilov volcano developed (Kastens *et al.*, 1990). A subsequent change to ESE-directed extensional stress in the Late Pliocene-Quaternary resulted in the emplacement of basaltic crust southeastwards, generating the Marsili backarc basin (2 Myr) also containing a large axial volcano, Marsili seamount, (Kastens *et al.*, 1990). In step with backarc basin development, the subduction-related island arc volcanism of the southern Tyrrhenian basin migrated from west to south-east, from Sardinia (32-13 Ma) to the currently active Aeolian island arc (Serri, 1997 and references therein), developing the present-day arc-backarc configuration of the southern Tyrrhenian region (Fig. 1). The Aeolian arc consists of seven islands and a number of submarine volcanoes west and northeast of the emerged arc (Fig. 2). The Aeolian arc, together with the Aegean arc, represents the only still active island arcs of the Mediterranean. The northeastern submerged portion of the arc, positioned on the Calabrian margin, consists of isolated cones and the large, Palinuro volcanic complex (Fig. 2). To the west of the emergent islands a number of submerged arc volcanoes are located on the Sicilian margin (Fig. 2). The Sicily channel is the foreland of the Apenninc-Maghrebian flod and thrust belt. It is the site of an intraplate rift interpreted as resulting from the displacement of Sicily away from Africa. As a consequence, tectonic trough such as the Pantelleria and Malta ones developed in the generally shallow water area of the Sicily Strait. Rifting processes have been accompanied by volcanism that is still active in the area. To the north of the Sicily channel rift zone the Mount Etna volcano also grows on continental crust and has its eastern flank in the coastal areas of eastern Sicily.

The following discussion will provide an account of the most recent volcanic events that occurred in Panarea and Stromboli Islands. It will then describe the morphology of the submarine arc volcanoes and provide a provisional analysis of their origin and their geohazard implications. Subsequently, the large, axially located backarc volcanoes, Marsili and Vavilov, will be illustrated in the same manner. Finally, an account of the volcanism in the Sicily Channel will be provided.

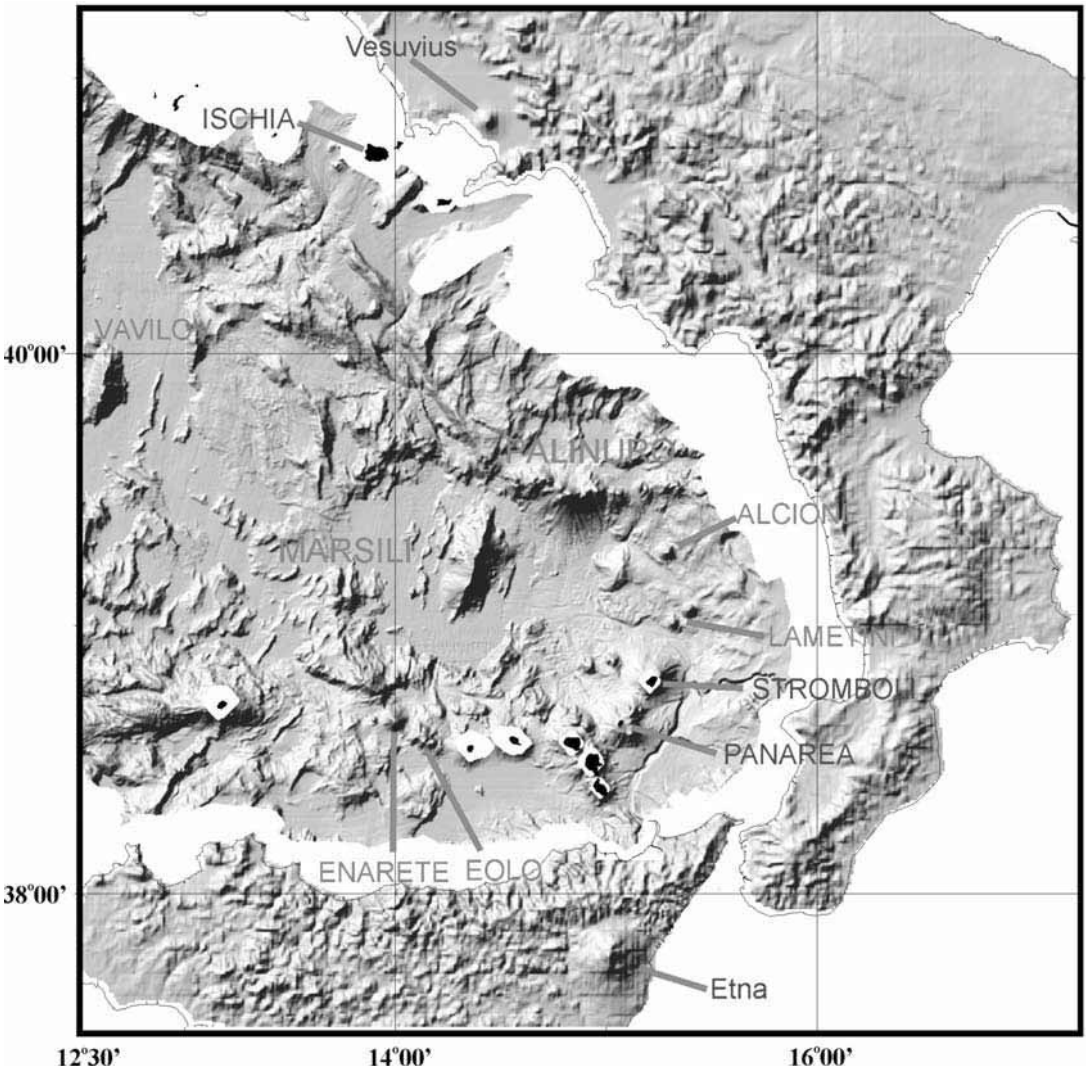

Fig. 2. Shaded relief of the southeastern Tyrrhenian Sea where the Aeolian arc and the Marsili backarc basin are developed. Locations treated in the text are indicated.

[see original colour illustration in Annex at end of volume]

3. The Aeolian arc

Panarea

Panarea volcano is the emergent portion of a submarine stratovolcano, 1,600 m high and 18 km across and is characterized by a large and ellipsoidal shaped platform area, at a depth of approximately 100 m (Gamberi *et al.*, 1997). The emergent portion of this platform forms Panarea Island (421 ma.s.l.) and a small archipelago with numerous islets to the east. Panarea and the Islets are made up of high-K calcalkaline, andesite to dacite and rhyolite rocks with age ranging from 149±5 to 20±2 ka (Dolfi *et al.*, 2007; Lucchi *et al.*, 2007). The volcano was considered extinct by the scientific community until 3 November 2002, when a very unusual phenomenon occurred in

the vicinity of the island. At least three large whitish plumes suddenly appeared at the sea surface in the islet area in a relatively shallow sea depth (10-15 m) where a submarine fumarolic field was known to be actively degassing (Fig. 3). About 20 low magnitude (Md≥1.0) and high frequency seismic events occurred on November 3, 2002, only a few hours before the local inhabitants of Panarea witnessed the boiling sea. It also caused vertical crustal deformation of 4.2±0.1 cm recorded 2.5 km to the west. The degassing event left a ''crater'' depression with a conical shape, about 20 and 14 m wide and 10 m deep, most likely the result of a submarine ''gas burst.'' The ''gas burst'' consisted of a mixture of gas mainly composed of CO2, fine-grained suspended sediments and colloidal S. Similar emissions had occurred in this area in historical times (126 B.C.). By May 2003, the hydrothermal conditions dominating the fluid reservoir prior to the degassing event were completely restored, The 2002 gas burst event suggests however that a significant contribution of fluids from a magmatic-related source (Capaccioni *et al.*, 2005; 2007) is possible in the Panarea area. This event highlighted the unexpected renewal of volcanic activity at Panarea Island, which until November 2002 was considered an extinct volcano. The most critical scenario, of the potential hazard, is related to phreatic eruptions that may occur offshore as well as on the inhabited island of Panarea.

Fig. 3. Photograph taken from ROV of the gas expulsion event at Panarea in Novembre 2002.

[see original colour illustration in Annex at end of volume]

Stromboli

The Stromboli volcano has been in continuous activity in the past 1,000-1,500 years. Several relatively large tsunamis, capable also to cause casualties, have been documented to have struck the Aeolian island in the last 100 year (Maramai *et al.*, 2005b). Their effects are often felt in the nearby Calabrian and Sicilian coasts (Maramai *et al.*, 2005a).

The recognition of the potential hazards associated with tsunamis in the Aeolian island was recently brought about by the events of 2002. In December 2002 during a period of intense volcanic activity of Stromboli, with lava flows spreading out both from the Sciara del Fuoco crater and midslope, a large amount of pyroclastic material and lava was present on the northern side of the volcano,

producing a lava delta at the shore (Fig. 4). Due to the weight of the new material and the steep gradient of the flank, downslope mass movements occurred on 30 December 2002 A first submarine landslide occurred just under the sea level and generated a large tsunami, followed, about 7-8 min later, by a second subaerial landslide in the Sciara del Fuoco at about 500 m a.s.l., probably driven by the submerged one, that also produced a tsunami. The total volume of the involved material was about 20,000,000 m^3, the largest contribution coming from the failure of the volcano submarine portion. The highest runup in the Stromboli Island was of approximately 11 m, causing much damage. The lack of casualties was only due to the period of the year being not a touristic season. Damages were also caused in the nearby Panarea Islands, and the effects of the tsunami were also felt in the surrounding Sicilian, Calabrian and Campanian coasts.

Fig. 4. Photograph taken from research vessel of the lava from the December/January eruption of Stromboli entering the sea to form a lava delta.

[see original colour illustration in Annex at end of volume]

Northeastern submerged Arc Volcanoes

Three volcanoes, Alcione and the twin cones of the Lametini seamounts (Figs. 2, 3), lie in the Calabrian slope delimited by the Palinuro volcanic complex to the north and Stromboli Island to the south. The volcanoes develop in the westerly deepening lower slope at a depth in the order of 2,000 m.

Alcione. Dredge hauls indicate a calc-alkaline basaltic composition for the seamount (Beccaluva *et al.*, 1985). The volcano is located on a seaward-sloping bench. This ~1,000 m high volcano is a textbook example of primary edifice gravitational instability. It's general conical shape is dissected by NNW-SSE trending, 100 m relief arcuate scarp (Fig. 5) that displaces downwards the western (seaward) half of the edifice.

The top of the volcano is characterised by two summit areas, separated by the scarp. Flank creep due to differential spreading of its western portion is the possible mechanism of volcano deformation, considering the E-W asymmetry of the volcano base, the basement drop beneath it and the thicker sediment pile to its west. Spreading or creep should be towards WSW, perpendicular to the edifice cutting scarp with a deep-seated decollement plane probably located within the weaker sedimentary material (Fig. 6a).

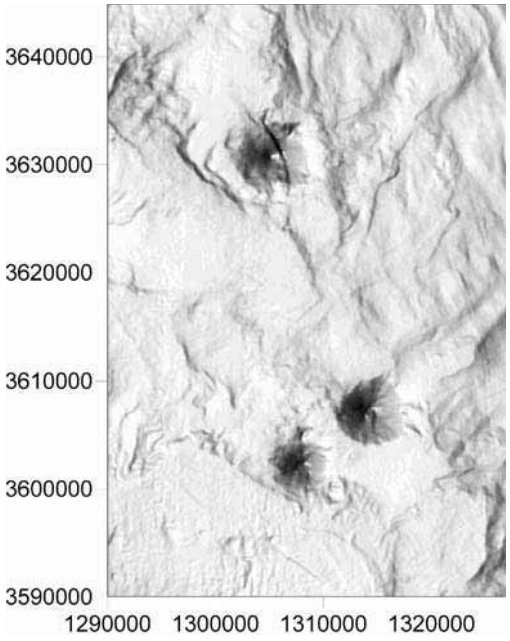

Fig. 5. Shaded relief bathymetry of the Alcione and Lametini volcanic seamounts, the eastern submarine arc volcanoes.

Lametini seamounts. The two conical edifices of the Lametini seamounts are located 20 km due south of Alcione on the same gently sloping bench area (Figs. 2, 5). They are aligned in a NE-SW direction 3 km apart. The NE volcano (LamN) is larger than the SW one (LamS). Dredge samples from LamN (Beccaluva *et al.*, 1985) recovered basalts. Both volcanoes display E-W asymmetry due to the sloping bench. Apart from its size, a distinctive characteristic of LamN is a prominent slide scar on its western flank (Fig. 5).

The slide scar on LamN is most probably related to a mass-wasting event along a shallow-seated detachment plane (Fig. 6b), evidence of gravitational instability due to the sloping (~15°) flanks of the volcano and not associated to any form of deep-seated source.

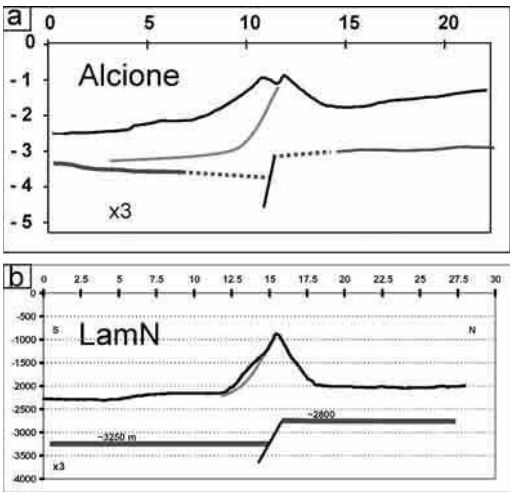

Fig. 6. Possible traces of detachment surfaces that explain volcano deformation. a) Deep detachment, aided by basement step and sloping bench, inducing volcano spreading of Alcione. b) Shallow detachment and slide affecting seaward slope of Lametini N.

Palinuro. Palinuro is made up of basalts and basaltic andesites and has been dated to 0.35 Ma (Beccaluva *et al.*, 1985). The composite Palinuro volcanic complex (PVC) stretchs E-W for 75 km. It stands between the lower slope at 2,000 m water depth to its north and the deep Marsili basin (3,400 m depth) to its south. The PVC delimits the north-western extent of Aeolian arc volcanism. At least eight single volcanic edifices can be recognised along the PVC (Fig. 7), their bases coalescing to form a near continuous volcanic ridge.

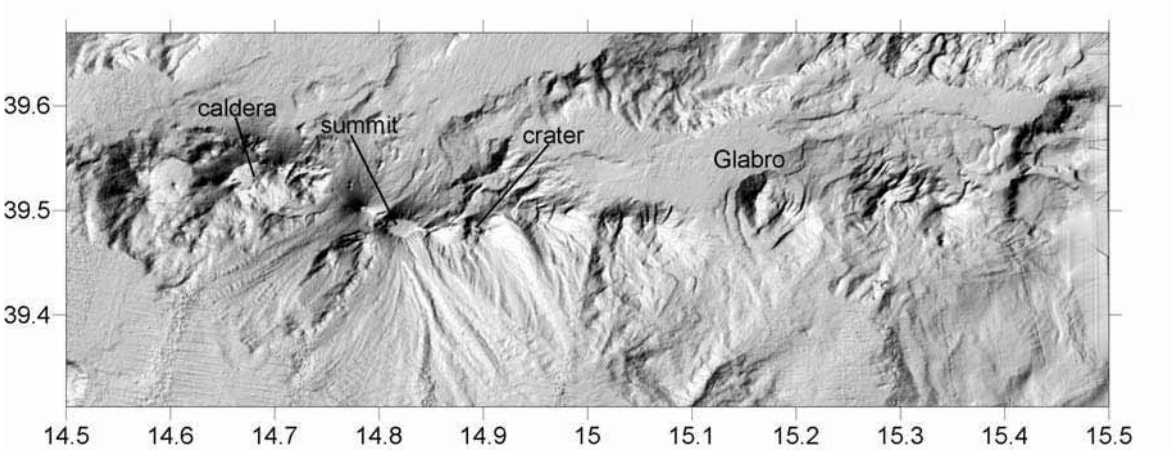

Fig. 7. Shaded relief bathymetry of the Palinuro volcanic complex.

Shallow water depths characterise the central portion of the PVC, with two volcanoes between 14.75° and 14.80° reaching 175 m and 70 m depths. They display flat tops, mostly due to emersion during glacial times. To the west of the two shallower volcanoes, clusters of small cones surround a depressed area (14.70°-14.75°) bordered by an arcuate northwestern ridge and smooth slope. This morphology could be related to a caldera forming gravitational collapse event of a pre-existing volcanic edifice, followed by the creation of resurgent domes. To the east, adjacent to the central area (14.90°- 15.00°), a series of smaller cones develop, mostly exhibiting horseshoe morphology and cratered summits. Further east, the PVC is affected by structures that are very prominent in the morphology of the last volcano, Glabro (centred on 15.20°), isolated from the PVC by a narrow moat. No samples are available for Glabro. The volcano is dissected by a series of arcuate fault scarps into two separate parts characterised by N-S elongated, linear summit zones. A possible process is directional gravitational spreading towards the E-NE.

4. Backarc volcanoes

Marsili. Marsili volcano rises 3,000 metres from the Marsili basin seafloor to a minimum depth of 489 metres (Fig. 8). It is elongated ~ 60 km NNE-SSW with mean width of 16 km. A narrow, 1 km wide linear region of lower gradient, approximately bounded by the 1,000 metre isobath, marks the summit zone that stretches 20 km along the main axis of the volcano. On the lower flanks of the volcano, particularly to the NW and SE, numerous seamounts develop while the adjacent basin areas to the west and to the east of the Marsili edifice are characterised by large fault scarps (Fig. 8).

These features, along with other morphological characteristics of the volcano and adjacent regional geology, led Marani and Trua (2002) to interpret Marsili volcano as a super-inflated spreading ridge, constructed due to robust volcanism during the last 0.7Ma. The volcano is active (D'Alessandro *et al.*, 2008), with activity localised in the summit zone and has an exceptionally low density in its upper region (Caratori Tontini *et al.*, 2010). These characteristics combined with its steep, kilometre-scale flanks imply that Marsili volcano exhibits processes that may trigger potentially severe flank destabilisation and collapse.

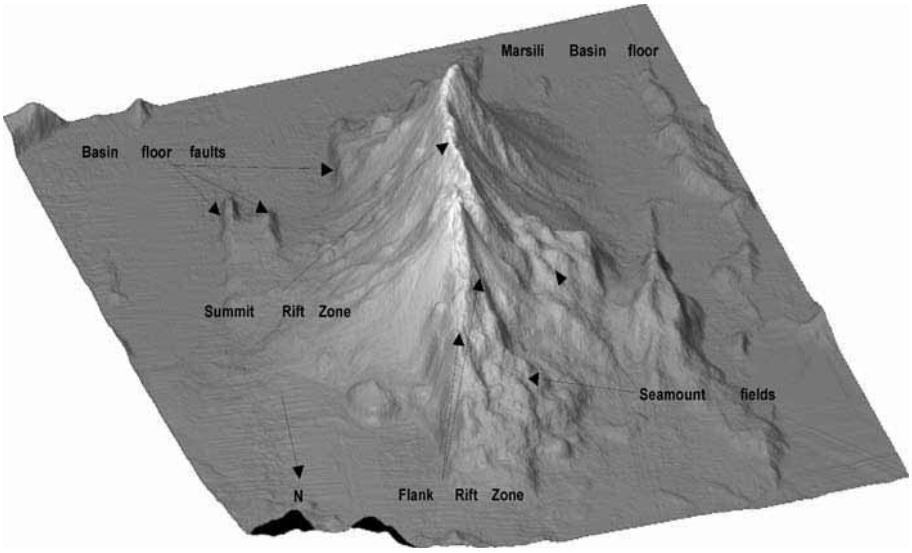

Fig. 8. Surface shaded relief of the Marsili volcanic seamount.

Vavilov. Vavilov volcano has a length of ~30 km, elongated in a N-S direction with a maximum width of ~14 km (Fig. 9). It rises 2,800 m from the flat Vavilov basin floor 3,600 m deep to minimum water depth of 800 m. Vavilov is a mature volcano, its formation occurring at the time of oceanisation of the Vavilov backarc basin at about 3Ma (Kastens *et al.*, 1988). The summit area, however, seems to have been subsequently active (Robin *et al.*, 1987) at 0.4 to 0.1Ma.

The overall morphology of Vavilov volcano is dominated by the strong asymmetry between its eastern and western flanks (Fig. 9). While the eastern flank, dipping on average 15°, displays irregular "volcanic" topography due to small cones, restricted terraces and ridges, a large portion of the western flank is steeply dipping (from >30° above 2,800 m depth to 20° along the lower flanks) and is remarkably smooth, displaying a complete lack of small scale topography. Considering the arcuate scar that bounds the high gradient western flank, it is likely that this portion of the volcano has been affected either by one or more flank collapses or by faulting that has resulted in the removal of a large volume of the pre-existing edifice.

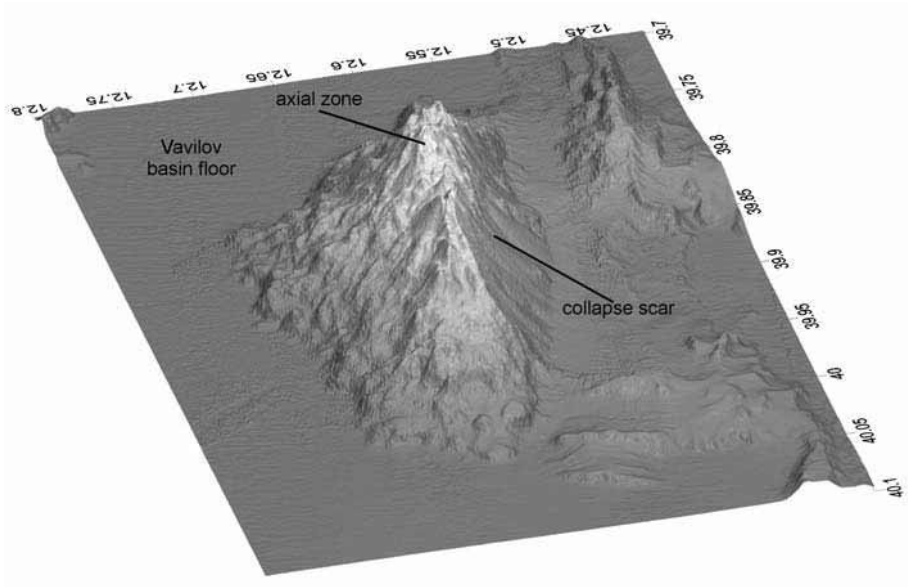

Fig. 9. Surface shaded relief of Vavilov volcanic seamount.

5. The campanian volcanic province

The Campanian area is a site of active volcanism that in historical time showed maximum powerful destructive potential during the Vesuvio's Plinian eruption of 79 A.D. which buried of the Roman cities of Pompei and Ercolano. The Campi Flegrei area is also active and its caldera has a submarine extension in the shallow Pozzuoli Bay. Although both Vesuvio and Campi Flegrei volcanoes can affect in the submarine environment and generate tsunami, their impact on land would be of much greater magnitude. This will be not treated here.

Within the Campanian volcanic province the volcanic island of Ischia is located to the west of the Campi Flegrei caldera and Vesuvio. Ischia Island is a volcanic complex forming the emerged section of a larger volcanic ridge located to the west of the Bay of Naples. Apart from the Mount Epomeo Green Tuff ignimbritic eruption that occurred around 55 ka, most of its recent activity is related to small-scale eruptions, the latest of which occurred in 1302 AD. A notable feature of this volcanic complex is the rapid uplift of Mount Epomeo, 787 m high, recently interpreted as a resurgent block inside a pre-existing caldera The block has been raised in the past 33 kyr of some 700-800 m. Clues of past tsunami events at Ischia Island may be found also in historical sources such as Strabo's Geographica where a sudden collapse with an associated tsunami is described to have occurred before the Greek period. In the southern submarine flank of the volcanic edifice, from the toe of the submarine slope at about 550 m, down to 1,100 m, a field of giant blocks is present. The hummocky topography covers an area about 200 km^2 as far as 50 km from the island and suggests a debris avalanche event related to a catastrophic failure on the island flank. The debris avalanche deposit would have been detached from a 2.2-km-wide horseshoe scar, bordered by two very steep sidewalls that correspond precisely to the Mt Epomeo block. This evidence supports the strong genetic link between uplift and failure. Provided the high tsunamigenic potential of the Ischia collapse, its prehistorical timing further raises the question of the impact on human communities that were already established along the coastal zone during that time.

6. The sicily channel

In the Sicily channel, volcanic activity is ongoing since the Pliocene with an alkaline signature (Carapezza *et al.*, 1979). It takes place in the Island of Pantelleria and Linosa and on several submarine edifices. Many submarine eruptions are in fact reported, although sometimes only with scant evidence, in historical time. The two most renowned ones are that of 1831 which caused the emergence of the Ferdinandea Island and that of 1891 in the Foerstner volcano offshore Pantelleria Island.

In 1831, the Ferdinandea Island was created in the area of the Graham Bank, due to a volcanic eruption; it had a brief life but at is maximum extension it reached a circumference of 3,700 m and an height of 65 m. Earthquakes accompanied the onset of the eruption that in the accounts of contemporaneous observers was also heralded by alternations of sea surface rising and sinking at regular intervals. The Ferdinandea Island mainly consisted of a cone of lapilli and scoriae due to explosive submarine volcanism. It was rapidly eroded away due to the action of the sea causing its disappearance approximately 6 months after its emergence. At present, the top of the volcano is at 7 m below sea surface and is part of a larger, 3 km long and 2 km wide edifice that is 180 m higher than the surrounding seafloor. Fumaroles are still active in the area and bubble eruptions are also observable at the sea surface.

The Foesrtener submarine volcano is located in the western offshore of Pantelleria Island. Its 1891 eruption was preceded by earthquakes and increased fumarolic activity in the Pantelleria Island that was also affected by local uplift of 80 cm. Columns of smoke were first seen rising from the sea surface 4 km west of the island. They were followed by more than 1 m large scoriaceous bombs that, being full of gas, reached the sea surface where they exploded, sometimes being thrown in the air. The eruption was not associated to the creation of an island.

7. Etna volcano

In the Aetnean offshore of the Ionian Sea, various landslide deposits are imaged. Amongst them, a large debris-avalanche deposit has been associated with the event that, approximately 8 kyr B.P. produced the Valle del Bove scar on the land portion of the volcano. The slide reaches a maximum

distance of 20 km offshore (35 km from the Valle del Bove scar on Mt. Etna), a maximum width of 20 km, and a maximum depth of 2000 m b.s.l.; 20 km offshore, the debris avalanche deposits are locally up to about 400 ms (TWTT) thick. The total area covered by the debris avalanche is about 250 km^2. The simulation of a possible tsunami associated with the 25 km^3 debris avalanche deposit off-shore of Etna, has shown that it had the potential to impact all of the Eastern Mediterranean. The model also shows that the resulting tsunami waves could have been able to destabilize soft marine sediments across the Ionian Sea floor. Generating the well-known, sporadically located, ''homogenite'' deposits of the Ionian Sea, and the widespread megaturbidite deposits of the Ionian and Sirte Abyssal Plains. Two other Pleistocenic megaturbidite deposits of the Ionian Sea can be explained by previous sector collapses from the Etna. It has also been hypothesized that, 8 ka B.P., the Neolithic village of Atlit-Yam (Israel) was abandoned because of impact by the same Etna tsunami. According to Galili *et al.* (2008), however, the destruction of the village some 8,300 years ago by a tsunami as proposed by PBF07, finds no support in the archaeological, anthropological, faunal, botanical or sedimentary record from the site.

8. Discussion and conclusions

In the Tyrrhenian Sea, the collapse of the flanks of volcanic islands is the largest hazard. It can cause tsunamis, as shown by the 2002 event in Stromboli, where the island coast was impacted with severe damage, and can also have impact on the nearby coasts of Sicily Calabria and Campania. Proofs of large debris avalanche deposits capable of originating large tsunamis have also been found around Ischia Island. In Panarea Island during the same year a submarine gas burst proved that the volcano is not quiescent as previously thought. In this area the hazard can be mainly related to phretomagmatic eruption occurring below the sea-surface. In the same area, earthquake and ground deformation are associated with the onset of gas burst event.

A variety of instability processes have affected several of the Tyrrhenian Sea volcanoes. In the arc sectors, these processes are linked to the ubiquitous basement faults that underlie the volcanoes. This framework could favour gravitational spreading, which causes the most outstanding morphological transformation in the arc. It may be incipient in the case of Alcione and in a mature stage in the case of Glabro. On the contrary to deep-seated spreading, the northern Lametini seamount displays a relatively large flank slide scar, most probably related to the failure along a slide surface limited to the edifice and due to the high gradient of the flanks. This type of instability evolves within a much more restricted time frame than that of gravitational spreading. Vavilov volcano is the most representative candidate for this style of gravitational instability, in this case leading to large-scale catastrophic sector collapse. Although no estimate can be made regarding the possibility of multiple events forming the scar, the sector failure would have been to all effects instantaneous. Marsili volcano is active, and, mirroring the youthful stage of volcanism, does not display important landslide events although the location of activity and other characteristics of the edifice have the capacity of posing significant hazards.

The Sicily channel volcanoes develop in shallow water areas, and are thus generally not associated with large edifice collapse. However, the records of historical submarine eruptions show that they can have large impact and are capable to cause hazard due to the possibility of pheratomagmatic eruptions that can also lead to tsunami generation.
The Etna volcano is also charactarized by large collapses. They have been shown to have caused tsunami although their impact is still debated.

Active faulting and slope failure in the Iberian margins: towards offshore geohazard mitigation

Valentí Sallarès [1], Eulàlia Gràcia [1] and Roger Urgeles [2]

[1] Unitat de Tecnologia Marina (CSIC), Centre Mediterrani d'Investigacions Marines i Ambientals, Barcelona, Spain

[2] Institut de Ciències del Mar (CSIC), Centre Mediterrani d'Investigacions Marines i Ambientals, Barcelona, Spain

Abstract

Several high-resolution marine geological and geophysical surveys have been carried out to investigate geohazards in the South and East Iberian Margins associated with slow-moving seismogenic faults and submarine landslides. Based on multiscale acoustic mapping, sub-seafloor seismic imaging, physical properties and dating methods, submarine fault systems and slope failure processes have been characterized with unprecedented resolution. Direct investigations of selected faults from the Mediterranean Sea and the external part of the Gulf of Cadiz yield their fault seismic parameters, suggesting that these faults are active and capable of generating large magnitude (Mw > 6) seismic events, representing an earthquake and tsunami hazard for the surrounding coastal areas.

Off-fault paleoseismic evidence in the SW Iberian Margin based on widespread synchronous turbidite deposits yields a regional recurrence rate of large magnitude earthquakes (Mw > 8) of 1800 – 2000 years. Submarine landslides are also ubiquitous in the Mediterranean margins of Iberia. Passive margins tend to have larger, but fewer landslides when compared to active margins. Most submarine landslides have areas in the range of 10 to 100 km^2. In general it is observed that submarine landslides in the western Mediterranean and Gulf of Cadiz originate beyond 2000 m water depth in slopes not exceeding 2º and display little vertical runout. Thus, only some infrequent large events are capable of tsunami generation. So far there are very little constraints on ages of most events. However, of these events that have been dated it is remarkable that a large number of them are reported as Holocene, which suggests a link to natural climate fluctuations. Detailed investigation of a few events suggests overpressures at depth in siliciclastic wedges and fluid seepage from sub-Messinian formations as important contributors for slope instability.

Introduction

Natural geohazards, such as earthquakes and landslides, are of immediate societal concern. In an oceanic setting they are capable of generating tsunamis that threaten coastal zones at distances of many thousands of kilometers (Morgan *et al.*, 2009). Since the deadly 2004 Sumatra-Andaman Islands earthquake (Mw=9.3) and subsequent tsunami there has been an increasing interest in understanding the recurrence, mechanics and processes associated with offshore geohazards in order to mitigate their effects. This has also raised public awareness of seismic, submarine landslide

and tsunami hazards. Most of the largest earthquakes are generated in submarine areas, essentially along subduction zones and other plate boundaries, while submarine landslides are ubiquitous but recurrence rates and typology vary according to geological setting, and so does their tsunamigenic potential (Camerlenghi *et al.*, 2010). This implies that offshore geohazards have a strong incidence near the coastline, where most of the world's population lives.

In the case of the Iberian Peninsula and margins, deformation is mainly controlled by the convergence between Africa and Eurasia, which is characterized by low to moderate magnitude seismicity (e.g. Buforn *et al.*, 1995; 2004; Stich *et al.*, 2003a; 2005) (Fig. 1). However, great earthquakes (Mw ≥ 8.0) such as the 1755 Lisbon Earthquake and Tsunami and the 1969 Horseshoe Earthquake have also occurred in this region (e.g. Buforn *et al.*, 2004; Baptista *et al.*, 1998; Martínez Solares and López Arroyo, 2004) (Fig. 1). Seismicity is also a major control in the distribution, magnitude and typology of submarine landslides (Camerlenghi *et al.*, 2010), but here other factors, mainly fluvial sediment input and margin progradation (Lastras *et al.*, 2007; Field and Gardner, 1990; Hampton *et al.*, 1996), come into play.

A multidisciplinary marine geological and geophysical dataset acquired during the last years offshore the Iberian Peninsula in the frame of National and European projects revealed a number of active faults and slope failures in the South and East Iberian margins which may represent a hazard to the coasts of Portugal, Spain and North Africa (e.g. Baraza, 1990; Rothwell *et al.*, 1996; Lastras *et al.*, 2002; 2004; 2007; Gràcia *et al.*, 2003a,b; 2006; 2010a; Terrinha *et al.*, 2003; 2010; Droz *et al.*, 2006; Urgeles *et al.*, 2006; 2007a; Vizcaino *et al.*, 2006; Dan *et al.*, 2007; Camerlenghi *et al.*, 2009; Zitellini *et al.*, 2009; Cattaneo *et al.*, 2010; Dan *et al.*, 2010). In this work we present an overview of the main submarine geological hazards that have the potential to affect the Iberian Margin, focusing on: a) active and seismogenic faults, and b) large slope failures. Final goals are the implications for seismic, slope failure and tsunami hazard assessment and recommendations for future actions, such as underwater long-term monitoring of active processes and deployment of early-warning systems near the Iberian Peninsula.

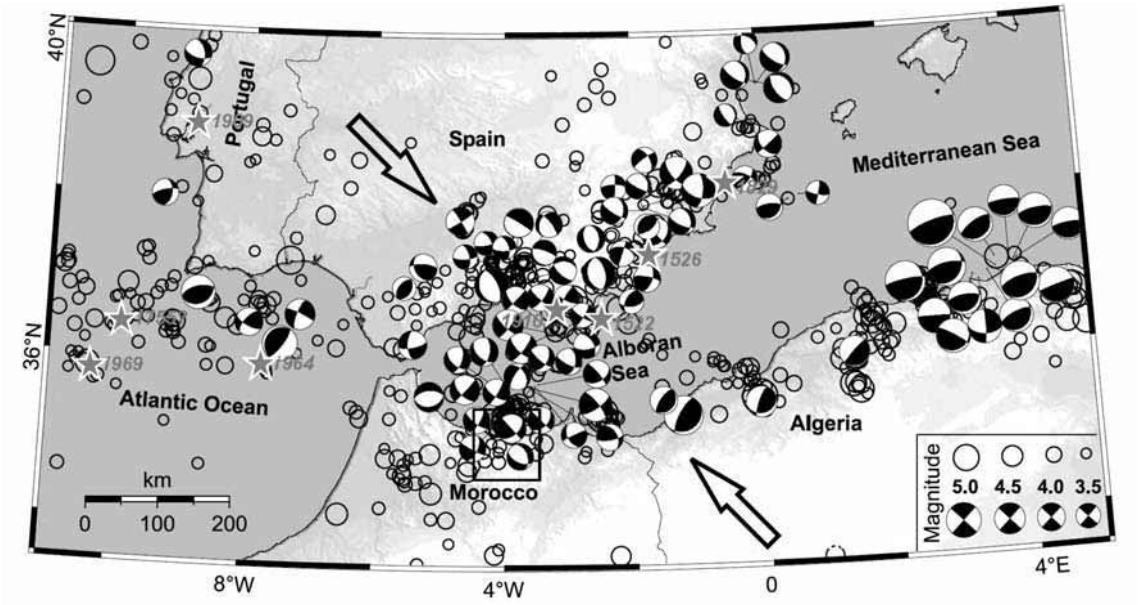

Figure 1. Seismicity and focal mechanism of Mw > 3.5 earthquakes occurred in the South Iberian and North African margins (Stich *et al.*, 2005), which include the Mediterranean Sea, Alboran Sea and Gulf of Cadiz. Stars depict large historical earthquakes occurred in the area.

Setting

The Western Mediterranean Sea comprises several basins defined by a structural framework related to the Alpine orogeny, the nature and age of the crust and their recent sedimentological development

(Biju-Duval and Montadert, 1976). Most deformation in the Western Mediterranean presently occurs in the South Iberian margin, Alboran basin and North African margin (Stich *et al.*, 2005). Crustal deformation in the south Iberian margin, which includes the offshore Atlantic and Mediterranean regions, is driven mainly by the NW-SE convergence (4-5 mm/year) between the African and Eurasian plates (e.g. Argus *et al.*, 1989). Convergence is accommodated over a wide active deformation zone suggesting distributed deformation among a number of tectonic structures. Earthquake mechanisms reveal that reverse to strike-slip faulting style dominates along the eastern Alboran Sea and external Gulf of Cadiz (e.g. Buforn *et al.*, 2004; Stich *et al.*, 2003; 2005), as corroborated by marine geological and geophysical data (e.g. Comas *et al.*, 1999; Gràcia *et al.*, 2003a,b; 2006; Terrinha *et al.*, 2003; 2009; Zitellini *et al.*, 2004; 2009) (Figure 1). Regional seismicity is characterized by shallow to deep earthquakes of low to moderate magnitude ($Mw < 5.5$) (Buforn *et al.*, 2004; Stich *et al.*, 2003a; 2005; 2010). However, large and destructive earthquakes ($Mw \geq 8.0$ and MSK Intensity X-XI) such as the 1755 Lisbon Earthquake, have also occurred in the region, and may represent a significant earthquake and tsunami hazard along the Iberian Peninsula and North African coasts. In South Iberia, assessment of seismic hazard is largely based on the relatively short period of instrumental and historical earthquake catalogues. This is not enough to assess seismic hazard in the region, especially when considering high-magnitude earthquakes with long recurrence intervals (> 1000 years) (e.g. Masana *et al.*, 2004; Gràcia *et al.*, 2010).

The Valencia Trough (VT), in eastern Iberia, is not as seismically active as its southern counterpart, but it has been recently shown that a number of faults have produced large earthquakes in historical and pre-historical times (Quaternary) (Perea *et al.*, 2006). It formed on the stretched continental crust that extends between the northeastern margin of the Iberian Plate and the Balearic promontory, the northeastern extension of the Betic thrust-belt (Roca *et al.*, 1999). The VT evolved as the southwestern branch of the oceanic Liguro-Provençal Basin, a late Oligocene-Miocene back-arc basin associated with the eastward roll-back of the west directed Apennines-Maghrebide subduction front (Doglioni *et al.*, 1997; Gueguen *et al.*, 1998). Rift-related tectonic extension of the eastern Iberian continental margin was controlled by major seaward-dipping listric faults that resulted from tectonic inversion of previous Paleogene reverse faults (Sàbat *et al.*, 1997; Roca *et al.*, 1999). The syn-rift stage resulted in the present horst-and-graben structure of the Catalan margin and it is recorded by thick (up to 2 km) Lower Miocene units restricted to the graben troughs.

The post-rift (Early Miocene to Recent) sedimentary history of the NE Iberian margin is characterized by the deposition of thick sedimentary sequences (Clavell and Berastegui, 1991). A major stratigraphic event on the Mediterranean continental margins of Iberia is the Messinian Salinity Crisis, which induced deposition of thick evaporitic deposits on the basin centers and major erosional unconformities on the proximal continental margins (Frey-Martínez *et al.*, 2004; Maillard and Mauffret, 2006; Maillard *et al.*, 2006; Ryan, 2008; Urgeles *et al.*, 2010).

The thick Pliocene and Quaternary sequence is up to 2500 m thick in the VT (Field and Gardner, 1990; Maillard *et al.*, 1992) and is characterized by numerous marine transgressive–regressive pulsations (Field and Gardner, 1990; Nelson and Maldonado, 1990; Evans and Arche, 2002; Bertoni and Cartwright, 2005). Abundant sediment supply from the Ebro River has resulted in particular clinoform geometries and a relatively wide continental shelf of the Ebro Margin, extending up to 80 km offshore compared to the 40 km of its northern and southern counterparts (Amblas *et al.*, 2006).

Active faults in the south iberian margins

Fault exploration of active regions integrates the most advanced technologies covering different scales of resolution (Díez and Gràcia, 2005; Bartolomé *et al.*, 2008). It requires acoustic mapping techniques (swath-bathymetry, sidescan sonar data) and sub-seafloor seismic imaging methods, ranging from high-resolution sub-bottom profiler (uppermost tens of meters of penetration) to multichannel seismic (MCS) data (several km of penetration), which allow identifying the geomorphic evidence of active faults and stratigraphic evidence of past seismic activity. In the SE Iberian Margin, Quaternary faulting activity is dominated by a large left-lateral strike-slip system of sigmoid geometry referred to as the Eastern Betic Shear Zone. The active fault system stretches

over more than 450 km, and its terminal splays extend further into the sea, corresponding to the Bajo Segura Fault to the north and the Carboneras Fault to the south (Fig. 2). Recent exploration of the Bajo Segura Fault reveal a thick Quaternary sedimentary sequence affected by folding and reverse faulting reaching up to the seafloor (Perea *et al.*, 2009). This fault has been suggested as a potential source of the historical 1829 Torrevieja earthquake (I=XI).

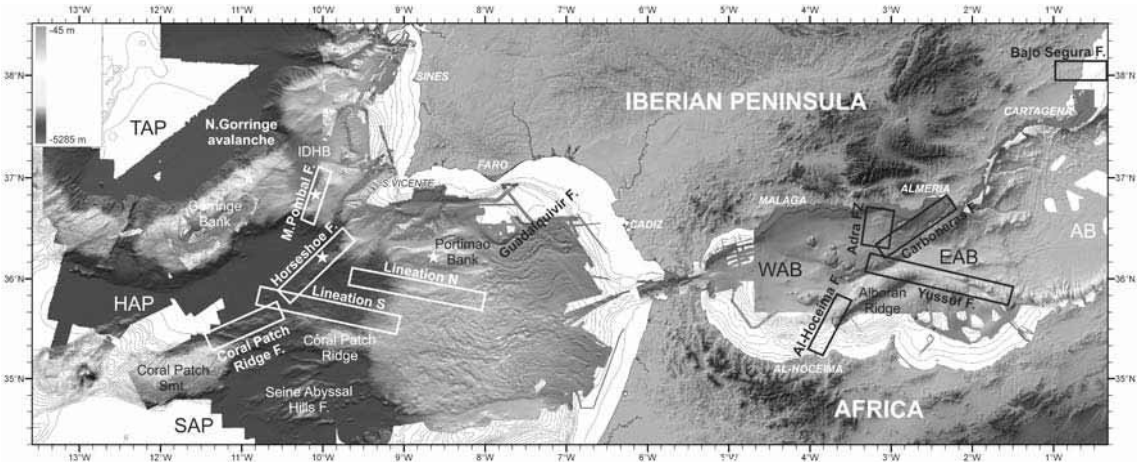

Figure 2. Topographic and bathymetric map of the Alboran Sea and Gulf of Cadiz. In the Alboran Sea (bathymetric map modified from MEDIMAP *et al.*, 2008), the fault systems presented are depicted by a black outlined box. WAB: Western Alboran Basin; EAB: Eastern Alboran Basin; AB: Algerian Basin. In the Gulf of Cadiz (bathymetric map modified from Zitellini *et al.*, 2009), the studied fault systems are marked by white outlined boxes. Yellow stars depict large landslides. TAP: Tagus Abyssal Plain; IDHB: Infante Don Henrique Basin; HAP: Horseshoe Abyssal Plain; SAP: Seine Abyssal Plain (Gràcia *et al.*, 2010b).

[see original colour illustration in Annex at end of volume]

In the Alboran Sea, the offshore Carboneras Fault (100 km long) is characterized by seafloor ruptures, deflected channels, pressure ridges, water gaps and push-ups typically found on active transpressional fault systems. A dense grid of high-resolution multichannel seismic (MCS) profiles allowed us to characterize the along-fault geometry between the segments, and dip-slip rates of up to 0.1 mm/a for the last 128 ka have been suggested (Moreno *et al.*, 2008; 2010). Based on left-laterally offset gullies, a Quaternary strike-slip rate of 1.3 mm/a was obtained. The observed segmentation allowed us to suggest that the N45 segment, which runs onshore and partly offshore, is able to generate Mw~7.4 earthquakes (Gràcia *et al.*, 2006). Related structures, such as the NNW-SSE trending, closely spaced and short subvertical faults located to the west of the Carboneras Fault, referred here as Adra FZ (Fig. 2), have also been imaged and investigated using acoustic and multi-scale seismic data (TOPAS, Sparker and high-resolution MCS). One of these structures, trending NW-SE, is very likely to be the source of the 1910 Adra Earthquake of estimated Mw 6.0 (Stich *et al.*, 2003b) (Fig. 1).

Other relevant fault systems, such as the Yussuf and Al-Idrisi Faults, have recently been investigated to image and characterize their geomorphology and detailed structure in order to determine how they accommodate the present-day strain regime between the African and Eurasian Plates. High-resolution and deep penetration multichannel seismic reflection methods were used during the EVENT-DEEP cruise on board the R/V Sarmiento de Gamboa (Bartolomé *et al.*, 2010). The Yussuf Fault is a 250 km long WNW-ESE trending dextral strike-slip fault running from the Eastern Alboran Sea to the Algerian Basin. The fault is formed by two main segments, western and eastern, which overlap in a deep pull-apart basin (Fig. 3). Based on empirical relationships between fault rupture length and maximum magnitude (Wells and Coppersmith, 1994), each of the segments is able to generate Mw 7.4 earthquakes. The Al-Idrissi Fault is a 150 km long NNE-SSW trending left-lateral strike-slip structure located to the SW of the Alboran Ridge (Martínez-García *et al.*, 2010; Bartolomé *et al.*, 2010). This area is characterized by intense seismic activity (Fig. 1), and the Al-Idrissi Fault may be the source of large events, such as the 1994 Al Hoceima Mw 6.0 earthquake.

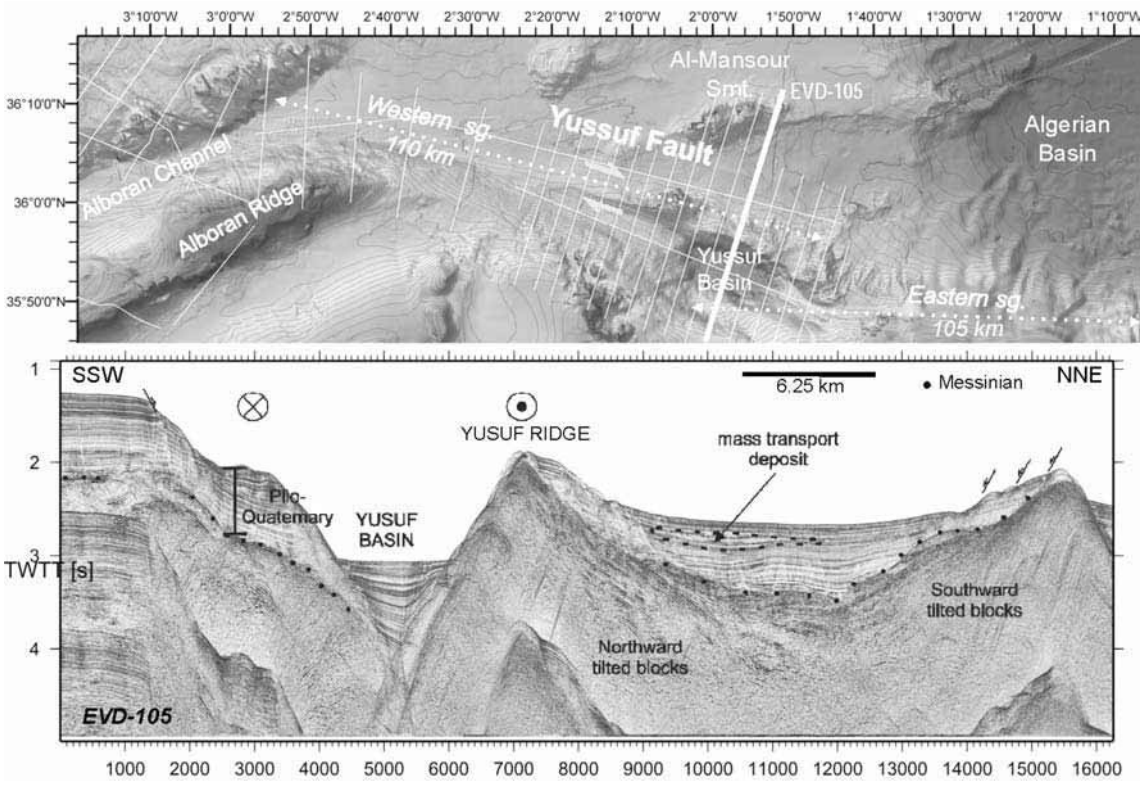

Figure 3. Top: Swath bathymetric map of the Yussuf Fault in the Alboran Sea, modified from MEDIMAP *et al.* (2008), where the main structures are located. Multi-channel seismic profiles acquired during the EVENT-DEEP survey are depicted by white lines. Bottom: Preliminary interpretation of the high-resolution seismic profile EVD105, which images with unprecedented resolution the Yussuf Fault at the pull-apart basin located in the eastern part of the Alboran Sea (Bartolomé *et al.*, 2010).

[see original colour illustration in Annex at end of volume]

In the SW Iberian Margin, fault investigations mainly focused on the active structures located at the external part of the Gulf of Cadiz, source of the largest earthquakes and tsunamis that have affected Western Europe. Recent surface ruptures have been recognized in this area, which correspond to the active NE-SW trending west-verging folds and thrusts of the Marques de Pombal Fault, Sao Vicente Canyon Fault, Horseshoe Fault and Coral Patch Ridge Fault (Zitellini *et al.*, 2004; Gràcia *et al.*, 2003a, 2010; Terrinha *et al.*, 2003). The Marques de Pombal Fault is a 50 km long west verging monocline thrust cutting through the Plio-Quaternary units (Fig. 1). Deformation is accommodated by a blind thrust to the south and a fold to the North. This fault, together with the Horseshoe Fault had been suggested as a potential source of the 1755 Lisbon earthquake (e.g. Gràcia *et al.*, 2003a; Zitellini *et al.*, 2004). The Horseshoe Fault is an 80-90 km west-verging thrust limited to the north by the NNE-SSW Sao Vicente Canyon Fault and to the south by the ENE-WSW trending Coral Patch Ridge Fault (Fig. 1). MCS data evidence that it is an active structure, as the fault reaches up to the surface cutting through the Plio-Quaternary units (Gràcia *et al.*, 2003a). The fault is also source of intermediate to large magnitude earthquakes, such as the 2007 Horseshoe event (Mw 6.0) (Stich *et al.*, 2007), and may be able to generate up to Mw 8.0 events. The Coral Patch Ridge Fault is an active 100 km long low-angle blind thrust verging to the NW (Fig. 1). The fault separates the Horseshoe Abyssal Plain from the Seine Abyssal Plain, generating a cumulated relief of 700 m (Martinez-Loriente *et al.*, 2009). To the south, the Seine Abyssal Hills Faults are a succession of highs and depressions, corresponding to conjugated ENE-WSW trending folds and thrusts verging to the NW and SE. Although this area is characterized by a subdued seismic activity, seismic data reveal that these thrusts are active and may be able to generate earthquakes up to magnitude Mw 7.

In addition, long WNW-ESE strike-slip faults referred as SWIM Lineations have recently been identified (e.g. Zitellini *et al.*, 2009; Terrinha *et al.*, 2009) (Fig. 1), and extend hundreds of km from the Horseshoe Abyssal Plain to the inner part of the Gulf of Cadiz (Terrinha *et al.*, 2009; Zitellini *et al.*, 2009) (Fig. 1). Recently acquired MCS data evidence that these structures correspond to large strike-slip faults, with a 3 to 6 km wide deformation zone and reaching up to 10 km deep (Bartolomé *et al.*, 2009a,b). TOPAS images reveal surface ruptures and morphologies of positive and negative flower structures. Moment tensor inversion of deep (40-50 km) Mw < 6.0 earthquakes occurred along one of these lineaments (Geissler *et al.*, 2010; Stich *et al.*, 2010), showing right-lateral strike-slip fault solutions, consistent with the geometry identified in the seismic data.

On the basis of geological evidence, geophysical data and tsunami modelling, different geodynamic models and mechanisms have been proposed as the source of the 1755 Lisbon Earthquake and Tsunami (e.g. Baptista *et al.*, 2003; Gutscher *et al.*, 2002; 2004; Gràcia *et al.*, 2003a; Terrinha *et al.*, 2003; 2009; Zitellini *et al.*, 2004; 2009; Stich *et al.*, 2007). However, none of these models satisfactorily accounts for the estimated magnitude of the earthquake and tsunami arrival times at the different localities onshore (Gràcia *et al.*, 2010).

Slope failures in the Iberian margins

Submarine landslides are ubiquitous on the Mediterranean margins of Iberia and adjacent areas (Fig. 4). Available marine geophysical data, comprising swath-bathymetry, side-scan sonar, high-resolution and deep penetration MCS profiles, and sediment cores evidence complex slope failure systems. Understanding the distribution of known submarine landslides is not straightforward because of incomplete coverage and lack of uniform studies in all areas. Nevertheless, during the last two decades, improvements in swath mapping and geophysical techniques, plus growing interest of both academia and industry in these processes, have allowed to identify hundreds of submarine landslides. With the aim to understand the causes of the submarine landslides mapped in recent years in the continental margins of the Western Mediterranean, we have undertaken a compilation of information from the scientific literature into a GIS-based framework (Camerlenghi *et al.*, 2010). This work provides a first step towards understanding the role of geology in controlling the patterns, frequency and magnitude of submarine slope failures, an essential part for

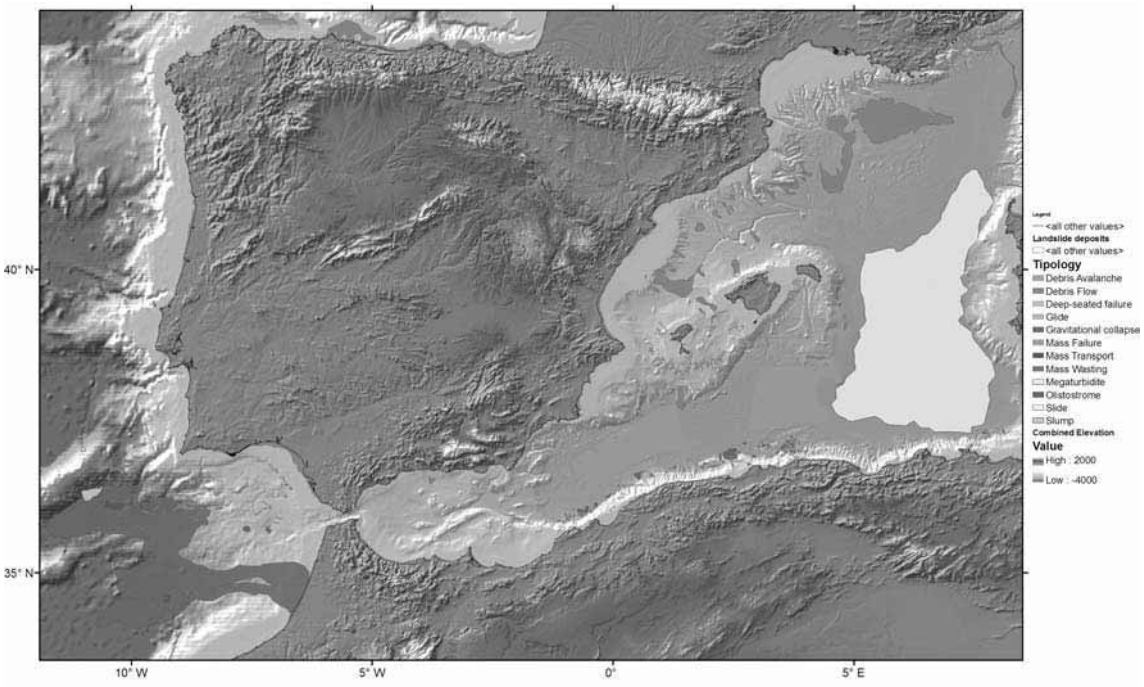

Figure 4. Display of all the submarine landslides in the eastern and southern Iberian margin, compiled from multiple sources, superimposed to the bathymetry shaded relief map (IOC, IHO and BODC 2003; Medimap Group *et al.*, 2008).

[see original colour illustration in Annex at end of volume]

assessing the geohazard from submarine landslides (e.g. Morgan *et al.*, 2009; Urgeles *et al.*, 2007b) in the W Mediterranean basin.

The largest mass transport deposits in the Western Mediterranean and Gulf of Cadiz are the Upper Miocene olistostromal bodies associated with the westward advance of frontal thrusts of the Gibraltar Arc (e.g. Maestro *et al.*, 2003; Iribarren *et al.*, 2007) and the megaturbidite that deposited on the Balearic Abyssal Plain at ~22 ka cal BP with a volume of ~500 km^3 and an area ~6x10^4 km^2 (Rothwell *et al.*, 1998) (Fig. 4). The latter remains however an enigmatic event as the source area has not been identified yet. Quaternary submarine landslides in the Western Mediterranean have modest to medium sizes, with the deposits involving areas generally smaller than 200 km^2 (Fig. 5A). 64% of the landslides display depositional areas in the range of 10 to 100 km^2 (Fig. 5B). The most tectonically active margins display the largest number of slope failure events but, on the other hand, the landslides tend to be smaller (Fig. 4). In the Algerian Margin, for example, 146 submarine landslides are reported with a mean area of 23,37 km^2 (Cattaneo *et al.*, 2010). In the Alboran Sea the number of reported failures is small (7), but similar in terms of deposit surface (30,82 km^2), and in the Gulf of Cadiz, a total of 29 submarine landslides are reported with a mean surface of 153,405 km^2. On the opposite side, are the areas displaying lower seismicity, but fed by large river systems: in the Ebro Margin the numbers are 41 events and a mean surface of 187,97 km^2, and finally for the Gulf of Lions and Ligurian Slope 53 events have been reported with a mean area of 402,40 km^2. For the Algerian margin, Cattaneo *et al.* (2010) indicate that there appears to be a relationship in the distribution of landslides with seafloor morphologies and structures of tectonic origin (Fig. 4). However, the distribution of recent earthquake epicenters versus submarine landslides offers no immediate comprehension.

Most landslides in the western Mediterranean originate in water depths exceeding 2000 m on slopes of 2º and most of them arrest only in slightly deeper water depths (Fig. 5C). This is also shown by the relatively short vertical runout that most landslide deposits show, with most of the

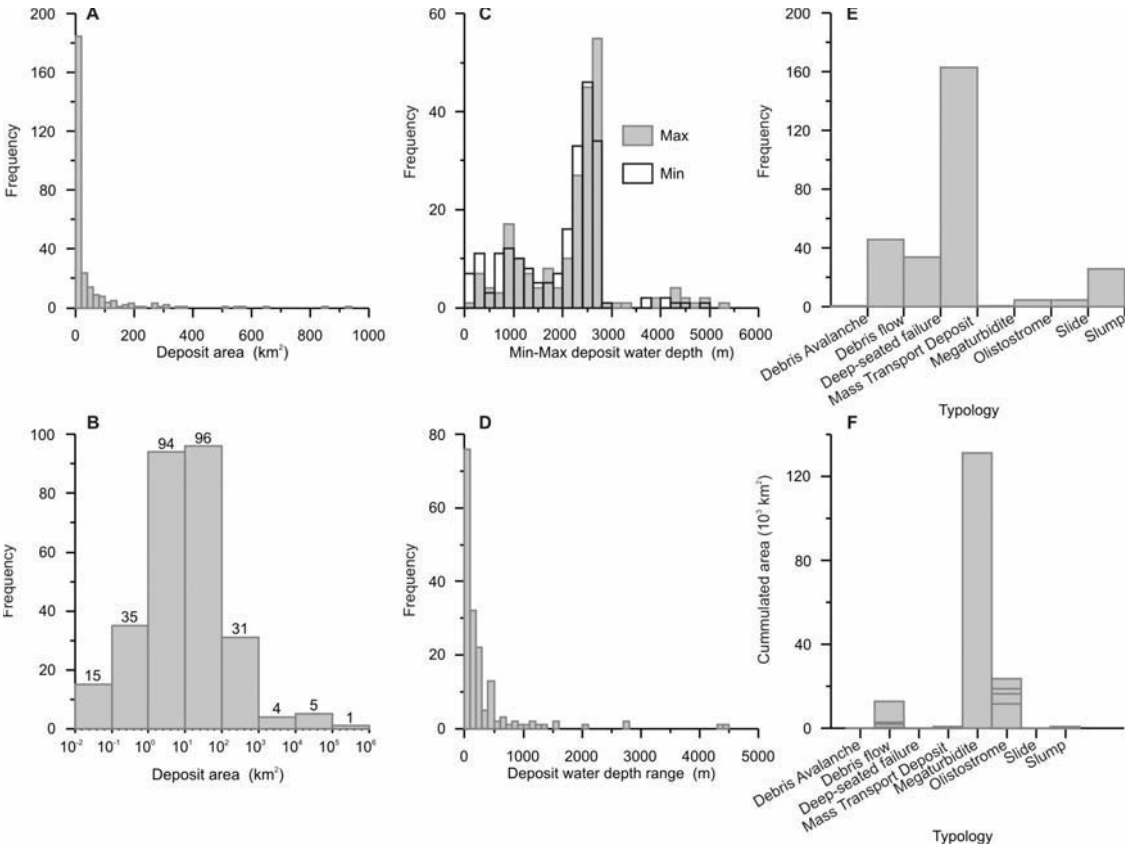

Figure 5. Statistical distribution of significant parameters of submarine landslides in the Western Mediterranean basin.

events (44%) displaying vertical runouts not exceeding 100 m, while 85% of the landslides have a vertical runout shorter than 500 m (Fig. 5D). This illustrates that a) most of the landslides in the database are relatively small landslides, but also b) that the continental rise is a place of higher slope instability compared to the continental slope; and c) that limited energy is available for down-slope sediment transport, with most failures arresting shortly after triggering and/or producing almost null sediment transport, as illustrated for the Eivissa Slides (Lastras *et al.*, 2004). Most submarine landslides have been generically identified as Mass Transport Deposits, but debris flows, deep-seated failures and slumps are common failure styles in the Western Mediterranean (Fig. 5E,F).

With regard to the age of the failure events little is known so far, stressing how little we know on the recurrence of these phenomena. Of the 282 submarine landslides events reported in Fig. 4 only 14 of them have somewhat accurate age determinations. The age of 66 events are simply reported in the literature with a geologic epoch, which induces a large error bar and makes almost impossible to establish a relationship with triggering mechanisms and environmental factors. Nevertheless, the large amount of these 66 events that are reported as Holocene (53 events mostly in the Ebro, Gulf of Lions and Ligurian Margins) is surprising. It suggests that climate induced stress changes (sea level and bottom temperature changes, and their effect on gas hydrate and gas systems, sedimentary load, etc.) have had a major role in triggering slope failures.

In tectonically active areas such as the Gulf of Cadiz, a detailed characterization of the mass-wasting deposits indicates that submarine landslides are associated with active faults and may therefore yield information of fault past activity (Gràcia and Lo Iacono, 2008). For instance, a

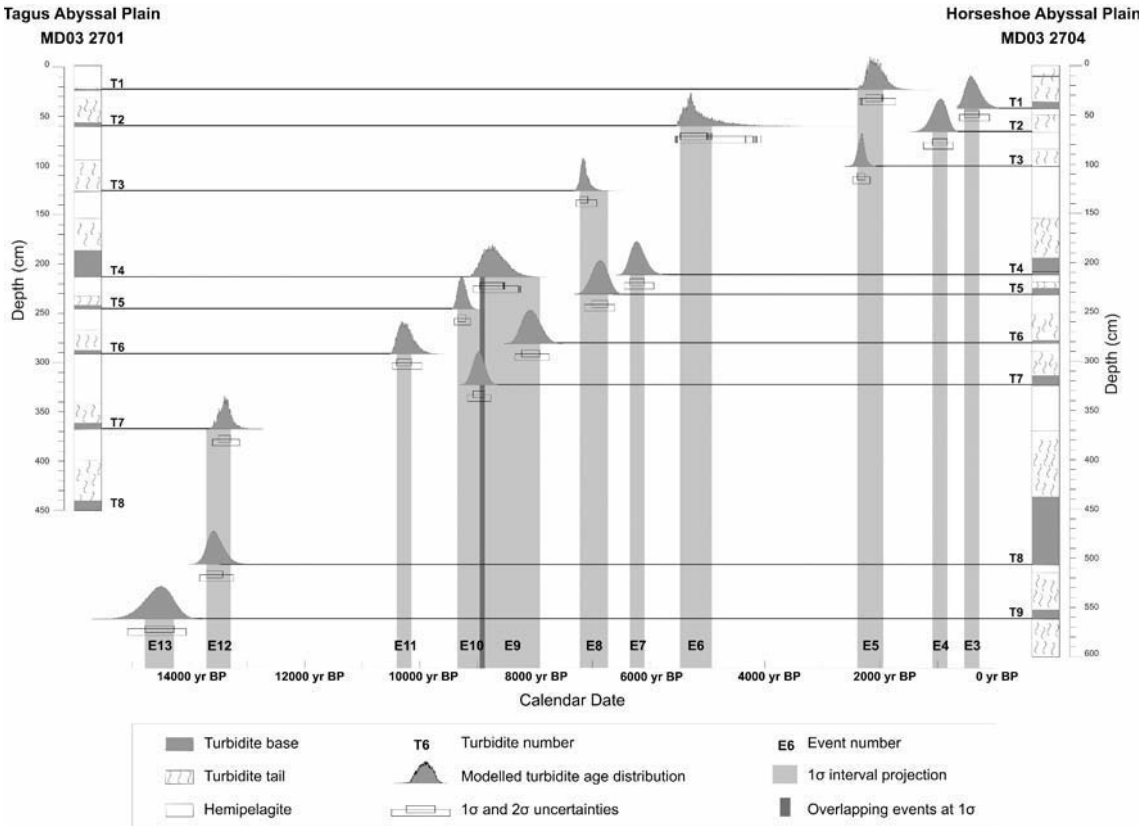

Figure 6. Age correlation of turbidites from the Tagus Abyssal Plain (MD03 2701) and the Horseshoe Abyssal Plain (MD03 2704). Probability distribution curves of modelled turbidite ages (orange) were obtained using OxCal 4.0 calibration software. Black horizontal lines link turbidite bases and their respective calibrated ages. Modelled turbidite ages (1s) are projected on the time axis by a purple band, where event numbers are indicated (Gràcia *et al.*, 2010).

[see original colour illustration in Annex at end of volume]

large (260 km^2) translational landslide and debris flow is associated to the Marques de Pombal Fault. The most recent slide has an age of about 230 yr BP, and it may have been triggered by the AD 1755 Lisbon earthquake (Gràcia *et al.*, 2010). By dating previous slide deposits a recurrence

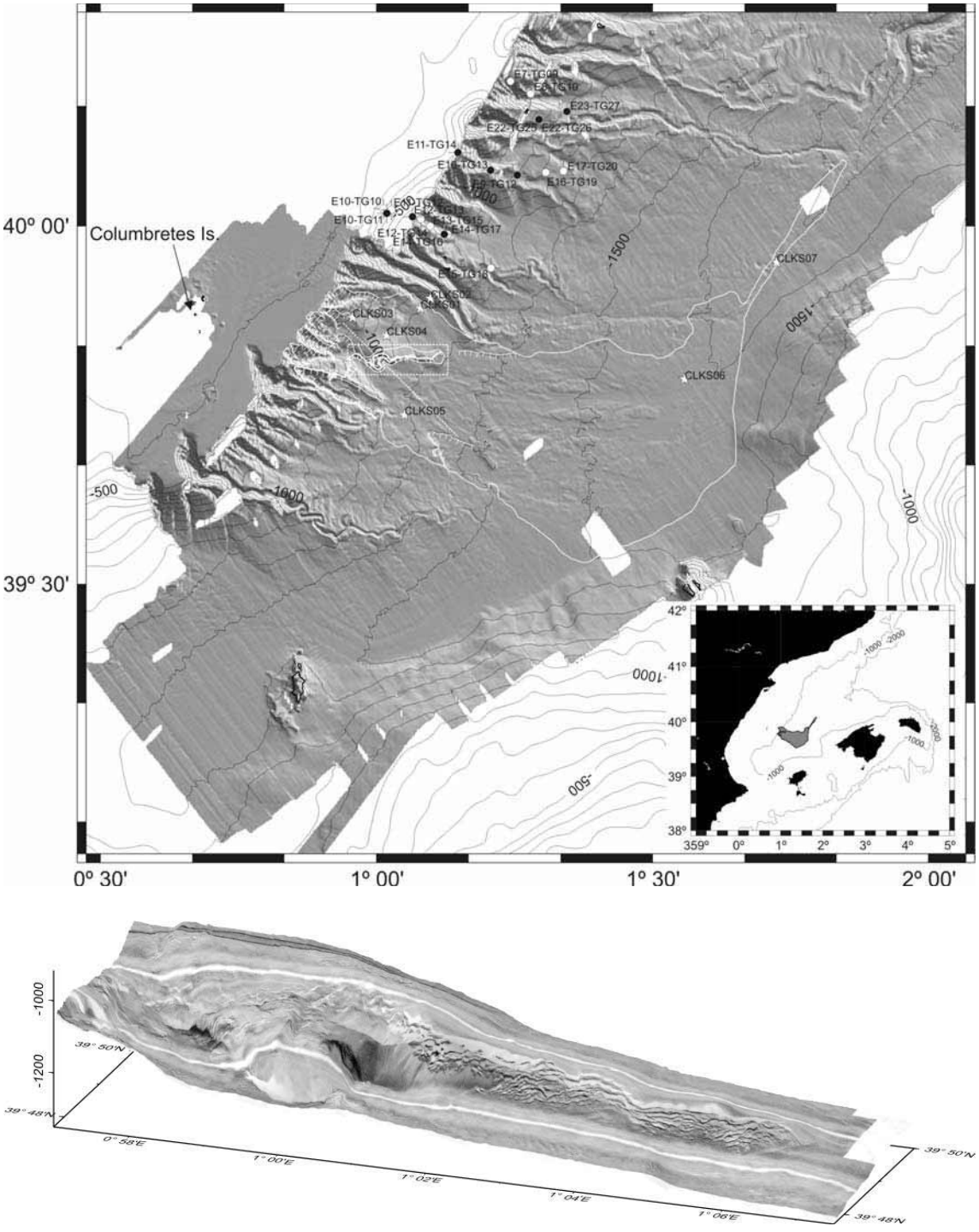

Figure 7. Top: Swath bathymetry of the BIG'95 debris flow area with location of the landslide boundaries. Debris flow deposit is shown as white solid line, main scar as white, thick solid hatched line, secondary scars are shown as white, thin hatched lines. Box with dashed outline provides location of Bottom figure. Stars show location of cores collected for geotechnical tests. Circles with crosses show the location of cores described in Baraza *et al.* (1990). Bottom: MAK-1M deep-towed side-scan sonar sonograph draped on EM-12 swath bathymetry showing the complex morphology of the BIG'95 headwall scar. See dashed box in Top Figure for location.

period of 2000 yr has been obtained (Vizcaino *et al.*, 2006), suggesting a cyclic activity of the Marques de Pombal Fault.

Turbidite deposits are also key to investigate the recurrence rate of great magnitude (Mw > 8) Holocene events, such as the AD 1755 Lisbon earthquake. The "turbidite paleoseismology" concept has been applied to the SW Iberian margin (Gràcia *et al.*, 2010). Sediment cores collected in the Tagus Abyssal Plain, Infante Don Henrique Basin, Horseshoe and Seine Abyssal Plains reveal that deep-sea basins preserve a record of episodic deposition of turbidites (Fig. 6). In the SW Iberian Margin, excluding specific climatic events, earthquakes are the most likely triggering mechanism for synchronous, widely-spaced distributed turbidites during the Holocene, when the sea level was relatively stable. Age correlation together with textural, physical properties and geochemical signatures of turbidite deposits reveals a total of seven widespread turbidite events for the Holocene. Precise dating of the most recent turbidite event based on ^{210}Pb and ^{137}Cs geochronology provides an age of AD 1971 ± 3 (Garcia Orellana *et al.*, 2006). This age corresponds to a high-magnitude instrumental earthquake in the region: the 1969 Horseshoe earthquake (Mw~8.0). Calibrated ^{14}C ages of subsequent widespread turbidite events correlate with the dates of important historical earthquakes and paleotsunami deposits in the Gulf of Cadiz area, such as AD 1755 and 218 BC, respectively. Taking into account older synchronous events, from 4960-5510 yr BP to 8715-9015 yr BP, a relatively large earthquake recurrence interval of about 1800 years is obtained for the Holocene (Gràcia *et al.*, 2010).

Finally, little is known on the actual slope conditions that led to occurrence of the observed slope failures. Physical properties of marine sediments of the Mediterranean margins of Iberia are scarce (Baraza *et al.*, 1990; Chassefiere, 1990; Urgeles *et al.*, 2003; Urgeles *et al.*, 2006; Sultan *et al.*, 2007; Lafuerza, 2009) and the continental margin hydrogeological regime is virtually unknown. Back-analysis of one of the largest submarine landslides in the region, the BIG'95 (Urgeles *et al.*, 2006; Fig. 7) suggests that large overpressures must be present at depth. In other instances fluid escape from sub-Messinian formations appears likely to produce significant stress reductions as to produce failure of the slope when additional environmental factors such as sea level lowering are added (Lafuerza *et al.*, 2009).

Potential tsunami genesis

The Western Mediterranean is vulnerable to marine geohazards due not only to the high density of coastal population, but also to its small dimensions. The latter results in close proximity between tsunami sources (induced by either co-seismic seafloor displacement or a submarine landslide) and impact areas (Camerlenghi *et al.*, 2010). All major active faults are potentially capable of generating large tsunamis, especially many of those located in the Gulf of Cadiz, such as the Marques de Pombal, Gorringe Bank, Horseshoe, São Vicente Canyon faults, Coral Patch Ridge and Portimao Bank faults (e.g. Baptista *et al.*, 1998b; 2003; Gjevik *et al.*, 1998; Barkan *et al.*, 2009; Lima *et al.*, 2010) or a postulated west-verging mega-thrust beneath the Gulf of Cadiz sedimentary wedge (Gutscher *et al.*, 2002; 2006; Barkan *et al.*, 2009; Lima *et al.*, 2010). A tsunami originated in any of these potentially seismogenic structures, capable of generating earthquakes of over Mw~8.0, would hit most of the southwestern Iberian coasts in less than 30 minutes (e.g. Baptista *et al.*, 1998; 2003). A clear example of the high tsunami hazard in the area is the occurrence of the huge tsunami that devastated the region in 1755, with a maximum observed run-up of ~15 m in Cape São Vicente (e.g. Baptista *et al.*, 1998a).

In order to better understand the current geodynamic setting of the area, characterize the most relevant tsunamigenic sources, and assess the present-day implications including seismic and tsunami hazard, successive national and European projects have been funded since 1998 (i.e. EU BIGSETS, ESF EuroMargins SWIM, IMPULS, VOLTAIRE, MATESPRO, DELILA and EU NEAREST). In the frame of the NEAREST project (NEAR shore sourcES of Tsunamis: towards an early warning system), a prototype of a tsunami early warning system (similar to GEOSTAR) has been developed and deployed offshore the Algarve coast (Portugal) for a year to direct monitoring tsunamigenic structures located near the coasts of SW Iberia (Zitellini *et al.*, 2011). Mass failures may also contribute to tsunami generation. However, as explained above, most failures have limited volume, short runout and originate in relatively deep water. Therefore only

the largest albeit infrequent events are likely to trigger tsunamis. The BIG'95 (Fig. 7), with a volume of 26 km^3 and 110 km runout, is one such event (Løvholt *et al.*, 2009; Tinti *et al.*, 2009; Iglesias *et al.*, 2010). Simulations show that maximum amplitudes follow the main sliding direction. The initial shores to be hit by the tsunami are the coasts of Eivissa (15 min) followed by Mallorca (20 min) and the Iberian Peninsula (45 min), which reflects the asymmetric bathymetry of the Valencia Trough and the shoaling effect caused by the wide continental shelf of the Ebro margin (Iglesias *et al.*, 2010). On the Gulf of Cadiz, the north Gorringe rock and debris avalanche with an estimated volume of 70-80 km^3, may also represent a potential threat for the surrounding coastal areas and beyond if a similar event occurs in the future. Numerical tsunami modeling results of this avalanche show that the Portuguese coast would be hit by 10 m high tsunami waves in around 30 minutes, and the Spanish and African coasts in about 60 minutes (Lo Iacono *et al.*, 2010; Zaniboni *et al.*, 2010).

Recommendation for future actions

Fault morphology and segmentation are well expressed underwater, as erosion is minimized and scarps are better preserved. Cross-cutting relationships revealed in map view (e g. offset channels) or in depth-section (e.g. faulted horizons) allow detailed fault recognition (Pantosti and Gràcia, 2010). However, large difficulties appear when dealing with slow-moving faults located in low sedimentation rate areas, such as the south Iberian margins. An important gap of knowledge concerns the identification of earthquake single ruptures and the obtention of vertical and strike-slip components per event (i.e. co-seismic slip). This is based on the ability to recognize and date individual event horizons, as is done in trenches on land. This is a topic for future research and technological development as it essentially depends on the vertical resolution of the underwater acoustic and seismic imaging methods. Moreover, difficulty rises when assigning historical and instrumental earthquakes to identified submarine faults, as earthquake location in oceanic areas has large uncertainties. Future implementation of long-term deployment of broadband seismic stations in active continental margins is needed.

Paleoseismic evidence based on identification and age of earthquake-triggered turbidite deposits may help obtain the recurrence rate of large magnitude (Mw > 6) earthquakes (i.e. Goldfinger *et al.*, 2003; Pantosti *et al.*, 2011), which is essential for seismic hazard assessment. However, the use of turbidites as paleoseismic indicators requires demonstrating that earthquakes are their most plausible triggering mechanism. Other gaps of knowledge are related to: (i) the selection of sediment coring sites, as events may be missing or under-represented depending on the depositional location; (ii) the link between the turbidite thickness and the magnitude of an earthquake as this relation is not straightforward; and (iii) the limitations to obtain accurate ages using radiocarbon techniques, due to the spatial and temporal variability of the ^{14}C reservoir age, essential for date calibration. Future lines of research may go in the line of modeling underwater active processes, such as turbidity flows, to better understand and tie paleoseismic observations. Paleoseismic parameters derived from subaqueous on-fault studies as well as recurrence intervals (regional or related to an individual fault) derived from off-fault earthquake triggered underwater mass transport deposits should be taken into account in any future seismic hazard assessment. This is especially important in active margins near highly populated areas, such as the Mediterranean Basin.

Besides information that a considerable number and relatively large (at least compared to their subaerial counterparts) submarine landslides are present along the Mediterranean continental margins of Iberia, and the whole Mediterranean (Camerlenghi *et al.*, 2010), little is known about the early phases of submarine landslide initiation, the materials that originate submarine landslides or the steady-state and/or transient conditions under which early deformation and subsequent slope failure evolve. Moreover there is a lack of understanding on early post-failure evolution of submarine slope failures, which is critical for assessing tsunami hazard from submarine landslides. Finally, a major gap in knowledge concerns the timing of failure processes and the precise age of failed sediment accumulations. It is therefore now time to start a new approach that includes not only sampling and high resolution geophysical data acquisition, but also in-situ measurements and long-term monitoring in addition to major modeling efforts. Major advances in our understanding of submarine landslides require capturing episodic events related to: seismology, slope deformation, gas venting and hydrogeology under steady-state and transient conditions that lead

to slope failure. Submarine slope failures have occurred recently in the western Mediterranean (El-Robrini *et al.*, 1985; Dan *et al.*, 2007) and past mapping efforts have shown evidence (cracks, depressions, partial failure, gas release…) which question how the stability of these margins is evolving (Urgeles *et al.*, 2006; Frey *et al.*, 2010; Sultan *et al.*, 2010), and at the same time offer a unique opportunity to study submarine slope failure development. Main actions should include identifying rates of seafloor deformation and precursory signs of slope instability, investigating the role of climate change in slope instability, better understand how continental margin development affects fluid flow focusing and pore pressure build-up and investigating post-failure evolution.

Acknowledgements: we acknowledge financial support from Spanish Ministry of Science and Innovation (MICINN) through Project EVENT (CGL2006-12861-C02-02), EDINSED3D (CTM2007-64880/MAR), AC NEAREST-SEIS (CGL2006-27098-E/BTE), AC EVENT-SHELF (CTM2008-03346-E/MAR), AC NEAREST-CORE (CTM2008-04938-E/MAR), AC SUBPALEOSIS (CTM2010-10179-E), CSIC grant PROINSED (200930I178), ESF-TOPOMED (CGL2008-03474-E), EU Specific Targeted Research Program NEAREST project (n. 037110) and IUGS-UNESCO International Geoscience Program for projects SMMTC (IGCP-511) and E-MARSHAL (IGCP-585). We wish to thank the captain, crew, technical and scientific team on board the R/V Hesperides, R/V Marion Dufresne, R/V Garcia del Cid and R/V Sarmiento de Gamboa for their assistance during the marine cruises. This work has been carried out within Grup de Recerca de la Generalitat de Catalunya Barcelona Centre of Subsurface Imaging (B-CSI) ref. 2009 SGR 146.

Tsunamis in the Euro-Mediterranean region: emergency and long term counter measures

Stefano Tinti [1], Alberto Armigliato [1], Gianluca Pagnoni [1], Filippo Zaniboni [1] and Roberto Tonini [2]

[1] *Dipartimento di Fisica, Settore di Geofisica, Università di Bologna, Italy*
[2] *Istituto Nazionale di Geofisica e Vulcanologia, Sezione di Bologna, Italy*

Abstract

Tsunamis are known to occur in the Mediterranean Sea where all types of sources – earthquakes, volcanic eruptions and landslides from the continental margins – are active. Despite a rich historical record, awareness of the threat posed by tsunamis was restricted to specialists until the Indian Ocean 2004 disastrous tsunami. This was a shock for the public even in Europe. The immediate effect was, among others, the planning of a number of regional and national Tsunami Warning Systems (TWS), the implementation of which was to be coordinated by the UNESCO/IOC (Intergovernmental Oceanographic Commission) through the intergovernmental group called ICG/NEAMTWS.

This paper analyses the efforts made by the international community to create the TWSs in the region, and the reasons why their implementation resulted to be a slow process that nowadays is still incomplete: five years after the establishment of the ICG/NEAMTWS, only a few national TWSs are in operations, while a few regional TWSs are in a pre-operational phase.

In addition to the efforts for building TWSs, countermeasures in the long term have to be developed and planned. In this category one can include all studies of tsunami hazard, tsunami vulnerability and tsunami risk, and the related plans for tsunami risk mapping, for evacuation, and for sustainability of coastal area development. Methods have been defined by recent research, but unfortunately they have not been given adequate attention by local authorities and have not been incorporated in any practical actions for defence from marine hazard of any coastal communities of southern Europe, not even in the one that happened to be the most exposed to tsunami attacks.

Today southern Europe is unprotected from tsunamis as it was in the last century, but it is much more vulnerable since the occupation of the coastal belt has grown enormously in the meantime.

1. Introduction

As detailed elsewhere in this volume, an ICG (Intergovernmental Coordination Group) for the Euro-Mediterranean region, denominated ICG/NEAMTWS was created in Europe in 2005 within the frame of the UNESCO/IOC (Intergovernmental Oceanographic Commission) to foster and harmonise all the initiatives for the creation of Tsunami Warning Systems (TWS). The main starting points or motivations to create the ICG/NEAMTWS were: 1) the Euro-Mediterranean region was theatre of large tsunamis in the past with disastrous effects, particularly in a southern belt running from Portugal and Morocco in the west to Turkey in the east (see the tsunami map in Figure 1); 2) most of the tsunami sources are very close to the coast, and therefore the leading time of the tsunami to the nearest coast is very short (less than 5-10 minutes); 3) the Mediterranean basin and its sub-basins (e.g. the Marmara sea) are small compared to the large oceans, and therefore even the remote coasts that are under the menace of disastrous waves in less than one hour (see Figure 2); 4) the Euro-Mediterranean region is among the most developed in the world with growing importance of the coastal belt for all the countries, both offshore and onshore, and with increasing usage and occupation of the coastal territories in terms of economic and industrial activities, including tourism and residential settlements; 5) hence the vulnerability and risk of the coasts has been enormously increased in the region, and the repetition of some of the largest historical tsunami occurrence could result under unfavourable circumstances (i.e. if it happens in coincidence with peak touristic season and in daily hours) in a disaster even larger than the Indian Ocean 2004 case; 6) tsunami can affect some mega-towns in the region (such as Istanbul, Alexandria).

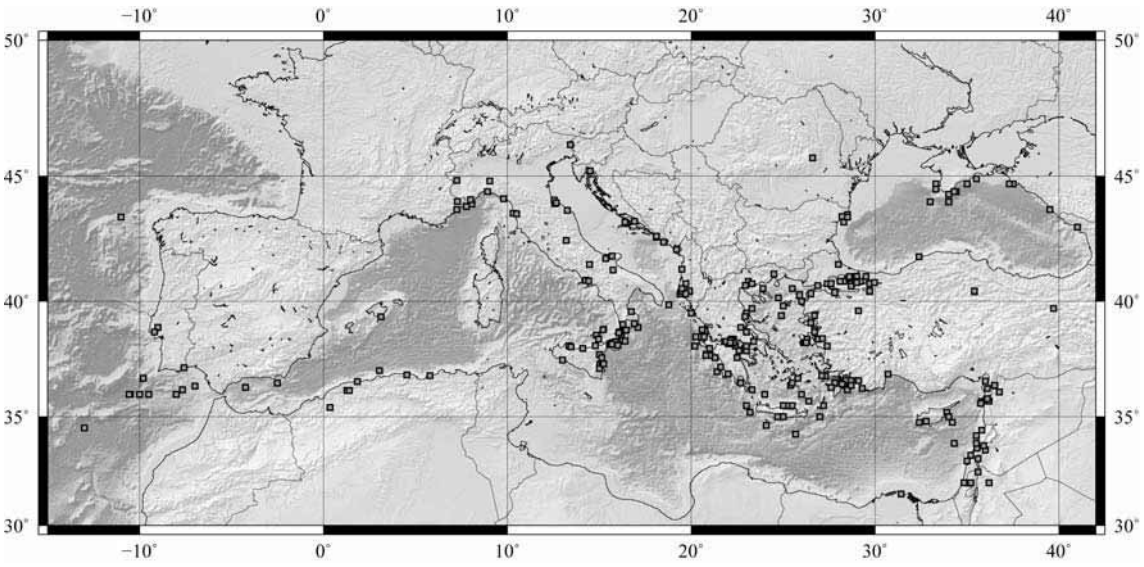

Figure 1. Distribution of tsunamis in the Mediterranean region, according to the recent catalogue of the European and Mediterranean tsunamis, covering the period from 1600 BP to 2006. The catalogue is strongly incomplete prior to 1000 AD, and probably complete only in the last century. The most important tsunamigenic region are in the Gulf of Cadiz, north of Algeria, in southern Italy, along the Hellenic Arc, with its eastern continuation involving Cyprus and the Marmara sea (see other papers in this volume, and also TRANSFER project, <http://www.transferproject.eu/>).

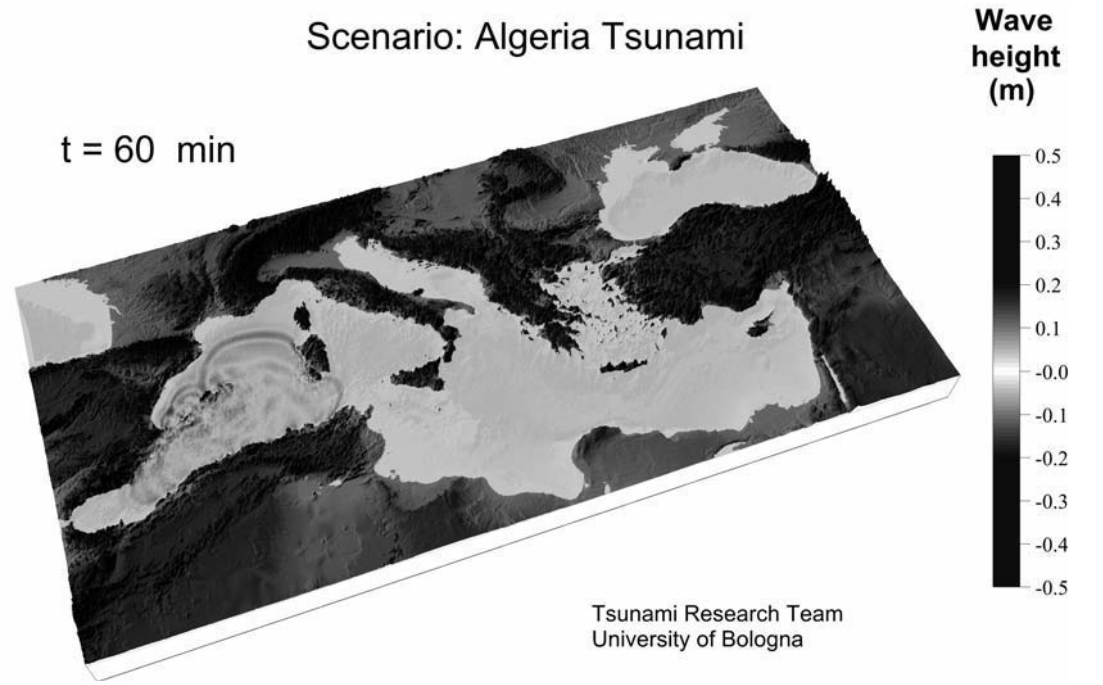

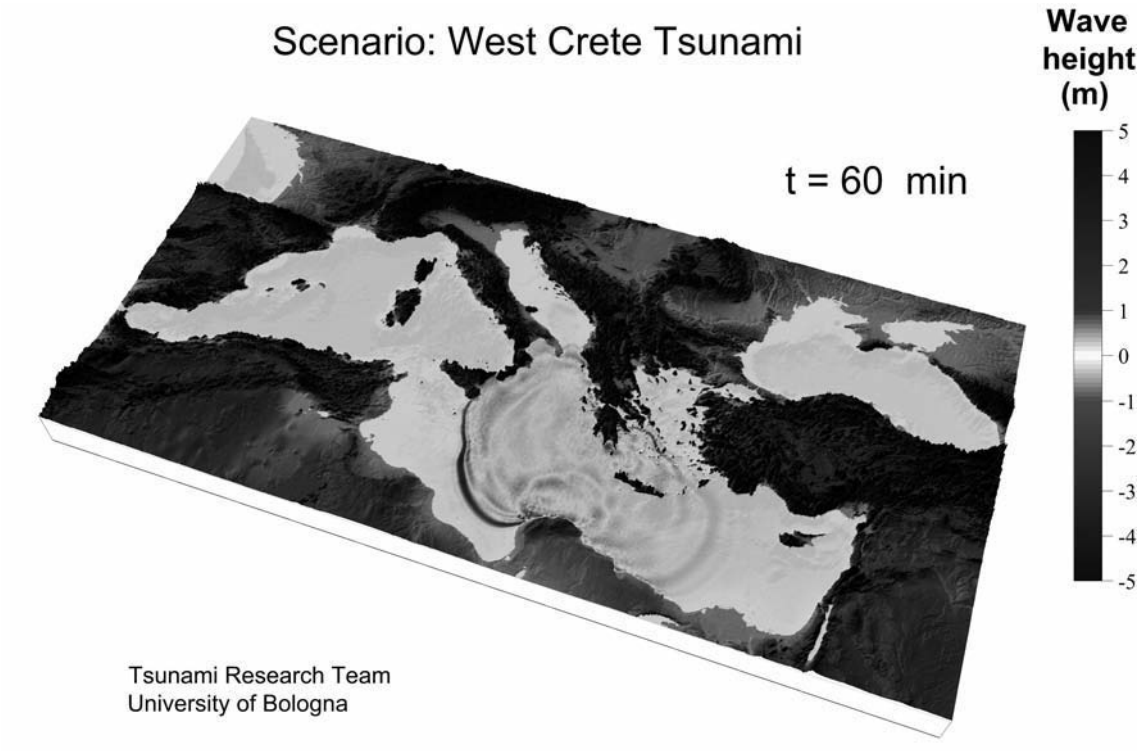

Figure 2. Propagation field of a tsunami generated off Algeria (a) and in the west Hellenic Arc (b) after one hour since the parent earthquake. These cases can be seen as examples of tsunamis occurred in 2003 and in 365 AD respectively. Observe that one hour is enough for the front to travel across the basin and reach the coasts opposite to the source.

2. Tsunami Warning System in the NEAM Region

The main objective of the ICG (http://www.ioc-tsunami.org/) was that of establishing as soon as possible a TWS covering the region and to foster the creation of the national TWS, according to an implementation plan that was adopted rather soon by the ICG and that dictated the steps and the related milestones to achieve the goal in the next years (see the implementation plan published as IOC/UNESCO, 2009 Technical Series Document). The chief idea was to create the TWS by building it on the existing national experiences and resources and to start a two-phase process, with the implementation of an initial or interim TWS (ITWS) in a two year-time (i.e. within 2007) and the establishment of the full operational system in the following four years (i.e. within 2011). These were the intents of the states forming the ICG. Unfortunately the process was slower than desired and the implementation of the ITWS is still to come, though a very large number of intermediate auxiliary steps have been taken and the process, that never stopped, is little by little approaching the target of a creation of the ITWS.

The reasons for such lack of success can be categorised in economical and organisational terms. The ICG is a coordination body, or, technically speaking, a subsidiary body of the IOC, with no specific budget apart from the support to some logistical and secretariat activities. Though solicited several times, no donations were ensured by the member states. This means that the ICG has the only possibility to provide directions and guidelines, or recommendations to the governments and to the authorities of the countries in the region, but that it cannot finance directly plans or projects, not even for the countries of the region with the weakest economies. In this optics, the ICG is bound to solicit the member states and the European Commission to finance plans, usually through their ordinary financing procedures, that can be seen as advancement and partial realisation of the ICG implementation plan. In this framework, a number of scientific projects have been run in recent years, with useful results included with significant impact in the list of the ICG achievement (examples can be given of projects on tsunamis funded by the European Commission, such as TRANSFER, DEWS, SCHEMA, SEAHELLARC, NEAREST, NERIES, SAFER and TRIDEC): The main contributions were especially in the field of numerical modelling and creation of tsunami scenarios, in the identification of the sources, in methodologies to assess vulnerability and risk, in improving the seismic monitoring network and exchange of data, in improving the performance in terms of quality and time of earthquake determination procedure, in devising platforms to support decision in the operational tsunami centres. These tasks were fulfilled thanks to results of projects born outside the ICG, had to respect their own deadlines and objectives, but that found in the ICG a strong which international frame providing harmonisation of the individual project goals and activities towards a common aim.

One of the consequences of this situation is that most achievements regard scientific advancements, since most tsunami projects were funded in the framework of basic or applied research financing schemes, but that progresses in developing adequate infrastructure for the TWS suffered from lack of specific plans of member states or international authorities. One interesting example comes from the monitoring network. The seismic monitoring network in the region was already very advanced before 2004 and was close to the requirement for a TWS, which mainly means real-time connection of an adequate number of stations, quick detection capability of large earthquakes with determination of location and magnitude in a few minutes for all the offshore and coastal source areas in the Euro-Mediterranean region. Progress made since the creation of ICG in terms of increasing coverage and performance by means of national and international programmes has ensured that the seismic monitoring system is today adequate to support the ITWS in the region. The picture is different if we consider the sea level monitoring network. Due to a number of reasons, its state in 2004 was quite far from the requirements for a quick tsunami detection system, particularly in terms of the characteristics of the single stations, of the number of distinct networks and micronetworks not mutually exchanging data, of the geographic distribution of the stations not ensuring general coverage, etc. (see Tinti *et al.*, 2005a). These drawbacks are slowly in the way of being eliminated in view of establishing a core network of real-time tsunami stations for the ITWS, as defined in the ICG implementation plan, but the process is ultimately in the hands of the agencies, usually national agencies, that have operational responsibility on the tide-gauge networks and have to harmonise this goal with their internal priority schemes. At the moment, one of the

main obstacles to create the ITWS for the Euro-Mediterranean region is the lack of a sea level network capable of detecting tsunamis in real time.

3. Weakness in the process of the TWS implementation

A second weakness lies in the organisational context. By this we mean here the uncertainty or lack of decision that still accompanies the construction of the architecture of the TWS. In order to understand this aspect better, it is convenient to recall how a TWS is expected to work. In principle, a basic TWS is formed by the seismic network that (sensu lato) detects the tsunamigenic earthquake, the sea level network that (sensu lato) detects the generated tsunami, a regional centre that collects and processes the real-time data, formulates the proper alert messages and transmits them to the national tsunami centres and to the national authorities that are in turn responsible for the dissemination of the messages (including cancellation) to the population. In this basic procedural scheme the role of the regional centre differs from the role of the national authorities since only these have the legal commitment to send the alert to the citizens of their territories. Therefore the regional centre can only transmit watches to the authorities, while the national states follow their own procedures to transform such watches into warnings, including evacuation orders and other emergency measures. The ICG has addressed correctly the problem of the architecture of the TWS and has also stated that it has to be a system of systems, meaning that at the top hierarchical level one places the regional tsunami watch centre (RTWC) and at the second level the national tsunami warning centres (NTWC). Moreover, functions and requirements of all these centres have been discussed and defined within the abovementioned Task Team of the ICG where also the interrelations among all these interacting centres has been properly figured out and is in course of further definition. But the weak point of the construction is that there are still a number of crucial unresolved organisational questions. The basic one is whether one or several regional centres are needed for the NEAMTWS ? and where, that is in which countries, will it or they be established? This point pertains to the organisation of the TWS, though the decision to be taken is essentially a political one, and the main actors are here the member states. The discussions so far have elucidated the existence of a number of candidates and the perspective of dividing the region into a number of subregions with possible marginal overlapping. In each one centre takes the role of RTWC: for example, an RTWC could be established in Lisbon with responsibility for the North-East Atlantic, a further RTWC could be placed in Paris with responsibility for the western Mediterranean, a third RTWC could be opened in Rome covering the Central Mediterranean, a fourth in Athens embracing the eastern Mediterranean, and a fifth in Istanbul with responsibility on the Marmara sea, the Black sea, and part of the eastern Mediterranean. The multiplicity of the RTWC poses the problem of their mutual relations. But, most importantly, it poses the problem of how to find the necessary resources to create the centres in the start-up phase and to sustain the role and function in the long term. No such centres could survive long if the system will be established only for tsunami defence. Tsunamis are very rare, and therefore those centres are expected to be most of the time in an idle state, which is not sustainable. All centres, as in the other TWS in the world, should be dedicated to a plurality of hazards, one of which is tsunami related. The choice of where these systems will be established is left to the nations. There are examples where they are attached to meteorological services, and other where they are attached to geohazard monitoring agencies covering earthquakes and volcanic eruptions cases.

It is clear that as long as no decision is taken on the number and location of the RTWCs to build, the process of establishing the Interim Tsunami Warning System lies in a sort of a suspension, which does not mean that all the ICG activities are in a waiting state, but certainly that all the operational aspects of the enterprise are suffering. The role of the ICG is to continue to stimulate the member states to make this decision as soon as possible and, in the same time, to induce them also to build the NTWC that are equally essential for the TWS in the region. Comparison with the other oceanic regions covered by ICGs is unfortunately unfavourable to the ICG/NEAMTWS. The Euro-Mediterranean region is today one of the few in the world with no TWS in function and hence with no protection given to the population, which should sound as a great incentive to pose new efforts and momentum to this undertaking in order to reduce and fill the gap with the other regions.

4. Long-term planning

Long-term policies should be mainly oriented to the involvement of the local population and should be mainly community based: they should embrace raising tsunami awareness, implementing local preparedness, ascertaining or favouring capacity buildings, etc. (see Tinti *et al.*, 2010a; see also the guidelines for reducing tsunami risk, adopted by the ICG/NEAMTWS in the 2010 Paris meeting, ICG/NEAMTWS, 2011). Here we focus on the formulation, adoption and implementation of tsunami vulnerability and risk reduction plans that should be of interest for all coastal communities exposed to the risk of tsunamis.

A methodology for tsunami hazard assessment and for damage evaluation has been recently proposed in the European project SCHEMA <http://www.schemaproject.org/> that is based on scenarios, and more precisely on individual worst-case credible scenarios to be aggregated in a final scenario. It is stressed that worst-case scenario approaches should be preferred to probabilistic scenarios when return periods of the tsunamigenic sources are far from being determined, which is almost always the case when in addition to earthquake sources also tsunamigenic landslides have to be considered.

One of the pillars of the SCHEMA method is the development of tsunami hazard scenarios, that is carried out by selecting the largest tsunami sources affecting a given target area, and then by running tsunami simulations in order to compute the tsunami impact. Tsunami modelling is therefore a basic tool, and this requires good models and good input data. As for the latter, it is stressed that bathymetric as well as topographic data of good quality (accuracy and resolution) are needed especially in the coastal belt zone (offshore and onshore), which usually implies a lot of efforts for data collection and data processing. The major interest resides in the computation of the tsunami behaviour at the coast, which includes interaction with small-scale features like harbour breakwaters and jetties, inundation of dry land, interaction with on-land structures, penetration along rivers. All these aspects are handled by the last-generation tsunami simulation models, but all such models imply approximations of the hydrodynamic equations, especially in the proximity

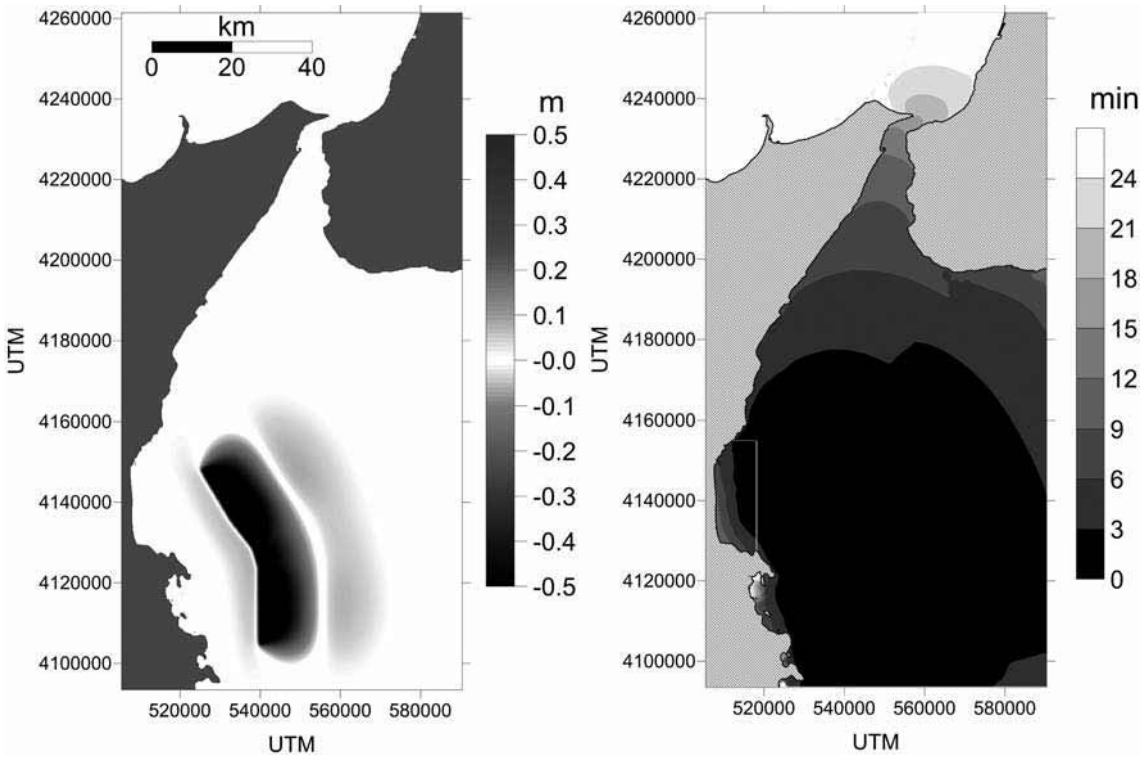

Figure 3. (Left) Initial field of tsunami induced by an earthquake source like the 1693 earthquake off Catania, taken as one of the worst-case scenarios for hazard studies. (Right) Travel times of the tsunami (in seconds). Simulations carried out with the code UBO-TSUFD.

of the mobile shoreline and of field discontinuities or field strong gradients that need to be managed with care to avoid that possible model artefacts be exchanged for real physical effects. A tsunami hazard scenario may be defined by means of the set of products that the analysis gives as output, in the form of maps and graphs, by distinguishing the propagation in the large scale (regional scenario) and in the small scale (local scenario), the latter being the most relevant for setting up scenarios of damage. Consequential to the possibility to define a multiplicity of tsunami sources and therefore of scenarios for a given target, is the concept of aggregation that combines all the scenarios in a single one. In the worst-case scenario approach, aggregation implies simply to select at each space position the most intense value among the ones computed for the various scenarios. One example of tsunami scenario is given in Figure 3 for the town of Catania, eastern Sicily. The source is a fault that is candidate to be the parent fault of the 11 January 1693 earthquake (Mw=7.3) and tsunami that hit all the eastern Sicily coast from Syracuse to Messina, causing deaths and destruction. Modelling results for such tsunami are given in Figure 3 (see Tonini *et al.*, 2010).

The second pillar of the method is the vulnerability analysis using earth observation imagery and field survey (see Tinti *et al.*, 2010b; see also Dall'Osso *et al.*, 2010). This basically is requested to identify the elements exposed to tsunami hazard and to define some relationships between the intrinsic features of these elements and the physical parameters describing the tsunami hazard. The SCHEMA method puts buildings at the centre of the scene, by defining a building classification, by introducing a qualitative damage scale, by determining damage functions for each building class (or equivalently a damage matrix) that relate the damage level to the depth of the tsunami flow, and by setting up inventories of the buildings' typology in coastal zones by photo-interpretation. Tsunami damage scenarios can be then built where the damage induced by each tsunami on the buildings on land can be mapped as is shown in Figure 4 (see Tinti *et al.*, 2010b).

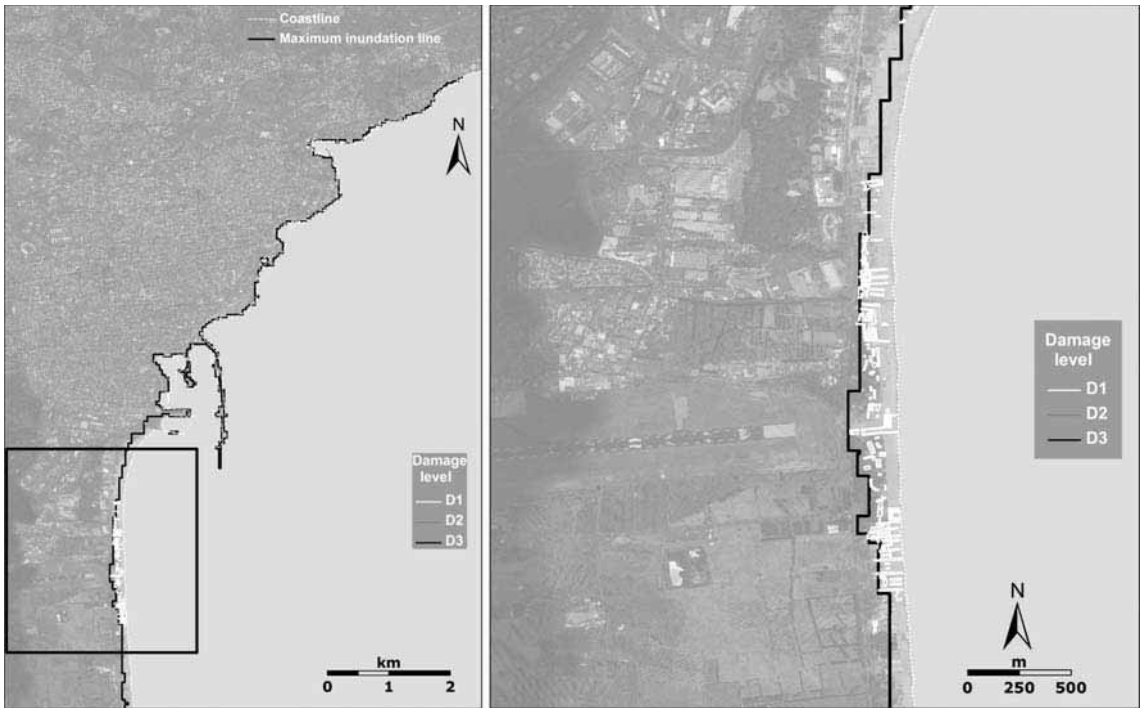

Figure 4. Damaged buildings as resulting from the attack by a tsunami like the 1693 case in the area of Catania and zooming on La Plaia, the beach south of Catania. Damage is classed from D1 (light) to D2 (important) and D3 (heavy). The solid line on land is the inundation line, marking the maximum penetration of the sea (flooded area).

Finally, collaboration with end users and local stakeholders is essential to refine the developed vulnerability-assessment methodology according to their needs.

Challenges start just here. They regard how to take into account other vulnerable elements in addition to buildings, and how to take into account other factors in addition to depth flow to better estimate damage to buildings. A possibility to tackle the problem is first to identify factors that can increase the damage level for buildings (aggravating factors such as sources of mobile, potentially floating, objects in the upstream side of buildings: open car parking places, marinas. Further strategic vulnerable elements can be identified such as lifelines, emergency service centres, and road networks. They can be mapped and crossed with the inundation line resulting from the tsunami hazard scenario in order to check if they happen to lie within or outside the flooded area. However, more complete answers are to be elaborated by future research and a more quantitative approach has to be devised for all categories of vulnerable objects and not only for buildings. This is quite complex because the reference physical model describing the interaction of tsunami with such objects is needed and because such objects may also interact with each other and not only with the water flow.

Separate considerations are to be made as regards human beings and human losses. The individual and societal aspects of a disaster in general and of a tsunami disaster in particular have been the subject of numerous studies especially after the 2004 Indian Ocean tsunami where it was recognised that local communities have their own proper dimension and that many actions (rehabilitation, resilience) and countermeasures (tsunami warning systems and evacuation plan implementation) cannot be solved without the direct involvement of local people. Such studies, so far, have not produced viable methods for defining vulnerability of persons and of coastal societies as a whole and not even for defining some damage multidimensional matrices on the basis of quantitative analyses.

A final remark on possible future extension of the method regards the multi-hazard approach. A tsunami scenario often has little value if it is examined alone. Indeed often a tsunami is caused by a local earthquake, so that the target area is affected both by seismic shaking and by tsunami waves. And vulnerable objects, such as buildings, must resist to both kinds of soliciting forces. The tsunami can affect a building after it has been weakened by the earthquake, and an aftershock in turn can affect a building after it has been attacked by a tsunami. Multi-hazard requires therefore that a more complicated physical model be used and also that different scientific communities talk to each other and cooperate in a multidisciplinary approach.

Acknowledgments: this paper is based in part on the experience gained by one of the authors (S. Tinti) in chairing the ICG/NEAMTWS in the first four years of activity. The results are also the fruit of the research undertaken in the frame of the EU projects TRANSFER and SCHEMA <http://www.transferproject.eu/>; <http://www.schemaproject.org/>

NEARTWARN – A proposal for near-field tsunamis in the Mediterranean Sea: potential assessment, early warning & risk mitigation

Gerassimos A. Papadopoulos

Institute of Geodynamics, National Observatory of Athens, Greece

Abstract

The early warning for near-field (local) tsunamis, with travel times of less than 1 hour, is today a hot topic of great importance in the international effort to reduce the loss of human lives and to mitigate other tsunami risks. Particularly, in the Mediterranean region earthquakes, volcanic eruptions and landslides produce near-field tsunamis threatening nearly all the coastal zones but mainly those in the Hellenic Arc and Trench (South Peloponnese, Cyclades, Crete, Rhodes, SW Turkey), in the Corinth Gulf, Central Greece, in the Messina strait and NE Sicily, Italy, in Algeria and the Balearic Islands, west Mediterranean basin, and the Cyprus-Lebanon area in the easternmost Mediterranean. So far no answer has been given on how to warn in conditions of time constraints of the order of 5 to 30 minutes maximum. For near-field warning it is unrealistic to rely on a unique system for the entire basin. Instead, several local systems working on the basis of some joint principles but with local adjustements is the most promising solution. To achieve progress in this prospect, the organization of the coordinated project NEARTWARN is proposed.

Introduction

The tragic experience from the devastating tsunami of 2004 in the Indian Ocean showed that if an Early Warning System (EWS) was in place many lives would be saved. That extreme event created a worldwide concern among the general public, the specialists and the relevant international organizations as regards the tsunami hazard even in regions considered of being of low hazard. Until 2004 only the Pacific Ocean was covered by an instrumental EWS operating since the 1960s under the supervision of the Intergovernmental Oceanographic Commission (IOC) of UNESCO.

In reaction, the national delegations participating at the General Assembly of IOC on June 2005 decided to develop instrumental tsunami EWSs in various parts of the globe, including the North East Atlantic and the Mediterranean Tsunami Warning System (NEAMTWS). These systems, which are under construction with the active participation of many country members and specialists under IOC coordination, already achieved the drastic improvement of the instrumental infrastructure and technology, the elaboration of requirements and protocols for the data, signal and message transmissions, and started pre-operational tests.

In the Pacific Ocean, the operational tsunami EWSs have proved effective in the far-field, that is in the regional and transoceanic domains, for issuing reliable warnings for coastal zones threatened by tsunami waves that may arrive more than 1 hour after their generation. Unfortunately, those

systems are not capable to provide warnings in the near-field (local) domain, that is for coastal zones which are inundated by tsunamis within a few minutes and certainly less than 1 hour after the wave generation. This is also the prospect foreseen for the other systems under development, including NEAMTWS, since they are designed to issue warnings only for far-field tsunamis. Yet, the most important tsunami sources around the world are situated very close to the coasts.

Near-field tsunamis and associated risks

The list of near-field, catastrophic tsunamis in several regions of the world is very long. In the last 20 years or so, characteristic examples come from the Okushiri Island, Hokkaido-Japan 1993, Java 1994 and 2006, Peru 1996, Sumatra 2004, Samoa 2009, Chile 2010. In fact, most of the fatalities due to tsunamis are caused in the near-field domain exactly because the first tsunami waves arrive very soon after their generation. In fact, global tsunami statistics show that 84% of the fatalities occurred within the first hour of tsunami propagation, 12% in the second hour and only 4% beyond two hours (Gusiakov, 2009). The important challenge for early warning in near-field (local) conditions in Japan and elsewhere was noted by several researchers recently (e.g. Murata *et al.*, 2010). These experiences highlight the urgent need to issue warnings for near-field tsunamis and for the mitigation of the associated risks. This issue, however, remains unsolved, even in countries such as Japan with very high tsunami hazard and in spite of the most sophisticated early warning systems developed there.

Near-field tsunamis in the Mediterranean Sea

Tsunami is one important marine hazard for most of the coastal zones of the Mediterranean region. Although the hazard is highest in the central and eastern Mediterranean Sea (Papadopoulos, 2009), it should not be ignored in the other coastal zones, as indicated in several research projects, the most important being the EU-funded projects GITEC (1992-1995), GITEC-TWO (1996-1998) and TRANSFER (2006-2009).

Tsunami waves in the Mediterranean Sea are generated mainly by submarine strong earthquakes but also by landslides or earth slumps and volcanic eruptions. Observational data and results of numerical modelling indicate that the near-field tsunamis in the Mediterranean region arrive in the nearest coasts in time intervals ranging between about 5 and 30 minutes. From a zonation of relative tsunami potential it comes out that the most tsunamigenic zones are the Hellenic Arc and Trench (HA-T) system and the Corinth Gulf, Central Greece (Papadopoulos and Fokaefs, 2005; Papadopoulos, 2009 ; Fig. 1).

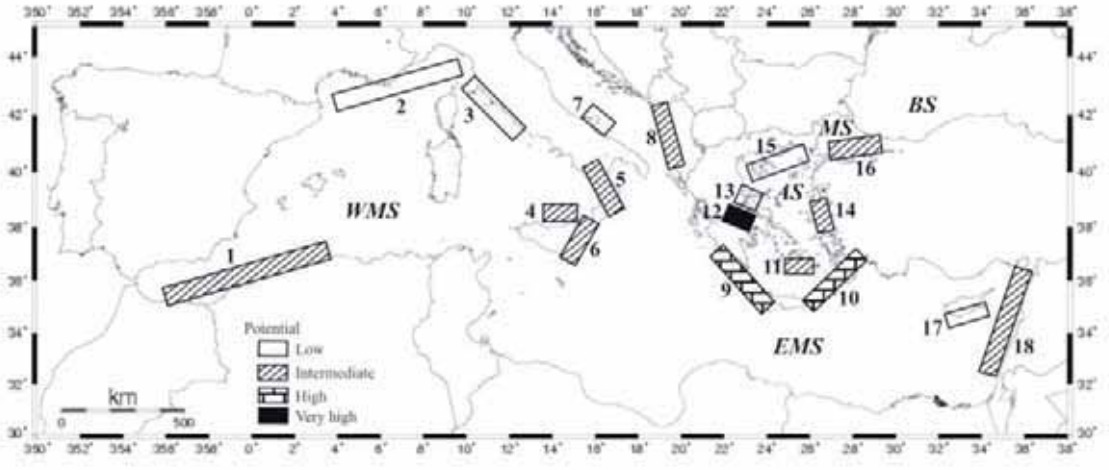

Figure 1. Tsunamigenic zones defined from documentary sources and their relative tsunami potential classification: *WMS*=Western Mediterranean Sea, *EMS*=Eastern Mediterranean Sea, *AS*=Aegean Sea *MS*=Marmara Sea. Black Sea (*BS*) is not included in this study. Zonation key; 1 = Alboran Sea, 2= Liguria and Côte d' Azur, 3 = Tuscany, 4=Aeolian Islands, 5=Tyrrhenian Calabria, 6= Eastern Sicily and Messina Straits, 7=Gargano, 8=east Adriatic Sea, 9=west Hellenic arc, 10=east Hellenic arc, 11=Cyclades, 12=Corinth Gulf, 13=Maliakos Gulf, 14=east Aegean Sea, 15=north Aegean Sea, 16=Marmara Sea, 17=Cyprus, 18=Levantine Sea.

The most active tsunamigenic structure is the HA-T system. This was the source of the large AD 365 and 1303 earthquakes (M~8) which ruptured the west and east HA-T segments, respectively. Very possibly they were the largest historical tsunamis in the European-Mediterranean region. In fact, from documentary sources it appears that the associated tsunamis hit Crete in the near-field but propagated also in the entire basin of the eastern Mediterranean Sea, causing destruction in long distances (Guidoboni and Comastri, 1997; Guidoboni *et al.*, 1994). Results of numerical modeling are consistent with the observations (Tinti *et al.*, 2005a; Loritto *et al.*, 2008). Highly tsunamigenic is also the area between the Dodecanese island complex, Greece, and SW Turkey, at the eastern termination of HA-T, where strong destructive tsunamis caused by earthquakes were reported on AD 144, 556, 1481, 1609 and 1749. A moderate tsunami was caused in 1851. In 2002 an aseismic, local but still damaging tsunami was reported in the city of Rhodes (Papadopoulos *et al.*, 2007c). In the west HA-T important were also the tsunamis of AD 62, 1630 and 1867 (Papadopoulos *et al.*, 2010).

In the Corinth Gulf strong tsunamis associated with earthquakes were reported in 373 BC and in AD 1402, 1748, 1817 (Papadopoulos, 2003b). A moderate tsunami was caused in 1981 and 1995. Aseismic earth slumps caused a destructive tsunami in 1963 and a moderate one in 1996. Since the Corinth Gulf is a closed bay, tsunamis do not propagate outside the Gulf. However, they threaten many coastal communities in the north and south coasts, making the most characteristic case of near-field tsunami hazard in the entire Mediterranean Sea.

In other parts of the Mediterranean Sea strong earthquakes caused destructive tsunamis (Tinti and Maramai, 1996; Soloviev *et al.*, 2000; Fokaefs and Papadopoulos, 2007; Salamon *et al.*, 2007): AD 551 in Lebanon, Syria and Palestine; 1201 in Cyprus, Israel and Syria; 1627 in the Gargano promontory of Italian Adriatic Sea; 1693 in NE Sicily; 1783 in Tyrrhenian Calabria; 1856 in Algeria; 1887 in the Ligurian Sea. In the present century, the largest and most destructive tsunamis were those of 1908 in Messina strait, South Italy, and of 1956 in Cyclades Islands, Greece. Other important tsunamis occurred in Dodecanese Islands, Greece, 1948 and in Bumerdes, 2003, in Algeria which affected the Balearic Islands. A aseismic earth slump caused a local but destructive tsunami in Nice, France, 1979.

A few but important tsunamis were associated with volcanic activity. The prehistoric large tsunami caused in the Late Bronge Age (17th century BC) by the giant eruption of Thera volcano, south Aegean, is well-known (e.g. Marinatos, 1939; McCoy and Heiken, 2000; Minoura *et al.*, 2000; Novikova *et al.*, 2011). The extra-caldera eruption of AD 1650 of Columbos submarine volcanic ediffice in the Thera Island complex caused a destructive tsunami in the entire South Aegean (Dominey-Howes *et al.*, 2000). The volcanic activity in Stromboli, Tyrrhenian Sea, caused several local but damaging tsunamis, most recently in 2002 (Tinti *et al.*, 2005b; Chiocci *et al.*, 2008).

The proposed project NEARTWARN

Tsunami detection is based on records by tide-gauges and sea bottom tsunameters. But the rapid determination of the tsunamigenic earthquake parameters by seismographs is also of great importance for the initiation of the warning procedure. The transmission of the seismic and sea-level signals to the monitoring centers require modern technologies of several types. Recently, promising research results were published about the possible contribution of GPS technologies in the warning procedures. The tsunami generation, propagation and inundation are simulated by advanced numerical models. Pre-calculated simulations are important tools for the tsunami early warning. The long-term preparedness of the threatened coastal zones require hazard, vulnerability and risk analysis and mapping with appropriate tools, such as numerical modelling, probabilistic assessments, digital files of coastal zones and of the bathymetry, GIS tools and others. The synergy between science, technology and operational applications is of fundamental importance for building up an effective tsunami warning system particularly in the near-field conditions.

The local nature of the tsunami sources in the Mediterranean Sea implies that for near-field early warning it is unrealistic to build up around a unique system. Instead, several local systems working on the basis of some joint principles but with local adjustements offer the most promising solution. The first efforts to built up local tsunami warning systems started by the end of the 1990s in the Kythira strait, South Greece, by NOA (Papadopoulos, 2003a). After the local tsunami of 2002 in

Stromboli a local, simplistic system was installed there by the local Volcanic Observatory for the needs only of that island. Currently, the RATCOM demontrator, pre-operational local tsunami warning system is under development in the Ligurian Sea under the lead of SME ACRI-ST, Sophia-Antipolis, France.

To achieve substantial progress in this prospect the organization of the coordinated project NEARTOWARN (NEAR-field Tsunami WARNing) is proposed to involve research, technological development and pre-operational demonstration for tsunami potential assessment, early warning in local conditions and risk mitigation actions. The main Work Packages of such a project may provisionally include the following:

WP 1: An initial report on the state-of-the-art about tsunami early warning systems internationally and particularly in the Mediterranean Sea.
WP 2: Review on the seismic and non-seismic sources which are of high tsunami potential and/or imply high risk for certain coastal communities in the Mediterranean Sea.
WP 3: Determination of the main test-sites in the Mediterranean Sea where local, pre-operational tsunami EWSs should be developed due to high tsunami potential and/or high risk associated with near-field tsunami waves.
WP 4: Development of a prototype tsunami EWS based on the synergy of a set of new technologies and advanced computational tools (e.g. forecasting algorithms, seismic alert devices, local tsunami detectors, immediate wave computation, camera-based systems) for the immediate detection of tsunami waves caused either by earthquakes and/or by earth slumps for near-field tsunami early warning.
WP 5: Early warning, preparedness and education, focusing on the rapid warning transmission to civil protection authorities; development of preparedness and education actions for the mitigation of near-field tsunami risk.

Concluding remarks

The early warning for near-field tsunamis with travel times of up to 30 minutes is a hot topic in the Mediterranean region where all the important tsunami sources are situated very close to populated coastal zones. The NEAMTWS/IOC/UNESCO system under construction is oriented to issue warnings only in regional scales. Therefore, no answer has been given so far on how to warn in conditions of time constraints of the order of 5 to 30 minutes maximum. For near-field warning it is unrealistic to rely on a unique system for the entire Basin. Instead, several local systems working on the basis of some joint principles but with local adjustements offer the most promising solution. To achieve progress in this prospect the organization of the coordinated project **NEARTWARN** is proposed to involve research, technological development and pre-operational demonstration for tsunami potential assessment, early warning in local conditions and risk mitigation actions.

Coastal geo-hazards around the Mediterranean Sea and disaster risk reduction

Nilgün Okay

Istanbul Technical University, Geological Eng. Department, and Earthquake Engineering and Disaster Management Institute, Turkey

"Neptune raises up huge waves and floods the countryside of Troy"
The Metamorphoses Book XI

Abstract

The Mediterranean region is one of the high risk areas in the world, as it attracts millions of tourists all the time of the year. According to historical records, many powerful events have taken the lives of thousands over the ages and affected disastrously the coastal civilizations and economies, even leading to the collapse of cultures. As more and more people choose to live along high-risk coastal areas, the region faces the possibility of large economic losses from structural and non-structural damages along densely populated coastlines. Tsunami warning systems, public awareness, risk mitigation strategies, planning and mitigation measurements are the ultimate goal to build "*coastal disaster-resilient cities*" around the Mediterranean region.

Devastating coastal geo-disasters around the Mediterranean Sea

The shorelines along southern Europe and northern Africa, from Spain, Algeria, Italy, Greece, Turkey, Egypt to Israel are affected by earthquakes, volcanic eruptions and collapses, mass failures generated by great fault zones and subduction systems in the area (Tinti, 2003; Mascle, this volume). Paleotsunamigenic sediments identified along the coasts of Italy, Greece and Anatolia indicate that the region has been repeatedly affected by tsunamis (Vött *et al*., 2009; De Martini *et al*., this volume; Sakellariou, this volume). Troy (Papadopoulos, 2009), Myous, Magnesia (Brückner *et al*., 2003), Cnidus, Miletus, Priene, Ephesus (Altunel, 2003) were major ancient Aegean coastal cities which were frequently hit by the earthquake associated tsunamis (Altınok *et al*., 2001; 2011; Sakellariou and Lykousis, 2003; Yolsal *et al.*, 2007).

In 1628 B.C. the coasts of the eastern Mediterranean were flooded by huge waves of up to 60 m high caused by a volcanic eruption on Santorini in the Aegean Sea. A major destructive earthquake in A.D. 365 had caused coastal uplift 9 m of more than 100 km long area in Crete and produced a tsunami which destroyed complete coastal regions as far as Cyprus, Libya and Sicily (Stiros, 2010), and reached the Egyptian coast, killing 50,000 lives in Alexandria. The best documented and most recent tsunamigenic earthquake in the Aegean Sea is the one that occurred near the Amorgos Island in 1956, killing 53 people, injuring 100 people and destroying hundreds of houses. The waves were reported to be almost 25 m high. A distinctive tsunami-prone area is associated with earthquake zone around Chios Island in the eastern Aegean Sea (Papadopoulos, 2009).

The Marmara Sea has a long history of severe hazards including earthquakes, submarine mass movements, and tsunami occurrences in the past. About 300 earthquakes (M>6) have occurred during the last four thousand years (Ambraseys, 2002). The tsunami problem in the Marmara Sea has been studied after the 1999 Kocaeli Earthquake (Altınok and Ersoy, 2000; Yalçıner *et al*., 2002; Tinti *et al.,* 2006a; Altınok *et al*., 2011). The observed tsunami run-up heights in the 1999 earthquake were almost 3 m and post-events were up to 15 m. The tsunami was damaging but not catastrophic. A part of the coast about 300 m long and 75 m wide slid into the sea, strong enough to carry multi-stored buildings.

Steep submarine scarps (15°-30°) of the northern margin of the Marmara Sea marked with deep basins bounding with continuous sediment transportation via submarine canyons (Okay and Ergün, 2005) carry a high risk associated with a large-scale slope failure with possibility to trigger tsunamis (Tinti *et al*., 2006a) in a possible Marmara earthquake in the Istanbul area (Özeren *et al*., 2010). Based on detailed multi-channel seismic data and bathymetry paleoearthquake-triggered underwater slides (Görür *et al*., 2010), gas releases (Geli *et al*., 2008) and fluid-venting (Zitter *et al*., 2008) have been identified. A possible earthquake may trigger sudden release of gases such as methane outflow in the water column associated with slope instabilities. Anoxic bottom conditions were observed after the 1999 earthquake in the Izmit Gulf area (Belkıs, 2003). There is strong evidence for active regional uplift of the northern margin of the Marmara Sea characterised by steep cliffs several tens of meters high with Pleistocene marine terraces (Yaltırak, 2002) and drainage reversals due to co-seismic uplift (Okay and Okay, 2002).

Impacts of tsunamis on coastal regions

Disasters cause impacts with both direct and indirect effects. Direct impacts immediately following the event are listed in Table 1. Indirect impacts are knock-on effects (after event) from reduced economic resources including worldwide ripple effects in different sectors caused by the tsunami and disrupted ecosystems, recovery of fishing industry, decline in tourist revenues.

Table 1. Direct impacts of tsunamis along coastal areas.

Population	• involves injury, death, and missing (including seasonal population) • causing life loss vulnerable residents such as children, the elderly (*almost 55% of recent tsunami victims in Japan were aged 65 or older*) and the sick or physically challenged or women even tourists suffer differently in tsunamis (*death rate of women in South Asian tsunami was at least three-four times higher than men*)
Physical damages	• damage to property • inundation (run-in) causing variable degrees of damage in flat areas along/nearby the coast (depending on the presence of waterways/rivers) • damage to costal morphology, landsliding and liquefaction due to seismic activity • local vertical tectonics has affected most of the known coastal cities of the ancient world around the Peloponese and along the Aegean and Marmara coastline which are vertically displaced by +3 m to -5 m relative to the present sea level (Sakellariou, 2003) • accumulation of tsunami debris/flooding materials (covers bodies, buildings, roads)
Structural damages	• Lifelines (water, gas, electricity) • Transportation lines (roads, bridges, tunnels, ports, airports, railways) • Telecommunication lines (fiber-optic cables) • Emergency Services (Safety, Fire, Hospitals) • Evacuation structures (vertical evacuation structures, evacuation and sheltering centres) • Tsunami coastal prevention/defence structures (seawalls and others) • Offshore infrastructures (harbors, storages, pipelines, platforms), hazardous facilities including power plants and onshore facilities (industry, fishing, boats, touristic) • Overturned, damaged residential and public buildings (administrative, educational) • Historical sites, structures, monuments
Contents	• Interiors and contents of buildings/offices/hospitals/museums, art galleries/touristic facilities • High-tech electronic equipment, machinery, historical, art and cultural values
Economic losses	• due to structural and contents damages (not insured) there will be losses • after response there will be indirect effects due to the costs of relief/reconstruction/rehabilitation • sectorel decrease in production, business interruptions, fishing, shipping, tourism, and other ripple effects worldwide
Environmental	Damage to ecosystem and coastal environment (fish, agriculture), contamination (soil, water), and fires
Social	interrupting social activities along coastal areas

TSUNAMI RISK REDUCTION: PUBLIC AWARENESS, PREPAREDNESS, PLANNING AND MITIGATION

It should continue to be focused on building tsunami-resilient communities around the world. A resilient community has capacities essentially in everything, economy, housing, life services such as energy, transportation, water, communication, health, rights, security, and emergency management. Multiple risk reduction and mitigation efforts are taken in order to reduce the vulnerabilities (structural, environmental, social and economic), and to build up the capacities of communities, infrastructures, and emergency response services (UNESCO, 2008; Okay, 2011). Based on Hyogo Framework of Action (HFA Implementation 2007-2009) coastal communities should be focused on five main issues of priorities for action (UNISDR, 2009):

1. making disaster risk a priority;
2. knowing and understanding hazards and risks;
3. taking action to reduce risks;
4. build understanding and awareness;
5. be prepared and ready to act.

Tsunami risk reduction requires continuous research (understanding of hazards in coastal areas, monitoring and designing coastal disaster scenarios), structural and non-structural public protection measurements and preparedness (combination of awareness and preventive disaster management "mitigation"). If one part of the system is over invested, like structural mitigation (building coastal defenses), and not invested in others, like building capacities, risk communication, legislation, risk transfer, then destructive disasters may strike. In order to achieve the preparedness and risk reduction that benefits the whole of society and social groups, such as governmental (central and local), and non-governmental organizations (national and international scientific communities and educational institutions), volunteers, business sector, public, media, all take part in mitigation actions (Okay, 2011).

Table 2. Recommendations for tsunami risk reduction and mitigation for the Mediterranean region.

Risk Reduction Action	*Mitigation Measures*
Data Management	• Improving basic data (*bathymetry, seismological, high-resolution shallow seismic, sea-level, temperature, pore-pressure and piezometer monitoring* at-risk areas) including *active fault zones, hydrocarbon gas releases, fluid ventilation, mud volcanoes, slope instability, along with archaeological and historical data* (paleo-disaster data and statistics) and **Marine Hazard Database** of Mediterranean Sea.
Hazard Maps	• Developing **Vulnerability and Risk Atlas** (*environmental, coastal forest, hazardous materials, industry, population, coastal infrastructures and critical facilities, transportation, emergency services, socio-economical, historic, touristic*) of the Mediterranean Sea. • Developing local **online *Tsunami Hazard Maps***, *Inundation Maps*, based on **worst case** coastal geo-disaster *scenarios.* • Improving *mitigation models* to manage risk (disaster information/forecast/warning systems based on 3S (Remote Sensing, GIS, GPS), **real-time tsunami damage and loss assessment** (before and after), ***Local Coastal Hazard Evacuation Maps.*** • Improving data, sharing of knowledge and related scientific studies, technologies.
Tsunami Early Warning Systems	• Establishing **National/Local Tsunami Information Centres** and building/improving the offshore/near shore *tsunami monitoring/warning systems* • Continuing to improve/upgrading and work towards tsunami monitoring/warning methods and standards. • Strengthening *emergency communications systems* not only through the wired system, but also through appropriate combinations of technologies such as satellite and mobile communications.
Social Mitigation and Preparedness	• Increasing the disaster resilient capacity of community: educating and training of all concerned public (government officials, disaster workers, volunteers, business sector, schools, women, children, local community as a whole), preparing guidance documents, creating a culture of

	public safety, risk reduction-mitigation, preparedness and raising public awareness (understand hazards and risks and *showing importance of mitigation*) in high-risk coastal areas. • Developing **awareness campaigns** and **sustainable awareness campaign strategy** locally implemented by different actors. • Warning systems are about people: educate the public and facilitate their understanding of tsunami warning/alert-related information. • Increasing protection of people and *Mediterranean Cultural Heritage* at risk-areas. • Promoting the community participation including gender-sensitivity to ensure the campaigns reach women, youth, school children, tourists and different groups to build sustained interest, to establish relationships for the involvement of local government, industry and public organizations, media professionals and other commercial and marketing interest groups, engage religious and community leaders in order to disseminate information. • Promoting educational campaigns in schools and community centres, community fairs, annual commemorative events or festivals, and neighbourhood safety drills and simulations, organising workshops, forums and educational activities for communities at local, social and cultural facilities (*Community Emergency Response Team* training, tsunami school programs). • There is a need for a strong community volunteer network to bring the people to shelters. Each villager is tasked with ensuring that elderly and other vulnerable neighbors have evacuated. • Improving participation in tsunami preparedness: public memorials and monuments in areas that have been struck by a tsunami, inundation maps, maps of evacuation sites and routes and evacuation procedures (used in pamphlets and display panels), high water marks and danger signs in local media sources (such as television, radio, newspapers, magazines, public bulletins and beach notices, security reports, displays, memorials, tsunami museums). • Organising education and training programs and technical staff to planning and voluntary potential and, defining scope and responsibilities.
Evacuation and Sheltering Systems	By the Local authorities • Planning *rapid and safe evacuation routes* from residential districts during a tsunami, and designating evacuation areas as part of local tsunami hazard mitigation plans. • Designating *evacuation sites* for temporary mass protection (schools, public and religious buildings, parks, sport and entertainment centres, stadiums). • Building evacuation structures (vertical, towers, dunes, green belts).
Evacuation Planning and Training	• Developing **exercise scenario** and conducting annual **tsunami evacuation exercises** and **drills** to **test planning** (organizational drill, tabletop, functional, and full-scale exercises) at various levels of agencies (Community Civil Defence or Protection, Local authorities including Municipalities, Education, Transportation, Coast Guard, and Disaster Management, and, Red Cross, Tourism Authority, and others (volunteers, utility companies, hotels, media), with coastal schools, community centres. • Planning for *special needs and requirements* during evacuation and sheltering for children, women, tourists, the elderly and the sick or physically challenged population (food, first-aid, clothing, gender-specific health needs and security to protect women and girls. Of women affected by the tsunami).
Local Integrated Tsunami Comprehensive Planning	• Developing preparedness actions and mitigation measurements, and increasing resources towards the tsunami risk reduction in the local plans. • To increase the efficiency of early-warning systems coping with **evacuation planning and testing** and improving the tsunami emergency response capacities. • Developing **tsunami preparedness plan**, as a part of a comprehensive local plan covering a broad range of tsunami awareness actions, public educational programmes, designing scenario, and the establishment of evacuation areas, maintenance of evacuation routes, testing and exercising evacuation planning, communication systems and the rapid dissemination of accurate tsunami warning information. • Developing **tsunami mitigation plan** for activities (structural/non-structural measures) to prevent and reduce the impact of tsunamis, increase the life safety, and improve at-risk communities' preparedness, o improving land-use and urban planning (*coastal buffer zones*/green zones) o conducting ***structural mitigation measurements*** to reduce the damaging effects of tsunamis, developing guidance for tsunami structural mitigation standards (resistant coastal housing and infrastructure, building evacuation mounds, vertical evacuation structures, evacuation towers and centres, tsunami defense structures (seawalls), maintaining beach development and coastal forests promoting coastal buffer zones,

	and safety platforms, natural sand dunes along high-risk coastal areas. o promoting continuous tsunami risk reduction research o implementing non-structural mitigation measures (development and application of **off-shore marine infrastructure design building-codes** for tsunami) o improving legislation (gender-sensitive policy development for tsunami risk mitigation, **coastal land use-planning**) o improving ***financial measurements*** (microfinance, gender-sensitive empowerment), increasing capacities of business sectors through mainstreaming risk management, and business continuity planning, risk transfer (insurance for structures and contents) to minimize the cost of damage from run-up and flooding, protecting coastal sectors, tourism, fishing and shipping industry o planning for damage and need assessment o increasing capacity of local emergency services, tsunami warning systems, communication, transportation infrastructure, lifelines, including **Planning for Emergency Response** (emergency relief, evacuating, sheltering, resources and volunteers, and tsunami debris management) and **Response** (loans, grants and services) o increasing emergency management capacities of organizational structure of local authorities in **communication, cooperation, capacity building and coordination** among the institutions at sufficient level, and improving **coordination** between central and local administrations and non-governmental/non-profit organizations **bilateral and multilateral cooperation** (agreements/partnership) that involves organizations (national and international scientific communities and educational organizations), volunteers, media, businesses, local communities **take part** in tsunami mitigation actions

Developments for Istanbul and Marmara Sea

The interest for the Marmara Sea Observatory is related to the growing research efforts and the link between fluid and seismicity investigated in terms of monitoring pore-fluid pressure as a possible precursor of earthquake (Cochonat and Person, 2008). Due to these considerations, in the frame of the **ESONET** Marmara project, a seafloor observatory, equipped with several sensors including a wide-band seismometer and methane sensor, was deployed recently. Turkey is also establishing the **Tsunami Warning Centre** under the IOC –Intergovernmental Coordination Group for the Tsunami Early Warning and Mitigation System in the North Eastern Atlantic, the Mediterranean and Connected Seas (NEAMTWS) initiative. Kandilli Observatory of Earthquake Research Institute (KOERI) as the Tsunami Warning and Emergency Rapid Response Centre is expected to act as a regional centre for an early warning system, monitoring both earthquake and tsunami hazard around the Mediterranean Sea (Özel *et al*., 2011).

Final remarks

We should have learned much more from the recent disasters. The destruction will lead to new building codes and better city planning, giving risky communities a chance for a new start. Safeguarding lifelines including power, water, gas, telecommunication and transportation after a disaster will also probably become a priority. One should be prepared for larger earthquakes. Policy makers should have a series of second best solutions, ranging from engineering to non-engineering, and technological and social based solutions. The future effect for disaster reduction can be improved significantly because the informed policy maker may take the best lessons from the events for a consistent and more sustainable reform in disaster reduction policy (Magnier, 2011). A moral responsibility to learn everything and implement it more broadly to understand and mitigate against likely hazards and risks. There is a need for further research, more solid knowledge and detailed data sets based reconstruction and disaster reduction policy and stronger policy enforcement to be demonstrated in the future.

Box 1. The reality of tsunami risk reduction

Hundreds of thousands of people having died in the 2004 tsunami in Indonesia, the 2010 tsunamis in Chile and Sumatra, and the 2011 devastating tsunami in Japan. This first world-shaking catastrophic event on 26 December 2004 was very difficult to predict without the tsunami warning system. The alert time of the tsunami was very short, the destructive power of the tsunami was very strong, there was no awareness, preparation, planning and mitigation to respond and cope with such a disaster. Huge chaos and mismanagement occurred and resulted in the death of nearly 300,000 people with huge impact and heavy loss. In Chile when the tsunami warning was issued, people evacuated on their own, and then the evacuation call was lifted at the same time as the tsunami was climbing up the Chilean coastline, and more than 200 died. In Sumatra most people did not feel the earthquake strong enough to begin self-evacuation, and the tsunami struck at night. All TV channels asked to evacuate were not seen by people because there was no electricity.

The Great Tohoku earthquake in March 2011 led to a series of disasters including the nuclear accidents which made the disaster response a complex, difficult and huge challenge. The subduction zone earthquake at 9.0 magnitude with landslides in 120 different place and significant level of soil liquefaction caused widespread damage. The earthquake triggered extremely destructive tsunami waves of more than 10 meters (even up to 38 m) along the 400 km long coast, in some cases traveling up to 10 km inland, and even reaching many other countries after several hours. The Japanese government temporarily confirmed almost 29, 000 people dead or missing, and over 125,000 buildings damaged or destroyed. The earthquake and tsunami caused extensive and severe structural damage in Japan, including heavy damage to roads (1450), bridges (51) and railways, and dam collapse as of 19th March based on Parashar *et al*. (2011). Early estimates of losses from the megadisaster may have far-reaching ripple effects in many sectors worldwide with cost in excess of $300 billion, making it the most expensive natural world's disaster (Revkin, 2011a).

It is important to recognize that one of the lessons to be learned is which efforts worked. There are important messages from the Great Tohoku earthquake and tsunami. The country survived the earthquake reasonably well, the good construction quality, building codes and other mitigation efforts stood up against the earthquake, but tsunami overrode coastal defenses significantly and caused tremendous damage. It would have been far worse had the Japanese governments and private firms not invested in monitoring capabilities, earthquake-resistant infrastructure and earthquake mitigation and preparedness over the years (EOS, 2011). They benefited from an earthquake early warning of tens of seconds. This means that the investment in disaster mitigation pays off as the Japanese earthquake early warning gave enough time for many households to switch off the gas lines to avoid more fire. Japan's tsunami warning system worked well, providing people with a 20- to 30-minute warning, which may have saved 100,000 or more lives. Tsunami mitigation measures have been constructed in some cities (almost 40% of Japan's coast; Marnier, 2011) such as massive concrete defense structures. The areas had a very high level of preparedness for a tsunami. People were educated and trained to evacuate with hazard maps. Many lives were saved by vertical evacuations by heading to the tops of buildings in the tsunami zone.

Japan is as a good example of seismic and tsunami resilience nation (Lassa, 2011), with excellent institutional frameworks and public awareness in terms of actions for Disaster Reduction Measures (DRR) as well as accessibility of disaster information to locals (Wisner, 2004). Despite strict building codes, early warning systems, and a disaster-resilient society what went wrong?

Size of the disaster: the tsunami disaster was not a simple problem, because it was extraordinary (boats, cars on top of buildings, overturned evacuation and sheltering structures, tsunami debris almost everywhere). The disaster prevention/mitigation seems to

have failed, but because there are limits to mitigation–especially when the exposure to risk is neither reduced nor considered.

Population and land use: coastal towns and cities are often densely populated, which means there is a higher level of exposure to disaster risks. More directly, people often live where they should not.

Disaster memory: Japan has not had such a large event in recent memory. Along the Japanese coastline hundreds of tsunami stones, some more than six centuries old, these ancient markers have warned generations of people of tsunami danger and reminded people not to build there. Then people, communities and goverments forget to assess their living conditions, allow building in risky areas (Revkin, 2011b).

Preparedness: Japan did prepare for the worst case earthquake, but not the worst case tsunami. They were prepared for tsunamis of smaller scales. There was no link to magnitude. On a flat coast there is no time for people to run. Vertical evacuation structures could not stand up against the tsunami. Most defenses were designed too low, because smaller waves were expected. More than half (55 %) of the tsunami victims were aged 65 or older (Kyodo News).

Hazard maps: most of the communities had made general hazard maps showing areas at risk, but no tsunami risks maps. Less than 15% of the Japan's coastal municipalities have produced tsunami hazard maps (a study in 2006 by Suganuma from Science and Technology Foresight Center, Japan). Maps were produced for tsunami of both 4 and 8 meters in height, but local residents may have only received the map and preparedness for a 4-meter tsunami.

Warning systems: the waves were so big that they even destroyed several of the tidal gauges used to measure wave size.

Prevention structures: more than 75% coastal defense structures (high as 6-8 meters) were destroyed because the tsunami heights (run-up) exceeded 10 meters.

Evacuation structures: a four-story reinforced concrete building that was knocked over by the tsunami. People went up to the tops of three- and four-story buildings and than died when the waves crested the buildings. Children at a school (the designated evacuation site) died, because they thought their school was safe. Most wooden buildings suffered full destruction.

Engineering and technology are not the only best solutions, physical infrastructure can create temporary security and also create a false sense of security because the people forget they are vulnerable and their responsibility of self-protection totally (Lassa, 2008). At the same time, it causes the public to underestimate non-structural measures such as community awareness and education, tsunami hazard maps, evacuation maps disaster drills, making communities more vulnerable. Tsunami risk reduction and preparedness is not just about building systems or constructing coastal protection, but also building institutional and communities disaster resilient capacity in the broad sense.

ANNEX

This section regroups the colour version of a number of illustrations found earlier in this volume so as to make them more easily interpretable than their black and white version.*

**the sequence adopted is that of the workshop communications*

From Mascle:

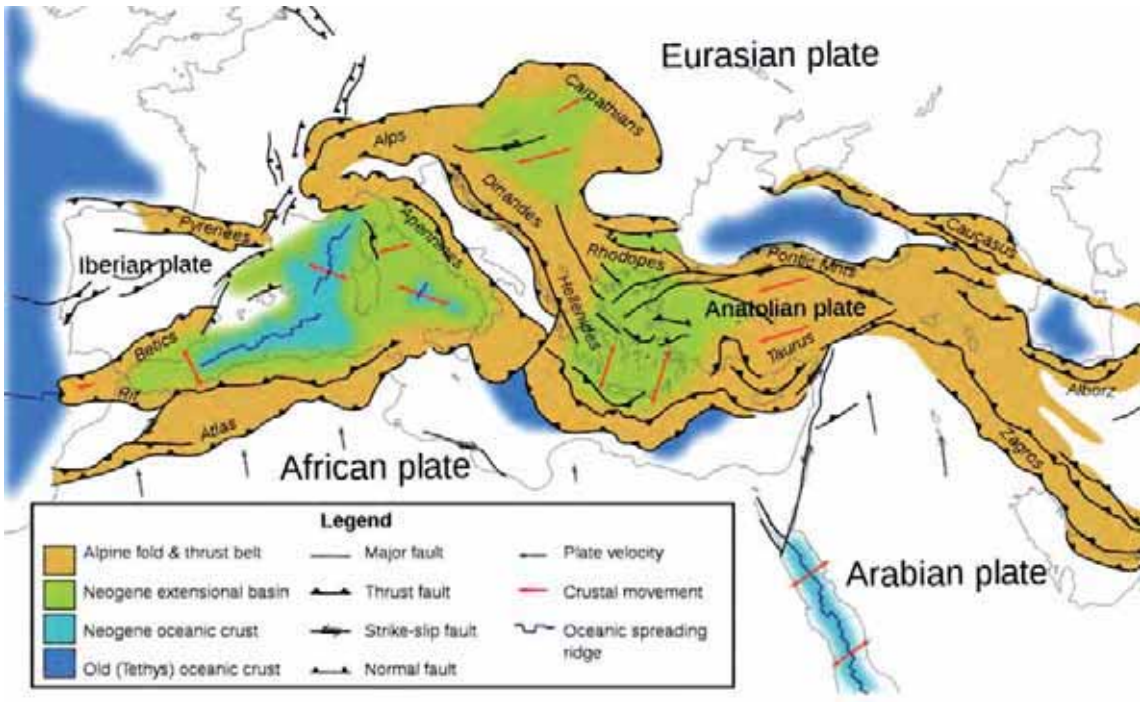

Figure 1. Tectonic setting of the Mediterranean Sea. *[refers to figure on p. 23]*

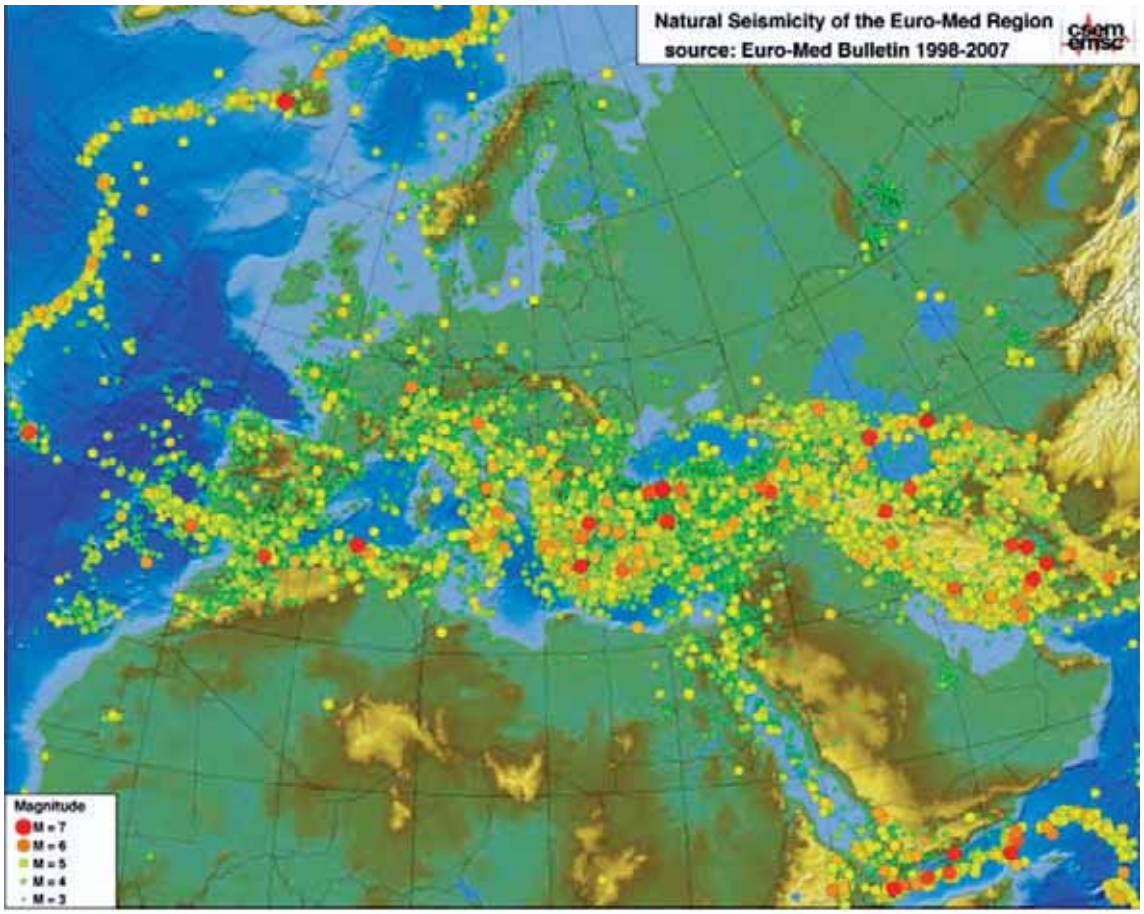

Figure 2. Repartition of seismic activity (epicenters of seisms from magnitude 3 to 7) on the Mediterranean domain and nearby areas. *[refers to figure on p. 24]*

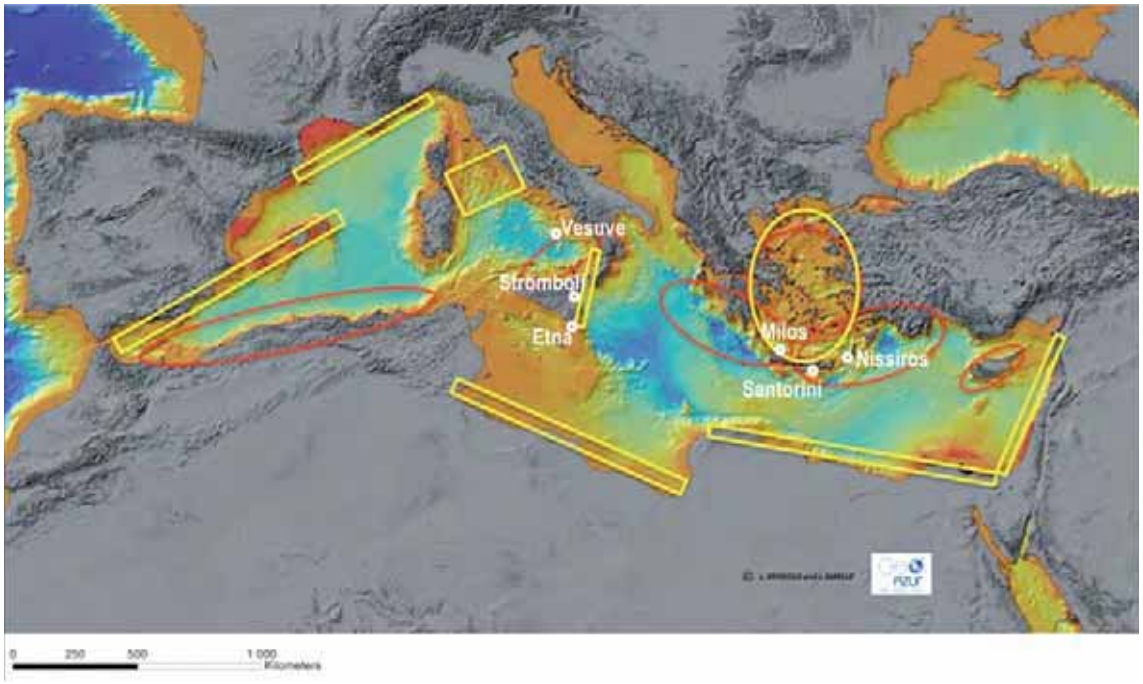

Figure 3. Main active, or recently active, volcanoes in the Mediterranean Sea, and location (in red) of the main earthquake-triggered tsunami areas and of main potentially impacted coastal zones (in yellow) within the Mediterranean Sea. *[refers to figure on p. 25]*

From Sakellariou:

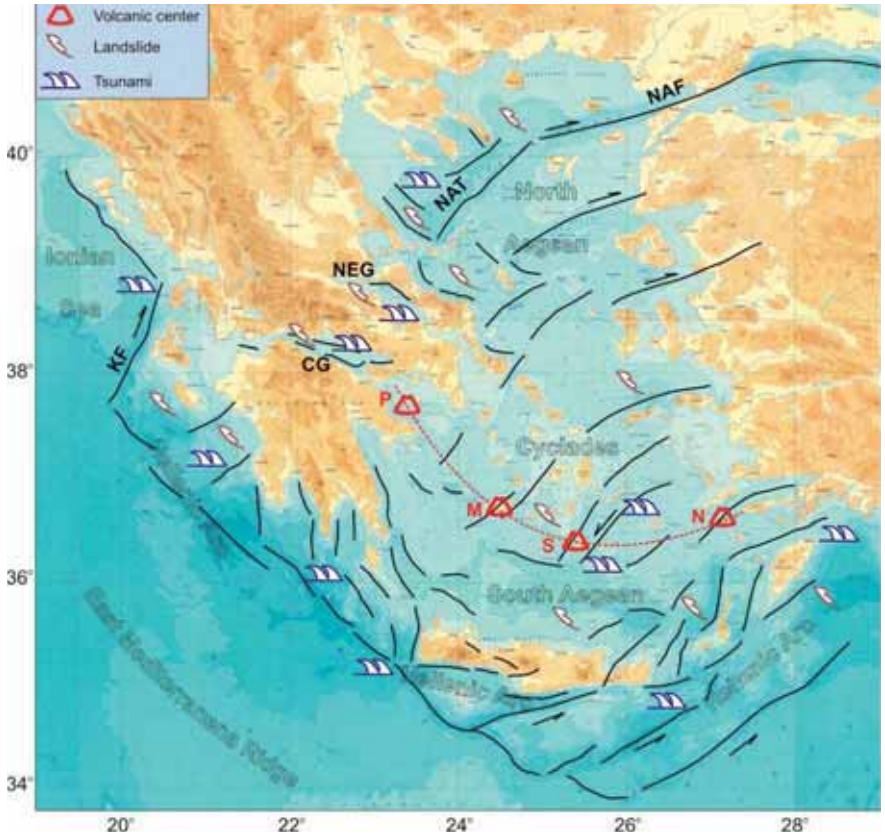

Fig. 1. Geodynamic structure of the Hellenic Arc and Back-Arc region with areas of major marine geohazards. Bathymetry extracted from the IBCM/IOC. *[refers to figure on p. 28]*

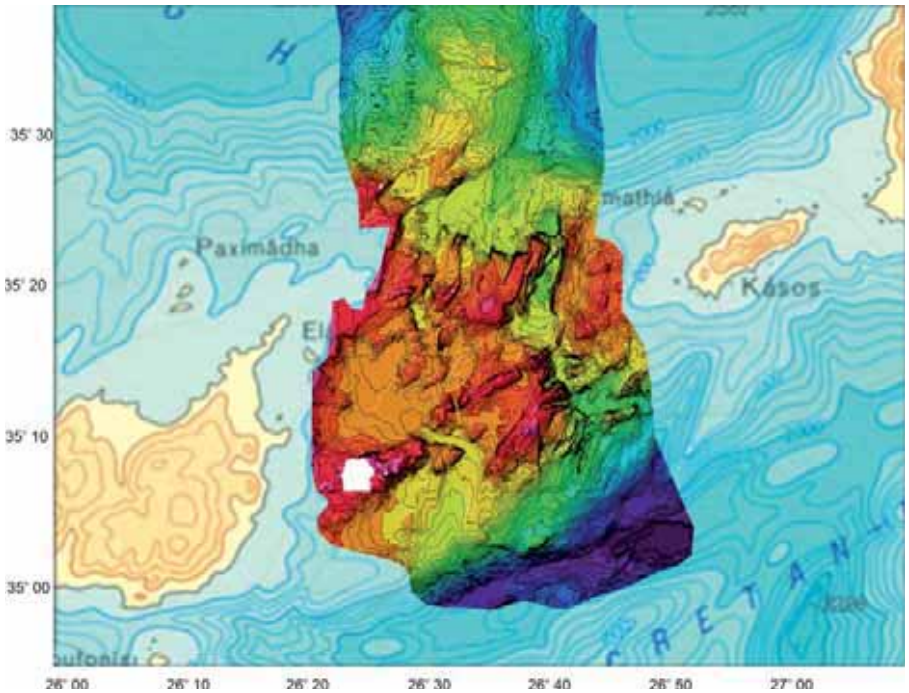

Fig. 3. Recently acquired swath bathymetry data in the Eastern Cretan Straits show extensive N70° faulting and N-S step-faulting. General bathymetry extracted from the International Bathymetric Chart of the Mediterranean IOC. *[refers to figure on p. 32]*

From Rosen:

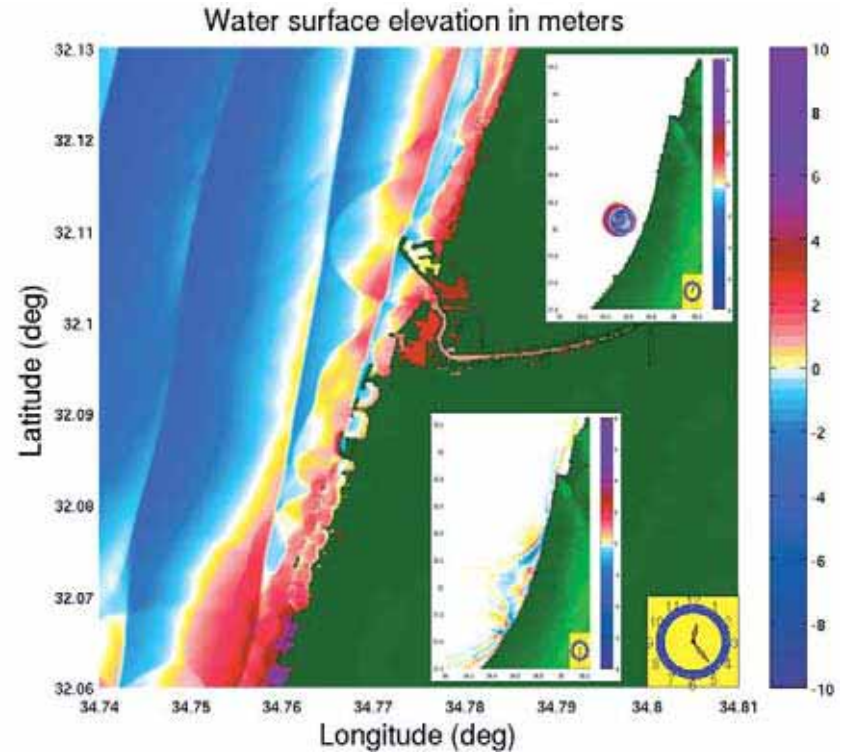

Figure 1. Example of earthquake induced landslide tsunami at the coastal shelf of Tel Aviv and the resulting inundation at the coast (after Galanti *et al.*, 2009). Landslide characteristics: volume 0.625 km^3 (50 m high x 2.5 km wide x 5 km long); initial fall speed 50 m/s. In the small frames are shown an earlier instance and a later instance of the tsunami wave, reaching neighboring countries coasts. *[refers to figure on p. 44]*

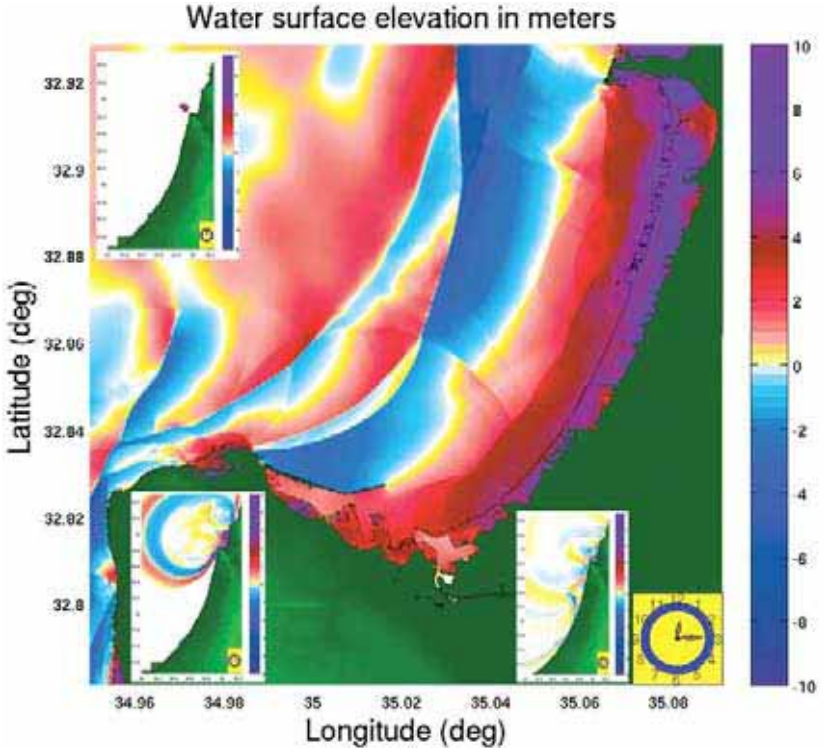

Figure 2. Example of earthquake induced landslide tsunami at the coastal shelf of Haifa and the resulting inundation at the Bay of Haifa coasts (after Galanti *et al.*, 2009). Landslide characteristics: volume 1.60 km^3 (50 m high x 4 km wide x 8 km long); initial fall speed 50 m/s. In the small frames are shown an earlier instance (up left) and two other instances of the tsunami wave. *[refers to figure on p. 44]*

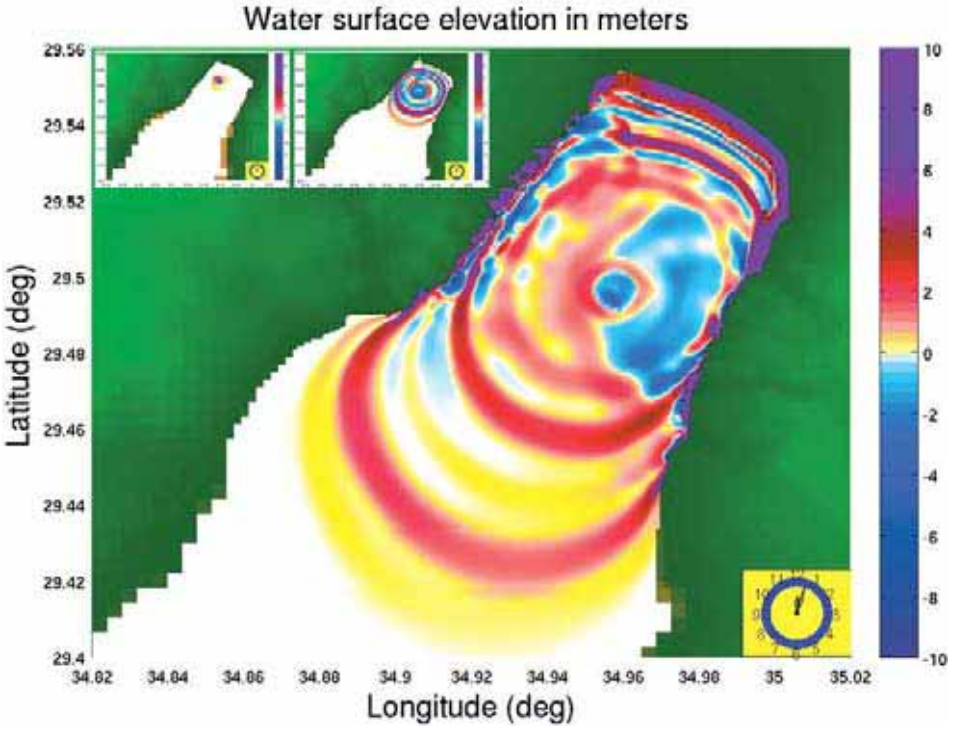

Figure 3. Example of earthquake induced landslide tsunami at the coastal shelf of the Gulf of Aqaba/Elat and the resulting inundation at the Gulf coasts. Landslide characteristics: volume 0.03 km^3 (30 m high x 1 km wide x 1 km long); initial fall speed 50 m/s. In the small frames are shown two earlier tsunami instances. *[refers to figure on p. 45]*

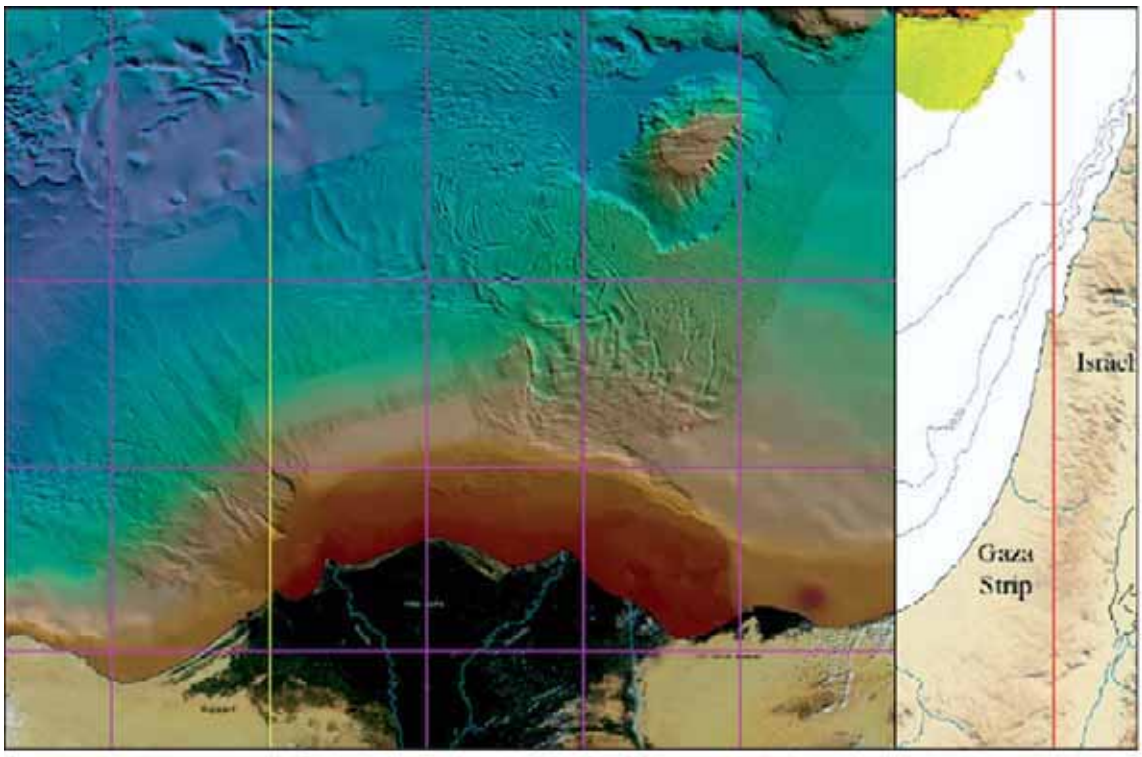

Figure 4. Underwater Nile delta fan as potential source of landslide induced tsunami for the Levantine basin (after Sardou and Mascle, 2003). *[refers to figure on p. 46]*

From Ceramicola *et al.*:

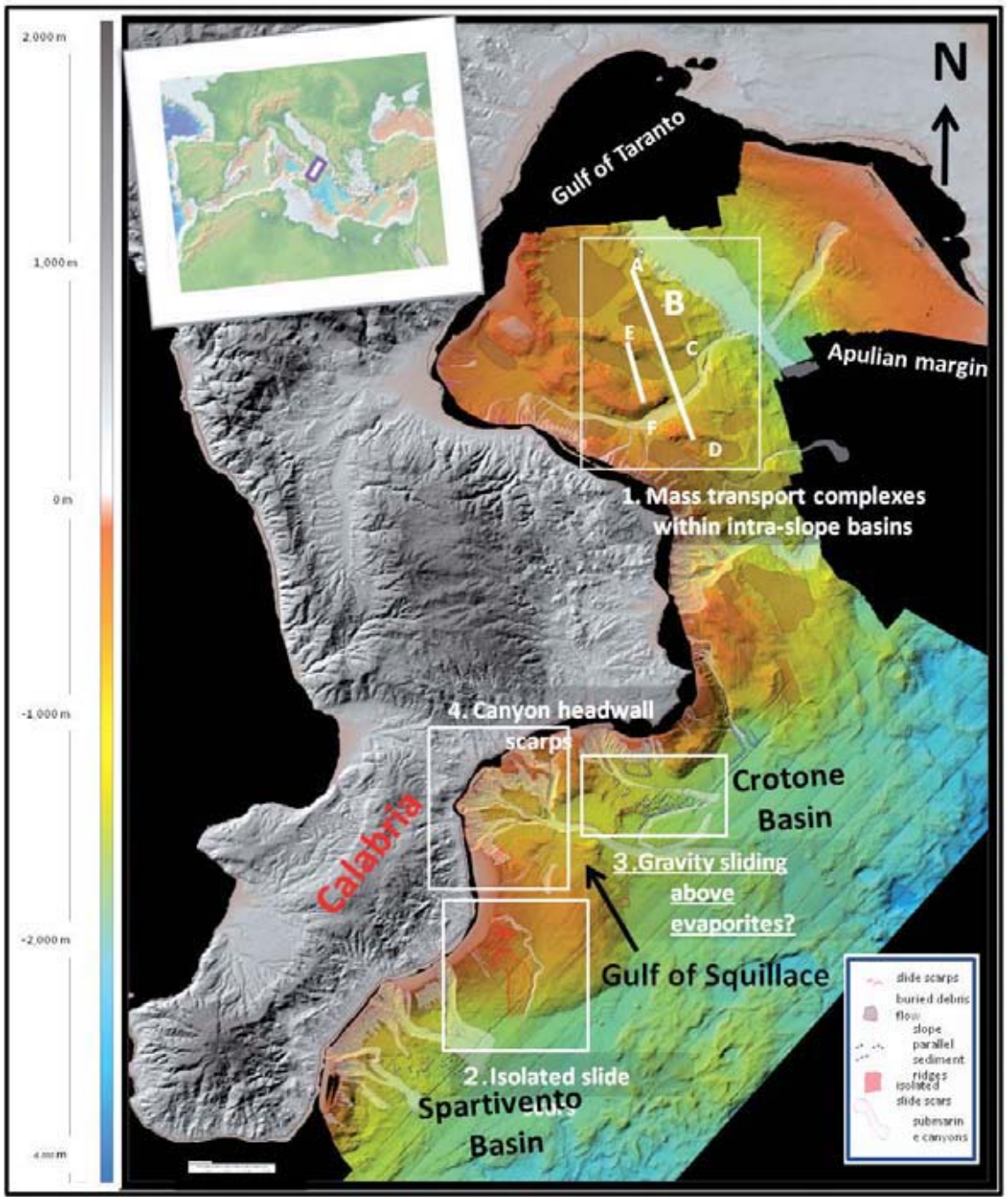

Fig. 1. Map of study area. *[refers to figure on p. 60]*

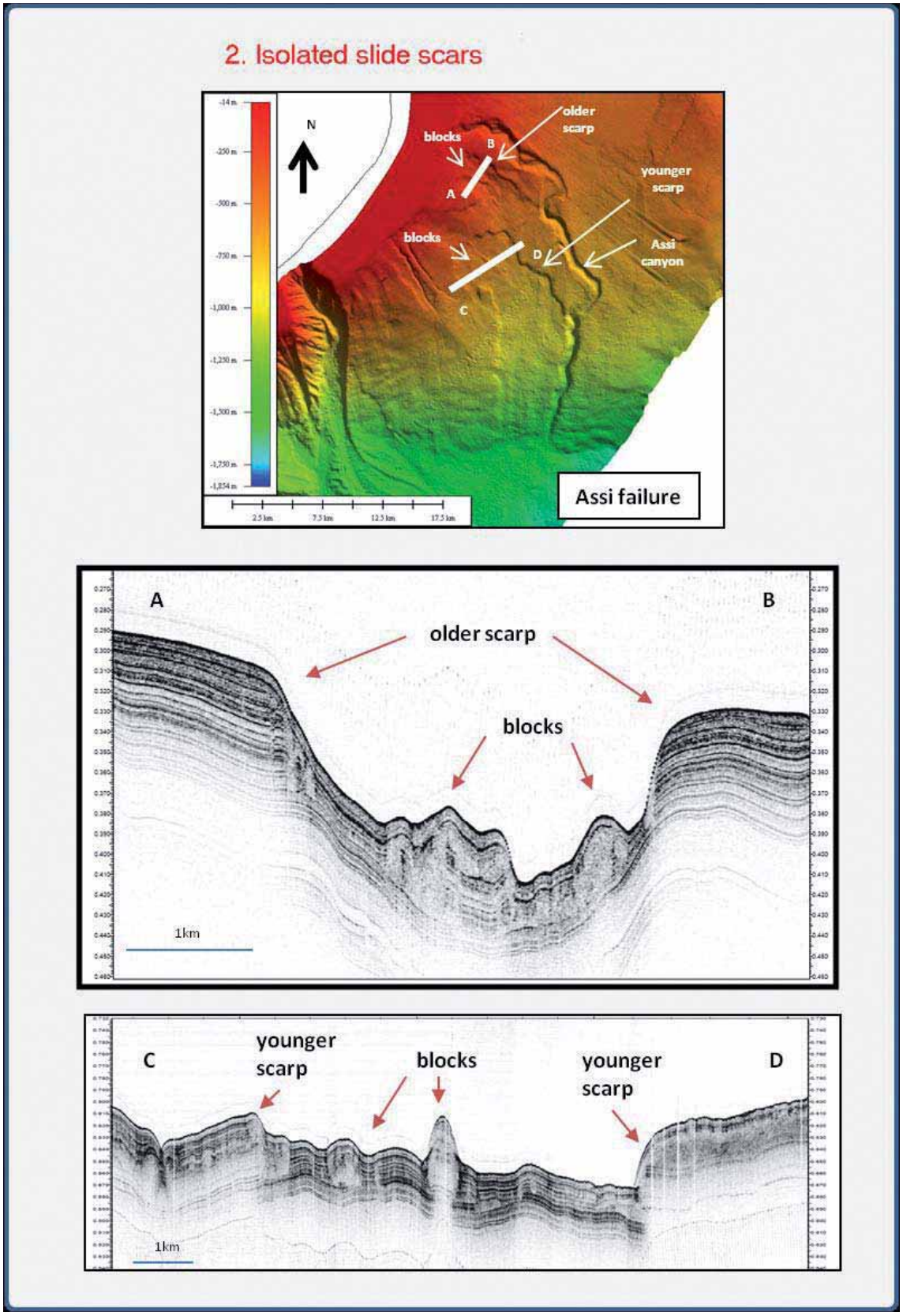

Fig. 3. Slide scars on open slopes. Location of swath bathymetry and sub-bottom profiles in Fig 1. *[refers to figure on p. 62]*

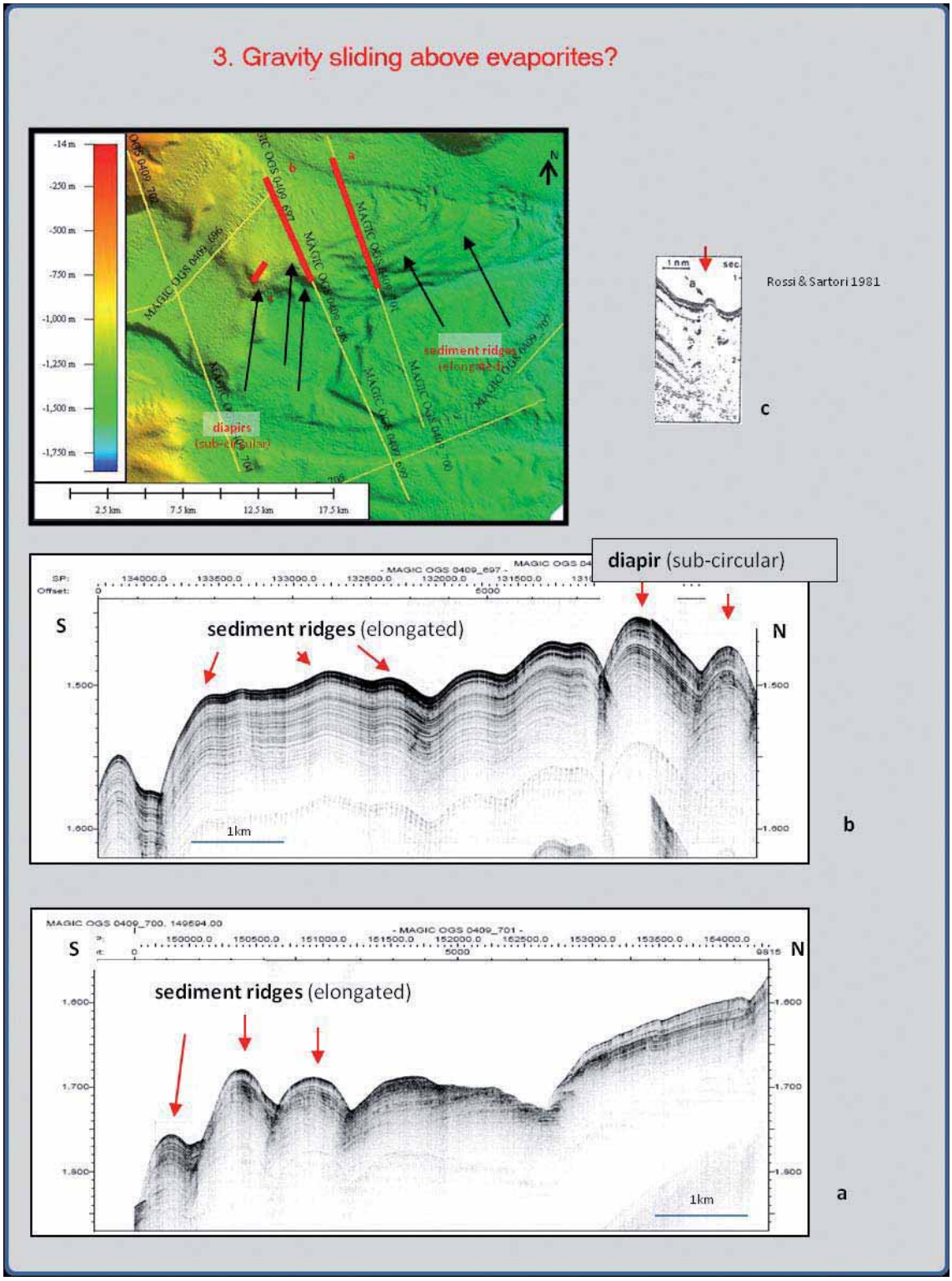

Fig. 4. Gravity sliding. Location of swath bathymetry and sub-bottom profiles in Fig 1.
[refers to figure on p. 63]

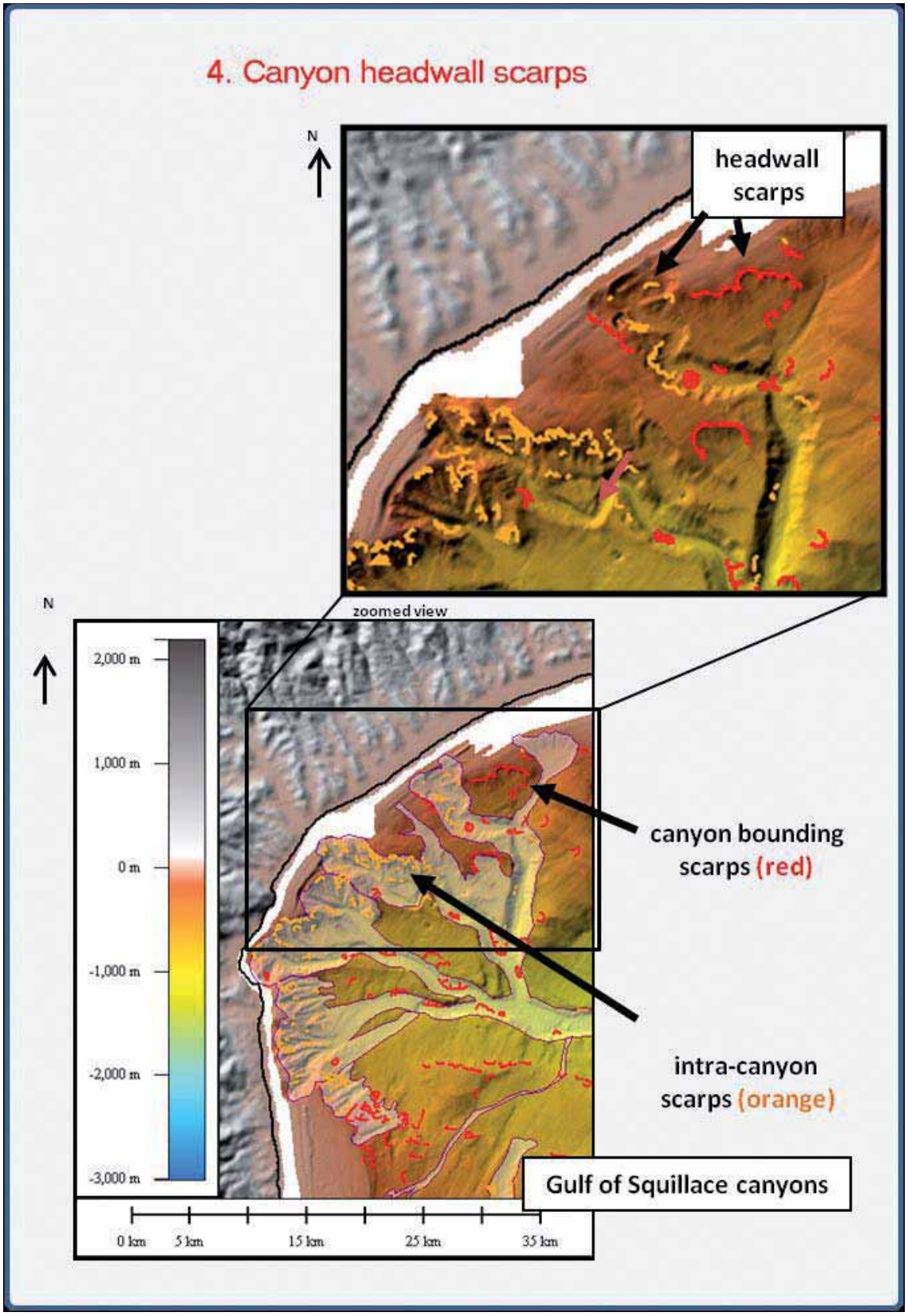

Fig. 5. Canyon headwall scarps. Location of swath bathymetry and sub-bottom profiles in Fig 1.
[refers to figure on p. 64]

From Migeon *et al.*:

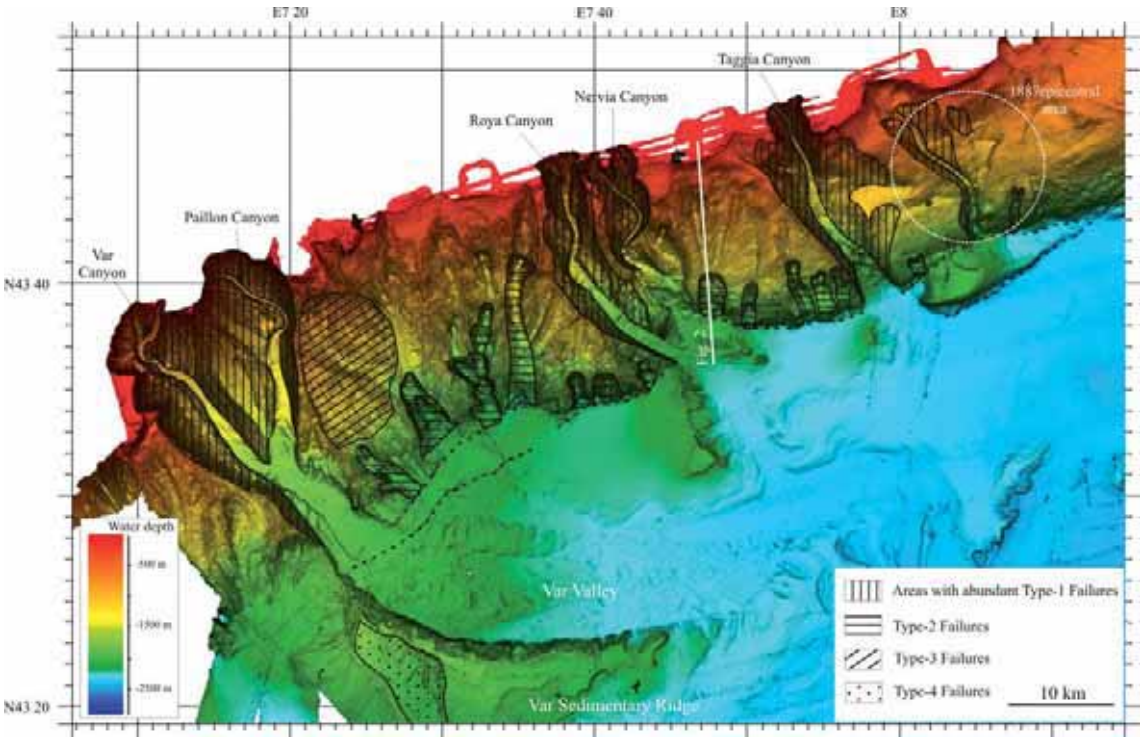

Figure 1. Bathymetric map illustrating the distribution and sizes of the main types of failures (see text for explanation) along the western segment of the northern Ligurian Margin. *[refers to figure on p. 69]*

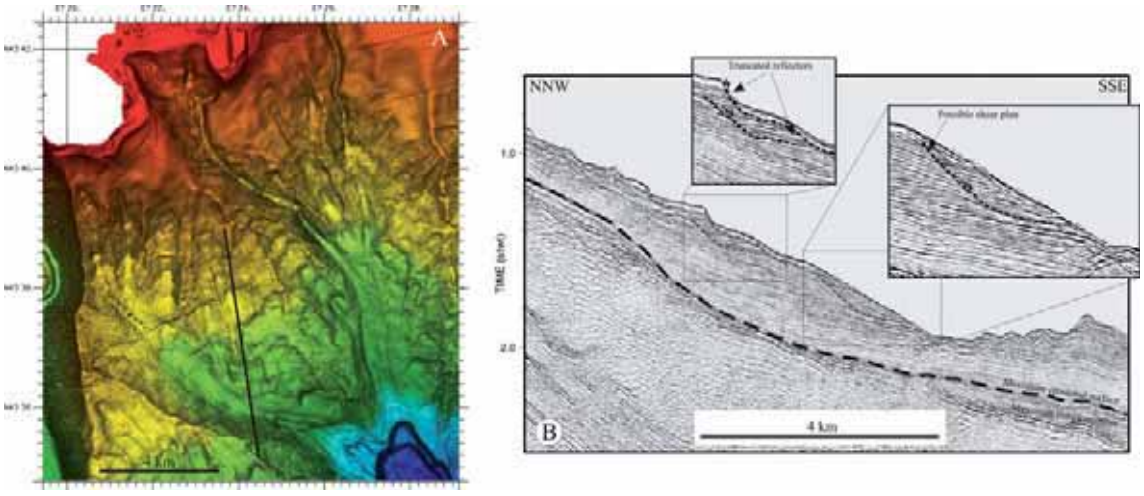

Figure 3. Shaded bathymetric map (A) and high-resolution seismic-reflection profile (B) illustrating the failures of type 3 located offshore Monaco. *[refers to figure on p. 71]*

From Sultan *et al.:*

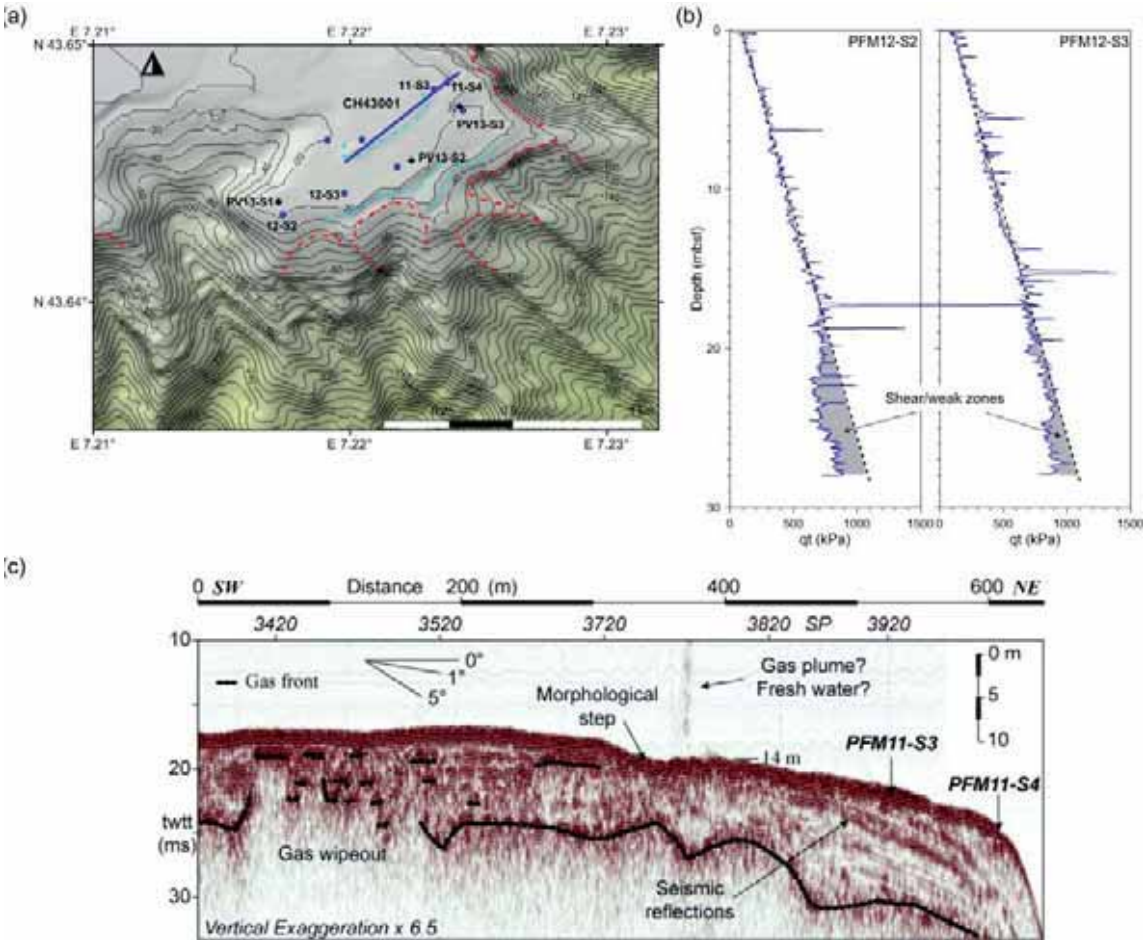

Figure 2. Nice slope study area: a) location of CH43001 Chirp sonar profile and available *in situ* geotechnical measurements projected on a shaded bathymetric map. Red dashed polylines indicate the uppermost headwall scarps of landslides and light blue dashed polylines highlight seafloor morphological steps. b) CPTu *in situ* data: corrected tip resistance (qt) versus depth from PFM12-S2 and PFM12-S3. For the 2 sites, shaded areas indicate significant decrease of the corrected tip resistance (possible shear zones). c) Profile CH43001 showing the presence of two seismic discontinuities to the NE at the edge of the slope. The two discontinuities fit with small seafloor morphological steps and correspond to a decrease in the sediment resistance measured at PFM11-S3 and PFM11-S4 (shear zones). A gas plume or fresh water flow can be observed in the water column above the morphological depression (trace: 3660-3670). *[refers to figure on p. 78]*

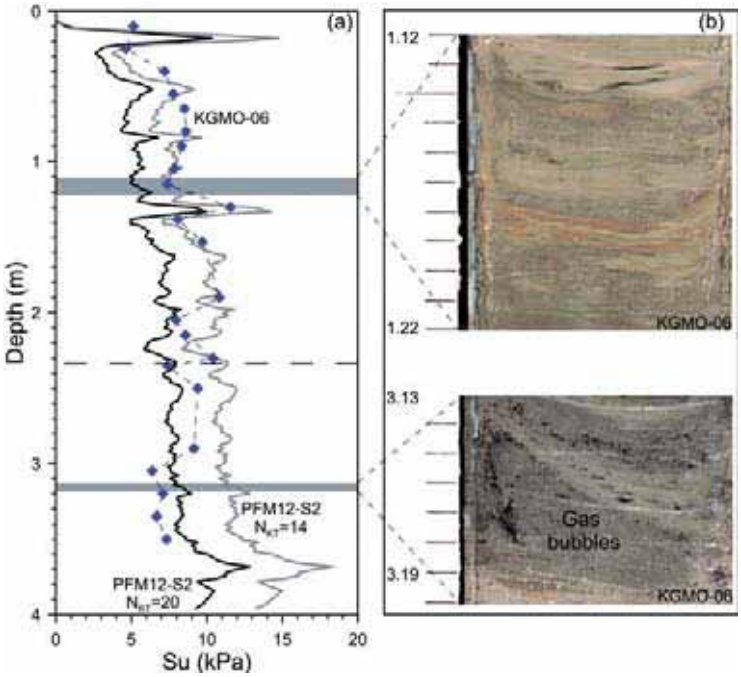

Figure 3. Free gas exsolution and expansion and degradation of the sediments' shear resistance: a) Undrained shear strength, Su, profiles derived from the piezocone test PFM12-S2 for empirical cone factor NKT of 14 and 20 compared with the Su values measured from laboratory vane shear tests. b) Photos of selected intervals from core KGMO-06 showing the vertical heterogeneity of the sediment. Note the disrupted sediment structures in the lower part of KGMO-06 and gas bubbles that exsolved during core retrieval.
[refers to figure on p. 79]

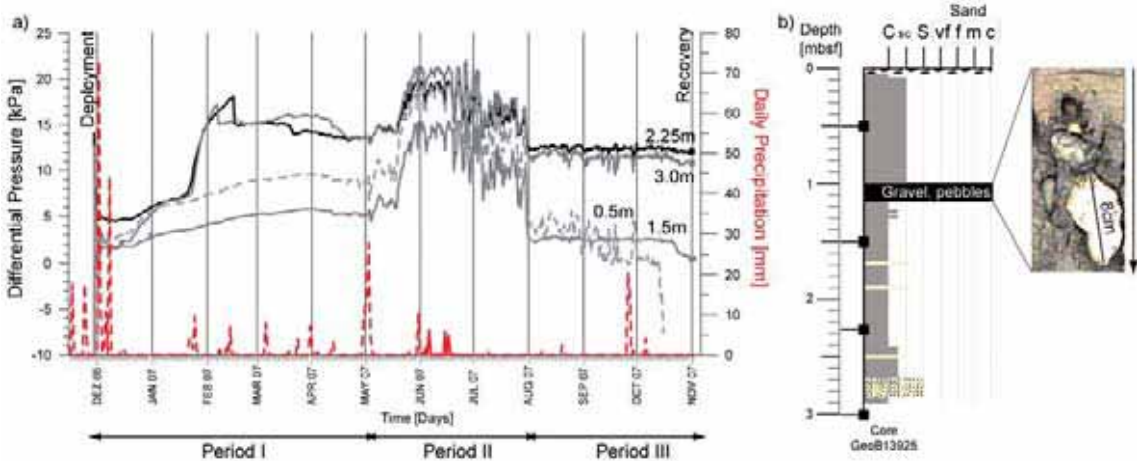

Figure 4. Excess pore pressure detection and quantification (from Stegmann *et al.*, 2011): a) Long-term pore pressure monitoring (1 year). Each curve represents one level of measurement (the corresponding depth is given in the graph). Annual pore pressure course is linked with hydrology by comparison with the daily precipitation rate measured at Nice Airport during the installation of the piezometer (<www.meteofrance.fr> b) Coarse-grained sediments and gravel recovered in the vicinity of the piezometer position. High permeable coarse grained portions imbedded in clayey-silty sediments favour the flow of fluids, due to the contrast of permeability hydraulic gradients. Pore water analyses here attest the occurrence of fresh water (Kopf *et al.,* 2009; 2010). *[refers to figure on p. 80]*

From De Martini *et al.*:

Figure 2. Two tsunami deposits found in the Augusta Bay sites. A) picture of a yellowish bioclastic layer (event AU-02) composed by few whole gastropods (*Hydrobia* spp., *P. conica*), abundant shell fragments (mollusks, corals and echinoderms), few ostracods, often broken benthic (*Ammonia* spp., *Bolivina* sp., *Cassidulina laevigata, Cibicides lobatulus, Haynesina germanica, Pullenia bulloides, Rosalina* spp., miliolids) and few badly preserved planktonic (*Globigerina* spp., *Globigerinoides* spp., *Globorotalia inflata, Turborotalita quinqueloba)* foraminifera; this layer shows a sharp erosional basal contact and no evidence for layering or grading. B) picture of a bioclastic layer with sharp (probably erosional) basal contact (event PR-02), with a huge amount of shell fragments, gastropods (*Pirenella conica*, with abrasions probably due to high energetic transport) and ostracods, benthic and few planktonic foraminifera (with a peculiar increment in the benthic foraminifera specific diversity with respect to adjacent deposits). *[refers to figure on p. 85]*

From Gamberi and Marani

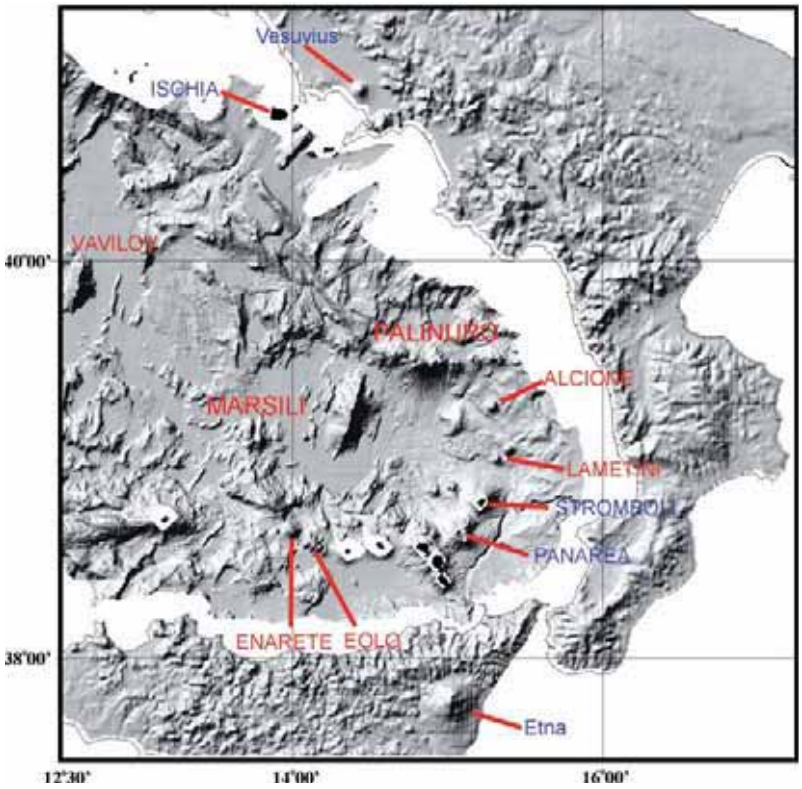

Fig. 2. Shaded relief of the southeastern Tyrrhenian Sea where the Aeolian arc and the Marsili backarc basin are developed. Locations treated in the text are indicated. *[refers to figure on p. 92]*

Fig. 3. Photograph taken from ROV of the gas expulsion event at Panarea in Novembre 2002.
[refers to figure on p. 93]

Fig. 4. Photograph taken from research vessel of the lava from the December/January eruption of Stromboli entering the sea to form a lava delta. *[refers to figure on p. 94]*

From Sallarès *et al.*:

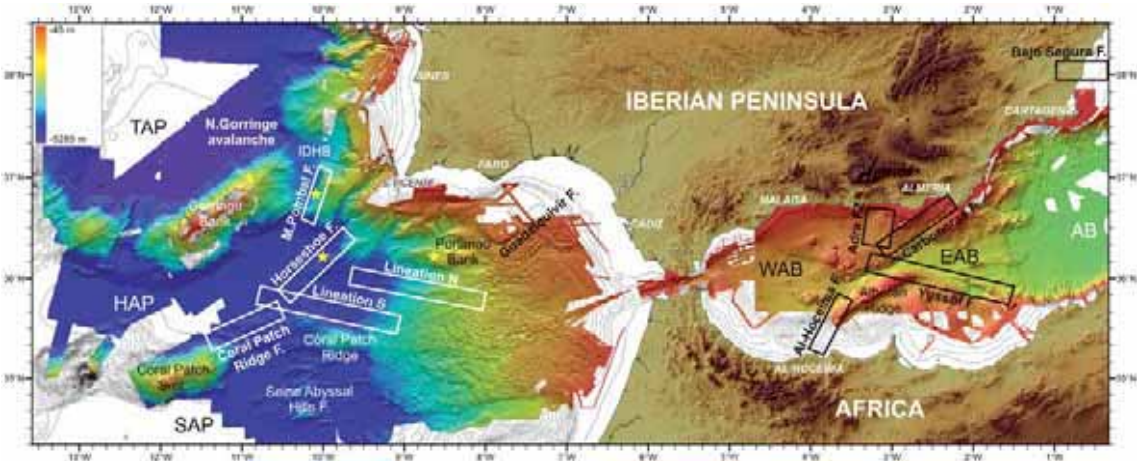

Figure 2. Topographic and bathymetric map of the Alboran Sea and Gulf of Cadiz. In the Alboran Sea (bathymetric map modified from MEDIMAP *et al*., 2008), the fault systems presented are depicted by a black outlined box. WAB: Western Alboran Basin; EAB: Eastern Alboran Basin; AB: Algerian Basin. In the Gulf of Cadiz (bathymetric map modified from Zitellini *et al*., 2009), the studied fault systems are marked by white outlined boxes. Yellow stars depict large landslides. TAP: Tagus Abyssal Plain; IDHB: Infante Don Henrique Basin; HAP: Horseshoe Abyssal Plain; SAP: Seine Abyssal Plain (Gràcia *et al*., 2010b).
[refers to figure on p. 104]

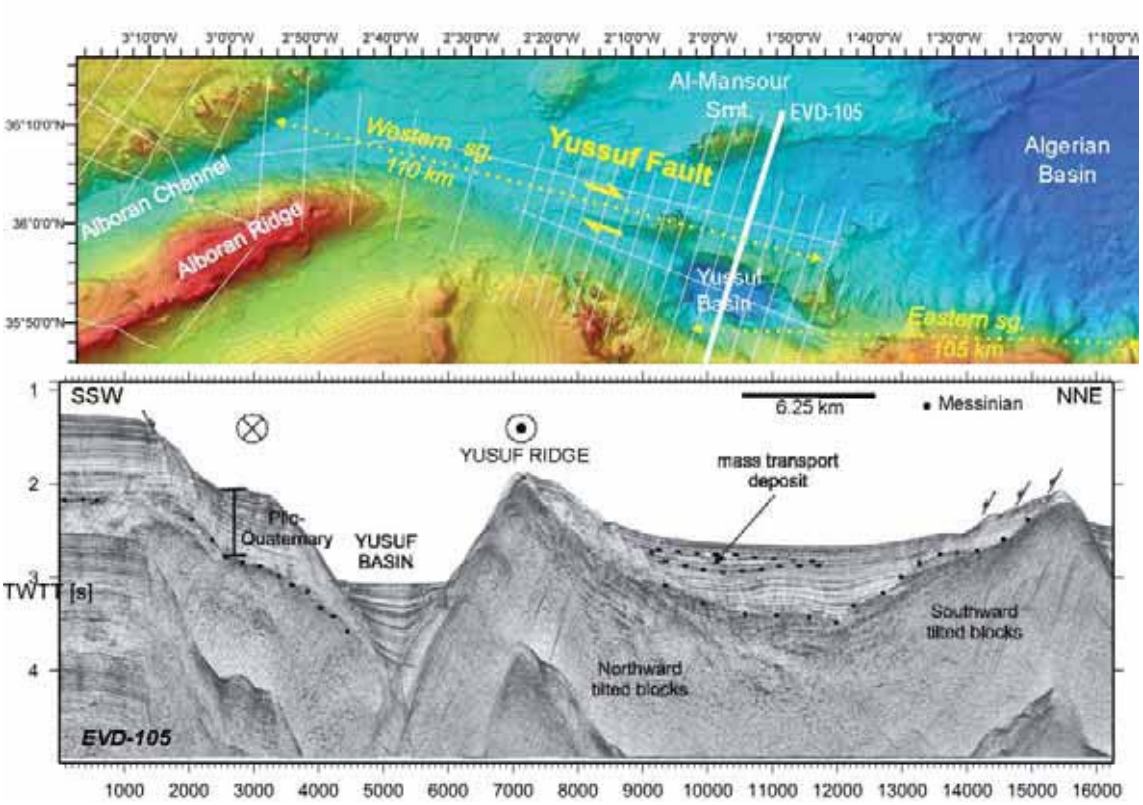

Figure 3. Top: Swath bathymetric map of the Yussuf Fault in the Alboran Sea, modified from MEDIMAP *et al.* (2008), where the main structures are located. Multi-channel seismic profiles acquired during the EVENT-DEEP survey are depicted by white lines. Bottom: Preliminary interpretation of the high-resolution seismic profile EVD105, which images with unprecedented resolution the Yussuf Fault at the pull-apart basin located in the eastern part of the Alboran Sea (Bartolomé *et al.,* 2010). *[refers to figure on p. 105]*

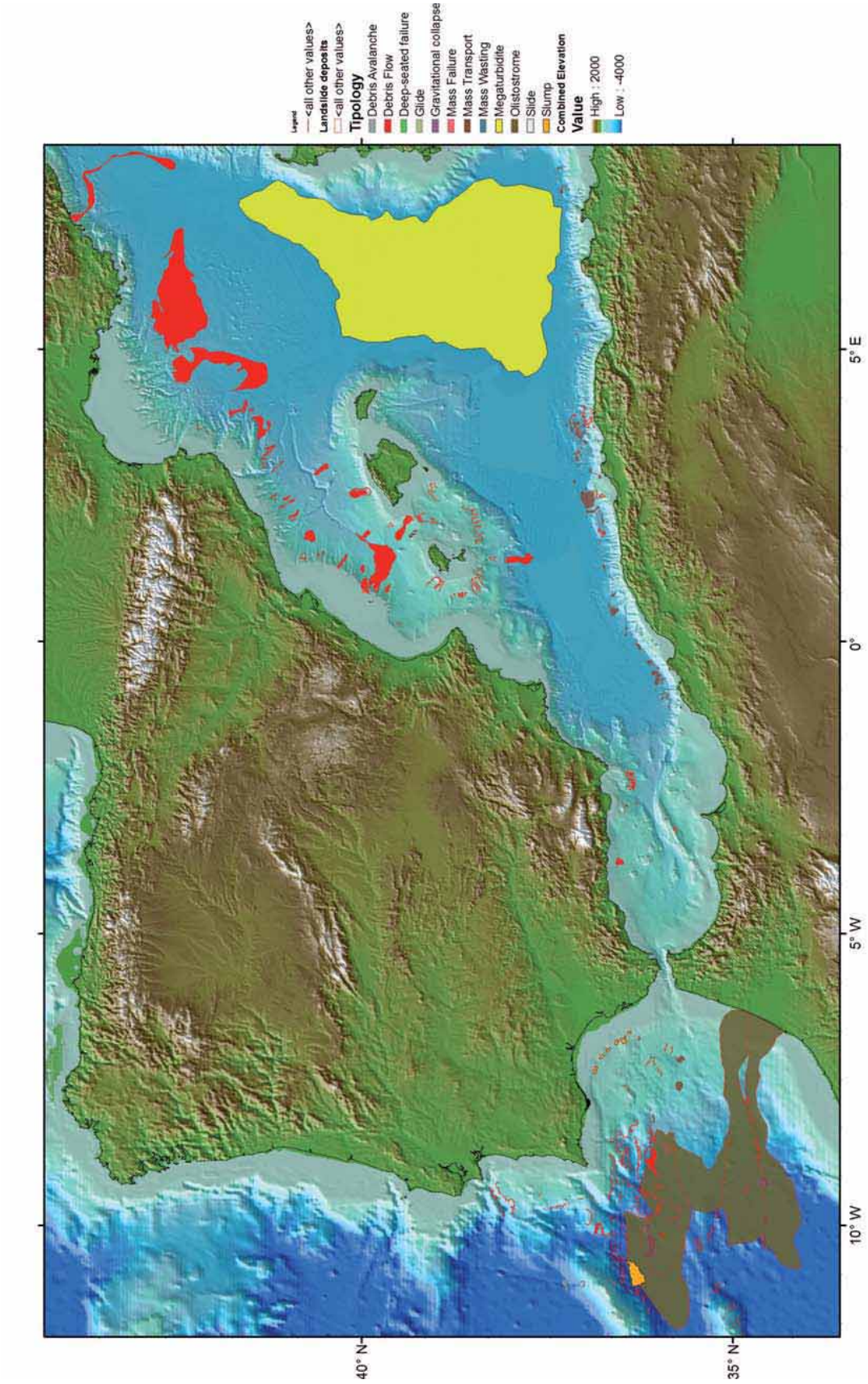

Figure 4. Display of all the submarine landslides in the eastern and southern Iberian margin, compiled from multiple sources, superimposed to the bathymetry shaded relief map (IOC, IHO and BODC 2003; Medimap Group *et al.*, 2008). *[refers to figure on p. 106]*

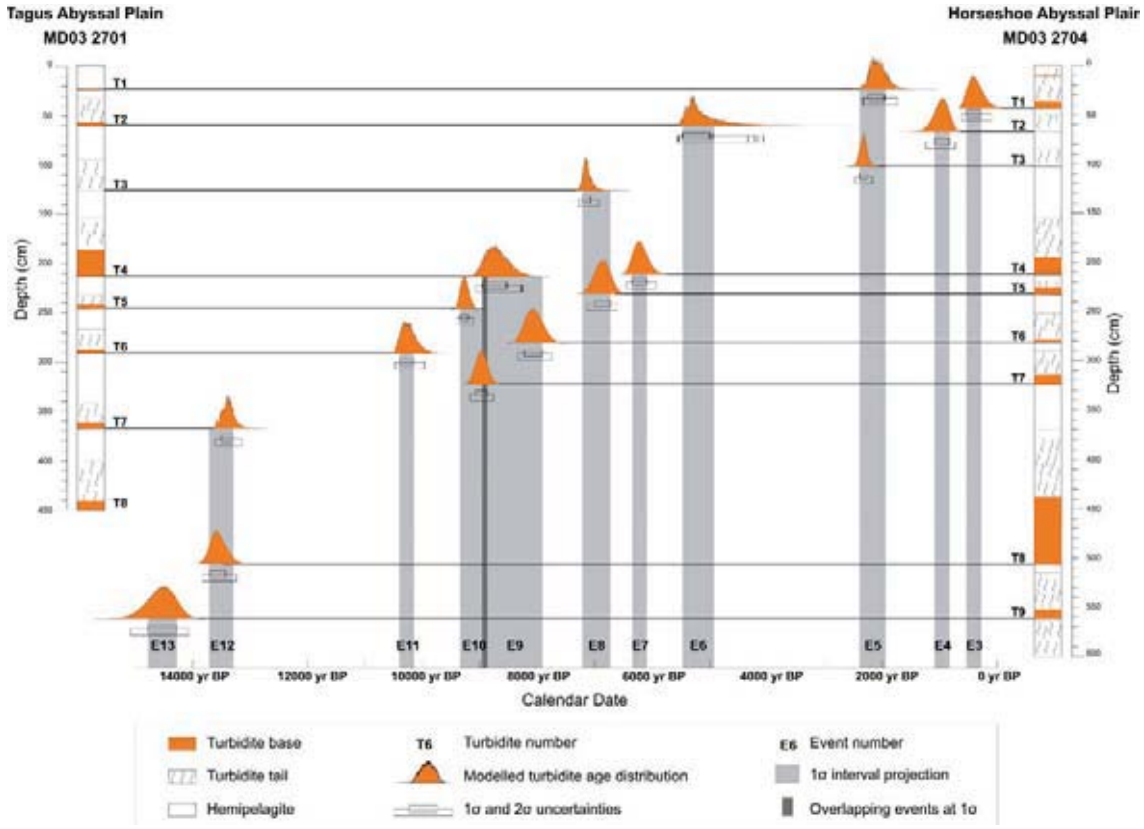

Figure 6. Age correlation of turbidites from the Tagus Abyssal Plain (MD03 2701) and the Horseshoe Abyssal Plain (MD03 2704). Probability distribution curves of modelled turbidite ages (orange) were obtained using OxCal 4.0 calibration software. Black horizontal lines link turbidite bases and their respective calibrated ages. Modelled turbidite ages (1s) are projected on the time axis by a purple band, where event numbers are indicated (Gràcia *et al*., 2010). *[refers to figure on p. 108]*

III - Bibliographic References

Abrantes F., Alt-Epping U., Lebreiro S., Voelker A. and Schneider R., 2008. Sedimentological record of tsunamis on shallow-shelf areas: the case of the 1969 AD and 1755 AD tsunamis on the Portuguese Shelf off Lisbon. *Mar. Geol.*, 249(3-4): 283-293.

Acosta J., Canals M., López-Martínez J., Muñoz A., Herranz P., Urgeles R., Palomo C. and Casamor J.L., 2002. The Balearic Promontory geomorphology (western Mediterranean): morphostructure and active processes. *Geomorphology*, 49: 177-204.

Aida I., 1975. Numerical experiments on tsunamis accompanied by landslide of Bisan, Shimabara, in 1792. *Zishin* (*Bull. Seismic. Soc. of Japan*), 28: 449-460.

Aksu A.E., Hall J.K. and Yaltirak C., 2005. Miocene to recent tectonic evolution of the eastern Mediterranean: new pieces of the old Mediterranean puzzle. Editorial, *Mar. Geol.*, 221: 1-13.

Alexander F. and Formichi R., 1993. Tectonic causes of landslides. *Earth. Surf. Proc. Land.*, 18: 311-338.

Almagor G., 1993. Continental slope processes off northern Israel and southernmost Lebanon and their relation to onshore tectonics. *Mar. Geol*., 112: 151-169.

Almagor G. and Garfunkel Z., 1979. Submarine slumping on the continental margin of Israel and Northern Israel. *Am. Assoc. Petrol. Geol*. Studies in Geology, 63: 324-340.

Altınok Y. and Ersoy S., 2000. Tsunamis observed on and near the Turkish coast. *Nat. Hazards*, 21: 185-205.

Altınok Y., Tinti S., Alpar B., Yalçıner A.C., Ersoy S., Bortolucci E. and Armigliato A., 2001. The tsunami of August 17, 1999 in Izmit Bay, Turkey. *Nat. Hazards,* 24: 133-146.

Altınok Y., Alpar B., Özer N. and Gazioğlu C., 2005. 1881 and 1949 earthquakes at the Chios-Çeşme Strait (Aegean Sea) and their relation to tsunamis. *Nat. Hazards Earth Syst. Sci*., 5: 717-725.

Altınok Y., Alpar B., Özer N. and Aykurt H., 2011. Revision of the tsunami catalogue affecting Turkish coasts and surrounding regions. *Nat. Hazards Earth Syst. Sci*., 11: 273-291.

Altunel E., 2003. Impacts of historical seismicity on major coastal cities in the southwestern Turkey. *In:* Human records of recent geological evolution in the Mediterranean, CIESM Workshop Monographs n° 24 [F. Briand ed.], Monaco, pp. 71-76.

Amblàs D., Canals M., Urgeles R., Lastras G., Liquete C., Hughes-Clarke J.E., Casamor J.L. and Calafat A.M., 2006. Morphogenetic mesoscale analysis of the northeastern Iberian margin, NW Mediterranean Basin. *Mar. Geol.*, 234: 3-20.

Ambraseys N.N., 1960. The seismic sea wave of July 9, 1956, in the Greek Archipelago. *J. Geophys. Res.*, 65(4): 1257-1265.

Ambraseys N.N., 1962. Data for the investigation of the seismic sea-waves in the Eastern Mediterranean. *Bull. Seismol. Soc. Am.*, 52(4): 895-913.

Ambraseys N.N., 1989. Temporary seismic quiescence: SE Turkey. *Geophys. J.*, 96: 311-331.

Ambraseys N.N., 1992a. Reappraisal of the seismicity in Cyprus (1894-1991), *In:* The seismicity of Cyprus, Ambraseys N.N. (ed.), ESEE Res. Report 92-9, published report, published by: Imperial College, London, pp. 1-46.

Ambraseys N.N., 1992b. The seismicity of Cyprus - Reappraisal of the seismic activity in Cyprus: 1894-1991, in ESEE Imperial College, London Research Report, No. 92, published report.

Ambraseys N.N., 1992c. Reappraisal of the seismic activity in Cyprus; 1894-1991. *B. Geofis. Teor. Appl.*, 34(133): 41-80.

Ambraseys N.N., 2002. The seismic activity of the Marmara Sea region over the last 2000 years. *Bull. Seism. Soc. Am.*, 92(1): 1-18.

Ambraseys N.N., 2009. Earthquakes in the Mediterranean and Middle East, a multidisciplinary study of seismicity up to 1900. Cambridge University Press, Cambridge, UK.

Ambraseys N.N. and Adams R.D., 1992. Seismicity of the Cyprus region. *In:* The seismicity of Cyprus, Ambraseys N.N. (ed.), ESEE Res. Report 92-9, published report, published by: Imperial College, London, pp. 47-67.

Ambraseys N.N., Melville C.P. and Adams R.D., 1994. The Seismicity of Egypt, Arabia and the Red Sea: an historical review, Cambridge University Press, Cambridge.

Ambraseys N. and Synolakis C., 2010. Tsunami catalogs for the Eastern Mediterranean, revisited. *J. Earthq. Eng.*, 14: 309-330.

Andersen K.H., Lunne T., Kvalstad T.J. and Forsberg C.F., 2008. Deep water geotechnical engineering, *In:* Proceedings of the XXIV National Conference of the Mexican Society of Soil Mechanics, Aguascalientes, 26-29 Nov. 2008, Mexican Society of Soil Mechanics, pp. 1-57.

Andresen A. and Bjerrum L., 1967. Slides in subaqueous slopes in loose sand and silt. Marine Geotechnique, Richards A. (ed.), Univ. Illinois Press, Urbana, pp. 221-239.

Anthony E.J. and Julian M., 1997. The 1979 Var Delta landslide on the French Riviera: a retrospective analysis. *J. Coastal Res.*, 13(1): 27-35.

Argus D.F., Gordon R.G., DeMets C. and Stein S., 1989. Closure of the Africa- Eurasia-North America plate motion circuit and tectonics of the Gloria fault. *J. Geophys. Res.*, 94: 5585-5602.

Armijo R., Lyon-Caen H. and Papanastassiou D., 1992. East-West extension and Holocene normal-fault scarps in the Hellenic Arc. *Geology*, 20: 491-494.

Armijo R., Flerit F., King G. and Meyer B., 2004. Linear elastic fracture mechanics explains the past and present evolution of the Aegean. *Earth Planet. Sci. Lett.*, 217(1-2): 85-95, doi: 10.1016/S0012-821X(03)00590-9.

Assier-Rzadkiewicz S., Mariotti C. and Heinrich P., 1997. Numerical simulation of submarine landslides and their hydraulic effects. *J. Waterway Port Coast. Oc. Eng.*, ASCE, 123(4): 149-157.

Assier-Rzadkiewicz S., Heinrich P., Sabatier P.C., Savoye B. and Bourillet J.F., 2000. Numerical modelling of a landslide-generated tsunami: the 1979 Nice event. *Pure Appl. Geophys.*, Birkhauser Verlag, Basel, 157: 1707-1727.

Auffret G.A., Auzende J.M. e*t al.*, 1982. Recent mass wasting processes on the Provencal Margin (Western Mediterranean). Contribution No. 719 of Centre Oceanologique de Bretagne, *In:* Marine slides and other mass movements, Saxon S. & Nieuwenhuis J.F. (eds), Plenum Press, New York, published in cooperation with NATO Scientific Affairs Division, pp. 52-58.

Austin B.J., 2006. Late Neogene mass transport deposits of the West Nile Delta, Egypt. Abstracts, Am. Assoc. Petrol Geol. Annual Meeting, Houston, Texas, <http://www.searchanddiscovery.net:16080/documents/2006/06088houston_abs/abstracts/austin.htm>

Baptista M.A., Heitor S., Miranda J.M., Miranda P. and Mendes Victor L., 1998. The 1755 Lisbon tsunami; evaluation of the tsunami parameters. *J. Geodyn.*, 25 (2): 143-157.

Baptista M.A., Miranda J.M., Chierici F. and Zitellini N., 2003. New study of the 1755 earthquake source based on multichannel seismic survey data and tsunami modeling. *Nat. Hazard Earth Sys.*, 3: 333-340.

Baraza J., Lee H.J., Kayen R.E. and Hampton M.A., 1990. Geotechnical characteristics and slope stability on the Ebro margin, Western Mediterranean. *Mar. Geol.*, 95: 379-393.

Barbano M.S., Pantosti D., De Martini P.M., Smedile A., Gerardi F. and Pirrotta C., 2007. Historical, archaeological and geological records of strong earthquakes at Capo Peloro (Southern Italy), GNGTS, Sessione 2.1, <http://www2.ogs.trieste.it/gngts/gngts/convegniprecedenti/2007/riassunti/tema-2/2-sess-1/21-barb.pdf>

Barbano M.S., Pirrotta C. and Gerardi F., 2010. Large boulders along the south-eastern Ionian coast of Sicily: storm or tsunami deposits? *Mar. Geol.*, 275: 140-154. doi:10.1016/j.margeo.2010.05.005.

Barkan R., Ten Brink U.S. and Lin J., 2009. Far field tsunami simulations of the 1755 Lisbon earthquake: Implications for tsunami hazard to the U.S. East Coast and the Caribbean. *Mar. Geol.*, 264:109-122.

Bartolomé R., Gràcia E., Stich D., Martínez–Loriente S., Klaeschen D., Masana E., Diez S., Lo Iacono C., Moreno X., Zitellini N., Mànuel A. and Dañobeitia J.J., 2009a. Seismic evidence of active strike-slip faulting in the external Gulf of Cadiz (SW Iberian Margin. EOS Trans AGU, Fall Meeting Suppl., San Francisco (USA).

Bartolomé R., Lo Iacono C. and Gràcia E., 2009b. Multiscale seismic imaging of active faults at sea. *Sea Tech.*, 50(5): 10-14.

Bartolomé R., Gràcia E., Lo Iacono C., Martínez-Loriente S., Moreno X., Perea H., Masana E. and EVENT-DEEP team, 2010. Seismic imaging of active faults in the Southern Alboran Sea (SE Iberian Margin): first results of the 2010 EVENT-DEEP cruise. *In:* Contribución de la Geología al Análisis de la Peligrosidad Sísmica, Insúa J.M. & Martín-González F. (eds), pp. 155-158.

Beccaluva L., Gabbianelli G., Lucchini F., Rossi P.L. and Savelli C., 1985. Petrology and K/Ar ages of volcanics dredged from the Aeolian seamounts: implications for geodynamic evolution of the Southern Tyrrhenian basin. *Earth Planet. Sci. Lett.*, 74: 187-208.

Beer T. and Ismail-Zadeh A., 2003. Risk science and sustainability, Kluwer Publ.

Behrens J., Androsov A., Babeyko A.Y., Harig S., Klaschka F. and Mentrup L., 2010. A new multi-sensor approach to simulation assisted tsunami early warning. *Nat. Hazards Earth Syst. Sci.*, 10: 1085-1100.

Beisel S.A., Chubarov L.B., Kit E., Levin A., Shokin Yu.I. and Sladkevich M., 2008. Tsunami near the Israeli coast: preliminary results of numerical modeling. *In:* Proceedings of the IX All-Russian Conference "Applied technologies of hydroacoustics and hydrophysics", St. Petersburg: Nauka, (750 p.), pp. 432-436.

Beisel S., Chubarov L., Didenkulova I., Kit E., Levin A., Pelinovsky E., Shokin Y. and Sladkevich M., 2009. The 1956 Greek tsunami recorded at Yafo, Israel, and its numerical modeling. *J. Geophys. Res.*, 114, C09002, doi:10.1029/2008JC005262.

Belkis N., 2003. The effect of Marmara (Izmit) earthquake on the chemical oceanography of Izmit Bay, Turkey. *Mar. Pollut. Bull.*, 46: 865-878.

Ben-Avraham Z., Tibor G., Limonov A.F., Leybov M.B., Ivanov M.K., Tokarev M.Y. and Woodside J.M., 1995. Structure and tectonics of the eastern Cyprean Arc. *Mar. Petrol. Geol.*, 12: 263-271.

Ben-Menahem A., 1991. Four thousand years of seismicity along the Dead Sea Rift. *J. Geophys. Res.*, 91: 20195-20216.

Ben-Menahem A. and Roseman M., 1972. Amplitude patterns of tsunami waves from submarine earthquake. *Jour. Geophys. Res.*, 77(17): 3,097-3,128.

Berger M.J., George D.L., LeVeque R.J. and Mandeli K., 2010. The GeoClaw software for depth-averaged flows with adaptive refinement. Preprint submitted to Elsevier.

Bertoni C. and Cartwright J., 2005. 3D seismic analysis of slope confined canyons from the Plio-Pleistocene of the Ebro Continental Margin (Western Mediterranean). *Basin Res.*, 17: 43-62.

Biju-Duval B. and Montadert L., 1976. Structural history of the Mediterranean Basins. Paris, ed. Technip, 464 p.

Billi A., Funiciello R., Minelli L., Faccenna C., Neri G., Orecchio B. and Presti D., 2008. On the cause of the 1908 Messina tsunami, southern Italy. *Geophys. Res. Lett.*, 35, L06301, doi:10.1029/2008GL033251.

Biscotin G., Pestana J.M. and Nadim F., 2004. Seismic triggering of submarine slides in soft cohesive soil deposits. *Mar. Geol.*, 203(3-4): 341-354.

Boldini D., Wang F., Sassa K. and Tommasi P., 2009. Application of large scale ring shear tests to the analysis of tsunamigenic landslides at Stromboli. *Landslides*, 6(3): 231-240.

Börner T., Galletti M., Marquart N.P. and Krieger G., 2010. Concept study of radar sensors for near-field tsunami early warning. *Nat. Hazards Earth Syst. Sci.*, 10: 1957-1964, <www.nat-hazards-earth-syst-sci.net/10/1957/2010/> doi:10.5194/nhess-10-1957-2010>

Bronk Ramsey C., 2009. Bayesian analysis of radiocarbon dates. *Radiocarbon*, 51(1): 337-360.

Brooks N. and Ferentinos G., 1984. Tectonics and sedimentology in the Gulf of Corinth and Zakynthos and Kefallinia Chanels, western Greece. *Tectonophysics*, 101: 25-54.

Brosolo L. and Mascle J., 2008. Shaded bathymetry of the Mediterranean Sea, DTM at 500 m grid from swath bathymetric data and Gebco DTM. *In:* CNRS-INSU Terre, Planète Mystérieuse, Editions Le Cherche Midi, 125 p.

Brückner H., Müllenhoff M., VanDer Borg K. and Vött A., 2003. Holocene coastal evolution of Western Anatolia-the interplay between natural factors and human impacts. *In:* Human records of recent geological evolution in the Mediterranean. CIESM Workshop Monograph n° 24 [F. Briand ed.], Monaco, pp. 51-56.

Bruins H.J., MacGillivray J.A., Synolakis C.E., Benjamini C., Keller J., Kisch H.J., Kluegel A. and Van der Plicht J., 2008. Geoarchaeological tsunami deposits at Palaikastro (Crete) and the Late Minoan IA eruption of Santorini. *J. Archaeol. Sci.*, 35: 191-212.

Budillon F., Ferraro L., Hopkins T.S., Iorio M., Tonielli R., Bellonia A., D'Isanto C. and Scotto P., 2005. Morphology and surface geology of the Augusta Bay (Eastern Ionian Sea): results of geophysical surveys. *Geophysical Research Abstracts*, 7: 10128.

Budillon F., Ferraro L., Hopkins T.S., Iorio M., Lubritto C., Sprovieri M., Bellonia A., Marzaioli F. and Tonielli R., 2008. Effects of intense anthropic settlement of coastal areas on sea-bed and sedimentary systems: a case study from the Augusta Bay (Southern Italy). *Rendiconti online della Società Geologica Italiana*, 3: 142-143.

Buforn E., Sanz de Galdeano C. and Udías A., 1995. Seismotectonics of the Ibero-Maghrebian region. *Tectonophysics*, 248: 247-261.

Buforn E., Bezzeghoud M., Udías A. and Pro C., 2004. Seismic sources on the Iberia-African Plate boundary and their tectonic implications. *Pure Appl. Geophys.*, 161: 623-646.

Burwell D., Tolkova E. and Chawla *A.*, 2007. Diffusion and dispersion characterization of a numerical tsunami model. *Ocean Model.*, 19: 10-30.

Camerlenghi A., Accettella D., Costa S., Lastras G. Acosta J., Canals M. and Wardell N., 2009. Morphogenesis of the SW Balearic continental slope and adjacent abyssal plain, Western Mediterranean Sea. *Int. J. Earth Sci.* (Geol Rundsch), 98: 735-750.

Camerlenghi A., Urgeles R. and Fantoni L., 2010. A database on submarine landslides of the Mediterranean Sea. *In:* Submarine mass movements and their consequences, advances in natural and technological hazards research, Mosher D.C., Moscardelli L., Shipp R.C., Chaytor J.D., Baxter C.D.P., Lee H.J. & Urgeles R. (eds), Spinger, Dordrecht (The Netherlands), 28: 491-501.

Capaccioni B., Tassi F., Vaselli O., Tedesco D. and Poreda R., 2007. Submarine gas burst at Panarea Island (southern Italy) on 3 November 2002: a magmatic versus hydrothermal episode. *J. Geoph. Res.*, 112: 567-582.

Capone T., Panizzo A. and Monaghan J., 2008. SPH modeling of water waves generated by submarine deformable landslides. Proc. ICCE 2008, Hamburg.

Caratori Tontini F., Cocchi L., Muccini F., Carmisciano C., Marani M., Bonatti E., Ligi M. and Boschi E., 2010. Potential field modeling of collapse-prone submarine volcanoes in the southern Tyrrhenian Sea (Italy). *Geophys. Res. Lett.*, 37, L03305, Doi:10.1029 /2009 gl0417 57

Cattaneo A., Babonneau N., Dan G., Déverchère J., Domzig A., Gaullier V., Lepillier B. and de Lépinay B.M., Nouguès A., Strzerzynski P., Sultan N. and Yelles K., 2010. Submarine landslides along the Algerian margin: A review of their occurrence and potential link with tectonic structures. *In:* Submarine mass movements and their consequences, advances in natural and technological hazards research, Mosher D.C., Moscardelli L., Shipp R.C., Chaytor J.D., Baxter C.D.P., Lee H.J. & Urgeles R. (eds), Spinger, Dordrecht (The Netherlands), 28: 515-525.

Ceramicola S., Civile D., Caburlotto A., Cova A., Accettella D., Caffau M., Cotterle D., Diviacco P., Wardell N. and Ramella R., 2008. Dinamiche morfo-sedimentarie del margine calabro ionico settentrionale per definire il rischio geologico (Progetto MaGIC). Extended abstract of the 84° Congresso della Società Geologica Italiana, 15-17 settembre 2008 Sassari, Italy, pp. 210-11.

Ceramicola S., Caburlotto A., Coste M., Cova A., Migeon S., Forlin E. Praeg D., Diviacco P., Cotterle D., Romeo R., Facchin L., Civile D., Ramella R., Critelli S. and Chiocci F.L., 2010a. Seabed features in relation to geohazards on the Ionian Calabrian margin: results from the MAGIC Project. *Rapp. Comm. int. Mer Médit.*, 39: 13.

Ceramicola S., Forlin E., Coste M., Cova A., Praeg D., Fanucci F. and Critelli S., 2010b. Submarine mass wasting on the Ionian Calabrian margin. American Geophysical Union, Fall Meeting 2010, abstract #OS13E-1295

Chassefiere B., 1990. Mass-physical properties of surficial sediments on the Rhône continental margin: implications for the nepheloid benthic layer. *Cont. Shelf Res.*, 10(9-11): 857-867.

Chester D., 1993. Volcanoes and society, Arnold, London, 351 p.

Chiocci F.L. and DeAlteriis G., 2006. The Ischia debris avalanche: first clear submarine evidence in the Mediterranean of a volcanic Island prehistorical collapse. *Terra Nova*, 18: 202-209.

Chiocci F.L., Romagnoli C., Tommasi P. and Bosman A., 2008. The Stromboli 2002 tsunamigenic submarine slide: characteristics and possible failure mechanisms. *J. Geophys. Res.*, 113, B10102, doi:10.1029/2007JB005172

CIESM, 2003. Human records of recent geological evolution in the Mediterranean Basin - historical and archeological evidence. CIESM Workshop Monograph n° 24, [F. Briand ed.], 152 p., Monaco.

Clarke S.H., Greene H.G. and Kennedy M.P., 1985. Identifying potentially active faults and unstable slopes offshore. *In:* Evaluating earthquake hazards in the Los Angeles region - An Earth-science perspective, Ziony J.I. (ed.), U.S. Geological Survey Professional Paper 1360, U.S. Gov't. Printing Office, Washington D.C., pp. 347-374; references, pp. 494-496.

Clavell E. and Berastegui X., 1991. Petroleum geology of the Gulf of Valencia. *In:* Spencer, A.M. (ed.), Generation, accumulation and production of Europe's hydrocarbons: Special Publication EAPG, Oxford University Press, 1: 355-368.

Cochonat P., Bourillet J.F., Savoye B. and Dodd L., 1993. Geotechnical characteristics and instability of submarine slope sediments, the Nice slope (N–W Mediterranean Sea). *Mar. Georesour. Geotec.*, 11(2): 131-151.

Cochonat P. and Person R., 2008. Deep seafloor observatories: a new tool for monitoring geohazards, climate change, ecosystem life and evolution. *In:* Towards an integrated system of Mediterranean marine observatories. CIESM Workshop Monographs n° 34, [F. Briand ed.], Monaco, pp. 43-52.

Collot J.Y., Lewis K., Lamarche G. and Lallemand S., 2001. The giant Ruatoria debris avalanche on the northern Hikurangi margin, New Zeland: result of oblique seamount subduction. *J. Geophys. Res.*, 106(B9): 19271-19297.

Comas M.C., Platt J.P., Soto J.I. and Watts A.B., 1999. The origin and tectonic history of the Alboran Basin: insights from leg 161 results. *In:* Proc. ODP, Sci. Res., Zahn R., Comas M.C. & Klaus A. (eds), Ocean Drilling Program, College Station TX, 161: 555-580.

Comninakis N., Delibasis and Galanopoulos A., 1964. A tsunami generated by an earth slump set in motion without shock, on February 7, 1963. *Annales Geologiques des Pays Helleniques*, Athens, Greece, 3 p.

Corti G., Cuffaro M., Doglioni C., Innocenti F. and Maneti P., 2006. Coexisting geodynamic processes in the Sicily Channel. Geological Soc. of America, special paper, 409: 83-96.

CPTI Working group, 2004. Catalogo Parametrico dei Terremoti Italiani, version 2004 (CPTI04). INGV, Bologna <http://emidius.mi.ingv.it/CPTI/>

D'alessandro A., D'anna G., Luzio D. and Mangano G., 2008. Polarization and high resolution parametric spectral analysis applied to the seismic signals recorded on the Marsili submarine volcano. Geophysical Research Abstracts, Vol. 10, EGU2008-A-06733, 2008 SRef-ID: 1607-7962/gra/EGU2008-A-06733. EGU General Assembly 2008.

Daëron M., Klinger Y., Tapponnier P., Elias A., Jacques E. and Sursock A., 2005. Sources of the large A.D. 1202 and 1759 Near East earthquakes. *Geology*, 33: 529-532.

Dall'Osso F., Maramai A., Graziani L., Brizuela B., Cavalletti A., Gonella M. and Tinti S., 2010. Applying and validating the PTVA-3 Model at the Aeolian Islands, Italy: assessment of the vulnerability of buildings to tsunamis. *Nat. Hazard Earth Sys.*, 10: 1547-1562.

Dan G., Sultan N. and Savoye B., 2007. The 1979 Nice harbour catastrophe revisited: trigger mechanism inferred from geotechnical measurements and numerical modelling. *Mar. Geol.*, 245: 40-64.

Das K., Green S., Basu D., Janetzke R. and Stamatakos J., 2009. Effect of slide deformation and geometry on waves generated by submarine landslides: a numerical investigation, offshore technology conference, Houston, Texas, USA, 4-7 May 2009., OTC paper 20293.

Dawson A.G. and Stewart I., 2007. Tsunami deposits in the geological record. *Sediment. Geol.*, 200(3-4): 166-183.

Delange W.P., Prasetya G.S. and Healy T.R., 2001. Modelling of tsunamis generated by pyroclastic flows (ignimbrites). *Nat. Hazards*, 24: 251-266.

De Martini P.M., Burrato P., Pantosti D., Maramai A., Graziani L. and Abramson H., 2003. Identification of tsunami deposits and liquefaction features in the Gargano area (Italy): paleoseismological implication. *Ann. Geophys-Italy,* 46(5): 883-902.

De Martini P.M., Barbano M.S., Smedile A., Gerardi F., Pantosti D., Del Carlo P. and Pirrotta C., 2010. A 4,000 yrs long record of tsunami deposits along the coast of the Augusta Bay (eastern Sicily, Italy): paleoseismological implications. *Mar. Geol.*, 276: 42-57, doi: 10.1016/j.margeo.2010.07.005

Demers D., Leroueil S. and d'Astous J., 1999. Investigation of a landslide in Maskinonge, Quebec. *Can. Geotech. J.*, 36(6): 1001-1014.

Dewey J.F. and Sengoer C.A.M., 1979. Aegean and surrounding regions: complex multiplate and continuum tectonics in a convergent zone. *Geol. Soc. Am. Bull.*, 90: 84-92.

Di Leonardo R., Bellanca A., Capotondi A., Cundy A. and Neri R., 2007. Possible impacts of Hg and PAH contamination on benthic foraminiferal assemblages: an example from the Sicilian coast, central Mediterranenan. *Sci. Total. Environ.*, 338: 168-183.

Didenkulova I., Nikolkina I., Pelinovsky E. and Zahibo N., 2010. Tsunami waves generated by submarine landslides of variable volume: analytical solutions for a basin of variable depth. *Nat. Hazards Earth Syst. Sci.*, 10: 2407-2419 <www.nat-hazards-earth-syst-sci.net/10/2407/2010/>

Diez S. and Gràcia E., 2005. Submarine mapping using multibeam bathymetry and acoustic backscatter: illuminating the seafloor. *Instrumentation Viewpoint*, 3: 10-14.

Dimitriadis I., Papazachos C., Panagiotopoulos D., Hatzidimitriou P., Bohnhoff M., Rische M. and Meier T., 2010. P and S velocity structures of the Santorini- Coloumbo volcanic system (Aegean Sea, Greece) obtained by non-linear inversion of travel times and its tectonic implications. *J. Volcanol. Geoth. Res.*, 195: 13-30.

Doglioni C., Gueguen E., Sàbat F. and Fernàndez M., 1997. The Western Mediterranean extensional basins and the Alpine orogen. *Terra Nova*, 9: 109-112.

Dolfi D., De Rita D., Cimarelli C., Mollo S., Soligo M. and Fabbri M., 2007. Dome growth rates, eruption frequency and assessment of volcanic hazard: insight from new U/Th dating of the Panarea and Basiluzzo dome lava and pyroclastics, Eolian Islands, Italy. *Quat. Int.*, 162(13): 182-194.

Dominey-Howes D., 2002. Documentary and geological records of tsunami in the Aegean Sea region of Greece and their potential value to risk assessment and disaster management. *Nat. Hazards*, 25: 195-224.

Dominey-Howes D., 2004. A re-analysis of the Late Bronze Age eruption and tsunami of Santorini, Greece, and the implications for the volcano-tsunami hazard. *J. Volcanol. Geoth. Res.*, 130: 107-132.

Dominey-Howes D., Papadopoulos G.A. and Dawson A.G., 2000. Geological and historical investigation of the 1650 Mt. Columbo (Thera Island) eruption and tsunami, Aegean Sea, Greece. *Nat. Hazards*, 21: 83-96.

Droz L., dos Reis A.T. and Rabineau M., 2006. Quaternary turbidite systems on the northern margins of the Balearic Basin (Western Mediterranean): a synthesis. *Geo-Mar. Lett.*, 26: 347-359.

Druitt T.H., Edwards L., Mellors R.M., Pyle D.M., Sparks R.S.J., Lanphere M., Davies M. and Barreirio B., 1999. Santorini volcano. *Geol. Soc. London Mem.*, 19: 165 p. and 1:20,000 geol. map.

Dubar M. and Anthony E.J., 1995. Holocene Environmental Change and River-Mouth Sedimentation in the Baie des Anges, French Riviera. *Quaternary Res.*, 43: 329-343.

Dzvonkovskaya A. and Gurgel K.W., 2009. Future contribution of HF radar WERA to tsunami early warning systems. *European Journal of Navigation*, 7(2): 7 p.

Edison G., Teng M.H., Liu P.L.F., Titov V. and Zhou H., 2007. Sensitivity analysis of source parameters for earthquake-generated distant tsunamis. *J. Waterway Port Coast. Oc. Eng.*, 133(6): 429-441.

Elias A., Tapponnier P., Singh S.C., King G.C.P., Briais A., Daëron M., Carton H., Sursock A., Jacques E., Jomaa R. and Klinger Y., 2007. Active thrusting offshore Mount Lebanon: source of the tsunamigenic A.D. 551 Beirut-Tripoli earthquake. *Geology*, 35(8): 755-758, DOI: 10.1130/G23631A.1

El-Robrini M., Gennesseaux M. and Mauffret A., 1985. Consequences of the El-Asnam earthquakes: turbidity currents and slumps on the Algerian margin (Western Mediterranean. *Geo-Mar. Lett.*, 5: 171-176.

EOS, 2011. Lessons from Japan's earthquake and tsunami, 92(12): 97-99.

Esposito A., Giordano G. and Anzidei M., 2006. The 2002-2003 submarine gas eruption at Panarea volcano (Aeolian Islands, Italy): volcanology of the seafloor and implications for the hazard scenario. *Mar. Geol.*, 277: 119-134.

Esposito A., Anzidei M., Aztori S., Devoti R., Giordano G. and Pierantonio G., 2010. Modelling ground deformations of Panarea volcano hydrothermal/geothermal system (Aeolian Islands, Italy) from GPS data. *Bull. Volcan.*, 72: 609-621.

Etienne S., Buckley M., Paris R., Nandasena A.K., Clark K., Chaque-Goff C., Goff J. and Richmond B., 2011. The use of boulders for characterizing past tsunamis: lessons from the 2004 Indian Ocean and 2009 South Pacific tsunamis. *Earth-Sci. Rev.*, 107: 75-89.

Evans G. and Arche A., 2002. The flux of siliciclastic sediment from the Iberian peninsula, with particular reference to the Ebro. *In:* Sediment flux to basins: causes, controls and consequences, Jones S.J. & Frostick L.E. (eds), Geological Society, London, Special Publications, 191: 199-208.

Favalli M., Boschi E., Mazzarini F. and Pareschi M.T., 2009. Seismic and landslide source of the 1908 Straits of Messina tsunami (Sicily, Italy). *Geophys. Res. Lett.*, 36: L16304, doi:10.1029/2009GL039135.

Ferentinos G., Papatheodorou G. and Collins - .- ., 1988. Sediment transport processes on an active submarine fault escarpment: Gulf of Corinth, Greece. *Mar. Geol.*, 83: 43-61.

Fernandez-Nieto E.D., Bouchut F., Bresch D., Castro Diaz M.J. and Mangeney A., 2008. A new Savage-Hutter type model for submarine avalanches and generated tsunami. Spain, 40 p.

Field M.E. and Gardner J.V., 1990. Pliocene-Pleistocene growth of the Rio Ebro margin, northeast Spain: a prograding-slope model. *GSA Bull.*, 102: 721-733.

Finn W. and Liam D., 2003. Landslide-generated tsunamis: geotechnical considerations. *Pure Appl. Geophys*, 160(10-11): 1,879-1,894.

Fleming J.G., Walters R.A., Sue L.P. and Nokes R.I., 2005. Experimental design for solid block and granular submarine landslides: a unified approach. *In:* Tsunamis: case studies and recent developments, Satake K. (ed.), Springer, Series VIII, 23: 259-277.

Fokaefs A. and Papadopoulos G.A., 2007. Tsunami hazard in the Eastern Mediterranean: strong earthquakes and tsunamis in Cyprus and the Levantine Sea. *Nat. Hazards*, 40: 503-526, doi: 10.1007/s11069-006-9011-3.

Folkman Y. and Mart Y., 2008. Newly recognized eastern extension of the Nile deep-sea fan. *Geology*, 12: 939-942, doi: 10.1130/G24995A.1.

Fouqué F., 1879. Santorin et ses éruptions, Masson et Cie, Paris.

Freundt A., 2003. Entrance of hot pyroclastic flows into the sea: experimental observations. *B. Volcanol.*, 65: 144-164.

Frey-Martínez J., 2010. 3D seismic interpretation of mass transport deposits: implications for basin analysis and geohazard evaluation. *In:* Submarine mass movements and their consequences, advances in natural and technological hazards research, Mosher D. *et al.* (eds), Springer, 28: 553-568.

Frey-Martínez J., Cartwright J.A., Burgess P.M. and Vicente-Bravo J., 2004. 3D seismic interpretation of the Messinian Unconformity in the Valencia Basin, Spain. *In:* 3D seismic technology: application to the exploration of sedimentary basins, Davies R.J., Cartwright J.A., Stewart S.A., Lappin M. & Underhill J.R. (eds), Geological Society, London, Memoirs, 29: 91-100.

Frey-Martinez J., Cartwright J.A. and Hall B., 2005. 3D seismic interpretation of slump complexes: examples from the continental margin of Israel. *Basin Res.*, 17: 83-108, doi: 10.1111/j.1365-2117.2005.00255.x.

Friedrich W., 2000. Fire in the sea, the Santorini Volcano: natural history and the legend of Atlantis. Cambridge University Press, Cambridge.

Fritz H.M., Hager W.H. and Minor H.E., 2001. Lituya Bay case: rockslide impact and wave run-up. *Science of Tsunami Hazards*, 19(1): 3-22.

Fritz H.M., Hager W.H. and Minor H.E., 2004. Near field characteristics of landslide generated impulse waves. *J. Waterway Port Coast. Oc. Eng.*, ASCE, 130(6): 287-310.

Galanti B., Rosen D.S. and Salamon A., 2009. Tsunami models adaptation and various scenarios simulations to aid early tsunami warning for Israel, Final Report. Ministry Of National Infrastructures Publ. No. ES-67A-2008, (IOLR Report H63/2010. GSI Report TR-GSI/23/2009), April. 2009, 195p. (in Hebrew with English summary)

Galanti B., Rosen D.S. and Salamon A., 2010a. Simulations of two additional high resolution tsunami scenarios in the framework of a digital data bank development of tsunami arrival time and inundation results at the Mediterranean coast of Israel, for the National Tsunami Early Warning System, Final Report. Ministry Of National Infrastructures Publ. No. ES-45-2010, (IOLR Report H48/2010. GSI Report GSI/25/2010), Nov.

Galanti B., Rosen D.S. and Salamon A., 2010b. High resolution earthquakes and landslides induced tsunami generation and inundation modeling at the Mediterranean coast of Israel, towards an early warning tsunami scenarios data bank.

Galili E., Horwitz L.K., Hershkovitz I., Eshed V., Salamon A., Zviely D., Weinstein-Evron M. and Greenfield H., 2008. Comment on "Holocene tsunamis from Mount Etna and the fate of Israeli Neolithic communities" by Pareschi, Boschi, and Favalli. *Geoph. Res. Lett.*, 35: L08311.

Gamberi F., Marani M.P. and Savelli, 1997. Tectonic, volcanic and hydrothermal features of a submarine portion of the Eolia Islands (Tyrrhenian Sea). *Mar. Geol.*, 140: 167-181.

Garcia-Orellana J., Gràcia E., Vizcaino A., Masqué P., Olid C., Martínez Ruiz F., Piñero E., Sanchez-Cabeza J.A and Dañobeitia J.J., 2006. Identifying instrumental and historical earthquake records in the SW Iberian Margin using 210Pb turbidite chronology. *Geophys. Res. Lett.*, 33(24): L24601, doi: 10.1029/2006GL028417

Garfunkel Z., 1984. Large-scale Submarine Rotational Slumps and Growth Faults in the Eastern Mediterranean. *Mar. Geol.*, 55: 305-324.

Garziglia S., Ioulalen M., Migeon S., Ducassou E., Mascle J., Sardou O. and Brosolo L., 2007. Triggering factors and tsunamigenic potential of a large submarine mass failure on the Western Nile margin (Roseta area, Egypt). *In:* Submarine mass movements and their consequences, Lykousis V., Sakellariou D. & Locat J. (eds), pp. 347-355.

Garziglia S., Migeon S., Ducassou E., Loncke L. and Mascle J., 2008. Mass-transport deposits on the Rosetta province (NW Nile deep-sea turbidite system, Egyptian margin): characteristics, distribution, and potential causal processes. *Mar. Geol.*, 250: 180-198.

Geissler W.H., Matias L., Stich D., Carrilho F., Jokat W., Monna S., IbenBrahim A., Mancilla F., Gutscher M.A., Sallarès V. and Zitellini N., 2010. *Geophys. Res. Lett.*, 37: L18309, doi:10.1029/2010GL044289

Gelfenbaum G. and Jaffe, B., 2003. Erosion and sedimentation from the 17 July 1998 Papua New Guinea tsunami. *Pure Appl. Geophys*, 160: 1969-1999.

Géli L., Henry P., Zitter T., Dupre S. *et al*., 2008. Gas emissions and active tectonics within the submerged section of the North Anatolian Fault zone in the Sea of Marmara. *Earth Planet Sci. Lett.,* 274(1-2): 34-39.

Gennesseaux M., 1962. Une cause probable des écoulements turbides dans le canyon sous-marin du Var. *C.R. Ac. Sc. Paris*, 254: 2409-2411.

Gennesseaux M., Mauffret A. and Pautot G., 1980. Les glissements sous-marins de la pente continentale niçoise et la rupture de câbles en mer Ligure (Méditerranée occidentale). *C.R. Ac. Sc. Paris*, 290: 959-962.

George D.L., 2006. Finite volume methods and adaptive refinement for tsunami propagation and inundation*,* PhD thesis, University of Washington.

George D.L., 2008. Augmented Riemann solvers for the shallow water equations over variable topography with steady states and inundation. *J. Comput. Phys*., 227(6): 3089-3113.

Gerardi F., Barbano M.S., De Martini P.M. and Pantosti D., 2008. Discrimination of tsunami sources (earthquake vs. landslide) on the basis of historical data in eastern Sicily and southern Calabria. *B. Seismol. Soc. Am.*, 98(6): 2795-2805.

Gjevik B., Pedersen G., Dybesland E., Harbitz C.B., Miranda P.M., Baptista M.A., Mendes-Victor L., Heinric P., Roche R. and Guesmia M., 1997. Modeling tsunamis from earthquake sources near Gorringe Bank southwest Portugal. *J. Geophys. Res.*, 102: 27931-27949.

Goff J., McFadgen B.G. and Chagué-Goff C., 2004. Sedimentary differences between the 2002 Easter storm and the 15th Century Okoropunga tsunami, southeastern North Island, New Zealand. *Mar. Geol.*, 204: 235-250, doi: 10.1016/S0025-3227(03)00352-9

Goldfinger C., Kulm L.D., McNeill L.C. and Watts P., 2000. Super-scale failure of the southern Oregon Cascadia Margin. *Pure Appl. Geophys.*, 157: 1189-1226.

Goldfinger C., Nelson C.H., Johnson J.E. and Shipboard Scientific Party, 2003. Holocene earthquake records from the Cascadia subduction zone and northern San Andreas Fault based on precise dating of offshore turbidites. *Ann. Rev. Earth Planet. Sci.*, 31: 555-577.

Goldsmith V. and Gilboa M., 1986. Tide and low in Israel. *Ofakim Be'Geographia*, 15: 21-47 (in Hebrew).

Gomez F., Meghraoui M., Darkal A.N., Sbeinati R., Darawcheh R., Tabet C., Khawlie M., Charabe M., Khair K. and Barazangi M., 2001. Coseismic displacements along the Serghaya fault: an active branch of the Dead Sea fault system in Syria and Lebanon. *J. Geol. Soc. London*, 158: 405-408.

Goodman-Tchernov B.N., Dey H.W., Reinhardt E.G., McCoy F. and Mart Y., 2009. Tsunami waves generated by the Santorini eruption reached Eastern Mediterranean shores. *Geology*, 37: 943-946.

Görür N., Papadopulos G.A. and Okay N., 2002. Integration of science research on the 1999 Turkish and Greek earthquakes, NATO Science Series IV, EES, 9: 71-85.

Gràcia E., Dañobeitia J.J., Vergés J. and PARSIFAL Team, 2003a. Mapping active faults offshore Portugal (36º N-38ºN): implications for seismic hazard assessment along the southwest Iberian margin. *Geology*, 31(1): 83-86.

Gràcia E., Dañobeitia J.J., Vergés J., Bartolomé R. and Córdoba D., 2003b. Crustal architecture and tectonic evolution of the Gulf of Cadiz (SW Iberian Margin) at the convergence of the Eurasian and African Plates. *Tectonics*, 22(4): 1033-1058.

Gràcia E., Pallàs R., Soto J.I., Comas M., Moreno X., Masana E., Santanach P., Diez S., García M. and Dañobeitia J.J., 2006. Active faulting offshore SE Spain (Alboran Sea): implications for earthquake hazard assessment in the Southern Iberian Margin. *Earth Planet. Sci. Lett.*, 241(3-4): 734-749.

Gràcia E., Vizcaino A., Escutia C., Asioli A., Rodés A., Pallàs R., Garcia-Orellana J., Lebreiro S. and Goldfinger C., 2010a. Holocene earthquake record offshore Portugal (SW Iberia): testing turbidite paleoseismology in a slow-convergence margin. *Quaternary Sci. Rev.*, 29: 1156-1172.

Gràcia E., Bartolomé R., Lo Iacono C., Moreno X., Martínez-Loriente S., Perea H., Masana E., Pallàs R., Diez S., Dañobeitia J.J., Terrinha P. and Zitellini N., 2010b. Characterizing active faults and associated mass transport deposits in the South Iberian Margin (Alboran Sea and Gulf of Cadiz): on-fault and off-fault paleoseismic evidence. *En:* Contribución de la geología al análisis de la peligrosidad sísmica (Insúa J.M. & Martín-González F. (eds), IBERFAULT, Sigüenza (Guadalajara), 27-29 Octubre 2010, pp. 163-166.

Grilli S. and Watts P., 2005. Tsunami generation by submarine mass failure. I: Modeling, experimental validation, and sensitivity analyses. *J. Waterway Port Coast. Oc. Eng*., 131: 283-297.

Group on Earth Observations, The GEO Geohazards Supersite, Tohoku-oki Event Supersite Website, <http://supersites.earthobservations.org/honshu.php#Sun3>

Gueguen E., Doglioni C. and Fernàndez M., 1998. On the post-25 Ma geodynamic evolution of the western Mediterranean. *Tectonophysics*, 298: 259-269.

Guglielmi Y. and Mudry J., 1996. Estimation of spatial and temporal variability of recharge fluxes to an alluvial aquifer in a fore land area by water chemistry and isotopes. *Ground Water*, 34(6): 1017-1023.

Guidoboni E., Comastri A. and Traina G., 1994. Catalogue of ancient earthquakes in the Mediterranean area up to the 10th century. ING-SGA, Bologna, Italy, 504 p.

Guidoboni E. and Comastri A., 1997. The large earthquake of 8 August 1303 in Crete: seismic scenario and tsunami in the Mediterranean area. *J. Seismology*, 1: 55-72.

Guidoboni E. and Comastri A., 2005. Catalogue of earthquakes and tsunamis in the Mediterranean area from the 11th to the 15th Century, INGV-SGA, Italy.

Gusiakov V., 2009. Tsunami history. *In:* The sea, Harvard University Press, 15: 23-53.

Gutscher M.A., Malod J., Rehault J.P., Contrucci I., Kingelhoefer F., Mendes Victor L. and Spakman W., 2002. Evidence for active subduction beneath Gibraltar. *Geology*, 30(12): 1071-1074.

Gutscher M.A., Baptista M.A. and Miranda J.M., 2006. The Gibraltar Arc seismogenic zone: Part 2. Constraints on a shallow east dipping fault plane source for the 1755 Lisbon earthquake provided by tsunami modeling and seismic intensity. *Tectonophysics*, 426: 153-166.

Habib P., 1983. Report of Mr. Pierre Habib, Referee - Expert on the accident of the port of Nice, 16th of October 1970, of Conseil General des Ports et Chaussees, France, translated by Guy Lengagne, report to H.B. Seed dated 21 June 1983, 51 p. and 3 app.

Habib P., 1994. Aspects géotechniques de l'accident du nouveau port de Nice. *Revue Française de Géotechnique*, 65: 2-15.

Hamilton T.S., 1987. The foreslope hills of the Fraser Delta: implications for tsunamis in Georgia Strait. *Science of Tsunami Hazards*, 5(1): 15-33.

Hampton M.A., Lee H.J. and Locat J., 1996. Submarine landslides. *Reviews in Geophysics*, 34: 33-59.

Harbitz C.B., 1992. Model theory and analytical solutions for large water waves due to landslides. Dept. of Math., Univ. Oslo, Norway, Preprint Series No. 4.

Harry Y., Robertson I. and Preuss J., 2005. Development of design guidelines for structures that serve as tsunami vertical evacuation sites. Washington State Dept. Natural Resources, Washington Division of Geology and Earth Resources, Open File Report 2005-4, Nov. 34 p.

Hasegawa S., Dahal R.K., Nishimura T., Nonomura A. and Yamanaka M., 2008. DEM-based analysis of earthquake-induced shallow landslide susceptibility. *Geotech. Geol. Eng.*, DOI 10.1007/s10706-008-9242-z, Springer Science+Business Media.

Head J.W. and Wilson L., 2003. Deep submarine pyroclastic eruptions: theory and predicted landforms and deposits. *J.Volcanol. Geotherm. Res.*, 121: 155-193.

Heezen B.C., 1957. 1908 Messina earthquake, tsunami, and turbidity current. *Bull. Geological Soc. Amer.*, 68(12): 1,743 (abstract).

Helgerud M.B., Dvorkin J., Nur A., Sakai A. and Collett T.S., 1999. Elastic-wave velocity in marine sediments with gas hydrates: effective medium modelling. *Geophys. Res. Lett.*, 26: 2021-2024.

Helzel Messtechnik, 2011. WERA ocean radar in chile observed tsunami signatures after the earthquake in Japan on March 11, 2011. Press release, May 2011 <http://www.helzel.com/files/432/upload/Tsunami/Press-Release-Tsunami-WERA-2011.pdf>

Hollenstein C., Müller M.D., Geiger A. and Kahle H.G., 2008. Crustal motion and deformation in Greece from a decade of GPS movements. *Tectonophysics*, 449: 17-40.

Huhnerbach V. and Masson D.G., 2004. Landslides in the North Atlantic and its adjacent seas: an analysis of their morphology, setting and behaviour. *Mar. Geol.*, *213*: 343-362.

Hutton E.W.H. and Syvitski J.P.M., 2004. Advances in the numerical modeling of sediment failure during the development of a continental margin. *Mar. Geol.*, 203(3-4): 367-380.

ICG/NEAMTWS (Intergovernmental Coordination Group for the Tsunami Early Warning and Mitigation System in the North Eastern Atlantic, the Mediterranean and Connected Seas), 2009. Interim operational users guide for the tsunami early warning and mitigation system in the north-eastern Atlantic, the Mediterranean and connected seas (NEAMTWS), Version 1.1g, Istanbul, Turkey <http://www. ioc-unesco.org/index.php?option=com_oe&task=viewDocumentRecord&docID= 4516>

ICG/NEAMTWS (7th Session of the Intergovernmental Coordination Group for the Tsunami Early Warning and Mitigation System in the North-eastern Atlantic, the Mediterranean and Connected Seas, Paris, France), 2010. Report of WG1, Hazard Assessment and Modeling, by Behrens, J. and Gonzáles, M., <http://ioc-unesco.org/index.php?option=com_oe&task=viewDocumentRecord&docID=6403>

ICG/NEAMTWS, 2011. Reducing and managing the risk of tsunamis, Guidance for National Civil Protection and Disaster Management Organisations as Part of the Tsunami Early Warning and Mitigation System in the North-eastern Atlantic, the Mediterranean and Connected Seas Region – NEAMTWS, Working Group 4 Public Awareness, Preparedness and Mitigation.

Iglesias O., Lastras G., Canals M., Olabarrieta M. and González M., 2010. Numerical simulation of the potential tsunami generated by the BIG'95 debris flow, Northwestern Mediterranean Sea. EGU 2010, Geophysical Research Abstracts, 12, Abstract EGU2010-9096-1, Vienna, Austria.

Imbo Y., De Batist M., Canals M., Prieto M.J. and Baraza J., 2003. The Gebra Slide: a submarine slide on the Trinity Peninsula Margin, Antarctica. *Mar. Geol.*, 193: 235-252.

IOC/UNESCO, 2009. Tsunami Early Warning and Mitigation System in the North Eastern Atlantic, the Mediterranean and Connected Seas, NEAMTWS, Implementation Plan, Version 3.4, Technical Series, October 2009.

Ioualalen M., Migeon S. and O. Sardoux, 2010. Landslide tsunami vulnerability in the Ligurian Sea: case study of the 1979 October 16 Nice international airport submarine landslide and of identified geological mass failures. *Geophys. J. Int.*, 181: 724-740.

Iribarren L., Verges J., Camurri F., Fullea J. and Fernandez M., 2007. The structure of the Atlantic-Mediterranean transition zone from the Alboran Sea to the Horseshoe Abyssal Plain (Iberia-Africa plate boundary. *Mar. Geol.*, 243(1-4): 97-119.

Jerome, 380. Chonicon Eusebii, Eusebius Chonicon, Helm R. (ed.), GSC 47, Berlin 1956.

Jolivet L., 1991. Extension of thickened continental crust, from brittle to ductile deformation: examples from Alpine Corsica and Aegean Sea. *Ann. Geofis.*, 36: 139-153.

Jolivet L., 2001. A comparison of geodetic and finite strain pattern in the Aegean, geodynamic implications. *Earth Planet. Sci. Lett.*, 187: 95-104, doi: 10.1016/S0012-821X(01)00277-1

Jongsma D., 1977. Pliny and Strabo trenches, south of the Hellenic Arc. *Geol. Soc. Am. Bull.*, 88: 797-805.

Jorry S., Jégou I., Emmanuel L., Silva Jacinto R. and Savoye B., 2011. Turbiditic levee deposition in response to climate changes: the Var sedimentary ridge (Ligurian Sea). *Mar. Geol.*, doi:10.1016/j.margeo.2010.10.021.

Kastens K.A., Mascle J., Auroux C., Bonatti E., Broglia C., Channell J., Curzi P., Emeis K., Glacon G., Hasegawa S., Hieke W., Mascle G., McCoy F., McKenzie J., Mendelson J., Muller C., Rehault J.P., Robertson A., Sartori R., Sprovieri R. and Torii M., 1988. ODP Leg 107 in the Tyrrhenian Sea: insights into passive margin and back-arc basin evolution. *Geol. Soc. Amer. Bull.*, 100: 1140-1156.

Kastens K.A. and Mascle J., 1990. The geological history of the Tyrrhenian Sea: an introduction to the scientific results of ODP Leg 107. *In:* Kastens K.A. & Mascle J. *et al.* (eds), Proc. ODP, Scientific Results, College Station, TX (Ocean Drilling Program), 107: 3-26.

Kawaguchi T., Itoh S. and Takeuchi T., 1995. Case studies of tsunami countermeasure considering coastal environment. *In:* Tsunamis: progress in prediction, disaster prevention and warning, Tsuchiya Y. & Shuto N. (eds), Kluwer Academic Pub., The Netherlands, pp. 249-262.

Kawamura K., Yamada Y., Ikehara K., Yamamoto Y., Kanamatsu T. and Sakaguchi A., 2009. White paper for geohazard (submarine landslides and mass movements) at INVEST09 from Japanese research group. Aug. 2009.

Keefer D.K.,1984. Landslides caused by earthquakes. *Geological Soc. Amer. Bull.*, 95: 406-421.

Kelletat D., 2002. Tsunamis on Cyprus: field evidences and 14C dating results, Zeitschrift fur. *Geomorphologie N. F.*, 46(1): 19-34.

Kelletat D. and Schellmann G., 2001. Kustenforschung auf zypern: tsunami-ereignisse und chronostratigraphische untersuchungen. *Essener Geographische Arbeiten* (32), Universitat Essen, Germany.

Kiyoshi H. and Shuto N., 1983. Tsunami disasters and protection measures in Japan. *In:* Tsunamis - Their science and engineering, Iida K. & Iwasaki T., Terra Scientific Pub. Co., Tokyo, pp. 9-22.

Klaucke I. and Cochonat P., 1999. Analysis of past seafloor failures on the continental slope off Nice (SE France). *Geo-Mar. Lett.*, 19: 245-253.

Klaucke I., Savoye B. and Cochonat P., 2000. Patterns and processes of sediment dispersal on the continental slope off Nice, SE France. *Mar. Geol.*, 162: 405-422.

Koike K., 1996. The countermeasures against coastal hazards in Japan. *Geo Journal*, 38(3): 301-312.

Kontogianni V., Tsoulos N. and Stiros S., 2002. Coastal uplift, earthquakes and active faulting of Rhodes Island (Aegean Arc): modeling based on geodetic inversion. *Mar. Geol.*, 186: 299-317.

Kopf A. and shipboard party, 2008. Report and preliminary results of Meteor Cruise M73/1: Lima-Lamo. Berichte aus dem Fachbereich Geowissenschaften der Universität Bremen, 264: 169.

Kopf A. and shipboard party, 2009. Report and preliminary results of Poseidon Cruise P386: NAIL (Nice Airport Landslide). Berichte aus dem Fachbereich Geowissenschaften der Universität Bremen, 271: 161.

Kopf A., Kasten S. and Blees J., 2010. Geochemical evidence for groundwater-charging of slope sediments: The Nice Airport 1979 landslide and tsunami revisited. Proc. IGCP511, Submarine mass movements and their consequences, Houston (TX), 2009.

Kortekaas S. and Dawson A.G., 2007. Distinguishing tsunami and storm deposits: an example from Martinhal, SW Portugal. *Sediment. Geol*, 200: 208-221.

Kreemer C. and Chamot-Rooke N., 2004. Contemporary kinematics of the southern Aegean and the Mediterranean Ridge. *Geophys. J. Int.*, 157: 1377-1392, doi: 10.1111/j.1365-246X.2004.02270.x

Kyodo News, 2011. 38-meter-high tsunami triggered by March 11 quake: survey <http://english.kyodonews.jp/news/2011/04/82888.html>

Kyoto University Team, 2011. See report at <http://www.iedm.ges.kyoto-u.ac.jp/report/2011/IEDM%202%20Week%20Report%20Japan%20EQT.pdf>

La Rocca M., Galluzzo D., Saccorotti G., Tinti S., Cimini G.B. and Del Pezzo E., 2004. Seismic signals associated with landslides and with a tsunami at Stromboli Volcano, Italy. *B. Seismol. Soc. Am.*, 94(5): 1850-1867.

Laberg J.S., Vorren T.O., Dowdeswell J.A., Kenyon N.H. and Taylor J., 2000. The Andøya Slide and the Andøya Canyon, north-eastern Norwegian-Greenland Sea. *Mar. Geol.*, 162: 259-275.

Lafuerza S., 2009. Aplicacions del CPTU en Geociències Marines: estudi de casos de la Mediterrània, PhD Thesis, University of Barcelona, 152 p.

Lassa J., 2011. Japan's resilience to tsunamis and the lessons for Japan and the world: an early observation <http://www.zef.de/module/register/media/b4d0_Japantsunami%20resilience31mar2011.pdf>

Lastras G., Canals M., Hughes Clarke J.E., Moreno A., De Batist M., Masson D.G. and Cochonat P., 2002. Seafloor imagery from the BIG'95 debris flow, western Mediterranean. *Geology*, 30(10): 871-874.

Lastras G., Canals M., Urgeles R., Hughes-Clarke J.E. and Acosta J., 2004. Shallow slides and pockmark swarms in the Eivissa Channel, Western Mediterranean Sea. *Sedimentology*, 51: 1-14.

Lastras G., Canals M., Amblas D., Frigola J., Urgeles R., Calafat A.M. and Acosta J., 2007. Slope instability along the northeastern Iberian and Balearic continental margins. *Geol. Acta*, 5: 35-47.

Lauterjung J., Münch U. and Rudloff A., 2010. The challenge of installing a tsunami early warning system in the vicinity of the Sunda Arc, Indonesia. *Nat. Hazards Earth Syst. Sci.*, 10: 641-646.

Le Pichon X. and Angelier J., 1979. The Hellenic arc and trench system: a key to the neotectonic evolution of the Eastern Mediterranean area. *Tectonophysics*, 60: 1-42.

Le Pichon X., Angelier J. and Sibuet J.C., 1982. Plate boundaries and extensional tectonics. *Tectonophysics*, 81: 239-256, doi: 10.1016/0040-1951(82)90131-7.

Leroueil S., 2001. Natural slopes and cuts: movement and failure mechanisms. *Geotechnique*, 51(3): 197-243.

Leroueil S., Demers D., La Rochelle P., Martel G. and Virely D., 1995. Practical use of the piezocone in eastern Canada clays. *In:* CPT'95, Proceedings of the International Symposium on Cone Penetration Testing, Linköping, 4-5 October 1995. Swedish Geotechnical Institute, pp. 515-521.

Leroueil S., Vaunat J., Picarelli L., Locat J., Lee H. and Faure R.M., 1996. Geotechnical characterisation of slope movements, *In:* Senneset K. (ed.), Proc. of 7th Int. Symp. on Landslides, Balkema, Rotterdam, pp. 53-74.

LeVeque R.J., 2006. Clawpack software <http://www.clawpack.org>

Leynaud D. and Sultan N., 2010. 3-D slope stability analysis: a probability approach applied to the nice slope (SE France). *Mar. Geol.*, 269: 89-106.

Li T., Troch P. and De Rouck J., 2008. Numerical simulation of landslide-induced waterwave kinematics by LVOF. Abst. ICCE 2008, Hamburg, Aug. 31-Sept. 5.

Lima V.V., Miranda J. M., Baptista M.A., Catalão J., Gonzalez M., Otero L., Olabarrieta M., Álvarez-Gómez J.A. and Carreño E., 2010. Impact of a 1755-like tsunami in Huelva, Spain. *Nat. Hazards Earth Syst. Sci.*, 10: 139-148.

Liu P.L.F., Lynett P. and Synolakis C.E., 2003. Analytical solutions for forced long waves on a sloping beach. *J. Fluid Mech.*, 478: 101-109.

Liu P.L.F., Wu T.R., Raichlen F., Synolakis C.E. and Borrero J.C., 2005. Runup and rundown generated by three-dimensional sliding masses. *Journal Fluid Mechanics*, 536: 107-144.

Lo Iacono C., Gràcia E., Zaniboni F., Pagnoni G., Tinti S., Dañobeitia J.J., Lourenço N. and Pinto de Abreu M., 2010. Geology and tsunamigenic potential of the North-Gorringe rock avalanche (Gulf of Cadiz, SW Iberia). ESF Research Conference "Submarine Paleoseismology: The Offshore search of large Holocene earthquakes". Obergurgl (Austria), 11-16 September 2010.

Lorito S., Tiberti M.M., Basili R., Piatanesi A. and Valensise G., 2008. Earthquake-generated tsunamis in the Mediterranean Sea: scenarios of potential threats to Southern Italy. *J. Geophys. Res.*, 113, B01301, doi:10.1029/2007JB004943

Løvholt F., de Blasio F., Harbitz C.B., Urgeles R., Canals M., Vanneste M., Iglesias O., Lastras G., Glimsdal S. and Pedersen G.K., 2009. Tsunami hazard studies in the eastern Hellenic Arc and Balearic Islands. EGU 2009, Geophysical Research Abstracts, vol. 11 Abstract EGU2009-2728-4, Vienna, Austria.

Lunne T., Robertson P.K. and Powell J.J.M., 1997. Cone penetration test in geotechnical practice. Blackie Academic and Professional, UK.

Lykousis V., Roussakis G., Alexandri M., Pavlakis P. and Papoulia I., 2002. Sliding and regional slope stability in active margins: North Aegean Trough (Mediterranean). *Mar. Geol.*, 186: 281-298.

Lykousis V., Sakellariou D., Moretti I. and Kaberi H., 2007a. Late Quaternary basin evolution of the Gulf of Corinth: sequence stratigraphy, sedimentation, fault-slip and subsidence rates. *Tectonophysics*, 440: 29-51.

Lykousis V., Sakellariou D., Rousakis G., Alexandri S., Kaberi H., Nomikou P., Georgiou P. and Ballas D., 2007b. Sediment failure processes in active grabens: the Western Gulf of Corinth (Greece). *In:* Submarine mass movements and their consequences, Lykousis V., Sakellariou D. & Locat J. (eds), Springer, pp .297-305.

Lykousis V., Rousakis G. and Sakellariou D., 2008. Slope failures and stability analysis of shallow water prodeltas in the active margins of Western Greece, northeastern Mediterranean. *Int. J. Earth Sci.*, DOI 10.1007/s00531-008-0329-9.

Lynett P., 2009. ISEC workshop 2009, ISEC Community Workshop: Simulation & Large-Scale Testing of Nearshore Wave Dynamics, July 8-10, 2009, Corvallis, Oregon, USA, <http://isec.nacse.org/workshop/isec_workshop_2009/pres_thurs/1_lynett_bmark>

Maestro A., Somoza L., Medialdea T., Talbot C.J., Lowrie A., Vázquez J.T. and Díaz-del-Río V., 2003. Large-scale slope failure involving Triassic and Middle Miocene salt and shale in the Gulf of Cádiz (Atlantic Iberian Margin. *Terra Nova*, 15: 380-391.

Magnier M., 2011. Japan rethinks tsunami safety, Los Angeles Times, March 29, 2011.

Mahmoud M., Woeller D. and Robertson P.K., 2000. Detection of shear zones in a natural clay slope using the cone penetration test and continuous dynamic sampling. *Can. Geotech. Can. Geotech. J.*, 37(3): 652-661.

Maillard A., Mauffret A., Watts A.B., Torné M., Pascal G., Buhl P. and Pinet B., 1992. Tertiary sedimentary history and structure of the Valencia Trough (western Mediterranean. *Tectonophysics*, 203: 57-75.

Maillard A. and Mauffret, A., 2006. Relationships between erosion surfaces and Late Miocene Salinity Crisis deposits in the Valencia Basin (NW Mediterranean): evidences for early sea-level fall. *Terra Nova*, 18: 321-329.

Maillard A., Gorini C., Mauffret A., Sage F., Lofi J. and Gaullier V., 2006. Offshore evidence of poliphase erosion in the Valencia Basin (NW Mediterranean): scenario for the Messinian Salinity Crisis. *Sed. Geol.*, 188-189: 69-91.

Makris J., Ben-Avraham Z., Behle A., Ginzburg A., Giese P., Steinmetz L., Whitmarsh R.B. and Eleftheriou S., 1983. Seismic refraction profiles between Cyprus and Israel and their interpretation. *Geophys. J. Roy. Astr. S.*, 75: 575-591.

Maramai A., Graziani L., Alessio G., Burrato P., Colini L., Cucci L., Nappi R., Nardi A. and Villardo G., 2005a. Near- and far-filed survey report of the 30 December 2002 Stromboli tsunami. *Mar. Geol.*, 215: 93-106.

Maramai A., Graziani L. and Tinti S., 2005b. Tsunamis in the Aeolian Islands (southern Italy): a review. *Mar. Geol.*, 215: 11-21.

Marani M.P. and Trua T., 2002. Thermal constriction and slabtearing at the origin of a super inflated spreading ridge: Marsili volcano (Tyrrhenian Sea). *J. Geophys. Res.*, 107: B9, doi:10.1029/2001JB000285

Marinatos S., 1939. The volcanic destruction of Minoan Crete. *Antiquity*, 13: 425-439.

Martel S.J., 2004. Mechanics of landslide initiation as a shear fracture phenomenon. *Mar. Geol.*, 203(3-4): 319-340.

Martínez Solares J.M. and López Arroyo A., 2004. The great historical 1755 earthquake: effects and damage in Spain. *J. Seism.*, 8: 275-294.

Martínez-García P., Soto J.I. and Comas M.C., 2010. Recent structures in the Alboran Ridge and Yusuf fault zones based on swath bathymetry and sub-bottom profiling: evidence of active tectonics. *Geo-Mar. Lett.*, DOI 10.1007/s00367-010-0212-0

Martínez-Loriente S., Gràcia E., Bartolomé R., Sallarès V. and Terrinha P., 2009. Active tectonics at the external part of the Gulf of Cadiz based on depth and time migrated MCS profiles. 6º Simposio sobre el Margen Ibérico Atlántico, Oviedo (Spain).

Mas V., Mulder T., Dennielou B., Schmidt S., Khripounoff A. and Savoye B., 2010. Multiscale spatio-temporal variability of sedimentary deposits in the Var turbidite system (North-Western Mediterranean Sea). *Mar. Geol.*, 275: 37-52.

Masana E., Martínez-Díaz J.J., Hernández-Enrile J.L. and Santanach P., 2004. The Alhama de Murcia fault (SE Spain), a seismogenic fault in a diffuse plate boundary: Seismotectonic implications for the Ibero–Magrebian region. *J. Geophys. Res.*, 109: 1-17.

Mascle J., Jongsma D., Campredon R., Dercourt J., Glacon G., Lecleach A., Lyberis N., Malod J.A. and Mitropoulos D., 1982. The Hellenic margin from eastern Crete to Rhodes: preliminary results. *Tectonophysics*, 86: 133- 147.

Mascle J. and Martin L., 1990. Shallow structure and recent evolution of the Aegean Sea: A synthesis based on continuous reflection profiles. *Mar. Geol.*, 94: 271-299.

Mascle J., Huguen C., Benkhelil J., Chamot-Rooke N., Chaumillon E., Foucher J.P., Griboulard R., Kopf A., Lamarche G., Volkonskaia A., Woodside J. and Zitter T., 1999. Images may show start of European-African Plate collision. *EOS Trans. AGU 80*, pp. 421-428.

Mascle J., Sardou O., Loncke L., Migeon S., Caméra L. and Gaullier V., 2006. Morphostructure of the Egyptian continental margin: Insights from swath bathymetry surveys. *Mar. Geophys. Res.*, 27: 49-59.

Maslin M., Vilela C., Mikkelsen N. and Grootes P., 2005. Causes of catastrophic sediment failures of the Amazon Fan. *Quaternary Sci. Rev.*, 24: 2180-2193.

McAdoo B.G., Pratson L.F. and Orange D.L., 2000. Submarine landslide geomorphology, US continental slope. *Mar. Geol.*, 169: 103-136.

McCoy F. and Heiken G., 2000. Tsunami generated by the Late Bronze Age eruption of Thera (Santorini), Greece. *Pure Appl. Geophys.*, 157: 1227-1256.

McKenzie D.P., 1970. Plate tectonics of the Mediterranean region. *Nature*, 226: 239-243.

McKenzie D.P., 1978. Active tectonics of the Alpine-Himalayan belt: the Aegean Sea and surrounding regions. *Geophys. J. R. astron. Soc.*, 55: 217-254.

MEDIMAP Group, Loubrieu B. and Mascle J., 2008. Morpho-bathymetry of the Mediterranean Sea. CIESM / Ifremer edition.

Meijer P.Th. and Wortel M.J.R., 1997. Present-day dynamics of the Aegean region: a model analysis of the horizontal pattern of stress and deformation. *Tectonics*, 16(6): 879-895, doi: 10.1029/97TC02004

Meulenkamp J.E., Wortel M.J.R., Van Wamel W.A., Spakman W. and Hoogerduyn Strating E., 1988. On the Hellenic subduction zone and the geodynamical evolution of Crete since the late Middle Miocene: Tectonophysics.146: 203-215, doi: 10.1016/0040-1951(88)90091-1

Minoura K., Imamura F., Kuran U., Nakamura T., Papadopoulos G.A., Takahashi T. and Yalciner A.C., 2000. Discovery of Minoan tsunami deposits. *Geology,* 28(1): 59-62.

Moore,J.G., Clague D.A., Holcomb R.T., Lipman P.W., Normark W.R. and Torresan M.E., 1989. Prodigious submarine landslides on the Hawaiian Ridge. *J. Geophys. Res.*, *94*(B12): 17,465-417,484.

Moreno X., Masana E., Gràcia E., Bartolomé R. and Piqué-Serra O., 2008. Estudio paleosismológico de la Falla de Carboneras: evidencias tierra-mar de actividad tectónica reciente. *GeoTemas*, 10: 1035-1038.

Moreno X., Masana E., Gràcia E., Bartolomé R., Rodés A. and Pallàs R., 2010. Onshore-offshore active tectonics along the Carboneras Fault Zone (Eastern Betic Cordilleras. *En:* Contribución de la geología al análisis de la peligrosidad sísmica, Insúa J.M. & Martín-González F. (eds), IBERFAULT, Sigüenza, 27-29 Octubre 2010, pp. 105-107.

Morgan J., Silver E., Camerlenghi A., Dugan B., Kirby S., Shipp C. and Suyehiro K., 2009. Addressing geohazards through ocean drilling. *Scientific Drilling*, 7: 25-30.

Morton R.A., Gelfenbaum G. and Jaffe B.E., 2007. Physical criteria for distinguishing sandy tsunami and storm deposits using modern examples. *Sediment. Geol.*, 200: 184-207.

Mulder T., 1992. Aspects géotechniques de la stabilité des marges continentales: Application à la Baie des Anges, Nice, France. Doctoral thesis, Nancy: Institut National Polytechnique de Lorraine, 457 pp.

Mulder T., Tisot J.P., Cochonat P. and Bourillet J.F., 1994. Regional assessment of mass failure events in the Baie des Anges, Mediterranean Sea. *Mar. Geol.*, 122: 29-45.

Mulder T., Savoye B. and Syvitski J.P.M., 1997. Numerical modelling of a mid-sized gravity flow: the 1979 Nice turbidity current (dynamics, processes, sediment budget and seafloor impact). *Sedimentology*, 44: 305-32.

Mulder T., Migeon S., Savoye B. and Jouanneau J.-M., 2001a. Twentieth century floods recorded in the deep Mediterranean sediments. *Geology*, 29(11): 1011-1014.

Mulder T., Migeon S., Savoye B. and Faugeres J.C., 2001b. Inversely graded turbidite sequences in the deep Mediterranean: a record of deposits from flood-generated turbidity currents? *Geo-Mar. Lett.*, 21(2): 86-93.

Murata S., Imamura F., Katoh K., Kawata Y., Takahashi Sh. and Takayama T., 2010. Tsunami – To survive from tsunami. *Adv. Series on Ocean Engin.*, World Scientific, 32: 302 p.

Nagai, T., A., Nozu2, J.H., Lee, M., Kudaka, S., Adachi, and T., Ohmachi, 2008. Characteristics of the observed pre-tsunami seabed pressure records obtained by the nationwide wave gauge network. Coastal Engineering, pp. 1360-1370.

Nanayama F., Shigeno K., Satake K., Shimokawa K., Koitabashi S., Miyasaka S. and Ishii M., 2000. Sedimentary differences between the 1993 Hokkaido–Nansei–Oki tsunami and the 1959 Miyakojima typhoon at Taisei, southwestern Hokkaido, northern Japan. *Sediment. Geol.*, 135: 255-264.

Nelson C.H. and Maldonado A., 1990. Factors controlling late Cenozoic continental margin growth from the Ebro Delta to the western Mediterranean deep sea. *Mar. Geol.*, 95: 419-440.

Noller J., Panayides I. and Zomeni Z., 2005. Report on the preliminary assessment of tsunami hazard in Cyprus. Cyprus Geological Survey, internal report, 27 p.

Novikova T., Papadopoulos G.A. and McCoy F.W., 2011. Modeling of tsunami generated by the giant late Bronze Age eruption of Thera, South Aegean Sea, Greece. *Geoph. J. Internat.,* 186(2): 665-680.

Okal E.A., Synolakis C.E., Uslu B., Kalligeris N. and Voukouvalas E., 2009. The 1956 earthquake and tsunami in Amorgos, Greece. *Geophys. J. Int.*, 178: 1533-1554.

Okay N., 2011. Seasurges *In:* Encyclopedia of disaster relief , Penuel K.B. & Statler M. (eds), Thousand Oaks, CA: SAGE Publ. <http://atgstg01.sagepub.com/refbooks/Book233446?>

Okay N. and Okay A.I., 2002. Tectonically induced Quaternary drainage diversion in the northeastern Aegean. *J Geol. Soc. Lond*., 159: 393-399.

Okay N. and Ergün B., 2005. The source of basinal sediments in the Marmara Sea. *Mar. Geol.*, 216: 1-15.

Ortolani F., Pagliuca S. and D'Agostino G., 2005. Tsunami and rapid catastrophic environmental change. the hazard along the Italian coastal area. Final Meeting, Dark Nature - Rapid Natural Change and Human Responses, Villa Olmo, Como, Italy, <http://atlas-conferences.com/cgi-bin/abstract/caqy-42>

Özel N.M., Ocal N., Yalciner A.C., Dogan K. and Erdik M., 2011. Tsunami hazard in the Eastern Mediterranean and its connected seas: Toward a tsunami warning center in Turkey. *Soil Dynam. Earthq. Eng*., 31: 598-610.

Özeren M.S., Çagatay M.N., Postacıoglu N., Sengör A.M.C., Görur N. and Eris K., 2010. Mathematical modelling of a potential tsunami associated with a late glacial submarine landslide in the Sea of Marmara. *Geo-Mar. Lett*., 30: 523-539.

Panizzo A. and Dalrymple R.A., 2005. SPH Modelling of underwater landslide generated waves. Proc. ICCE 2004, McKee Smith J. (ed.), World Scientific, New Jersey, 2: 1,147-1,159.

Pantosti D. and Gràcia E., 2010. Submarine paleoseismology: the offshore search of large Holocene earthquakes. Scientific report of the ESF-FWF Conference in partnership with LFUI, Obergurgl 11-16 September 2010, 20 p. <http://www.esf.org/index.php?id=6484>

Pantosti D., Gràcia E. and Nelson C.H., 2011. Searching for records of past earthquakes under water. *Eos*, 92(6): 48.

Papadopoulos G.A., 2003a. Tsunami hazard in the Eastern Mediterranean: strong earthquakes and tsunamis in the Corinth Gulf, Central Greece. *Nat. Hazards,* 29: 437-464.

Papadopoulos G.A., 2003b. A tsunami warning system in the SW Aegean Sea, Greeece. *In:* Early warning systems for natural disaster reduction, Zschau J. & Küppers A.N. (eds), Springer-Verlag, pp. 549-552.

Papadopoulos G.A., 2009. Tsunamis. *In:* The physical geography of the Mediterranean, Woodward J.C. (ed.), Oxford Univ. Press, Oxford, pp. 493-512.

Papadopoulos G.A. and Fokaefs A., 2005. Strong tsunamis in the Mediterranean Sea: a re-evaluation. *ISET J. of Earthquake Technology,* 42(4): 159-170.

Papadopoulos G.A., Lobkovsky L.I., Mazova R.Kh., Garagash I.A., Karastathis V., Kataeva L. Yu. and Kaz'min V.G., 2007a. Numerical modeling of sediment mass sliding and tsunami generation: the case of February 7, 1963, in Corinth Gulf, Greece. *Mar. Geod.*, 30: 315-331.

Papadopoulos G.A., Daskalaki E. and Fokaefs A., 2007b. Tsunami generation by coastal and submarine landslides in the Mediterranean Sea. *In:* Submarine mass movements and their consequences, Lykousis V., Sakellariou D. & Locat J. (eds), pp. 415-422.

Papadopoulos G.A., Daskalaki E., Fokaefs A. and Giraleas N., 2007c. Tsunami hazards in the Eastern Mediterranean: strong earthquakes and tsunamis in the East Hellenic Arc and Trench system. *Nat. Hazards Earth Syst. Sci.,* 7: 57-64.

Papadopoulos G.A., Charalambakis M., Daskalaki E., Fokaefs A. and Orfanogiannaki K., 2009. The decision matrix for early tsunami warning in the Mediterranean Sea revisited. *Geophys. Res. Abstr.*, 11, EGU2009-3476.

Papadopoulos G.A., Daskalaki E., Fokaefs A. and Giraleas N., 2010. Tsunami hazards in the Eastern Mediterranean: strong earthquakes and tsunamis in the West Hellenic Arc and Trench system. *J. Earthquakes and Tsunamis*, 4: 145-179, DOI: 10.1142/S1793431110000856.

Parashar S., Uy N., Glenn F., Nguyen H., Mulyasari F., Joerin J. and Shaw R., 2011. Mega disaster in a resilient society: the Great East Japan (Tohoku Kanto) earthquake and tsunami of 11th March 2011. Synthesis and initial observations, International Environment and Disaster Management, Graduate School of Global Environmental Studies, Kyoto University, 25th March 2011, <http://www.iedm.ges.kyoto-u.ac.jp/report/2011/IEDM%202%20Week%20Report%20Japan%20EQT.pdf>

Pareschi M., Favalli M. and Boschi E., 2006a. Impact of the Minoan tsunami of Santorini: Simulated scenarios in the eastern Mediterranean. *Geophys. Res. Lett.*, 33, L18607, doi:10.1029/2006GL027205.

Pareschi M.T., Boschi E., Mazzarini F. and Favalli M., 2006b. Large submarine landslides offshore Mt. Etna. *Geoph. Res. Lett.*, 33, L13302.

Pareschi M.T., Boschi E. and Favalli M., 2006c. Lost tsunami. *Geoph. Res. Lett.*, 33, L22608.

Pareschi M.T., Boschi E. and Favalli M., 2007. Holocene tsunamis from Mount Etna and the fate of Israeli Neolithic communities. *Geophys. Res. Lett.*, 34, L16317, doi:10.1029/2007GL030717.

Pasotti J., 2006. Ancient cataclysm marred the Med, (Mount Etna). *Science*, 314(5805): 1527.

Pautot G., 1981. Carte morphologique de la Baie des Anges, modèle d'instabilité de pente continentale. *Oceanol. Acta*, 4(2): 203-212.

Perea H., Masana E. and Santanach P., 2006. A pragmatic approach to seismic parameters in a region with low seismicity: the case of eastern Iberia. *Nat. Hazards*, 39: 451-477.

Perea H., Gràcia E., Bartolomé R., Lo Iacono C., Masana E. and EVENT-SHELF Team, 2009. Structure and potential seismogenic and tsunamigenic sources of the offshore Bajo Segura Fault zone, SE Iberian Peninsula (Mediterranean Sea). European Geosciences Union, Vienna (Austria), 19-24 April.

Perissoratis C. and Papadopoulos G.A., 1999. Sediment instability and slumping in the Southern Aegean Sea and the case history of the 1956 tsunami. *Mar. Geol.*, 161: 287-305.

Picarelli L., 2009. Understanding to predict, *In:* Landslides – disaster risk reduction, Sassa K. & Canuti P. (eds), Springer, Berlin, pp. 63-88.

Pino N.A., Piatanesi A., Valensise G. and Boschi E., 2009. The 28 December 1908 Messina Straits Earthquake (Mw 7.1): a great earthquake throughout a century of seismology. *Seismol. Res. Lett.*, 80(2): 243-259, doi: 10.1785/gssrl.80.2.

Piper D.J.W., Pirmez C., Manley P.L., Long D., Flood R.D., Normark W.R. and Showers W., 1997. Mass-transport deposits of the Amazon Fan, *In:* Proceedings of the Ocean Drilling Program, Scientific Results, Flood R.D., Piper D.J.W., Klaus A. & Peterson L.C. (eds), pp. 109-146.

Pirazzoli P.A., Montaggioni L.F., Saliege J.F., Segonzac G., Thommeret Y. and Vergnaud-Grazzini C., 1989. Crustal block movements from Holocene shorelines: Rhodes Island (Greece). *Tectonophysics*, Elsevier Sc. Publ., 170: 89-114.

Prior D.B. and Coleman J.W., 1982. Active slides and flows in underconsolidated marine sediments on the slopes of the Mississippi Delta. *In:* Marine slides and other mass movements, Saxov S. & Nieuwenhuis J.K. (eds), Plenum Press, pp. 21-49.

Rabinovich A.B. and Monserrat S., 1996. Meteorological tsunamis near the Balearic and Kuril Islands: descriptive and statistical analysis. *Nat. Hazards,* 13(1): 55-90.

Reilinger R., McClusky S., Vernant P., Laurence S., Ergintav S., Cakmak R., Ozener H., Kadirov F., Guliev I., Stepanyan R., Nadariya M., Hahubia G., Mahmoud S., ArRajehi A., Abdulaziz K., Paradissis D., Al-Aydrus A., Prilepin M., Guseva T., Evren E., Dmitrotsa A., Filikov S.V., Gomez F., Al-Ghazzi R. and Karam G., 2006. GPS Constraints on Continental deformation in the Africa-Arabia-Eurasia continental collision zone and implications for the dynamics of plate interactions. *J. Geophys. Res*., 111(B5), doi:10.1029/2005JB004051

Reimer P.J. and Reimer R.W., 2001. A marine reservoir correction database and on-line interface. *Radiocarbon*, 43: 461-463. [suppl. mat. <http://www.calib.org>]

Reimer P.J. and McCormac F.G., 2002. Marine radiocarbon reservoir corrections for the Mediterranean and Aegean Seas. *Radiocarbon*, 44: 159-166.

Reinhardt E.G., Goodman B.N., Boyce J.I., Lopez G., van Hengstum P., Rink W.J., Mart Y. and Raban A., 2006. The tsunami of 13 December A.D. 115 and the destruction of Herod the Great's harbor at Caesarea Maritima, Israel. *Geology*, 34: 1061-1064.

Revkin A.C., 2011a. The varied costs of catastrophe. NY Times, March 29.

Revkin A.C., 2011b. Disaster memory' and the flooding of Fukushima. NY Times, April 4.

Robin C., Colantoni P., Gennesseaux M. and Rehault J.P., 1987. Vavilov seamount: a mildly alkaline Quaternary volcano in the Tyrrhenian Sea. *Mar. Geol.*, 78: 125-136.

Roca E., Sans M., Cabrera L. and Marzo M., 1999. Oligocene to Middle Miocene evolution of the central Catalan margin (northwestern Mediterranean). *Tectonophysics*, 315: 209-233.

Rohricht R., 1882. Testimonia minora de Quinto Bello Sacro. Soc. de l'Orient Latin, Geneva, 9: 240 p.

Rosen D.S., 2007. Detection of tsunami and other sea level induced hazards using low latency sea level measurements - a conceptual approach. Workshop on Real-time Transmission and Processing Techniques: Improving the Global Sea Level Observing System's contribution to multi-hazard warning systems, IOC/UNESCO, Paris, 5 June 2007. (<http://www.gloss-sealevel.org/technical_forum/ge10_workshop.html>)

Rosen D.S. and Raz S., 2010. *In situ* detection of tsunami and other sea level related hazards – From a conceptual approach to implementation at MedGLOSS stations. *Rapp. Comm. int. Mer Médit.*, 39: 170.

Rossi S. and Sartori R., 1981. A seismic reflection study of the external Calabrian Arc in the northern Ionian Sea (eastern Mediterranean). *Mar. Geophys. Res.*, 4: 403-426.

Rothwell R.G., 1998. Low-sea-level emplacement of a very large Late Pleistocene "megaturbidite" in the western Mediterranean Sea. *Nature*, 392: 377-380.

Ryan W.B.F., 2008. Decoding the Mediterranean salinity crisis. *Sedimentology*, 56: 95-136.

Sàbat F., Roca E., Muñoz J.A., Vergés J., Santanach P., Sans M., Massana E., Estévez A. and Santisteban C., 1997. Role of extension and compression in the evolution of the eastern margin of Iberia: the ESCI-València trough seismic profile. *Rev. Soc. Geol. Esp.*, 8: 431-448.

Sakellariou D. and Lykousis V., 2003. Impact of geological processes and hazards on the Aegean civilizations in prehistorical and ancient time. *In:* Human records of recent geological evolution in the Mediterranean Basin - historical and archaeological evidence. CIESM Workshop Series n°24 [F. Briand ed.], Monaco, pp. 85-91.

Sakellariou D., Lykousis V., Alexandri S., Kaberi H., Rousakis G., Nomikou P., Georgiou P. and Ballas D., 2007a. Faulting, seismic-stratigraphic architecture and Late Quaternary evolution of the Gulf of Alkyonides basin – East Gulf of Corinth, Central Greece. *Basin Res.*, 19(2): 273-295.

Sakellariou D., Rousakis G., Kaberi H., Kapsimalis V., Georgiou P., Kanellopoulos Th. and Lykousis V., 2007b. Tectono-sedimentary structure and late quaternary evolution of the north Evia Gulf basin, Central Greece: preliminary results. *Bulletin of the Geological Society of Greece*, 37(1): 451-462.

Sakellariou D., Sigurdsson H., Alexandri M., Carey S., Rousakis G., Nomikou P., Georgiou P. and Ballas D., 2010. Active tectonics in the Hellenic Volcanic Arc: the Kolumbo submarine volcanic zone. *Bulletin of the Geological Society of Greece*, 63(2): 1056-1063.

Salamon A., 2010. Patterns of seismic sequences in the Levant - Interpretation of historical seismicity. *J. Seismol.*, 14(2): 339-367. doi: 10.1007/s10950-009-9168-9

Salamon A., Hofstetter A., Garfunkel Z. and Ron H., 2003. Seismotectonics of the Sinai subplate - The Eastern Mediterranean region. *Geophys. J. Int.*, 155: 149-173.

Salamon A., Rockwell T., Ward S.N., Guidoboni E. and Comastri A., 2007. Tsunami hazard evaluation of the easterm Mediterranean: historical analysis and selected modeling. *Bull. Seismol. Soc. Am.,* 97(3): 705-724, doi:10.1785/0120060147

Sardou O. and Mascle J., 2003. Cartography by multibeam echo sounder of the Nile deep sea fan and surrounding areas, special publication CIESM / Ifremer, série carte et atlas.

Sartori R., 1990.The main results of ODP Leg 107 in the frame of Neogene to Recent geology of peri-Tyrrhenian areas. *In:* Proceedings of the ODP, Scientific Results, Kastens K.A., Mascle J. *et al.* (eds), 107: 715-730.

Sartori R., 2003. The Tyrrhenian back-arc basin and subduction of the Ionian lithosphere. *Episodes*, 26(3): 217-221.

Savoye B. and Piper D.J.W., 1991. The Messinian event on the margin of the Mediterranean Sea in the Nice area, southern France. *Mar. Geol.*, 97: 279-304.

Scicchitano G., Monaco C. and Tortorici L., 2007. Large boulder deposits by tsunami waves along the Ionian coast of south-eastern Sicily (Italy). *Mar. Geol.*, 238: 75-91.

Scicchitano G., Costa B., Di Stefano A., Longhitano S. and Monaco C., 2010. Tsunami and storm deposits preserved within a ria-type rocky coastal setting (Siracusa, SE Sicily). *Zeitschrift für Geomorphologie N.F.*, 54(3): 51-77.

Seed H.B., Seed R.B., Schlosser F., Blondeau F. and Juran I., 1988. The Landslide at the port of Nice on October 16, 1979. Earthquake Engineering Research Center, report No. CB/EERC-88/10.

Serri G., 1997. Neogene-Quaternary magmatic activity and itsgeodynamic implications in the Central Mediterranean region. *Annali di Geofisica*, XL(3): 681-703.

Shalem N., 1956. Seismic tidal waves (tsunamis) in the Eastern Mediterranean. *Bull. Isr. Explor. Soc.*, XX(3-4): 159-170 (in Hebrew).

Shaw B., Ambraseys N.N., England P.C., Floyd M.A., Gorman G.J., Higham T.F.G., Jackson J.A., Nocquet J.M., Pain C.C. and Piggott M.D., 2008. Eastern Mediterranean tectonics and tsunami hazard inferred from the AD 365 earthquake. *Nat. Geosci.*, 1: 268-276, <www.nature.com/naturegeoscience> Published online: 9 March 2008, doi:10.1038/ngeo151

Shiki T., Tachibana T., Fujiwara O., Goto K., Nanayama F. and Yamazaki T., 2008. Characteristic features of tsunamiites. *In:* Tsunamiites - features and implications, Shiki T., Tsuji Y., Yamazaki T. & Minoura K. (eds), Elsevier, Amsterdam, pp. 319-340.

Sigurdsson H., 2000. Encyclopedia of volcanoes. Academic Press, Florida, U.S.A., 1417 p.

Sigurdsson H. and Carey S., 1989. Plinian and coignimbrite tephra fall from the 1815 eruption of Tambora volcano. *Bull. Volcanol.*, 51: 243-270,84.

Sigurdsson H., Carey S., Mandeville C. and Bronto S., 1991. Pyroclastic flows of the 1883 Krakatau eruption. *Eos Trans. AGU*, 72(36): 377, 380-381.

Sigurdsson H., Carey S., Alexandri M., Vougioukalakis G., Croff K., Roman C., Sakellariou D., Anagnostou C., Rousakis G., Ioakim C., Gogou A., Ballas D., Misaridis T. and Nomikou P., 2006. Marine Investigations of Greece's Santorini Volcanic Field. *EOS*, 87(34): 22 August.

Singer J., 2011. Disaster expert seeks better tsunami defense. The Japan Times, April 23, 2011.

Smedile A., De Martini P.M., Pantosti D., Bellucci L., Del Carlo P., Gasperini L., Pirrotta C., Polonia A. and Boschi E., 2011. Possible tsunamis signatures from an integrated study in the Augusta Bay offshore (Eastern Sicily-Italy). *Mar. Geol.,* doi: 10.1016/j.margeo.2011.01.002.

Smid T.C., 1970. 'Tsunamis' in Greek Literature. *Greece & Rome*, 2nd Ser., 17(1): 100-104.

Soloviev S.L., Solovieva O., Go C., Kim K. and Shchetnikov A., 2000. Tsunamis in the Mediterranean Sea, 2000 B.C. to 2000 A.D., Kluwer, Dordrecht, 237 p.

Stegmann S., Sultan N. and Kopf A., 2011. Hydrogeology and its effect on slope stability along the coastal acquifer of Nice, France. *Mar. Geol.*, doi: 10.1016/j.margeo.2010.12.009.

Stich D., Ammon C.J. and Morales J., 2003a. Moment tensor solutions for small and moderate earthquakes in the Ibero-Maghreb region. *J. Geophys. Res.*, 108: 2148-2168.

Stich D., Batlló J., Morales J., Macià R. and Dineva S., 2003b. Source parameters of the MW = 6.1 1910 Adra earthquake (southern Spain). *Geophys. J. Int.*, 155: 539-546.

Stich D., Mancilla F. and Morales J., 2005. Crust mantle coupling in the Gulf of Cadiz (SW Iberia). *Geophys. Res. Lett.*, 32: L13306.

Stich D., Mancilla F., Pondrelli S. and Morales J., 2007. Source analysis of the February 12th, Mw 6.0 Horseshoe earthquake: implications for the 1755 Lisbon earthquake. *Geophys. Res. Lett.*, 34: L12308.

Stich D., Martín R. and Morales J., 2010. Moment tensor inversion for Iberia-Maghreb earthquakes 2005-2008. *Tectonophys.*, 483: 390-398.

Stiros S.C., 2010. The 8.5+ magnitude, AD365 earthquake in Crete: coastal uplift, topography changes, archaeological and historical signature. *Quatern. Int*., 216: 54-63.

Stiros S.C. and Pirazzoli P.A., 2009. Earthquake cycle anomalies in the Aegean Arc. Int'l Symposium on Historical Earthquakes in the Eastern Mediterranean Region, 500th Anniversary of the 1509 Sept. 10th Marmara Earthquake. 10-12 Sept. 2009. Istanbul, p. 142-147.

Striem H.L. and Miloh T., 1976. Tsunami induced by submarine slumping off the coast of Israel. Israel Atomic Energy Commission, 1975, 23 p.; also, *Inter. Hydrogr. Rev.*, 53(2): 41-53.

Stuiver M. and Reimer P.J., 2005. Radiocarbon calibration program CALIB REV5.0.2, copyright, available at <http://calib.cub.ac.uk/calib/>

Sugawara D., Minoura K. and Imamura F., 2008. Tsunamis and tsunami sedimentology. *In:* Shiki T., Tsuji Y., Yamazaki T. & Minoura K., (eds), Tsunamiites - features and implications, Elsevier, Amsterdam, pp. 9-49.

Sultan N., Cochonat P., Canals M., Cattaneo A., Dennielou B., Haflidason H., Laberg J., Long D., Mienert J. and Trincardi F., 2004. Triggering mechanisms of slope instability processes and sediment failures on continental margins: a geotechnical approach. *Mar. Geol.*, 213: 291-321.

Sultan N., Gaudin M., Berné S., Baztán J., Canals M., Urgeles R. and Lafuerza S., 2005. Slope failures in canyon heads. *J. Geophys. Res.*, 112(F1): Art. No. F01009.

Sultan N., Voisset M., Marsset B., Marsset T., Cauquil E. and Colliat J.L., 2007. Potential role of compressional structures in generating submarine slope failures in the Niger Delta. *Mar. Geol.*, 237(3-4): 169-190.

Sultan N. and shipboard party, 2008. Prisme Cruise (R/V Atalante Toulon - Toulon; 2007): Reports and Preliminary Results. IFREMER Internal Report, Ref: IFR CB/GM/LES/08-11.

Sultan N., Savoye B., Jouet G., Leynaud D., Cochonat P., Henry P., Stegmann S. and Kopf A., 2010. Investigation of a possible submarine landslide at the Var delta front (Nice slope, SE France). *Canadian Geotech. J.*, 47: 486-496.

Tani K., Fiske R.S., Tamura Y., Kido Y., Naka J., Shukuno H. and Takeuchi R., 2008. Sumisu volcano, Izu-Bonin arc, Japan: site of a silicic caldera-forming eruption from a small open-ocean island. *Bull. Volcanol.*, 70: 547-562

Tassi F., Capaccioni, B., Caramanna G., Cinti D., Montegrossi G., Pizzino L., Quattrocchi F. and Vaselli O., 2009. Low-pH waters discharging from submarine vents at Panarea Island (Aeolian Islands, southern Italy) after the 2002 gas blast: origin of hydrothermal fluids and implications for volcanic surveillance. *Appl. Geochem.*, 24: 246-254.

Ten Veen J.H. and Kleinspehn K.L., 2003. Incipient continental collision and plate-boundary curvature: Late Pliocene–Holocene transtensional Hellenic forearc, Crete, Greece. *Journal of the Geological Society*, London, 160: 161-181.

Ten Veen J.H., Woodside J.M., Zitter T.A.C., Dumont J.F., Mascle J. and Volkonskaia A., 2004. Neotectonic evolution of the Anaximander Mountains at the junction of the Hellenic and Cyprus arcs. *Tectonophysics*, 391: 35-65.

Terrinha P., Pinheiro L.M., Henriet J.P., Matias L., Ivanov M.K., Monteiro J.H., Volkonskaya A., Cunha T., Shaskin P. and Rovere M., 2003. Tsunamigenic-seismogenic structures, neotectonics, sedimentary processes and slope instability on the southwest Portuguese Margin. *Mar. Geol.*, 195(1-4): 55-73.

Terrinha P., Matias L., Vicente J., Duarte J., Luiss J., Pinheiro L., Lourenço N., Diez S., Rosas F., Magalhaes V., Valadares V., Zitellini N., Roque C., Mendes Victor L. and MATESPRO Team., 2009. Morphotectonics and strain partitioning at the Iberia-Africa plate boundary from multibeam and seismic reflection data. *Mar. Geol.*, 267: 156-174.

Thio H.K., 2009. Tsunami hazard in Israel, URS Corp., Pasadena, USA report for Geological Survey of Israel, January 2009.

Tibor G., Niemi T.M., Ben-Avraham Z., Al-Zoubi A., Sade R.A., Hall J.K., Hartman G., Akawi E., Abueladas A. and Al-Ruzouq R., 2010. Active tectonic morphology and submarine deformation of the northern Gulf of Eilat/Aqaba from analyses of multibeam data. *Geo-Mar Lett*., DOI 10.1007/s00367-010-0194-y

Tinti S., 2003. Needs and perspectives of tsunami research in Europe. *In:* Submarine landslides and tsunamis, Yalçıner A.C. *et al.* (eds), Kluwer publ., pp. 9-16.

Tinti S. and Maramai A., 1996. Catalogue of tsunamis generated in Italy and in Côte d'Azur, France: a step towards a unified catalogue of tsunamis in Europe. *Annali di Geofisica*, 39: 1253-1299.

Tinti S., Bortolucci E. and Romagnoli C., 1999. Modeling a possible holocenic landslide-induced tsunami at Stromboli Volcano, Italy. *Phys. Chem. Earth*, Part B: Hydrology, Oceans and Atmosphere, 24(5): 423-429.

Tinti S. and Armigliato A., 2003. The use of scenarios to evaluate tsunami impact in South Italy. *Mar. Geol.*, 199: 221-243.

Tinti S., Maramai A. and Graziani L., 2004. The new catalogue of the Italian tsunamis. *Nat. Hazards*, 33: 439-465.

Tinti S., Armigliato A., Pagnoni G. and Zaniboni F., 2005a. Scenarios of giant tsunamis of tectonic origin in the Mediterranean. *ISET J. Earthq.Technol.*, 42(4): 171-188.

Tinti S., Manucci A., Pagnoni G., Armigliato A. and Zambinoni F., 2005b. The 30 December 2002 landlside-induced tsunami in Stromboli: sequence of events reconstructed from the eyewitness accounts. *Nat. Hazards Earth Syst. Sci.*, 5: 763-775.

Tinti S., Armigliato A., Manucci A., Pagnoni G., Zaniboni F., Yalçiner A.C. and Altinok Y., 2006a. The generating mechanisms of the Aug.17. 1999 Izmit Bay (Turkey) tsunami: regional (tectonic) and local (mass instabilities) causes. *Mar. Geol.*, 225: 311-330.

Tinti S., Maramai A., Armigliato A., Graziani L., Manucci A., Pagnoni G. and Zaniboni F., 2006b. Observations of physical effects from tsunamis of December 30, 2002 at Stromboli volcano, southern Italy. *Bull. Vocan.*, 68: 450-461.

Tinti S., Canals M., Pagnoni G., Zaniboni F., Iglesias O. and Lastras G., 2009. The BIG'95 event, Balearic Islands, Western Mediterranean Sea: numerical simulation of the possibly generated tsunami. EGU 2009, Geophysical Research Abstracts, vol. 11 Abstract EGU2009-13365, Vienna, Austria.

Tinti S., Armigliato A. and Zaniboni F., 2010a. Tsunami Early Warning System in Italy and involvement of local Communities, *In*: EGU General Assembly 2010, Vienna, Austria, Geophysical Research Abstracts, Vol. 12, EGU2010-8108.

Tinti S., Tonini R., Bressan L., Armigliato A., Gardi A., Guillande R., Valencia N. and Scheer S., 2010b. Handbook on Tsunami Hazard and Damage Scenarios, EUR XXXXX EN, JRCXXXXX, Luxembourg (Luxembourg): OP, 2010.

Todorovska M.I., Hayir A. and Trifunac M.D., 2002. A note on tsunami amplitudes above submarines slides and slumps. *Soil Dyn. Earthquake Eng.*, 22: 129-141.

Tokyo Earthquake Research Institute, 2011. 2011 Tohoku earthquake. <http://outreach.eri.u-tokyo.ac.jp/eqvolc/201103_tohoku/eng/>

Tonini R., Armigliato A., Pagnoni G. and Tinti S., 2010. Tsunami inundation scenarios of the city of Catania, Eastern Sicily, Italy, *In*: EGU General Assembly 2010, Vienna, Austria, Geophysical Research Abstracts, Vol. 12, EGU2010-7000.

Tonini R., Armigliato A., Pagnoni G., Zaniboni F. and Tinti S., 2011. Tsunami hazard and risk assessment for the city of Catania, eastern Sicily, Italy. Part I: hazard maps based on worst credible tsunami scenarios. *Nat. Hazard Earth Sys.*, 11: 1217-1232.

Tuttle M.P., Ruffman A., Anderson T. and Jeter H., 2004. Distinguishing tsunami from storm deposits in eastern North America: The 1929 Grand Banks tsunami versus the 1991 Halloween storm. *Seismol. Res. Lett.*, 75: 117-131.

UNESCO, 2008. Tsunami preparedness: information guide for disaster planners. IOC Manuals and Guides No. 49. Paris, UNESCO, 26 p. <http://www.ioc-tsunami.org/images/stories/documents/manualandguides49_e.pdf>

UNISDR, 2009. Global risk assessment report on disaster risk reduction, United Nations, Geneva.

Urciuoli G., Picarelli L. and Leroueil S., 2007. Local soil failure before general slope failure. *Geotechnical and Geological Engineering*, 25: 103-122.

Urgeles R., Canals M., Baraza J., Alonso B. and Masson D.G., 1997. The most recent megalandslides of the Canary Islands: El Golfo debris avalanche and Canary debris flow, west El Hierro Island. *J. Geophys. Res.*, *102*(B9), 20,305-320,323.

Urgeles R., Lastras. G., Canals M., Willmott V., Moreno A., Casas D., Baraza J. and Berné S., 2003. The BIG'95 debris flow and adjacent unfailed sediments in the NW Mediterranean Sea: geotechnical-sedimentological properties and dating, *In:* Submarine mass movements and their consequences, Locat J. & Mienert J. (eds), Kluwer Academic Publishers, Dordrecht (The Netherlands), pp. 479-487.

Urgeles R., Leynaud D., Lastras G., Canals M. and Mienert J., 2006. Back-analysis and failure mechanisms of a large submarine slide on the Ebro continental slope, NW Mediterranean. *Mar. Geol.*, 226: 185-206.

Urgeles R., Camerlenghi A., Ercilla G., Anselmetti F., Brückmann W., Canals M., Gràcia E., Locat J., Krastel S. and Solheim A., 2007a. Scientific ocean drilling behind the assessment of geo-hazards from submarine slides. *EOS Trans. Am. Geoph. Union*, 88(17): 192.

Urgeles R., De Mol B., Liquete C., Canals M., De Batist M., Hughes-Clarke J.E., Amblàs D., Arnau P.A., Calafat A.M., Casamor J.L., Centella V., De Rycker K., Fabrés J., Frigola J., Lafuerza S., Lastras G., Sànchez A., Zuñiga D., Versteeg W. and Willmott V., 2007b. Sediment undulations on the Llobregat prodelta: signs of early slope instability or bottom current activity?, *J. Geophys. Res.*, 112: B05102.

Urgeles R., Camerlenghi A., Garcia-Castellanos D., De Mol B., Garcés M., Vergés J., Haslam I. and Hardman M., 2010. New constraints on the Messinian sealevel drawdown from 3D seismic data of the Ebro Margin, western Mediterranean. *Basin Res.*, doi:10.1111/j.1365-2117.2010.00477.x.

Valensise G., 2004. Source characteristics of the 28 December 1908, Messina Straits earthquake (Mw 7.1): a review. 1st International Conference of Applied Geophysics for Engineering, Osservatorio Sismologico – Università di Messina
Messina, Italy.

Van der Bergh G.D., Boer W., Haas H., van Weering T. and van Wijhe R., 2003. Shallow marine tsunami deposits in Telik Banten (NW Java, Indonesia), generated by the 1883 Krakatau eruption. *Mar. Geol.*, 197: 13-34.

Van Dorn W.G., 1987. Tide gage response to tsunamis. Part II: other oceans and smaller seas. *J. Phys. Oceanogr.*, 17: 1507-1516.

Vaunat J. and Leroueil S., 2000. Analysis of post-failure slope movements within the framework of hazard and risk analysis. *In:* Canadian Workshop on Geotechnique and Natural Hazards. Montreal, Canada, pp. 83-109.

Vidal N. and Merle O., 2000. Reactivation of basement faults beneath volcanoes: a new model of flank collapse. *J. Volcanol. Geotherm. Res.*, 99: 9-26.

Vilibic´ I. and Šepic J., 2009. Destructive meteotsunamis along the eastern Adriatic coast: overview. *Phys. Chem. Earth*, 34: 904-917.

Vizcaino A., Gràcia E., Pallàs R., Garcia-Orellana J., Escutia C., Casas D., Willmott V., Diez S. and Dañobeitia J.J., 2006. Sedimentology, physical properties and ages of mass-transport deposits associated to the Marquês de Pombal Fault, Southwest Portuguese Margin. *Norw. J. Geol.*, 86: 173-182.

Voett A., May M., Brueckner H. and Brockmueller S., 2006. Sedimentary evidence of Late Holocene tsunami events near Lefkada Island (NW Greece). *Zeitschrift f. Geomorphologie N.F.*, 146(Suppl.): 139-172.

Voett A., Brueckner H., Brockmueller S., May M., Fountoulis I., Gaki-Papanastassiou K., Herd R., Lang F., Maroukian H., Papanastassiou D. and Sakellariou D., 2007. Tsunami impacts on the Lefkada coastal zone during the past millennia and their palaeogeographical implications. *In:* Papadatou-Giannopoulou H. (ed.), Proceedings of the International Conference Honouring Wilhelm Doerpfeld, August 6-9, 2006, Lefkada.

Vött A. *et al*., 2009. Traces of Holocene tsunamis across the Sound of Lefkada, NW Greece. *Global Planet. Change*, 66: 112-128.

Washington H.S., 1909. The submarine eruption of 1831 and 1891 near Pantelleria. *Am. Journ. Sc.*, 27: 131-150.

Watts P., 2004. Probabilistic predictions of landslide tsunamis off southern California. *Mar. Geol.*, 203: 281-301.

Weiss R. and Bahlburg H., 2006. A note on the preservation of offshore tsunami deposits. *J. Sediment. Res*, 76: 1267-1273.

Westaway R., 1993. Quaternary uplift of southern Italy. *J. Geophys. Res.*, 98: 21741-21772.

Whelan F. and Kelletat D., 2002. Geomorphic evidence and relative and absolute dating results for tsunami events on Cyprus. *Science of Tsunami Hazards*, 20(1): 3-18.

Wiegel R.L., 1964. Oceanographical engineering, Englewood Cliffs, New Jersey: Prentice Hall.

Wiegel R.L., 2007. Technical information resources on tsunamis with a section on landslide generated waves. California Shore and Beach Preservation Association, Northern California Conference, Pacifica, California, USA. April 26. updated May 9, 2007.

Wisner B., Blaikie P., Cannon T. and Davis I., 2004. At risk. London: Routledge, 2nd Edition 2004.

Wust H., 1997. The November 22, 1995, Nuweiba earthquake, Gulf of Elat (Aqaba), Post-seismic analysis of failure features and seismic hazard implications. *Isr. Geol. Surv.,* Rep. GSI/3/97, 58 p.

Yalciner A.C., Synolakis C.E., Borrero J.C., Altinok Y., Watts P., Imamura F., Kuran U., Ersoy S., Kanoglu U. and Tinti S., 1999. Tsunami generation in Izmit bay by the 1999 Izmit Earthquake. *In:* Proc. Conference on the 1999 Kocaeli Earthquake, Istanbul Technical University Press, Turkey, pp. 217-221.

Yalcıner A.C., Alpar B., Altınok Y., Ozbay I. and Imamura F., 2002. Tsunamis in the Sea of Marmara: historical documents for the past, models for future. *Mar. Geol*., 190: 445-463.

Yalciner A.C., Pelinovsky E., Zaitsev A., Kurkin A., Ozer C., Karakus H. and Ozyurt G., 2007. Modeling and visualization of tsunamis: Mediterranean examples. *In:* Kundu A. (ed.), Tsunami and nonlinear waves tsunami and nonlinear waves, Springer Berlin Heidelberg, pp. 273-283, DOI 10.1007/978-3-540-71256-5.

Yaltırak C., 2002. Tectonic evolution of the Marmara Sea and its surroundings. *Mar. Geol*., 190: 493-529.

Yokoyama I., 1978. The tsunami caused by the prehistoric eruption of Thera. *In:* Thera and the Aegean World II, 2 (Doumas C., ed.) (London, Thera and Aegean World 1978), pp. 277-283.

Yolsal S., Taymaz T. and Yalçiner A.C., 2007. Understanding tsunamis, potential source regions and tsunami-prone mechanisms in the Eastern Mediterranean. *In:* The geodynamics of the Aegean and Anatolia, Taymaz T., Yilmaz Y. & Dilek Y. (eds). *Geol. Soc., London*, Special Publ. 291: 201-230, doi:10.1144/SP291.10.

Zaniboni F., Lo Iacono C., Tinti S., Gràcia E., Pagnoni G., Dañobeitia J.J., Lourenço N. and Abreu M.A., 2010. Numerical simulations of the North Gorringe Avalanche, Eastern Atlantic Ocean, and of the consequent tsunami impacting the Iberian coasts. EOS Trans AGU, Fall meeting Suppl., San Francisco (USA).

Zitellini N., Rovere M., Terrinha P., Chierici F., Matias L. and BIGSETS TEAM, 2004. Neogene through Quaternary tectonic reactivation of SW Iberian passive margin. *Pure Appl. Geophys.*, 161: 565-587.

Zitellini N., Gràcia E., Matias L., Terrinha P., Abreu M.A., De Alteriis G., Henriet J.P., Dañobeitia J.J., Masson D.G., Mulder T., Ramella R., Somoza L. and Diez S., 2009. The Quest for the Africa-Eurasia plate boundary west of the Strait of Gibraltar. *Earth Planet. Sci. Lett.*, 280: 13-50.

Zitellini N. and NEAREST TEAM, 2011. Development of a Tsunami Early Warning System (TEWS) Prototype based on the direct monitoring of a potential tsunamigenic structure located near the coasts of SW Iberia: Preliminary results of the EU Project NEAREST. European Geosciences Union (EGU)-11, Vienna (Austria).

Zitter T.A.C., Henry P., Aloisi G., Delaygue G. *et al*., 2008. Cold seeps along the main Marmara fault in the Sea of Marmara (Turkey). *Deep Sea Res.,* Part I, 55: 552-570.

IV - List of Participants

Frédéric Briand
Director General, CIESM
CIESM
16, bd de Suisse, Monaco
fbriand@ciesm.org

Silvia Ceramicola
Istituto Nazionale di Oceanografia e Geofisica Sperimentale (OGS), Sgonico, Italy
sceramicola@ogs.trieste.it

Gert de Lange
Chair, CIESM Committee on Marine Geosciences
Workshop Moderator
Faculty of Geosciences
Utrecht University, Netherlands
gdelange@geo.uu.nl

Paolo Marco De Martini
Istituto Nazionale di Geofisica e Vulcanologia
Gruppo di Tettonica Attiva, Roma, Italy
paolomarco.demartini@ingv.it

Fabiano Gamberi
ISMAR - CNR
Bologna, Italy
fabiano.gamberi@bo.ismar.cnr.it

Jean Mascle
Coordinator, CIESM Task Force on Deep Sea Research
GéoAzur
Villefranche-sur-Mer, France
mascle@geoazur.obs-vlfr.fr

Sébastien Migeon
GéoAzur
Villefranche-sur-Mer, France
migeon@geoazur.obs-vlfr.fr

Nilgun Okay
Dept. of Geological Engineering
Istanbul Technical University, Turkey
okayn@itu.edu.tr

Ioannis Panayides
Geological Survey Dpt.
Nicosia, Cyprus
ipanayides@gsd.moa.gov.cy

Gerassimos Papadopoulos
Institute of Geodynamics
National Observatory of Athens, Greece
papadop@noa.gr

Dov S. Rosen
Israel Oceanographic & Limnological Research
Haifa, Israel
rosen@ocean.org.il

Dimitris Sakellariou
Institute of Oceanography, HCMR
Athens, Greece
sakell@ath.hcmr.gr

Amos Salamon
Geological Survey of Israel
Jerusalem, Israel
salamon@gsi.gov.il

Valenti Sallarès
Barcelona-CSI, Marine Technology Unit (CSIC)
Barcelona, Spain
vsallares@cmima.csic.es

Nabil Sultan
Département Géosciences Marines
Ifremer, Plouzané, France
nabil.sultan@ifremer.fr

Stefano Tinti
Dipartimento di Fisica, Settore di Geofisica
Università di Bologna, Italy
stefano.tinti@unibo.it

MULTIPRINT - MONACO
Dépôt légal 75150